STRUCTURE/FUNCTION STUDIES OF THE *BORDETELLA PERTUSSIS* AUTOTRANSPORTER PROTEIN BRKA: SECRETION AND FOLDING

by

David C. Oliver

B.Sc., University of British Columbia, 1997

A THESIS SUBMITTED IN PARTIAL FULFILLMENT OF

THE REQUIREMENTS FOR THE DEGREE OF

DOCTOR OF PHILOSOPHY

in

THE FACULTY OF GRADUATE STUDIES

(DEPARTMENT OF MICROBIOLOGY AND IMMUNOLOGY)

THE UNIVERSITY OF BRITISH COLUMBIA

March 2005

Abstract

The autotransporter secretion system represents a fundamental strategy that Gram-negative bacteria have evolved to deliver an array of functionally diverse proteins to the cell surface. As the name implies, the autotransporter secretion system does not employ specific accessory factors; all of the information necessary for movement of a substrate polypeptide across the two membranes of the cell envelope is encoded within a single gene product. Autotransporters are modular multidomain proteins consisting of an N-terminal signal peptide, a passenger domain that contains the effector function(s) to be delivered to the cell surface, and a C-terminal domain termed the translocation unit. The signal peptide directs translocation across the inner membrane and the translocation unit facilitates export across the outer membrane. How this seemingly simple protein secretion strategy functions is largely unknown. This study addresses the secretion mechanism of the BrkA protein, a known virulence factor of *Bordetella pertussis* (the causative agent of whooping cough) and a putative autotransporter protein. Using a combination of genetic, biochemical, bioinformatic and cell biological approaches, BrkA was shown here to be a *bona fide* autotransporter protein and was established as a model system for studying autotransporter secretion. Structural and functional dissection of BrkA revealed a multidomain architecture consisting of a signal peptide, a passenger domain that contains the BrkA effector functions (serum resistance and adherence), and a C-terminal translocation unit. Significantly, a region termed the junction that is located at the C-terminus of the BrkA passenger domain was identified to be required for passenger folding during secretion. The conservation of this domain in a functionally

diverse group of autotransporter proteins suggested that it plays an important role in secretion. The demonstration that the junction region mediated BrkA passenger folding when supplied in *trans* as a separate polypeptide suggests that it can function as an intramolecular chaperone. Further dissection of the BrkA junction revealed a sub-region that is not required for passenger folding but is required for secretion of a "folding competent" native BrkA passenger. These findings have been integrated with our current knowledge of autotransporter secretion to generate a working model of BrkA secretion that may be applicable to other autotransporter proteins.

Table of Contents

Abstract ii

Table of Contents iv

List of Figures and Tables ix

List of Abbreviations xi

Acknowledgments xii

Chapter 1

1.1 Introduction and Overview 1

1.1.1 Protein secretion in Gram negative bacteria 1

1.1.2 Autotransporter secretion 3

1.1.3 Autotransporter domain structure 7

1.1.3.1 Signal peptides: variations on a theme 7
1.1.3.2 Passengers: scaffolds for hitching functional modules 8
1.1.3.3 The translocation unit: a *bona fide* portal? 9

1.1.4 Outer membrane translocation 12

1.1.4.1 Passenger targeting and orientation 13
1.1.4.2 Passenger conformation 14
1.1.4.3 What drives translocation? 16

1.1.5 At the surface: maturation, anchoring, release 17

1.1.6 AT1 vs. AT2 autotransporters 18

1.1.7 Thesis overview 19

1.1.8 References 22

Chapter 2: Initial characterization of BrkA secretion

2.1 Introduction 27

2.2 Materials and method 31

2.2.1 Bacterial strains and growth media 31
2.2.2 Recombinant DNA techniques 32
2.2.3 Purification of $rBrkA^{1-693}$ 33
2.2.4 Generation of polyclonal antibodies to $rBrkA^{1-693}$ 34
2.2.5 SDS-PAGE and immunoblot analysis 34
2.2.6 N-terminal sequencing 35
2.2.7 Immunofluorescence 36
2.2.8 Radial diffusion serum killing assay 37

2.3 Results 41

2.3.1 Expression and purification of functional recombinant $rBrkA^{1-693}$ 41
2.3.2 Antibodies to $rBrkA^{1-693}$ recognise surface-expressed BrkA in *B. pertussis* 44
2.3.3 Antibodies to $rBrkA^{1-693}$ neutralise serum resistance in *B. pertussis* 46
2.3.4 Expression of BrkA in *E. coli* 49
2.3.5 Identification of the BrkA signal peptide 52
2.3.6 Identification of the minimal BrkA translocation unit necessary for surface expression 53

2.4 Discussion

2.4.1 The BrkA signal peptide 59
2.4.2 The BrkA "translocation unit" 60
2.4.3 What cleaves the BrkA precursor at Asn^{731}-Ala^{732} to yield the α- and β- domains? 63
2.4.4 How does the BrkA α-domain remain anchored to the cell surface? 64

2.5 References 65

Chapter 3: Identification and initial characterization of a conserved domain required for folding of the BrkA passenger domain

3.1 Introduction 69

3.2 Materials and Methods 72

3.2.1 Bacterial strains and plasmids and growth conditions 72
3.2.2 Recombinant DNA techniques 72
3.2.3 SDS-PAGE and immunoblot analysis 75
3.2.4 Immunofluorescence analysis 75
3.2.5 Purification and refolding of BrkA fusion proteins 76
3.2.6 Far-UV circular dichroism spectroscopy of BrkA fusion proteins 77
3.2.7 *In vitro* limited proteolysis analysis 77
3.2.8 *In vivo* limited proteolysis analysis 78
3.2.9 Cell surface refolding of rBrkA(61-605)P fusion protein 78
3.2.10 Adherence assay 79

3.3 Results

3.3.1 BrkA Glu^{601}-Ala^{692} is necessary for passenger stability in the presence of endogenous outer membrane proteases 82
3.3.2 A conserved domain is found within the passenger region of several autotransporters 86
3.3.3 *In vivo trans* complementation of BrkA folding 91
3.3.4 *In vivo* evidence demonstrating that residues Glu^{601}-Ala^{692} of BrkA are required for folding of the BrkA passenger 95
3.3.5 BrkA (ΔGlu^{601}-Ala^{692}) *trans* complemented *in vivo* yields a proteolytic profile similar to wild type BrkA expressed in *E. coli* and *B. pertussis* 98
3.3.6 *In vitro* evidence demonstrating that residues Glu^{601}-Val^{699} of BrkA are required for folding of the BrkA passenger 101
3.3.7 Purified junction-deleted BrkA (Glu^{61}-Lys^{605}) passenger adopts a protease resistant conformation when added exogenously to *E. coli* UT5600 expressing the BrkA "junction" region 105
3.3.8 Summary of BrkA fusion protein refolding studies 107
3.3.9 Residues Ala^{681}-Gln^{707} are not required for BrkA passenger folding or stability 110
3.3.10 Co-expression of the pertactin junction (Phe^{470}-Ser^{607}) complements BrkA(ΔGlu^{601}-Ala^{692}) passenger folding 112

3.4 Discussion

3.4.1 The BrkA junction region mediates folding of the BrkA passenger domain 115
3.4.2 The role of the junction in BrkA secretion 119
3.4.3 Other functions of the junction 122
3.4.4 Do all autotransporters encode a "junction" region,

and are the "autochaperone" and "HSF" functions conserved? 132
3.4.5 Terminology: "junction" vs. "linker"

3.5 References 134

Chapter 4: Homologous translocation units are not required for *trans* complementation of BrkA passenger folding

4.1 Introduction 140

4.2 Materials and Methods 143

4.2.1 Bacterial strains and plasmids and growth conditions 143
4.2.2 Recombinant DNA techniques 143
4.2.3 SDS-PAGE and immunoblot analysis 144
4.2.4 *In vivo* limited proteolysis analysis 144

4.3 Results 146

4.3.1 Construction of BrkA, pertactin, IgA protease chimeras 146
4.3.2 Homologous translocation units are not required for *trans* complementation of BrkA(Gln^{43}-Ala^{600}) passenger folding 148

4.4 Discussion 151

4.5 References 153

Chapter 5: General Discussion

5.1 Autotransporter secretion: simply biochemistry 154

5.1.1 Targeting to the inner membrane 156
5.1.2 Translocation across the inner membrane and transit through the periplasm 158
5.1.3 Outer membrane translocation: working models 161
5.1.4 What is the driving force for translocation across the outer membrane?
5.1.5 What is the driving force for translocation across the outer membrane? 167
5.1.6 At the surface: the final station and destinations beyond... 171

5.2 Future directions in BrkA secretion 173

5.3 Practical potential 174

5.4 References 176

Appendix

A.1 Structural modeling of the BrkA passenger domain 180

A.2 Lipidation of autotransporters 185

A.3 Oliver DC, Fernandez RC.Antibodies to BrkA augment killing of *Bordetella pertussis*. Vaccine. 2001 Oct 12;20(1-2):235-41. 188

A.4 Oliver DC, Huang G, Fernandez RC. Identification of secretion determinants of the *Bordetella pertussis* BrkA autotransporter. J Bacteriol. 2003 Jan;185(2):489-95. 197

A.5. Oliver DC, Huang G, Nodel E, Pleasance S, Fernandez RC. A conserved region within the *Bordetella pertussis* autotransporter BrkA is necessary for folding of its passenger domain. Mol Microbiol. 2003 Mar;47(5):1367-83. 205

List of Figures and Tables

Figure 1-1	Model of autotransporter secretion	5
Figure 1-2	Structural features of autotransporter proteins	6
Table 2-1	Strains and plasmids	39
Table 2-2	Primer table	40
Figure 2-1	Purification and demonstration of functional activity of recombinant BrkA	43
Figure 2-2	Immunoblot analysis of the rBrkA$^{1-693}$ antiserum	45
Figure 2-3	The rBrkA$^{1-693}$ antiserum recognises surface expressed BrkA.	45
Figure 2-4	The rBrkA$^{1-693}$ antiserum neutralises serum resistance in wildtype *B. pertussis*.	48
Figure 2-5	BrkA expression in *E. coli* strain UT5600	51
Figure 2-6	BrkA passenger deletion constructs	57
Figure 2-7	Expression of BrkA deletion constructs in *E. coli* UT5600.	58
Figure 2-8	Comparison of the C-terminal regions of different autotransporters.	62
Table 3-1	Strains and plasmids	80
Figure 3-1	Expression of mutant forms of BrkA	85
Figure 3-2	Identification of a conserved domain within the passenger region of several autotransporter proteins.	88
Figure 3-3	Comparative analysis of the junction region found within several autotransporters	90
Figure 3-4	*In vivo trans* complementation of BrkA stability	94
Figure 3-5	Characterization of surface expressed forms of BrkA by trypsin analysis	97

Figure 3-6	Proteolytic profiles of surface expressed forms of BrkA	99
Figure 3-7	Limited proteolysis of surface exposed BrkA yields a stable 50-55 kDa fragment.	100
Figure 3-8	Characterization of refolded BrkA fusion peptides.	104
Figure 3-9	Exogenous addition of recombinant junction-deleted BrkA passenger to *E. coli* UT5600.	106
Table 3-2	Summary of refolding studies of BrkA fusion proteins.	109
Figure 3-10	Residues Glu^{681}-Gln^{707} are not required for BrkA passenger folding or stability	111
Figure 3-11	Expression of the pertactin junction region fused to the BrkA translocation unit complements BrkA(ΔGlu^{601}-Ala^{692}) passenger folding *in trans*	114
Figure 3-12	Model of BrkA secretion: the role of the "junction" region in promoting BrkA passenger folding concurrent with or following translocation across the outer membrane.	120
Figure 3-13	Comparison of the BrkA and EspP junction regions	127
Figure 3-14	Model of BrkA secretion: the role of residues Ala^{681}-Glu^{707} (the hydrophobic secretion facilitator (HSF) domain).	130
Figure 4-1	Experimental concepts	142
Figure 4-2	Autotransporter chimeras	147
Figure 4-3	Homologous translocation units are not required for *trans* complementation of BrkA passenger folding	150
Figure 5-1	Overview of BrkA structure	155
Figure 5-2	Models of outer membrane translocation	162
Appendix A-1	Structural model of the BrkA passenger domain	183

Appendix A-2 Three dimensional structural model of the BrkA (Leu^{485}-Leu^{702}) passenger domain 184

List of Abbreviations

°C	celsius
µ	micro-
µg	microgram
AC	autochaperone
Amp	ampicillin
B.	*Bordetella*
BLAST	basic local alignment search tool
BrkA	*Bordetella* resistance to killing protein A
rBrkA	recombinant *Bordetella* resistance to killing protein A
Bvg	*Bordetella* virulence gene
Cm	chloramphenicol
Ctx-β	cholera toxin β subunit
Da	Dalton
dH_2O	distilled water
DMSO	dimethyl sulphoxide
DNA	deoxyribonucleic acid
DTT	dithiothreitol
E.	*Escherichia*
EDTA	ethylenediamenetetraacetic acid
e.g.	*exempli gratia*
et al.	*et alteri*
EtBr	ethidiumbromide
FHA	filamentous hemaglutinin
g	gram
Gm	gentamycin
HSF	hydrophobic secretion facilitator
i.e.	*id est*
k	kilo-
Kan	kanamycin
kDa	kilodalton
l	liter
LB	Luria-Bertani
nS	nanoSiemen
m	milli-
M	molar
mg	milligramm
min	minute
ml	milliliter
mM	millimolar
n	nano-
nm	nanometer
OD_x	optical density
PAGE	polyacrylamide gel electrophoresis
PBS	phosphate-buffered saline

PCR	polymerase chain reaction
pH	*pondus hydrogenii*
Prn	pertactin
r	resistance
rpm	revolutions per minute
RT	room temperature
SDS	sodium dodecylsulfate
sec	second
SS	Stainer-Scholte
TEMED	N,N,N‘,N‘-Tetramethylendiamin
Tet	tetracyclin
Tris	Tri-(hydroxymethyl)-aminomethane
U	unit(s)
V	volt
vag	virulence activated gene
w/v	weight per volume
wt	wildtype

Acknowledgements

... my supervisor and mentor Dr. Rachel Fernandez for her support, patience, and guidance. This was truly and invaluable and exciting learning experience – thank-you.

... my committee members, Drs. Dana Devine, Brett Finlay and Francois Jean, for guidance and support during the course of my doctoral studies and for critical reading of this manuscript.

... the support and friendship of past and present members of the Fernandez laboratory. In particular, I thank George Huang, Alina Gerrie and Barb Turner whom I had the privilege of working with during their undergraduate studies. Steve Pleasance, Elena Nodel, Jody Yue and Nico Marr are thanked for technical assistance, discussion, and collaboration on bioinformatic approaches, BrkA binding studies, region III studies, and structural modeling of the BrkA passenger domain, respectively.

... my friend and partner Kim for her constant support, tremendous patience and companionship.

And Zoe and Kevin, thank-you for letting me see the world through your eyes – you gave me balance, direction, motivation and inspiration.

Chapter 1

1.1 Introduction

1.1.1 Protein secretion in Gram-negative bacteria

The delivery of proteins to their correct cellular location is a fundamental aspect of cell biology. For many proteins, localization involves traversing membranes and transiting through distinct aqueous environments before reaching a targeted destination. In Gram-negative bacteria proteins destined for locations beyond the cytoplasm must contend with the barrier imposed by the cell envelope defined by the inner membrane and the outer membrane, which delimit the compartment known as the periplasm. This barrier presents a real challenge for Gram-negative bacterial pathogens whose ability to infect, multiply and survive in a host depends largely on interactions mediated by variety of protein-based virulence factors that are expressed at the cell surface and/or released into the surrounding environment (e.g. toxins, adhesins, enzymes). On the other hand, the cell envelope performs a myriad of critical physiological functions and affords protection from the surrounding environment, making its integrity essential.

To satisfy these requirements Gram-negative bacteria have evolved a number of strategies to shuttle proteins across the cell envelope (Thanassi and Hultgren, 2000). These strategies involve (i) sophisticated systems for moving protein substrates from the cytosol to the cell surface, and (ii) protein substrates that encode defined information for targeting to, and transiting through, specific systems. It is worth keeping in mind that the system and its substrate(s) have co-evolved to achieve optimal recognition and secretion

---

Portions of this chapter have been submitted for publication in the journal Molecular Microbiology.

efficiency. At the center of these systems are protein-based molecular machines termed translocons that form semi-permeable hydrophilic conduits to facilitate substrate translocation across the plane of a membrane. The process of translocation is tightly coordinated with events of substrate targeting, folding, maturation, assembly, and modification, which often involve the participation of additional factors such as chaperones and proteases (Economou, 2002).

In Gram negative bacteria, six distinct protein secretion systems have been identified, termed Types I-IV, autotransporters and two partner transporters (Jacob-Dubuisson *et al.*, 2001) (Thanassi and Hultgren, 2000). In the Types I and III systems, and also in most examples of Type IV secretion, protein cargo is delivered directly from the cytoplasm to the extracellular environment via a contiguous channel created by a multiprotein translocon that spans the inner membrane, the periplasm, and the outer membrane. In the Type II, autotransporter, two-partner system, and a small number of Type IV systems, proteins cross the cytoplasmic membrane and outer membrane using independent translocons. Inner membrane translocation occurs via the Sec translocon or the Tat translocon. Outer membrane translocation is mediated by several distinct translocons that define the specific secretion systems (Desvaux *et al.*, 2004b).

Proteins that employ an autotransporter and two partner strategies are translocated across the outer membrane via a dedicated translocon (Jacob-Dubuisson *et al.*, 2004) (Desvaux *et al.*, 2004a) (Jacob-Dubuisson *et al.*, 2001). This structure adopts a β-barrel fold in the outer membrane that facilitates translocation of a passenger (substrate) to the cell surface.

While autotransporter secretion and two-partner secretion appear to employ convergent strategies to export proteins across the outer membrane, the systems differ in that the autotransporter secretion system is encoded within a single polypeptide (the passenger and 'translocator' are covalently linked) whereas the two-partner secretion system is comprised of two proteins (a passenger and cognate translocator). This thesis will focus on the autotransporter secretion system.

1.1.2 Autotransporter Secretion

The autotransporter secretion system was discovered during studies of the IgA protease of *Neisseria gonnorhoeae*. The secreted form of IgA protease was initially described as a protein of approximately 105 kDa (Halter *et al.*, 1984), however upon sequencing of the cloned *iga* locus, an open reading frame encoding for a protein with a predicted mass of 169 kDa was revealed (Pohlner *et al.*, 1987). In an effort to resolve this size discrepancy, Pohlner *et al.* made several observations related to the secretion of IgA protease. It was determined that the 169 kDa *iga* gene product represents a precursor protein that contains at least three functional domains: an amino-terminal signal peptide for targeting to the inner membrane, the mature protease to be secreted, and a ~ 45 kDa carboxy-terminal region predicted to form an amphipathic β barrel structure that is required for export across the outer membrane. Significantly, secretion of IgA protease was demonstrated in both *N. gonnorhoeae* and *E. coli*, indicating that specific accessory proteins are not required for export.

Based on these seminal observations, a model was proposed for IgA protease secretion where the inner and outer membranes are traversed in two separate steps. The N-terminal signal peptide directs export of the preproprotein from the cytoplasm to the periplasm via the Sec system. In the periplasm the signal peptide is cleaved and the protein is released into the periplasmic compartment where the C-terminal domain folds into the outer membrane forming a β-barrel structure that facilitates translocation of the protease domain across the outer membrane. On the surface, the protein undergoes autoproteolysis to release the mature IgA protease from the membrane bound C-terminal domain.

Since the introduction of this model, hundreds of proteins that share a similar tripartite domain organization and mode of secretion (Fig. 1-1) have been identified in the available genomic sequences (Yen *et al.*, 2002). Indeed, autotransporters represent the largest family of Gram-negative secreted proteins (Pallen *et al.*, 2003) and phylogenetic analyses reveal that these proteins are widely distributed throughout the Gram-negative bacterial world, including the α-, β-, γ-, and ε-proteobacteria, and *Chlamydiae* (Yen *et al.*, 2002).

Experimental and *in silico* comparative approaches have begun to reveal some of the structural and functional attributes of autotransporter proteins. Using the tripartite domain architecture as a framework (Fig 1-1), these attributes are described below.

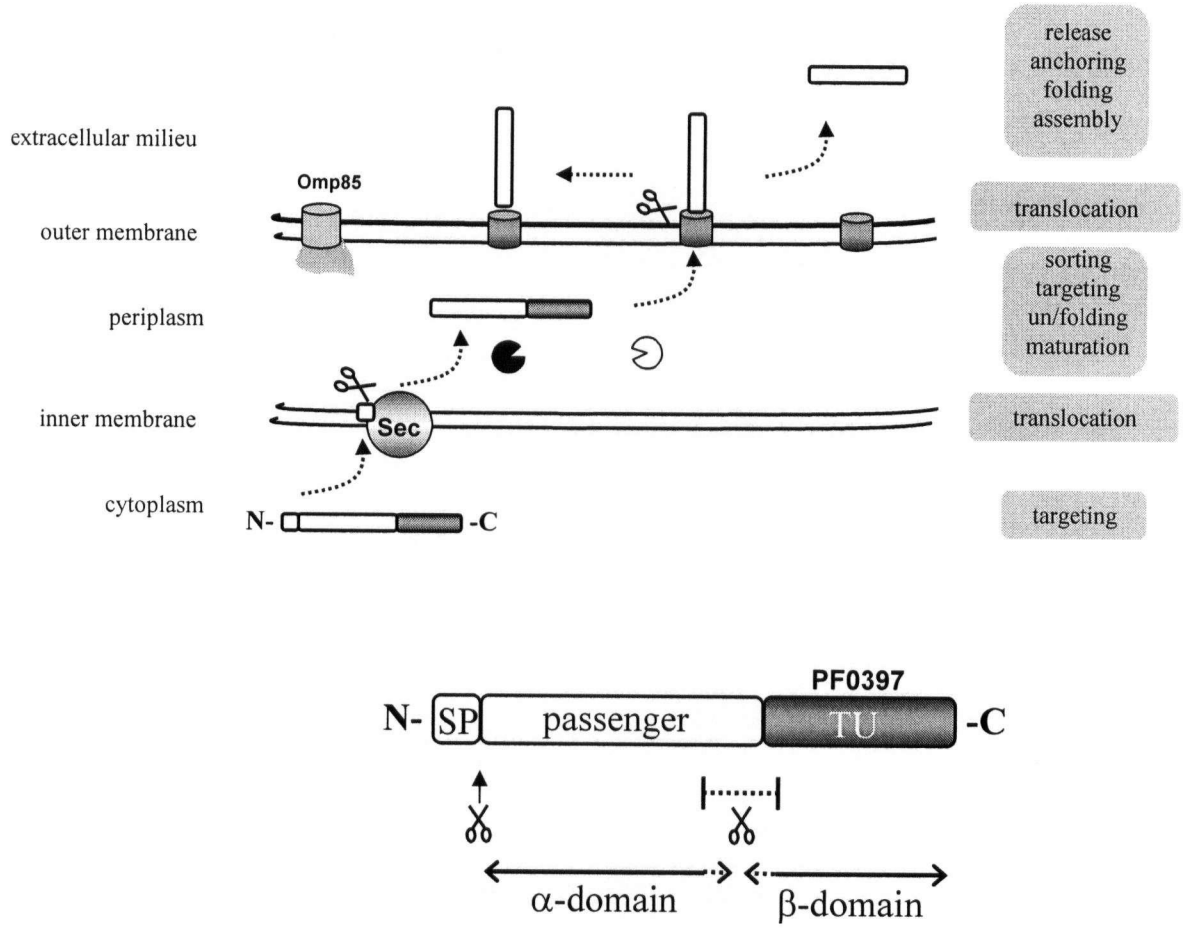

Figure 1-1. Autotransporter Secretion

Top: Two step model of autotransporter secretion across the Gram negative cell envelope. Following synthesis in the cytoplasm the precursor is targeted to the inner membrane by its N-terminal signal peptide and exported via the Sec system into the periplasm. In the periplasm the signal peptide is cleaved and the proprotein is released into the periplasmic compartment. The C-terminal translocation unit inserts into the outer membrane forming a β-barrel structure which facilitates translocation of the passenger domain. On the cell surface the passenger domain is most often cleaved to yield the α-domain and β-domain. The α-domain can be released into the surrounding environment or remain non-covalently associated with the cell surface. Putative periplasmic chaperones and proteases are depicted as white and black pies. The conserved outer membrane protein Omp85 is shown in the outer membrane. **Right panel:** The autotransporter secretion pathway can be viewed as a series of interconnected molecular processes. How translocation across the inner and outer membrane is coordinated with events of protein folding, maturation, sorting, targeting, and assembly are only beginning to be dissected. **Bottom:** Tripartite domain architecture of an autotransporter protein: signal peptide (SP), passenger containing the effector function(s) (white box), and translocation unit (grey box). Cleavage sites/events are denoted by scissors. The translocation unit has been assigned PFAM domain PF0397. Note: The PFAM database represents a collection of multiple sequence alignments and hidden Markov models covering many common protein domains and families (http://www.sanger.ac.uk/Software/Pfam/).

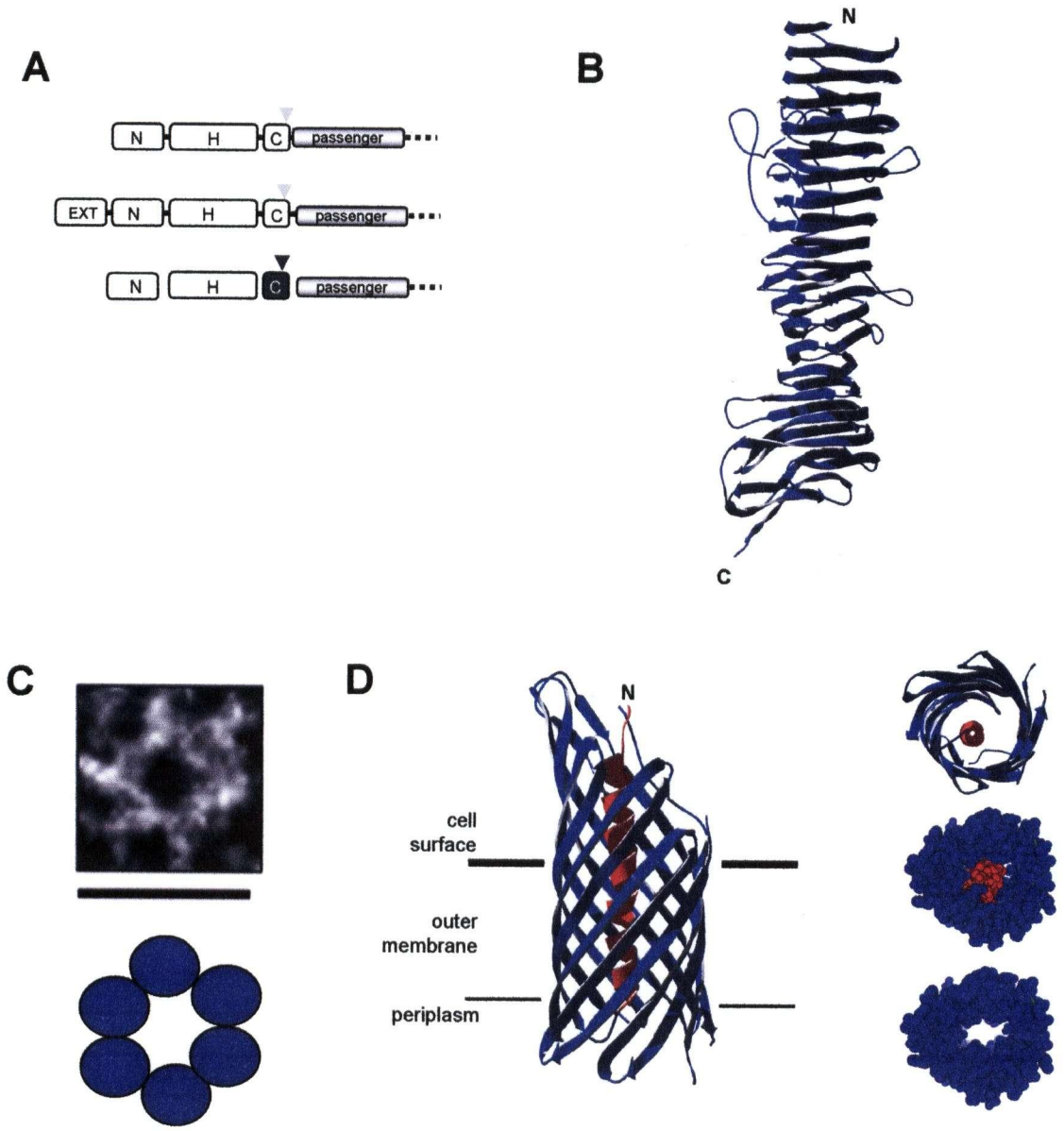

Figure 1-2. Structural features of autotransporter proteins.
A. Architectures of autotransporter signal peptides. N-terminal extension (EXT); charged N-domain (N), hydrophobic H-domain (H); and signal peptidase I (white box) or signal peptidase II cleavage site (grey box) (C). **B.** Structure of the passenger domain (residues 35-573) of the autotransporter protein pertactin (Emsley *et al.*, 1996). **C.** High molecular weight complex formed by the β-domain of IgA protease. Top: Image captured by cryo-electron microscopy (Veiga *et al.*, 2003). Bottom: Interpretation of putative secretion complex. Individual β-domain subunits are depicted as blue circles and central secretion channel is depicted as a white space in center of the complex. **D.** Crystal structure of the C-terminal region of the autotransporter NalP (residues 777 - 1084) (Oomen *et al.*, 2004). Left: Side view showing 12-stranded β-barrel in blue and the α-helical linker region in red. Right: Periplasmic view of NalP structure. Top: Cartoon diagram depicting α-helical linker within 1 nm channel. Middle: Space filling model showing α-helical linker region occluding channel. Bottom: Space filling model with α-helical linker region removed.

1.1.3 Autotransporter domain structure

Autotransporters are multidomain proteins with their functional attributes and secretion determinants organized as modules. Autotransporters comprise (i) an N-terminal signal sequence containing the orthodox information required for targeting to the Sec translocase: a basic N-terminal region (N-domain), a hydrophobic core region (H-domain) and a C-terminal cleavage site (C-domain), (ii) a passenger domain, and (iii) a translocator domain predicted to form a 12-14 stranded β-barrel (Henderson *et al.*, 1998) (Fig. 1-2A). The signal peptide and translocation unit define the minimal determinants required to export a passenger across the inner membrane and outer membrane, respectively.

1.1.3.1 Signal Peptides: variations on a theme

All known autotransporters bear N-terminal signal sequences, however closer inspection reveals that some autotransporters bear signal peptide variants (Fig. 1-2A). These include (i) N-terminal extensions (a subset of which are conserved) (Henderson *et al.*, 1998) (Sijbrandi *et al.*, 2003) and (ii) signals for lipoprotein modification (Coutte *et al.*, 2003b) (Odenbreit *et al.*, 1999).

(i) It has been suggested (Henderson *et al.*, 1998) (Sijbrandi *et al.*, 2003) that N-terminal extensions observed in the signal peptides of autotransporter proteins might promote co-translational translocation across the inner membrane by preferentially engaging signal recognition particle (SRP), rather than the cytosolic chaperone SecB. However, the exact role of this feature in autotransporter secretion remains

controversial. In this regard, Peterson *et al.* (2003) have shown that the hydrophobicity of the H-domain, rather than the N-terminal extension, of the autotransporter EspP is the principle determinant of SRP-mediated targeting to the inner membrane. Further, Brandon *et al.* (2003) have shown that the *Shigella* autotransporter IcsA, which has a 52 residue signal peptide with a 25 residue N-terminal extension, is preferentially targeted to the inner membrane via SecB.

(ii) Autotransporter signal peptides can also include a consensus lipoprotein modification signal (LA(G,A)↓C)) for modification and presumably trafficking by the Lol system (Juncker *et al.*, 2003) (Takeda *et al.*, 2003). Evidence exists to show that autotransporters bearing lipoprotein modification signals actually undergo lipid modification (Coutte *et al.*, 2003b) (Odenbreit *et al.*, 1999) (van Ulsen *et al.*, 2003). How this modification affects trafficking through the periplasm and translocation across the outer membrane remains to be determined.

1.1.3.2 Passengers: scaffolds for hitching functional modules

Autotransporter passengers are functionally diverse and include proteases, adhesins, cytotoxins, lipases, esterases, serum resistance factors, and mediators of actin polymerization (Henderson and Nataro, 2001). They can be amongst the largest secreted proteins (Yen *et al.*, 2002) and many have a modular organization as suggested by PFAM (Bateman *et al.*, 2004) annotation. The only known structure of an autotransporter passenger is the *B. pertussis* adhesin pertactin (Emsley *et al.*, 1996). Pertactin (residues 35-573) forms a monomeric right-handed parallel β-helix consisting of 16 rungs (or structurally repetitive units) (Fig. 1-2B). Repetitive units characteristic of a β-helix fold

have been identified in other autotransporters (Kajava *et al.*, 2001) (Klemm *et al.*, 2004) (Vandahl *et al.*, 2002) (Yen *et al.*, 2002) suggesting that the β-helix fold may represent a versatile scaffold to display functional motifs and modules on the cell surface where functionality is achieved by duplicating groups of rungs to form a module (Ciccarelli *et al.*, 2002), or by adding loops to turns between particular β-sheets on the β-helix scaffold (Jenkins *et al.*, 1998).

Underscoring the versatility of the autotransporter secretion mechanism, a variety of non-native (heterologous) passengers have been surface displayed using different autotransporters. Heterologous passengers include: antigenic determinants (Konieczny *et al.*, 2000), important enzymes (Lattemann *et al.*, 2000), heavy metal detoxifying agents (Valls *et al.*, 2000), and platforms for steroid biosynthesis (Jose *et al.*, 2002).

1.1.3.3 The Translocation Unit: a *bona fide* portal?

How is the translocation unit defined?

Most autotransporters are proteolytically processed into 2 domains: the α-domain corresponding to the passenger and the β-domain encompassing the "translocator" (Fig. 1-1). The β-domain can vary in size depending on the positioning of the processing site; however the translocon itself is usually of a defined size. The minimal translocation unit is comprised of the terminal 255-294 amino acids that make up the membrane-embedded β-core, preceded by a so-called linker domain that is made up of an α-helical region of 21-30 amino acids (Oliver *et al.*, 2003a). The β-core is predicted to form 12-14 amphipathic β-strands (Loveless and Saier, 1997). In addition, the C-terminus of the

translocation unit has a consensus motif (Tyr/Val/Ile/Phe/Trp)-X-(Phe/Trp) characteristic of many outer membrane proteins (Loveless and Saier, 1997) (Henderson *et al.*, 1998).

Does the translocation unit form a channel?

The capacity for an AT1 β-domain to form a channel was first shown with the *B. pertussis* autotransporter protein BrkA. A refolded, histidine-tagged recombinant β-domain formed channels with an average single conductance of 3 nanoSiemens (nS) in black lipid bilayers (Shannon and Fernandez, 1999). In subsequent studies using liposome swelling assays the β–domains from IgA protease (Veiga *et al.*, 2002) and *Pseudomonas aeruginosa* lipase PalA (Lee and Byun, 2003) were both shown to form 2 nm pores. Interestingly, a refolded form of the NalP translocation unit, an autotransporter of *Neisseria meningitides*, produced channels with conductances of 0.15 nS and 1.3 nS that were calculated to correspond to a channel diameter of 0.24 nm and 0.84 nm, respectively (Oomen *et al.*, 2004). The larger NalP channel appears to be half the size of the channels from the other autotransporter proteins, with the smaller sized channel postulated as being the result of a translocon that was blocked by its linker region. It should also be noted that channel activity of the *E. coli* adhesion AIDA-I could not be observed in planar lipid bilayer experiments perhaps, as the authors suggest, because the pore is blocked, or that the β-domain does not form a channel (Konieczny *et al.*, 2001).

What are the structural constraints of the translocation unit?

Heterologous (i.e. non-native) passengers have been useful tools to probe the conformational constraints of translocation across the outer membrane. Veiga *et al.* have shown that a soluble camel single chain antibody passenger domain with a 2 nm diameter fused to the IgA protease β-domain can be translocated efficiently, presumably in a folded conformation (Veiga *et al.*, 2004). Importantly, a 2nm passenger size is in accordance with the 2 nm channel size for the IgA protease β-domain (Fig. 1-2C). Heterologous passengers that are either not secreted or are only inefficiently secreted by IgA protease β-domain (unless placed in a reducing environment) include the 15 kDa cholera toxin B subunit (Ctx-β) (Klauser *et al.*, 1990), and metallothionein, a protein of only 8 kDa (Valls *et al.*, 2000). In the case of the CtxB fusion, Veiga *et al.* suggested that the subunits might have formed oligomers or aggregates that were too large to be translocated (Veiga *et al.*, 1999) (Veiga *et al.*, 2004), although translocation intermediates were found to be to be surface expressed (Klauser *et al.*, 1992).

The structure of the translocator: multimer or monomer?

Two studies have investigated the structure of the autotransporter translocation unit (Veiga *et al.*, 2002) (Oomen *et al.*, 2004). First, a cryo-electron microscopy study of the IgA protease β-domain isolated from *E. coli* membranes revealed a ring-shaped complex formed by several (~ 6-8) β-domain subunits. The structure had an outer diameter of 9 nm and a stained-filled central cavity with a diameter measuring approximately 2 nm (Fig. 1-2C). The observation of a multimeric complex was consistent high molecular species observed in gel filtration and crosslinking experiments. The 2 nm stain-filled

cavity is in accordance with biophysical measurement of channel formation suggesting that this may represent the actual secretion channel through which multiple passengers are translocated. The idea was supported by an experiment that employed 2 constructs where different passengers were fused to the IgA protease β-domain: one was a bulky scFv (single chain Fv) passenger that is inefficiently translocated and the other was a small (hexahistidine) passenger that is translocated efficiently. The experiment showed that the bulky passenger prevented surface presentation (translocation) of the smaller passenger (Veiga *et al.*, 2002).

More recently the crystal structure of the NalP translocation unit was reported (Oomen *et al.*, 2004). The NalP β-domain (Asp^{777}-Phe^{1084}) was renatured from cytoplasmic inclusion bodies. The structure revealed a monomeric 12-stranded β-barrel with a large region predicted to protrude beyond the outer membrane surface. The exterior surface of the β-barrel that would face the membrane is hydrophobic. The core of the β-barrel forms a 10 x 12.5 Å hydrophilic channel that is fully occupied by an N-terminal α-helix (Fig. 1-2D), and thus could represent a snapshot of translocation proceeding through the translocator. The diameter of channel (1 nm) is in close agreement with size predicted by the biophysical measurements of NalP (Asp^{777}-Phe^{1084}).

1.1.4 Outer Membrane Translocation

The problem of protein translocation is multifaceted and must take into account the nature of the channel and the substrate, as well as the nature of the environments that are separated by the membrane interface. For autotransporter secretion, the nature of the

outer membrane channel through which passengers are translocated remains controversial (see discussion above, monomer vs. multimer). However, the channel represents only one aspect of the translocation problem; indeed substrate targeting signals, orientation, conformation, the periplasmic and cell surface environment, as well as the source of energy required to drive translocation across the outer membrane should also be considered.

1.1.4.1 Passenger Targeting and Orientation

Several observations support the notion that (i) covalent linkage supersedes the need for substrate encoded targeting signals and (ii) that passengers are translocated across the outer membrane in a C-terminal to N-terminal orientation. First, the fact the heterologous passengers can be exported when fused to an autotransporter translocation unit indicates that specific targeting signals are not required to initiate translocation. Thus, it is likely that passenger targeting to the translocon is mediated through a covalent linkage to the C-terminal translocator, rather than by an affinity based targeting motif or signal present on the passenger. In this regard, the linker region would be ideally positioned to initiate a C-terminal to N-terminal translocation process using a hairpin fold where the C-terminal part of the linker interacts with residues lining one side of the β-core cavity (Oomen *et al.*, 2004) allowing the N-terminal part of the linker to be the first to emerge from the translocator. Indeed, analysis of CtxB-IgA β-domain fusions in which Ctx-β translocation is blocked (due to disulphide bond formation) indicates that portions of the linker region (plus some upstream residues) are exposed on the surface of the cell, which might represent a trapped translocation intermediate (Klauser *et al.*, 1990).

1.1.4.2 Passenger conformation

Whether native autotransporter passengers are translocated in a folded or an unfolded conformation has yet to be determined. As mentioned above, studies using non-native heterologous passengers suggest that folded domains with a diameter less than ~ 2 nm can be translocated efficiently (Veiga *et al.*, 2002), implying that larger domains (> 2 nm) would be translocated in an unfolded or partially folded conformation. This idea raises two questions: (i) is there any evidence to suggest that native autotransporter passengers fold in the periplasm, and (ii) do the structural dimensions of native autotransporter passengers exceed 2 nm? Brandon and Goldberg have shown that a protease resistant form of the *Shigella* autotransporter IcsA passenger can be detected in periplasmic extracts suggesting that some degree of passenger folding can occur in the periplasm. However, as the authors point out, whether IcsA is translocated across the outer membrane in a folded or unfolded conformation is not known. As previously mentioned, the only known structure of an autotransporter passenger is that of pertactin. The pertactin passenger adopts a β-helix fold with a length of 10nm and an average diameter of 2.7 nm (minimum 1.7 nm and maximum 3.8 nm) (Veiga *et al.*, 2004) (Emsley *et al.*, 1996). The β-helix fold is comprised of an elongated hydrophobic core of stacked aliphatic and aromatic residues which is further stabilized by a network of inter-rung hydrogen bonds, suggesting that the flexibility of this molecule would be limited (Jenkins *et al.*, 1998). Thus, given the properties (rigid rod) and dimensions (width > 2 nm) of the pertactin passenger, it seems likely that translocation of this structure would proceed in an unfolded or at most a partially folded conformation.

The notion that passengers are translocated in a partially folded or unfolded conformation raises the intriguing question of how a translocation competent folding state would be maintained (i.e. how folding is prevented) in the periplasm. Periplasmic chaperones such as DegP, FkpA and DsbA have been shown to play a role in the biogenesis of native and heterologous autotransporter proteins (Brandon and Goldberg, 2001) (Purdy *et al.*, 2002) (Veiga *et al.*, 2004), however the exact role of these factors remains to be elucidated. Another question that arises is how an unfolded passenger would be folded as it emerges on the cell surface, ostensibly in the absence of chaperones. In this regard, Ohnishi *et al.* have shown that the protease activity of the *Serratia marcescens* autotransporter PrtS (previously known as SSP protease) is dependent on a pro-peptide region of approximately 100 amino acids located at the C-terminus of its passenger domain (Ohnishi *et al.*, 1994). The demonstration that this region could rescue the PrtS protease activity when supplied in *trans* suggested that it functions as an intramolecular chaperone to mediate PrtS passenger folding following translocation to the cell surface. Whether a similar region exists in other autotransporters was not known; this question is the major focus of the work presented in Chapter 3 of this thesis.

Factors within the outer membrane could also play role in passenger secretion. In this regard, Vouloux *et al.* have shown that the highly conserved bacterial outer membrane protein Omp85 is required for the correct folding and assembly of a variety of outer membrane proteins in *Neisseria gonorrhoeae* (Voulhoux *et al.*, 2003) (Voulhoux and Tommassen, 2004). With IgA protease, the defect is manifested by the accumulation of unprocessed (full-length) protein, and no processed passenger is seen. If processing

occurs on the surface (see below) then this implies that IgA protease is not secreted. Whether Omp85 facilitates IgA protease β-barrel insertion or passenger translocation is not known.

Further, it is possible that the translocation unit itself might influence passenger folding. Two residues within the PalA translocation unit (Pro^{478} and Gly^{576}) which are highly conserved in autotransporter translocation units (Loveless and Saier, 1997), appear to influence channel size and passenger function but are not involved in surface expression (Lee and Byun, 2003). It is tempting to speculate that the translocation unit itself could have chaperone activity similar to the Tom40 β-barrel of the mitochondrial outer membrane translocation machinery that promotes protein unfolding to facilitate translocation of an unfolded polypeptide (Esaki *et al.*, 2003) (Voos, 2003).

1.1.4.3 What drives translocation?

An open question concerns the source of energy to drive passenger translocation across the outer membrane. Inner membrane translocation processes are driven by ATP hydrolysis and electrochemical gradients. However, an absence of ATP in the periplasm and the presence of open channels (porins) in the outer membrane make these options seem unlikely. It has been suggested that passenger folding and hydration on the cell surface might yield free energy to drive translocation (Klauser *et al.*, 1992). This theory was supported by (i) the notion that translocation proceeds in an unfolded conformation (Klauser *et al.*, 1990) and the (ii) low concentration of free water in the periplasm (Brass *et al.*, 1986).

1.1.5 At the surface: maturation, anchoring, release

Most autotransporters undergo cleavage during secretion to yield the α-domain and the β-domain. Cleavage has been shown to occur via several mechanisms, including: (i) autoproteolysis (if the passenger is a protease) (Fink *et al.*, 2001) (Pohlner *et al.*, 1987) (van Ulsen *et al.*, 2003), (ii) endogenous outer membrane proteases such as the omptins (Egile *et al.*, 1997) and other autotransporters (van Ulsen *et al.*, 2003), and (iii) by host proteases (Plaut *et al.*, 2000). However, for several autotransporters, the protease responsible for passenger processing has not been identified. The surface localization of the omptins and the hypothesis that passenger folding occurs concurrent with or following translocation across the outer membrane suggests that cleavage occurs on the cell surface. Although the vast majority of autotransporter proteins are processed or predicted to be processed, it does not appear that passenger processing is essential for translocation since there are examples of autotransporters such as Vag8 (Finn and Stevens, 1995) that remain uncleaved in its native host, IgA protease that remains uncleaved in the absence of OmpT and its native passenger domain (e.g. Chapter 4, Fig. 4-3), and since mutation of the cleavage site (e.g. in IcsA) does not abolish surface expression of the passenger domain (Fukuda *et al.*, 1995).

Cleavage of the passenger from the translocation unit serves to (i) release cytotoxins, proteases, and bioactive peptides into the surrounding environment, (ii) release adhesins from the bacterial surface thereby promoting bacterial dispersal (Fink *et al.*, 2001), (iii) maintain polar distribution of some autotransporter proteins such as IcsA (Egile *et al.*,

1997) and (iv) influence the assembly of ternary passenger complexes such as what has been observed for the *Helicobacter pylori* cytotoxin VacA (Papini *et al.*, 2001). The cleaved α-domain can also remain non-covalently anchored to the cell surface (Benz and Schmidt, 1992) (Coutte *et al.*, 2003a) (Oliver *et al.*, 2003a) (Owen *et al.*, 1996). For the most part, the mechanism of this interaction is unknown, but in some autotransporter proteins, this can occur via an N-terminal lipoprotein modification as has been shown for SphB1 (Coutte *et al.*, 2003b).

1.1.6 AT1 vs. AT2 autotransporters

It is also worth noting that a subfamily of autotransporter proteins, termed the AT2's (Jacob-Dubuisson *et al.*, 2004), has recently been discovered that includes YadA of *Yersinia enterocolitica* (Roggenkamp *et al.*, 2003) and Hia of *Haemophilus influenza* (Surana *et al.*, 2004). AT2's bear the characteristic tripartite domain architecture of an autotransporter but are distinguished by a short C-terminal translocation unit comprised of only 4 β-strands that forms a trimer in the outer membrane. The C-terminal domain of these proteins has been assigned the PFAM domain PF03895. This is in contrast with the "classic" autotransporters, termed the AT1's, which encode a translocation unit of 12 –14 predicted β-strands. For reference, the AT1's include IgA protease and BrkA. The AT2 autotransporters will not be discussed further in this thesis, and as such, the generic term "autotransporter" will be used to describe AT1 proteins (PF03797).

1.1.7 Thesis Overview

Increasing interest in autotransporter secretion derives from their being (i) the largest family of Gram-negative secreted proteins (Pallen *et al.*, 2003) that are often associated with virulence (Henderson and Nataro, 2001), thus making them potential vaccine targets, (ii) useful tools for surface displaying heterologous proteins for biotechnological applications, and (iii) a unique one-component genetic system from which to study the fundamental basis of protein translocation. A detailed understanding of autotransporter secretion mechanisms will not only shed light on the biological problem of traversing the outer membrane, seemingly in one step, but it will also contribute to the improved engineering of autotransporters for specific biotechnological purposes.

At the outset of this project only a small handful of autotransporters had been characterized experimentally (Klauser *et al.*, 1993) (Ohnishi and Horinouchi, 1996) (Maurer *et al.*, 1997) (Suzuki *et al.*, 1995) (Hendrixson *et al.*, 1997) and *in silico* comparative analyses were only beginning to emerge (Henderson *et al.*, 1998) (Loveless and Saier, 1997). A key question was (and remains) whether, or what parts, of the autotransporter secretion process apply universally to all proteins. Further, a myriad of questions remained to be addressed surrounding the translocation steps across the inner and outer membranes. Many of these questions have been highlighted in the preceding introduction (Fig. 1-1 and 1-2). A focal point of this study is an investigation of the folding state and secretion of a native autotransporter passenger.

The work described herein focuses on structural and functional studies of the virulence factor BrkA of *Bordetella pertussis*. An obligate human pathogen and the causative agent of whooping cough, *B. pertussis* secretes a variety of proteins that allow it to colonize the upper respiratory tract and to circumvent host defenses present on the mucosal surface. BrkA (*Bordetella* resistance to killing) confers resistance to killing by the classical antibody-dependent pathway of complement (Fernandez and Weiss, 1994) as well as certain classes of antimicrobial peptides (Fernandez and Weiss, 1996); it also represents one of several factors that contribute to adherence (Fernandez and Weiss, 1994). In order to fully understand the role of BrkA in the pathogenesis of *B. pertussis* an understanding of its biogenesis, structure and function are required. As such, the group of Dr. Rachel Fernandez has engaged in a structure/function analysis of BrkA. Early efforts aimed at elucidating aspects of BrkA function suggested that future progress on this project would be aided by a better understanding of its biogenesis. As such, the focus of this project turned towards characterizing BrkA secretion.

The initial goal was to (i) test the hypothesis that BrkA is surface expressed protein that is secreted by an autotransporter mechanism and (ii) to establish BrkA as a model system to study autotransporter secretion. The studies described in Chapter 2 demonstrate that BrkA is expressed and functions at the cell surface of *B. pertussis* (Oliver and Fernandez, 2001). Using a plasmid-based expression system BrkA is shown to be secreted in a *E. coli* host without the introduction of specific accessory genes. BrkA is also shown to bear the characteristic tripartite domain architecture of an autotransporter protein: an N-terminal signal peptide, a passenger domain to be secreted, and a C-terminal translocation

unit (Oliver *et al.*, 2003a). During the course of these studies a region located at the C-terminus of the BrkA passenger was identified that is required for stability in the presence of outer membrane proteases. The conservation of this region of BrkA in a functionally diverse group of autotransporter proteins suggested that it plays an important role in secretion. We hypothesized that this region might function as an intramolecular chaperone to facilitate BrkA passenger folding either concurrent with or following translocation across the outer membrane, perhaps similar to the junction region of PrtS protease (see discussion above) (Ohnishi *et al.*, 1994), despite a lack of sequence identity. Using a combination of biochemical, bioinformatic, genetic and cell biological approaches this region is shown (i) to be required for BrkA passenger folding both *in vitro* and *in vivo*, and (ii) to be capable of mediating BrkA passenger folding at the cell surface when supplied in *trans* as a separate polypeptide (Oliver *et al.*, 2003b). Taken together these experiments support the hypothesis that this region of BrkA functions as an intramolecular chaperone to affect passenger folding during secretion. Further dissection of the BrkA junction region has revealed a region important for secretion of a "folding competent" full length BrkA passenger. This region of BrkA shares sequence and positional identity with a recently described region within the passenger domain of the *E. coli* autotransporter EspP that was coined the hydrophobic secretion facilitator (HSF) domain (Velarde and Nataro, 2004). Based on these findings, a model of BrkA passenger secretion is proposed that may be applicable to secretion of other autotransporter proteins.

1.1.8 References

Bateman, A., Coin, L., Durbin, R., Finn, R.D., Hollich, V., Griffiths-Jones, S., Khanna, A., Marshall, M., Moxon, S., Sonnhammer, E.L., Studholme, D.J., Yeats, C., and Eddy, S.R. (2004) The Pfam protein families database. *Nucleic Acids Res* **32 Database issue**: D138-141.

Benz, I., and Schmidt, M.A. (1992) AIDA-I, the adhesin involved in diffuse adherence of the diarrhoeagenic *Escherichia coli* strain 2787 (O126:H27), is synthesized via a precursor molecule. *Mol Microbiol* **6**: 1539-1546.

Brandon, L.D., and Goldberg, M.B. (2001) Periplasmic transit and disulfide bond formation of the autotransported *Shigella* protein IcsA. *J Bacteriol* **183**: 951-958.

Brandon, L.D., Goehring, N., Janakiraman, A., Yan, A.W., Wu, T., Beckwith, J., and Goldberg, M.B. (2003) IcsA, a polarly localized autotransporter with an atypical signal peptide, uses the Sec apparatus for secretion, although the Sec apparatus is circumferentially distributed. *Mol Microbiol* **50**: 45-60.

Brass, J.M., Higgins, C.F., Foley, M., Rugman, P.A., Birmingham, J., and Garland, P.B. (1986) Lateral diffusion of proteins in the periplasm of *Escherichia coli*. *J Bacteriol* **165**: 787-795.

Ciccarelli, F.D., Copley, R.R., Doerks, T., Russell, R.B., and Bork, P. (2002) CASH--a beta-helix domain widespread among carbohydrate-binding proteins. *Trends Biochem Sci* **27**: 59-62.

Coutte, L., Alonso, S., Reveneau, N., Willery, E., Quatannens, B., Locht, C., and Jacob-Dubuisson, F. (2003a) Role of adhesin release for mucosal colonization by a bacterial pathogen. *J Exp Med* **197**: 735-742.

Coutte, L., Willery, E., Antoine, R., Drobecq, H., Locht, C., and Jacob-Dubuisson, F. (2003b) Surface anchoring of bacterial subtilisin important for maturation function. *Mol Microbiol* **49**: 529-539.

Desvaux, M., Parham, N.J., and Henderson, I.R. (2004a) The autotransporter secretion system. *Res Microbiol* **155**: 53-60.

Desvaux, M., Parham, N.J., Scott-Tucker, A., and Henderson, I.R. (2004b) The general secretory pathway: a general misnomer? *Trends Microbiol* **12**: 306-309.

Economou, A. (2002) Bacterial secretome: the assembly manual and operating instructions (Review). *Mol Membr Biol* **19**: 159-169.

Egile, C., d'Hauteville, H., Parsot, C., and Sansonetti, P.J. (1997) SopA, the outer membrane protease responsible for polar localization of IcsA in *Shigella flexneri*. *Mol Microbiol* **23**: 1063-1073.

Emsley, P., Charles, I.G., Fairweather, N.F., and Isaacs, N.W. (1996) Structure of *Bordetella pertussis* virulence factor P.69 pertactin. *Nature* **381**: 90-92.

Esaki, M., Kanamori, T., Nishikawa, S., Shin, I., Schultz, P.G., and Endo, T. (2003) Tom40 protein import channel binds to non-native proteins and prevents their aggregation. *Nat Struct Biol* **10**: 988-994.

Fernandez, R.C., and Weiss, A.A. (1994) Cloning and sequencing of a *Bordetella pertussis* serum resistance locus. *Infect Immun* **62**: 4727-4738.

Fernandez, R.C., and Weiss, A.A. (1996) Susceptibilities of *Bordetella pertussis* strains to antimicrobial peptides. *Antimicrob Agents Chemother* **40**: 1041-1043.

Fink, D.L., Cope, L.D., Hansen, E.J., and Geme, J.W., 3rd (2001) The *Hemophilus influenzae* Hap autotransporter is a chymotrypsin clan serine protease and undergoes autoproteolysis via an intermolecular mechanism. *J Biol Chem* **276**: 39492-39500.

Finn, T.M., and Stevens, L.A. (1995) Tracheal colonization factor: a *Bordetella pertussis* secreted virulence determinant. *Mol Microbiol* **16**: 625-634.

Fukuda, I., Suzuki, T., Munakata, H., Hayashi, N., Katayama, E., Yoshikawa, M., and Sasakawa, C. (1995) Cleavage of *Shigella* surface protein VirG occurs at a specific site, but the secretion is not essential for intracellular spreading. *J Bacteriol* **177**: 1719-1726.

Halter, R., Pohlner, J., and Meyer, T.F. (1984) IgA protease of *Neisseria gonorrhoeae*: isolation and characterization of the gene and its extracellular product. *Embo J* **3**: 1595-1601.

Henderson, I.R., Navarro-Garcia, F., and Nataro, J.P. (1998) The great escape: structure and function of the autotransporter proteins. *Trends Microbiol* **6**: 370-378.

Henderson, I.R., and Nataro, J.P. (2001) Virulence functions of autotransporter proteins. *Infect Immun* **69**: 1231-1243.

Hendrixson, D.R., de la Morena, M.L., Stathopoulos, C., and St Geme, J.W., 3rd (1997) Structural determinants of processing and secretion of the *Haemophilus influenzae* hap protein. *Mol Microbiol* **26**: 505-518.

Jacob-Dubuisson, F., Locht, C., and Antoine, R. (2001) Two-partner secretion in Gram-negative bacteria: a thrifty, specific pathway for large virulence proteins. *Mol Microbiol* **40**: 306-313.

Jacob-Dubuisson, F., Fernandez, R., and Coutte, L. (2004) Protein secretion through autotransporter and two-partner pathways. *Biochim Biophys Acta* **1694**: 235-257.

Jenkins, J., Mayans, O., and Pickersgill, R. (1998) Structure and evolution of parallel beta-helix proteins. *J Struct Biol* **122**: 236-246.

Jose, J., Bernhardt, R., and Hannemann, F. (2002) Cellular surface display of dimeric Adx and whole cell P450-mediated steroid synthesis on E. coli. *J Biotechnol* **95**: 257-268.

Juncker, A.S., Willenbrock, H., Von Heijne, G., Brunak, S., Nielsen, H., and Krogh, A. (2003) Prediction of lipoprotein signal peptides in Gram-negative bacteria. *Protein Sci* **12**: 1652-1662.

Kajava, A.V., Cheng, N., Cleaver, R., Kessel, M., Simon, M.N., Willery, E., Jacob-Dubuisson, F., Locht, C., and Steven, A.C. (2001) Beta-helix model for the filamentous haemagglutinin adhesin of *Bordetella pertussis* and related bacterial secretory proteins. *Mol Microbiol* **42**: 279-292.

Klauser, T., Pohlner, J., and Meyer, T.F. (1990) Extracellular transport of cholera toxin B subunit using *Neisseria* IgA protease beta-domain: conformation-dependent outer membrane translocation. *Embo J* **9**: 1991-1999.

Klauser, T., Pohlner, J., and Meyer, T.F. (1992) Selective extracellular release of cholera toxin B subunit by Escherichia coli: dissection of *Neisseria* Iga beta-mediated outer membrane transport. *Embo J* **11**: 2327-2335.

Klauser, T., Pohlner, J., and Meyer, T.F. (1993) The secretion pathway of IgA protease-type proteins in gram-negative bacteria. *Bioessays* **15**: 799-805.

Klemm, P., Hjerrild, L., Gjermansen, M., and Schembri, M.A. (2004) Structure-function analysis of the self-recognizing Antigen 43 autotransporter protein from *Escherichia coli*. *Mol Microbiol* **51**: 283-296.

Konieczny, M.P., Suhr, M., Noll, A., Autenrieth, I.B., and Alexander Schmidt, M. (2000) Cell surface presentation of recombinant (poly-) peptides including functional T-cell epitopes by the AIDA autotransporter system. *FEMS Immunol Med Microbiol* **27**: 321-332.

Konieczny, M.P.J., Benz, I., Hollinderbaumer, B., Beinke, C., Niederweis, M., and Schmidt, M.A. (2001) Modular organization of the AIDA autotransporter translocator: the N-terminal beta1-domain is surface-exposed and stabilizes the transmembrane beta2-domain. *Antonie Van Leeuwenhoek* **80**: 19-34.

Lattemann, C.T., Maurer, J., Gerland, E., and Meyer, T.F. (2000) Autodisplay: functional display of active beta-lactamase on the surface of *Escherichia coli* by the AIDA-I autotransporter. *J Bacteriol* **182**: 3726-3733.

Lee, H.W., and Byun, S.M. (2003) The pore size of the autotransporter domain is critical for the active translocation of the passenger domain. *Biochem Biophys Res Commun* **307**: 820-825.

Loveless, B.J., and Saier, M.H., Jr. (1997) A novel family of channel-forming, autotransporting, bacterial virulence factors. *Mol Membr Biol* **14**: 113-123.

Maurer, J., Jose, J., and Meyer, T.F. (1997) Autodisplay: one-component system for efficient surface display and release of soluble recombinant proteins from *Escherichia coli*. *J Bacteriol* **179**: 794-804.

Odenbreit, S., Till, M., Hofreuter, D., Faller, G., and Haas, R. (1999) Genetic and functional characterization of the alpAB gene locus essential for the adhesion of *Helicobacter pylori* to human gastric tissue. *Mol Microbiol* **31**: 1537-1548.

Ohnishi, Y., Nishiyama, M., Horinouchi, S., and Beppu, T. (1994) Involvement of the COOH-terminal pro-sequence of *Serratia marcescens* serine protease in the folding of the mature enzyme. *J Biol Chem* **269**: 32800-32806.

Ohnishi, Y., and Horinouchi, S. (1996) Extracellular production of a *Serratia marcescens* serine protease in Escherichia coli. *Biosci Biotechnol Biochem* **60**: 1551-1558.

Oliver, D.C., and Fernandez, R.C. (2001) Antibodies to BrkA augment killing of *Bordetella pertussis*. *Vaccine* **20**: 235-241.

Oliver, D.C., Huang, G., and Fernandez, R.C. (2003a) Identification of secretion determinants of the *Bordetella pertussis* BrkA autotransporter. *J Bacteriol* **185**: 489-495.

Oliver, D.C., Huang, G., Nodel, E., Pleasance, S., and Fernandez, R.C. (2003b) A conserved region within the *Bordetella pertussis* autotransporter BrkA is necessary for folding of its passenger domain. *Mol Microbiol* **47**: 1367-1383.

Oomen, C.J., Van Ulsen, P., Van Gelder, P., Feijen, M., Tommassen, J., and Gros, P. (2004) Structure of the translocator domain of a bacterial autotransporter. *Embo J* **23**: 1257-1266.

Owen, P., Meehan, M., de Loughry-Doherty, H., and Henderson, I. (1996) Phase-variable outer membrane proteins in *Escherichia coli*. *FEMS Immunol Med Microbiol* **16**: 63-76.

Pallen, M.J., Chaudhuri, R.R., and Henderson, I.R. (2003) Genomic analysis of secretion systems. *Curr Opin Microbiol* **6**: 519-527.

Papini, E., Zoratti, M., and Cover, T.L. (2001) In search of the *Helicobacter pylori* VacA mechanism of action. *Toxicon* **39**: 1757-1767.

Peterson, J.H., Woolhead, C.A., and Bernstein, H.D. (2003) Basic amino acids in a distinct subset of signal peptides promote interaction with the signal recognition particle. *J Biol Chem* **278**: 46155-46162.

Plaut, A.G., Qiu, J., and St Geme, J.W., 3rd (2000) Human lactoferrin proteolytic activity: analysis of the cleaved region in the IgA protease of *Haemophilus influenzae*. *Vaccine* **19 Suppl 1**: S148-152.

Pohlner, J., Halter, R., Beyreuther, K., and Meyer, T.F. (1987) Gene structure and extracellular secretion of *Neisseria gonorrhoeae* IgA protease. *Nature* **325**: 458-462.

Purdy, G.E., Hong, M., and Payne, S.M. (2002) *Shigella flexneri* DegP facilitates IcsA surface expression and is required for efficient intercellular spread. *Infect Immun* **70**: 6355-6364.

Roggenkamp, A., Ackermann, N., Jacobi, C.A., Truelzsch, K., Hoffmann, H., and Heesemann, J. (2003) Molecular analysis of transport and oligomerization of the *Yersinia enterocolitica* adhesin YadA. *J Bacteriol* **185**: 3735-3744.

Shannon, J.L., and Fernandez, R.C. (1999) The C-terminal domain of the *Bordetella pertussis* autotransporter BrkA forms a pore in lipid bilayer membranes. *J Bacteriol* **181**: 5838-5842.

Sijbrandi, R., Urbanus, M.L., ten Hagen-Jongman, C.M., Bernstein, H.D., Oudega, B., Otto, B.R., and Luirink, J. (2003) Signal recognition particle (SRP)-mediated targeting and Sec-dependent translocation of an extracellular *Escherichia coli* protein. *J Biol Chem* **278**: 4654-4659.

Surana, N.K., Cutter, D., Barenkamp, S.J., and St Geme, J.W., 3rd (2004) The *Haemophilus influenzae* Hia autotransporter contains an unusually short trimeric translocator domain. *J Biol Chem* **279**: 14679-14685.

Suzuki, T., Lett, M.C., and Sasakawa, C. (1995) Extracellular transport of VirG protein in *Shigella*. *J Biol Chem* **270**: 30874-30880.

Takeda, K., Miyatake, H., Yokota, N., Matsuyama, S., Tokuda, H., and Miki, K. (2003) Crystal structures of bacterial lipoprotein localization factors, LolA and LolB. *Embo J* **22**: 3199-3209.

Thanassi, D.G., and Hultgren, S.J. (2000) Multiple pathways allow protein secretion across the bacterial outer membrane. *Curr Opin Cell Biol* **12**: 420-430.

Valls, M., Atrian, S., de Lorenzo, V., and Fernandez, L.A. (2000) Engineering a mouse metallothionein on the cell surface of *Ralstonia eutropha* CH34 for immobilization of heavy metals in soil. *Nat Biotechnol* **18**: 661-665.

van Ulsen, P., van Alphen, L., ten Hove, J., Fransen, F., van der Ley, P., and Tommassen, J. (2003) A *Neisserial* autotransporter NalP modulating the processing of other autotransporters. *Mol Microbiol* **50**: 1017-1030.

Vandahl, B.B., Pedersen, A.S., Gevaert, K., Holm, A., Vandekerckhove, J., Christiansen, G., and Birkelund, S. (2002) The expression, processing and localization of polymorphic membrane proteins in *Chlamydia pneumoniae* strain CWL029. *BMC Microbiol* **2**: 36.

Veiga, E., de Lorenzo, V., and Fernandez, L.A. (1999) Probing secretion and translocation of a beta-autotransporter using a reporter single-chain Fv as a cognate passenger domain. *Mol Microbiol* **33**: 1232-1243.

Veiga, E., Sugawara, E., Nikaido, H., de Lorenzo, V., and Fernandez, L.A. (2002) Export of autotransported proteins proceeds through an oligomeric ring shaped by C-terminal domains. *Embo J* **21**: 2122-2131.

Veiga, E., de Lorenzo, V., and Fernandez, L.A. (2004) Structural tolerance of bacterial autotransporters for folded passenger protein domains. *Mol Microbiol* **52**: 1069-1080.

Velarde, J.J., and Nataro, J.P. (2004) Hydrophobic residues of the autotransporter EspP linker domain are important for outer membrane translocation of its passenger. *J Biol Chem* **279**: 31495-31504.

Voos, W. (2003) Tom40: more than just a channel. *Nat Struct Biol* **10**: 981-982.

Voulhoux, R., Bos, M.P., Geurtsen, J., Mols, M., and Tommassen, J. (2003) Role of a highly conserved bacterial protein in outer membrane protein assembly. *Science* **299**: 262-265.

Voulhoux, R., and Tommassen, J. (2004) Omp85, an evolutionarily conserved bacterial protein involved in outer-membrane-protein assembly. *Res Microbiol* **155**: 129-135.

Yen, M.R., Peabody, C.R., Partovi, S.M., Zhai, Y., Tseng, Y.H., and Saier, M.H. (2002) Protein-translocating outer membrane porins of Gram-negative bacteria. *Biochim Biophys Acta* **1562**: 6-31.

Chapter 2

Initial characterization of BrkA secretion

2.1 Introduction

Bordetella pertussis is an obligate human pathogen of the upper respiratory tract and the causative agent of whooping cough. Like most Gram negative bacterial pathogens, *B. pertussis* secretes a variety of proteins to its surface and into its surrounding environment that mediate specific interaction with host factors throughout the course of infection that allow it to colonize, multiply and survive. The expression of most *B. pertussis* virulence factors is positively regulated by the BvgA/S response-regulator system (Kerr and Matthews, 2000). As summarised by Kerr (Kerr and Matthews, 2000), *B. pertussis* virulence factors include the adhesins filamentous hemagglutinin (FHA), fimbriae, BrkA and pertactin; and the toxins adenylate cyclase toxin, pertussis toxin, and dermonecrotic toxin, and other factors such as tracheal colonisation factor and the muramyl peptide, tracheal cytotoxin. In 2003, the *B. pertussis* genome sequence was reported (Parkhill *et al.*, 2003). This publication (Parkhill *et al.*, 2003), and other genomic analyses (Locht *et al.*, 2001) (Locht *et al.*, 2004), have revealed an array of new genes that are likely to be involved in virulence, thus suggesting that the pathogenesis of *B. pertussis* is more complicated than previously thought (Locht *et al.*, 2001). Included in its genomic arsenal of virulence determinants are each of the known secretion systems (Types I-IV, two-partner secretion, and the autotransporter secretion system), including 16 open reading frames predicted to code for autotransporter proteins (Parkhill *et al.*, 2003), [1]

Portions of the chapter have been published in Vaccine and the Journal of Bacteriology.

some of which have previously been implicated in *B. pertussis* pathogenesis (e.g. pertactin, BrkA, Tcf, Vag8, SphB1 (Locht *et al.*, 2001).

BrkA (*Bordetella* resistance to killing) is a Bvg regulated protein that mediates serum resistance and adherence in *B. pertussis* (Fernandez and Weiss, 1994). BrkA mutants are 10-fold less virulent in an infant mouse model of infection, indicating a role in pathogenesis (Weiss *et al.*, 1983). BrkA inhibits lysis by the antibody-dependent pathway of complement (Fernandez and Weiss, 1994), probably by inhibiting an early step in the complement activation pathway (i.e. prior to C4 deposition) (Barnes and Weiss, 2001). Although its mechanism of action remains to be elucidated, it has been proposed that BrkA may mediate serum resistance by recruiting a complement regulatory factor to the surface of *B. pertussis* (Fernandez and Weiss, 1998). BrkA also contributes to *B. pertussis* adherence as mutants have been shown a two-fold decrease in binding to host cells (Ewanowich *et al.*, 1989) (Fernandez and Weiss, 1994). The host receptor(s) for BrkA is not yet known and is currently under investigation.

The observation that BrkA mediates resistance to complement and contributes to adherence is a strong indication that BrkA is probably expressed at the surface of *B. pertussis*. However, whether, or how, BrkA is expressed at the cell surface had not been determined experimentally. Several lines of evidence suggest that BrkA is secreted by an autotransporter mechanism. The closest relative to BrkA is the *B. pertussis* adhesin pertactin, a known autotransporter protein (Li *et al.*, 1991) (Charles *et al.*, 1993). BrkA and pertactin share 29 % identity, which rises to 54.5 % over the C-terminal 300 amino

acids (Fernandez and Weiss, 1994); a region predicted to form a 12-14 stranded β-barrel (Loveless and Saier, 1997) that is bounded by a conserved proteolytic cleavage site (Gotto *et al.*, 1993) (Fernandez and Weiss, 1994) and a conserved outer membrane localization motif (Loveless and Saier, 1997). Consistent with this prediction, the BrkA β-domain can be isolated from *B. pertussis* outer membrane fractions and is cleaved between residues Asn^{731} and Ala^{732} (Passerini de Rossi *et al.*, 1999). Finally, it has been shown that a recombinant form of the C-terminal region of BrkA encompassing the β-domain has the capacity to form channels with a conductivity of 3.2 nanoSiemens in planar lipid bilayer experiments (Shannon and Fernandez, 1999).

This study begun by developing tools and methods for studying BrkA secretion. Using an antibody raised against the region corresponding to the putative passenger domain (residues 1-693), BrkA is detected at the surface of *B. pertussis* by indirect immunofluorescence analysis. Western immunoblot analysis was used to confirm that the 103 kDa BrkA precursor is processed to yield a 73 kDa α-domain (Fernandez and Weiss, 1994). The observation that (i) a serum resistant phenotype is restored by a recombinant form of the BrkA passenger added exogenously to cell surface of a *B. pertussis brk*A mutant, and (ii) that *B. pertussis* serum resistance can be neutralized using an antibody raised against the BrkA passenger, supports the conclusion that the BrkA N-terminal region is involved in mediating *B. pertussis* serum resistance. The notion that BrkA is secreted by an autotransporter mechanism implies that accessory genes are not required for secretion. To test this hypothesis, *brkA* was introduced on a plasmid into *E. coli* strain UT5600 and BrkA expression was assessed. Indirect immunofluorscence

analysis and trypsin accessibility assays demonstrate the N-terminal 73 kDa region of BrkA is expressed at the surface of *E. coli* UT5600. BrkA was not detected in concentrated culture supernatants of *B. pertussis* or *E. coli* strain UT5600 suggesting that following secretion the cleaved 73 kDa α-domain remains non-covalently associated with the bacterial surface. Finally, the BrkA secretion determinants are defined: an N-terminal signal peptide and the C-terminal translocation unit.

2.2 Materials and methods

2.2.1 Bacterial strains and growth media.

The *Bordetella pertussis* strains used in this study are the wildtype Tohama1 derivative BP338 (Weiss *et al.*, 1983), BrkA mutant strains BPM2041 which has a transposon insertion within *brkA* (Fernandez and Weiss, 1994) (Weiss *et al.*, 1989) and RFBP2152 which has a gentamicin cassette disrupting *brkA* (Fernandez and Weiss, 1998), and the Bvg mutant strain BP347 (Weiss *et al.*, 1983). *E. coli* strains RF1066 (Fernandez and Weiss, 1996) and DO218 (Shannon and Fernandez, 1999) have been described previously. In brief, RF1066 contains the *brk* locus cloned into pBluescript SKII (Stratagene, La Jolla, CA) and transformed into DH5α (Canadian Life Technologies, Burlington, ON.). DO218 was constructed by cloning a fragment of the *brkA* gene from the *Afl*III site to the *Bam*HI site into pET30b (Novagen, Madison, WI), and transforming the resulting plasmid into BL21 (DE3) pLysS (Novagen). *B. pertussis* strains were maintained on Bordet-Gengou agar (Becton Dickinson Microbiology Systems, Franklin Lakes, NJ) supplemented with 15% sheep blood (RA Media, Calgary, AB) as described (Fernandez and Weiss, 1994). Forty-eight hour old cultures were used for the serum assays. *E. coli* strains and plasmids used in this study are listed in Table 2-1. *E. coli* strains were cultured at 37 °C on Luria broth or Luria agar supplemented with the appropriate antibiotics. Antibiotic concentrations were as follows: naladixic acid 30 μg/ml, kanamycin 50 μg/ml, ampicillin 100 μg/ml, gentamicin 30 μg/ml, and chloramphenicol 34 μg/ml.

2.2.2 Recombinant DNA techniques

All DNA manipulations were carried out using standard techniques (Sambrook, 1989). Restriction enzymes were purchased from New England BioLabs (Beverly, MA). Primers used in this study were purchased either from the University of British Columbia (UBC) Nucleic Acid Protein Services Unit (Vancouver, BC), Sigma-Genosys (The Woodlands, TX) or Alpha DNA (Montreal, PQ) (Table 2). DNA sequencing was done using an ABI Prism 377 DNA sequencer (Applied Biosystems, Foster City, CA) at the UBC Nucleic Acid Protein Services Unit (Vancouver, BC).

The *B. pertussis* strain BBC9DO was made by introducing a second copy of the *brkA* gene (on plasmid pUW2171) into the chromosome of strain BBC9, a pertactin mutant of *B. pertussis*, as described (Fernandez and Weiss, 1998).

Construct pDO6935, which constitutively expresses low levels of BrkA in *E. coli*, was derived by excision of a 476 *Aat*II base pair fragment of pRF0166. Plasmid pDO6935 was used as a template in all subsequent PCR reactions described in this study. All PCR was performed using Vent polymerase (New England BioLabs) with the following cycles: an initial denaturation step of 2 min at 94 °C, followed by 30 cycles of 45 s at 94 °C, 30 s at 60 °C and 1 min/kb at 72 °C. The last cycle was followed by an additional 10 min at 72 °C. Amplified PCR products were separated on an agarose gel and a band of the expected size was extracted and cloned as described below. Primers used in this study are listed in Table 2-2.

Construct pDO181 was made by PCR using primer pairs DO1210F/DO1614R and DO2894F/BRK-CR. The resulting products were digested with restriction enzyme pairs *Asc*I and *Xba*I, and *Xba*I and *Bam*HI, respectively. In a triple ligation reaction, these products were ligated into a 5 kb *Asc*I to *Bam*HI digested fragment of pDO6935 to yield pDO181. Construct pDO182 was generated via the same strategy using primer sets DO1210F/DO1893R and DO2894F/BRK-CR. Constructs pDO244 and pDO246 were made using primer pair DO1975F/BRK-CR to generate a PCR product that was subsequently digested with *Xba*I and *Bam*HI. The resulting 1.3 kb product was then ligated into either a 5.3 kb *Xba*I to *Bam*HI digested fragment of pDO181 or a 5.5 kb *Xba*I to *Bam*HI digested fragment of pDO182 to yield pDO244 and pDO246, respectively.

Constructs pGD1, pGD2, pGD3, pGD4, pGD5, pGD6, pGD7, pGD8, pGD9, pGD10, pGD10.5, pGD11, and pGD12 were made by PCR using forward primers BRK-2113F, BRK-2398F, BRK-2650F, BRK2752F, BRK-2821F, BRK-2890F, BRK-3010F, BRK-3184F, BRK-3238F, BRK-3289F, BRK-3310F, BRK-3370F, and BRK-3601F, respectively. BRK-CR was used as the reverse primer in each of the reactions. The amplified products were purified, digested with *Xba*I and *Hind*III, and ligated into a 4.3 kb *Xba*I to *Bam*HI digested fragment of pDO246.

2.2.2 Purification of rBrkA$^{1-693}$.

The recombinant fusion protein produced by DO218 consists of the first 693 amino acids of BrkA flanked by N- and C-terminal histidine tags and is designated as rBrkA$^{1-693}$.

DO218 was grown to an OD_{600} of approximately 0.6 and induced with 1 mM isopropyl-beta-D-thiogalactopyranoside (IPTG) for 2h. Recombinant $BrkA^{1-693}$was purified under denaturing conditions using the protocol in the Xpress System Protein Purification manual (Invitrogen, Carlsbad, CA) as described (Shannon and Fernandez, 1999). In brief, the bacteria were lysed in 6 M guanidine hydrochloride, and the lysate was applied to Ni^{2+}-nitrilotriacetic acid (NTA) agarose (Qiagen Inc., Mississauga, ON). After successive washes in 8 M urea of decreasing pH, purified $rBrkA^{1-693}$ was eluted at pH 4 and the fractions were pooled. The urea was removed by slow dialysis at 4 °C against 10 mM Tris, pH 8.0 in the presence of 0.1% Triton X-100 (Shannon and Fernandez, 1999). The final dialysis was either against 10 mM Tris, pH 8 or phosphate buffered saline. Protein concentrations were determined by the bicinchoninic acid (BCA) method following protocol TPRO-562 (Sigma Chemical Company, St. Louis, MO).

2.2.4 Generation of polyclonal antibodies to $rBrkA^{1-693}$.

Polyclonal antibodies to $rBrkA^{1-693}$ were generated at Harlan Bioproducts for Science (Indianapolis, IN) in a pathogen-free, barrier-raised New Zealand white rabbit. Harlan's standard 112-day production protocol was followed using 1 mg antigen per rabbit and 4 immunisations in total.

2.2.5 SDS-PAGE and immunoblot analysis.

SDS-PAGE was performed as described (Fernandez and Weiss, 1994) (Laemmli, 1970) and the separated proteins were visualised after staining with Coomassie brilliant blue. The low molecular weight markers were purchased from Amersham Pharmacia Biotech

(Baie d'Urfé, QC). For immunoblot analysis, whole-cell lysates of the *B. pertussis* strains were separated by SDS-PAGE and transferred to Immobilon-P membranes (Millipore, Bedford, MA) as described (Shannon and Fernandez, 1999). The dilutions for the rabbit anti-rBrkA antiserum and the horseradish peroxidase-conjugated goat anti-rabbit secondary antibody (Cappel, ICN Biomedicals, Costa Mesa, CA) were 1:50,000 and 1:10,000 respectively. The blots were developed with the Renaissance chemiluminescence reagent (NEN Life Science Products, Boston, MA). Kaleidoscope prestained molecular weight markers were obtained from Bio-Rad (Hercules, CA).

For detection of expressed BrkA via SDS-PAGE or immunoblot, *E. coli* cultures were grown to 0.7 optical density (OD_{600}) units and pelleted. Trypsin accessibility experiments were performed following a previously described protocol (Maurer *et al.*, 1997) with slight modifications. In brief, cell pellets were resuspended in 0.2 ml phosphate-buffered saline (PBS) to an OD_{600} of ~10. To 0.1 ml of cells, 2 µl of 10 mg/ml trypsin was added to yield a final concentration of 200 µg/ml trypsin. Cells were incubated in the presence of protease for 10 minutes at 37 °C, pelleted by centrifugation, washed three times with PBS containing 10% fetal calf serum to stop digestion, and once in PBS alone. As a control, cell pellets were simultaneously processed in the same manner in the absence of trypsin. Washed pellets were finally resuspended in sample buffer and immediately boiled for 5 minutes prior to SDS-PAGE.

2.2.6 N-terminal sequencing

Whole cell lysates of strains BBC9DO (a pertactin (*prn*) mutant with 2 copies of *brkA*), and BBC9BrkA (a *prn*, *brkA* double mutant (Fernandez and Weiss, 1994)) were resolved by SDS-PAGE and transferred to an Immobilon-P membrane (Millipore). A unique band migrating at approximately 73 kDa in the BBC9DO lane was excised from the membrane and sequenced using Edman degradation by the UBC Nucleic Acid and Protein Services core facility.

2.2.7 Immunofluorescence analyses

B. pertussis strains were incubated with a 1:200 dilution of the rabbit anti-rBrkA antiserum in phosphate-buffered saline (PBS) containing 1% bovine serum albumin (BSA) for 30 minutes at 37 °C. The bacteria were subsequently washed three times prior to incubating them with a 1:100 dilution of a FITC-conjugated goat anti-rabbit antibody (Jackson ImmunoResearch Laboratories, WestGrove, PA). After washing, the bacteria were immobilised on a glass slide that had been previously treated with 0.1% poly-L-lysine (Sigma). The bacteria were viewed under epi-fluorescence using a Zeiss Axioskop 2 microscope. Phase-contrast and fluorescent images were captured digitally. For UV microscopy, a constant exposure time of 18 seconds was used.

E. coli were grown to 0.7 OD_{600} units, pelleted by centrifugation, and resuspended in PBS. Resuspended cells were immobilized on a glass slide that had been previously treated with 0.1% poly-L-lysine (Sigma). Slides were washed 3 times with PBS to remove unbound bacteria and subsequently probed with a 1/200 dilution of heat inactivated rabbit anti-BrkA antiserum (Oliver and Fernandez, 2001) and a 1/100 dilution

of FITC-conjugated goat anti-rabbit antibody (Jackson ImmunoResearch Laboratories, West Grove, PA), respectively. Slides were washed 3 times with PBS containing 1% BSA between each step to remove unbound material. Bacteria were visualized under epi-fluorescence using a Zeiss Axioscop-2 microscope. Phase contrast and fluorescent images were captured digitally.

2.2.8 Radial diffusion serum killing assay.

The sera used in this study came from adults who had no recollection of exposure to *B. pertussis*. The bactericidal capacity of each of these samples was similar to previously published values from other individuals with "no recollection of disease" (Weiss *et al.*, 1999). The radial diffusion serum killing assay was performed essentially as described (Weiss *et al.*, 1999) (Fernandez and Weiss, 1994) (Fernandez and Weiss, 1998) with two notable modifications, described below. In general, the radial diffusion serum assay consists of adding 200 µl of bacteria (OD600 = 0.2) to 10ml of Stainer Scholte (SS) broth containing 1% molten agarose and pouring the mixture into an Integrid square Petri dish. The agarose is allowed to harden. Wells (3mm in diameter) are formed using an aspirator punch and 5 µl of serum is added to each well. After the serum is allowed to diffuse, an overlay of SS-agarose (lacking bacteria) is added and the plates are incubated for 24-48h at 37 °C. Zones of clearing are noted and the size of the zones, which is proportional to the killing capacity of the serum, is measured. For some experiments, 200 µl of strain BPM2041 were pelleted, and resuspended in 100 µl of PBS containing rBrkA$^{1-693}$ at a concentration of 2 mg/ml prior to the addition of the molten agarose. For other experiments, the conventional radial diffusion assay was done, except in this case,

various concentrations of rabbit anti-rBrkA antiserum (diluted in RPMI medium) were mixed with a constant amount of the human serum prior to adding the serum mix to the wells. The concentration of rabbit antiserum in the mix ranged from 20% to none. The control antiserum used in these experiments came from a rabbit that was immunised with an irrelevant antigen; in this case, a non-native form of the C-terminal (amino acids 694-1010) of BrkA. Unless otherwise stated, the experiments were repeated at least 3 times. Student's *t* test was used for statistical analysis of the data.

Table 2-1. Strains and plasmids.

Strain/Plasmid	Relevant Characteristics[a]	Reference/Source
B. pertussis		
BP338	wild type; Tohama background; Nal^r	(Weiss *et al.*, 1983)
RFBP2152	BP338 *brkA*::*gent*, Nal^r, Gent^r	(Fernandez and Weiss, 1998)
BBC9	W28 *prn*::*kan*, Kan^r	(Fernandez and Weiss, 1994)
BBC9DO	BBC9::pUW2171 *brkA*$^+$ *brkB*$^+$ duplication Nal^r , Gent^r , Amp^r	this study
E. coli		
UT5600	F$^-$ *ara-14 leuB6 azi-6 lacYI proC14 tsx-67 entA403 trpE38 rfbD1 rpsL109 xyl-5 mtl-1 thi1 ΔompT-fepC266*	(Elish *et al.*, 1988)
DH5αF'	K–12 cloning strain	Invitrogen
Plasmids		
pBluescriptII SK$^-$	Amp^r; Cloning vector	Stratagene
pRF1066	Amp^r, 4.5-kb *brk* locus	(Fernandez and Weiss, 1998)
pUW2171	pRF1066 + gent^r oriT cassette	(Fernandez and Weiss, 1998)
pDO6935	Amp^r, pRF1066 derivative; 476bp AatII fragment excised resulting Δ*brk*B	this study
pDO181	Amp^r, pDO6935 derivative; BrkA Δ(A136-Q562), XbaI linker	this study
pDO182	Amp^r, pDO6935 derivative; BrkA Δ(S229-Q562), XbaI linker	this study
pDO244	Amp^r, pDO181 derivative; BrkA Δ(A136-P255), XbaI linker	this study
pDO246	Amp^r, pDO182 derivative; BrkA Δ(S229-P255), XbaI linker	this study
pGD1	Amp^r, pDO246 derivative; BrkA Δ(S229-G301), XbaI linker	this study
pGD2	Amp^r, pDO246 derivative; BrkA Δ(S229-G396), XbaI linker	this study
pGD3	Amp^r, pDO246 derivative; BrkA Δ(S229-D480), XbaI linker	this study
pGD4	Amp^r, pDO246 derivative; BrkA Δ(S229-Q514), XbaI linker	this study
pGD5	Amp^r, pDO246 derivative; BrkA Δ(S229-A537), XbaI linker	this study
pGD6	Amp^r, pDO246 derivative; BrkA Δ(S229-A560), XbaI linker	this study
pGD7	Amp^r, pDO246 derivative; BrkA Δ(S229-P600), XbaI linker	this study
pGD8	Amp^r, pDO246 derivative; BrkA Δ(S229-A658), XbaI linker	this study
pGD9	Amp^r, pDO246 derivative; BrkA Δ(S229-A676), XbaI linker	this study
pGD10	Amp^r, pDO246 derivative; BrkA Δ(S229-E693), XbaI linker	this study
pGD10.5	Amp^r, pDO246 derivative; BrkA Δ(S229-W700), XbaI linker	this study
pGD11	Amp^r, pDO246 derivative; BrkA Δ(S229-A720), XbaI linker	this study
pGD12	Amp^r, pDO246 derivative; BrkA Δ(S229-G797), XbaI linker	this study

[a]Nal^r,Gent^r, Kan^r, Amp^r refer to resistance to naladixic acid, gentamicin, kanamycin and ampicillin, respectively.

Table 2-2. Primers used in this study[a].

BRK-CR	TATAAGCTTCGCTCAGAAGCTGTAGCG
DO2894F	ATTTCTAGATG-GGTGCTCCAGTCG
DO1614R	CATCTAGAAAT-ATCGATGGTCGAG
DO1893R	CATCTAGAAAT-ACCGCCGGCGACG
DO2374R	CATCTAGAAAT-GATGCGGGTCTGC
DO1210F	TAGTCCATGGCG-ATGTATCTCGATAG
DO1975F	ATTTCTAGAGTT-CTCGATCGCGTTGCC
BRK-2113F	ATTTCTAGA-ACAGTCAGCGTGCAGGGC
BRK-2398F	ATTTCTAGA-ATCTCCGTGCTGGGCTTC
BRK-2650F	ATTTCTAGA-ACGCCGCTGAAGCTGATG
BRK-2752F	ATTTCTAGA-CAGCATTCCACCATTCCG
BRK-2821F	ATTTCTAGA-GACGGCAACAAGCCCCTC
BRK-2890F	ATTTCTAGA-ACCCAGGTGCTCCAGTCG
BRK-3010F	ATTTCTAGA-GAGGCCTCTTACAAGACC
BRK-3184F	ATTTCTAGA-CGCCTGGGCCTGGTGCAT
BRK-3238F	ATTTCTAGA-AACGTCGGCAAGGCGGTT
BRK-3289F	ATTTCTAGA-GATCCGAAGACGCATGTC
BRK-3310F	ATTTCTAGA-AGCTTGCAGCGCGCG
BRK-3370F	ATTTCTAGA-GATCTTTCCAGCATCGCC
BRK-3601F	ATTTCTAGA-TACACCTATGCCGACCGC

[a]Noted in 5' to 3' direction. The *Hin*dIII and *Xba*I sites are underlined.

2.3 Results

2.3.1 Expression and purification of functional recombinant rBrkA$^{1-693}$

BrkA is a member of the autotransporter family of outer membrane proteins (Henderson *et al.*, 1998). It is synthesised as a 103 kDa precursor which is processed to yield a 73 kDa N-terminal passenger and a 30 kDa C-terminal porin-like transporter region (Shannon and Fernandez, 1999). When full-length BrkA is expressed in *B. pertussis* or in *E. coli*, it represents only a small fraction of the total protein in whole-cell lysates. Unlike many autotransported proteins whose N-terminal passenger domains are released into the culture media, the BrkA passenger domain remains tightly associated with the bacterium despite being processed. Over-expression of the full-length BrkA protein in *E. coli* is lethal. Thus in order to obtain sufficient quantities of BrkA for functional studies, it was necessary to uncouple the N-terminal passenger portion of BrkA from its outer-membrane embedded transporter moiety. BrkA comprising the first 693 amino acids was cloned with both amino and carboxy terminal histidine tags. Induction of this clone (DO218) with IPTG resulted in the production of approximately 2 mg of recombinant protein (rBrkA$^{1-693}$) per ml of culture (Fig. 2-1). Most of the recombinant protein was insoluble; therefore all purification steps were performed under denaturing conditions (Fig. 2-1A and B), and the peptides were refolded by diluting the urea in a drop-wise manner during dialysis (Shannon and Fernandez, 1999).

To determine whether the refolded rBrkA$^{1-693}$ was functional, we bathed *B. pertussis* strain BPM2041, a *brkA* mutant, with rBrkA$^{1-693}$ and assessed whether the protein could rescue the serum sensitive phenotype of this mutant. The effective concentration of

rBrkA$^{1-693}$ was 20 μg per ml for the assay. As shown in Fig. 2-1C, whereas the zone surrounding the well in BPM2041 panel was completely clear due to bacterial lysis, the bathing of BPM2041 with rBrkA$^{1-693}$ resulted in a significant restoration of serum resistance as indicated by a turbid zone, similar to what is seen with the wildtype, serum-resistant strain, BP338. While it is clear that the addition of the recombinant protein to BPM2041 mimics what is seen in the wildtype strain, it is not known how or whether rBrkA$^{1-693}$ physically associates with *B. pertussis* to protect it from serum killing since the mechanism of BrkA has not been deciphered. Restoration of serum resistance in BPM2041 was also observed when a wildtype copy of the *brkA* gene was recombined into its chromosome (data not shown).

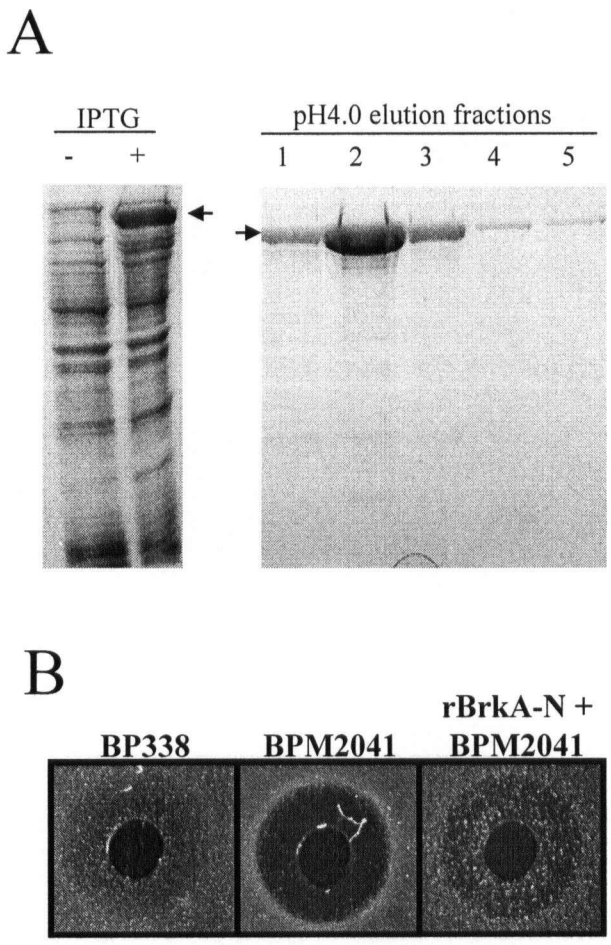

Figure 2-1. Purification and demonstration of functional activity of recombinant BrkA.

BrkA comprising the first 693 amino acids ($BrkA^{1-693}$) was expressed as a histidine-tagged fusion protein and purified under denaturing conditions. The left side of Panel A shows the SDS-PAGE (11% gel) and Coomassie Blue staining of whole cell lysates of strain DO218 before and after a one-hour induction with IPTG. The right side of Panel A shows the SDS-PAGE and Coomassie Blue staining of the pH 4 elution profile of $BrkA^{1-693}$ following Ni-NTA chromatography. The arrowheads show the histidine-tagged recombinant $BrkA^{1-693}$. In Panel B, purified recombinant $BrkA^{1-693}$ was added to *B. pertussis* strain BPM2041 (*brkA*) for 30 minutes prior to performing the radial diffusion serum assay with 5µl of undiluted human serum. For comparison, the wildtype strain BP338 and BPM2041 to which no $rBrkA^{1-693}$ was added are also shown. The dark area surrounding the well to which serum was added represents a zone of bacterial lysis. The light area represents the surviving bacteria. Figure from Oliver and Fernandez., Vaccine 2001.

2.3.2 Antibodies to rBrkA$^{1-693}$ recognise surface-expressed BrkA.

Antibodies to rBrkA$^{1-693}$ were made in a barrier-raised, pathogen-free rabbit. Immunoblot analysis showed that the antiserum recognises the N-terminal portion of BrkA in its unprocessed (103kDa) and processed (73kDa) forms. Other processed forms of BrkA are also evident. The antiserum was specific for BrkA as no cross-reactivity to any other *B. pertussis* antigens was evident (Fig. 2-2).

To assess whether the rabbit anti-rBrkA$^{1-693}$ antiserum was capable of recognising native BrkA, we performed an indirect immunofluorescence assay for surface-expressed BrkA. For this assay, bacteria were first stained and then immobilised on poly-L-lysine coated glass slides. Fig. 2-3 demonstrates that the rBrkA$^{1-693}$ antiserum is indeed capable of recognising native, surface-expressed BrkA on *B. pertussis*. This figure also shows that even at high concentrations of antiserum, there is no cross-reactivity with other *B. pertussis* antigens.

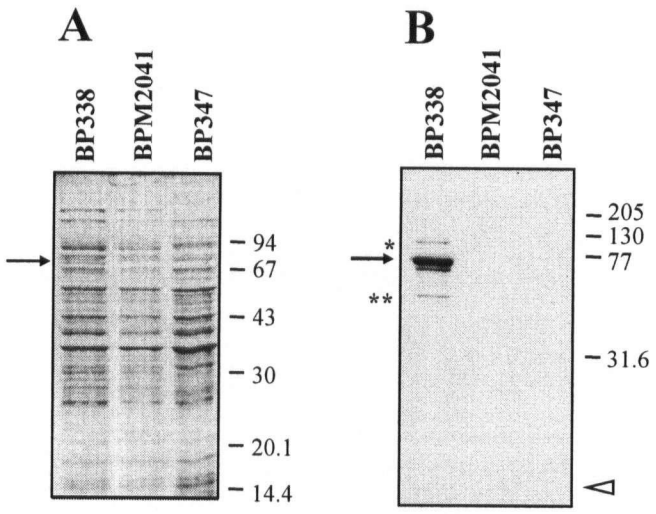

Figure 2-2. Immunoblot analysis of the rBrkA$^{1-693}$antiserum.

Panel A shows whole-cell lysates of *B. pertussis* strains characterised by SDS-PAGE (11% gel) and stained with Coomassie Blue. Panel B shows an immunoblot of a duplicate gel visualised by chemiluminescence. BP338 is the wildtype strain, BPM2041 is the BrkA mutant, and BP347 is the Bvg mutant. The arrow shows the 73kDa N-terminal portion of BrkA. The single asterisk is the 103 kDa full-length form of BrkA. The double asterisk denotes a minor band migrating at approximately 53 kDa, the identity of which is unknown. The open arrowhead shows the dye-front. Molecular sizes are in kilodaltons. Figure from Oliver and Fernandez., Vaccine 2001.

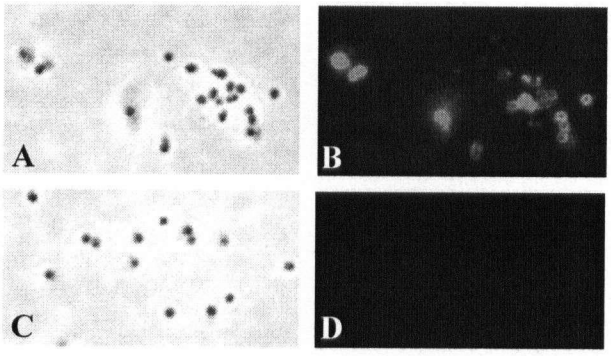

Figure 2-3. The rBrkA$^{1-693}$ antiserum recognises surface expressed BrkA.
B. pertussis strains were incubated with the rBrkA$^{1-693}$ antiserum followed by incubation with a FITC-conjugated goat anti-rabbit secondary antibody. The stained bacteria were immobilised on poly-L-lysine coated slides and visualised by phase-contrast (Panels A, C) and fluorescence (Panels B, D) microscopy. The exposure times for Panels B and D were identical. Panels A and B show strain BP338, Panels C and D show strain BPM2041. Figure from Oliver and Fernandez., Vaccine 2001.

2.3.3 Antibodies to rBrkA$^{1-693}$ neutralise serum resistance.

Because the rBrkA$^{1-693}$ antiserum was shown to recognise native BrkA, we asked whether it could neutralise serum resistance in wildtype *B. pertussis*. Radial diffusion serum killing assays were performed rather than the traditional killing assays (where the numbers of surviving bacteria are determined by colony counts) to circumvent potential agglutination of *B. pertussis* cells via the anti-BrkA antibodies; agglutinated bacteria would influence the colony counts. Various concentrations of the rBrkA$^{1-693}$ antiserum were added to a constant amount of an individual human serum sample and 5 µl of these mixtures were then dispensed into the wells of the radial diffusion serum assay that was seeded with either wildtype *B. pertussis*, or RFBP2152 another independent BrkA mutant (Fernandez and Weiss, 1998). In the absence of the rBrkA$^{1-693}$ antiserum, the wildtype strain was found to be resistant to killing by the human serum sample, whereas the same human serum killed the BrkA mutant strain very well (Fig. 2-4A and Fig. 2-4B, 4th column in the top panels; Fig. 2-4C). When the human serum spiked with the rBrkA$^{1-693}$ antiserum was added to wildtype *B. pertussis*, there was a dose-dependent neutralisation of serum resistance (Fig. 2-4A, top panel; Fig. 2-4C). Maximum neutralisation was achieved when the total concentration of the rBrkA$^{1-693}$ antiserum was 20% ($p<0.0001$), whereas little neutralisation was seen at 2% ($p<0.04$), and no neutralisation whatsoever was seen at 0.2%. The abrogation of serum resistance was specifically due to the neutralisation of BrkA, since a control rabbit antiserum which was raised against an irrelevant antigen (i.e. a non-native form of the C-terminal transporter moiety of BrkA) did not have any effect (Fig. 2-4A, bottom panel; Fig. 2-4C); the rBrkA$^{1-693}$ antiserum

was itself not bacteriolytic (data not shown); and there was no increased killing of the BrkA mutant strain (Fig. 2-4B, top panel; Fig. 2-4C).

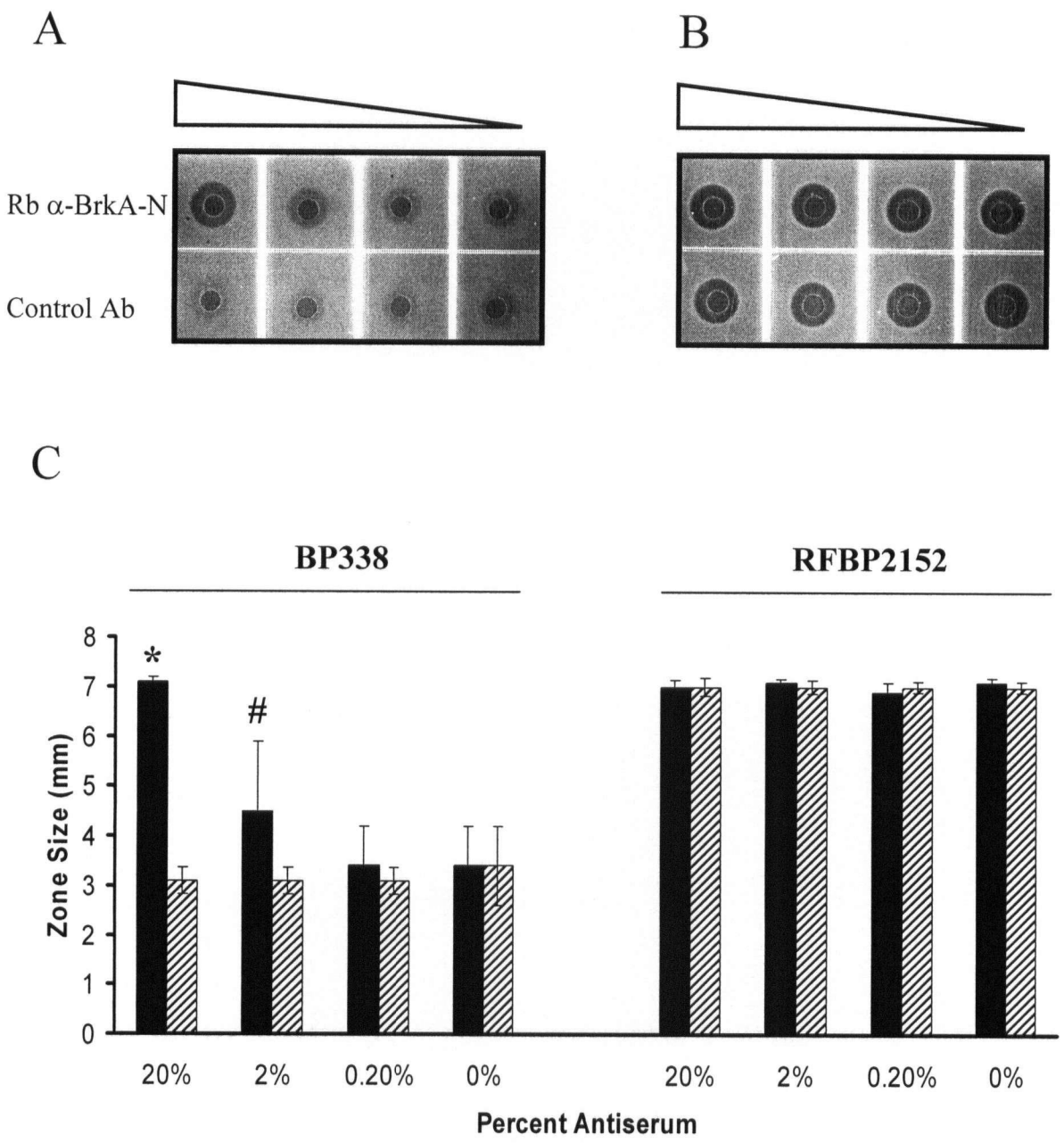

Figure 2-4. The rBrkA$^{1-693}$ antiserum neutralises serum resistance in wildtype *B. pertussis*.
Panels A and B show a representative radial diffusion killing assay. The radial diffusion serum killing assay was done in the presence or absence of the rabbit rBrkA$^{1-693}$ antiserum (designated as Rb α-BrkA-N), or a control rabbit serum. The rBrkA$^{1-693}$ antiserum (or control) in decreasing concentrations (20%, 2%, 0.2%, 0%), was added to 100% human serum. Five microliters of each mixture was added to the wells. Panel A shows the radial diffusion killing assay with wildtype strain BP338. Panel B shows the radial diffusion killing assay with strain BPRF2152, a *brkA* mutant. The control antibody is a rabbit antiserum which recognises a denatured (but not native) form of the C-terminal moiety of BrkA. Panel C shows the quantitation of the radial diffusion assay from 5 experiments using the same serum that was used in Panels A and B. Solid bars represent treatment with rBrkA$^{1-693}$ antiserum. Hatched bars represent treatment with control rabbit serum. $p<0.0001$(*) and $p<0.04$ (#) when the rBrkA$^{1-693}$ antiserum treatment is compared to control serum treatment at 20% and 2% serum respectively. Figure from Oliver and Fernandez., Vaccine 2001.

2.3.4 Expression of BrkA in *E. coli.*

We next asked whether BrkA can be secreted in an *E. coli* host, a background that has previously been used as a host to study secretion of a variety of autotransporters (Klauser *et al.*, 1993) (Klauser *et al.*, 1990) (Klauser *et al.*, 1992) (Maurer *et al.*, 1997) (Miyazaki *et al.*, 1989) (St Geme and Cutter, 2000) (Suzuki *et al.*, 1995) (Veiga *et al.*, 1999) (Veiga *et al.*, 2002) thus allowing comparisons to be made between different autotransporters, and because mutational analysis of BrkA is greatly facilitated in *E. coli.* Plasmid pDO6935 was derived from pRF1066 (Fernandez and Weiss, 1994), which carries the entire *brk* locus encoding the divergently transcribed *brkA* and *brkB* genes (Table 2-1). pDO6935 was generated by excision of a 476 base pair *Aat*II fragment from pRF1066 resulting in a deletion of the 5' region of the *brkB* gene. pDO6935 was transformed into *E. coli* strain UT5600 which is deficient for the outer membrane proteases OmpT and OmpP (Grodberg and Dunn, 1988). UT5600 has been used in the past to study secretion of the *Neisseria* IgA protease (Klauser *et al.*, 1993) (Veiga *et al.*, 1999) (Veiga *et al.*, 2002), the *E. coli* AIDA-1 adhesin (Maurer *et al.*, 1997) (Maurer *et al.*, 1999), and the *Shigella* VirG (IcsA) autotransporters (Suzuki *et al.*, 1995). BrkA expression was assessed using anti-BrkA polyclonal antiserum described in the section 2.4.2 (Oliver and Fernandez, 2001). Immunoblots of whole cell lysates resolved by SDS-PAGE show that BrkA was expressed to yield two major species migrating at approximately 103 kDa and 73 kDa. The 103 kDa product corresponds to the unprocessed full-length precursor and the species migrating at 73 kDa corresponds to the cleaved α-domain (Figure 2-5A and Figure 2-5B, lane 1). Although BrkA is Bvg-regulated in *B. pertussis*, the promoter region responsible for driving BrkA expression from pDO6935 in *E. coli* is not known.

Previously we had found that over-expression of full length BrkA in *E. coli* is toxic (Oliver and Fernandez, 2001), however, in the absence of IPTG induction, the levels of BrkA expression in *E. coli* with this construct are similar to what is seen in *B. pertussis* (Fernandez and Weiss, 1994) (Oliver and Fernandez, 2001).

To determine whether BrkA is translocated to the surface of *E. coli*, trypsin accessibility and immunofluorescence experiments were performed on whole cells. When cells were incubated with trypsin, a marked decrease in the 73 kDa moiety was observed and two products of approximately 40 kDa and 45 kDa were detected by Western immunoblot (Figure 3-5B, lane 2). The cleavage sites producing the 40 kDa and 45 kDa species are unknown, and over time, both species were lost. The intensity of the 103 kDa product remained constant following trypsin digestion suggesting that the 103 kDa band represents an intracellular form of the protein inaccessible to trypsin. Concomitant with this result, BrkA was detected on the surface of *E. coli* (Fig 2-5C) and appeared evenly distributed as shown by indirect immunofluorescence staining. Secreted BrkA could not be detected in concentrated culture supernatants suggesting that the cleaved passenger remains non-covalently associated with the bacterium (data not shown). Taken together these data indicate that BrkA is exported to the surface of *E. coli* strain UT5600 and is processed (independently of proteases OmpT or OmpP) in a manner similar to what is observed in *B. pertussis* (Oliver and Fernandez, 2001).

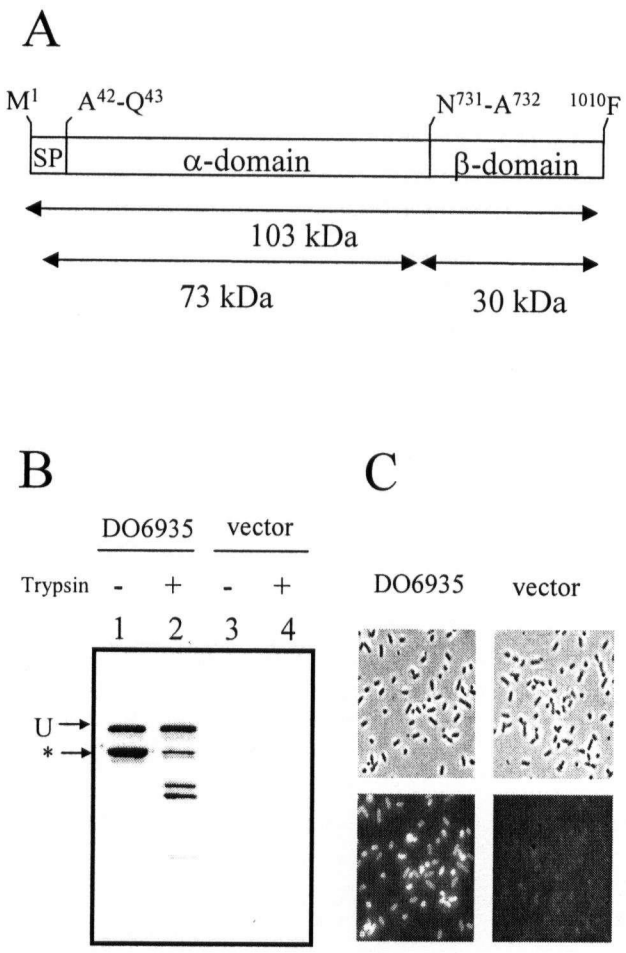

Figure 2-5. BrkA expression in *E. coli* strain UT5600.

A. BrkA domain organization. BrkA: SP (signal peptide) (residues 1-42); passenger or α-domain (residues 43-731); β-domain (residues 732-1010). **B.** Western immunoblot of *E. coli* UT5600 whole cell lysates resolved by 11% SDS-PAGE, probed with anti BrkA antiserum and detected using goat anti-rabbit antiserum conjugated to horseradish peroxidase. Lanes 1 and 2, pDO6935 (wild type copy of *brk*A gene); lanes 3 and 4, pBluescript (vector control). Specific BrkA bands are indicated; U refers to the unprocessed 103 kDa precursor protein, * 73 kDa processed passenger moiety. Cells were processed in the presence (+) or absence (-) of trypsin as described in the Materials and Methods. **C.** Surface expression of BrkA in *E. coli* UT5600 detected via indirect immunofluorescence. Top panels: phase contrast images. Bottom panels: Epifluorescence images. Figure from Oliver *et al.*, J. Bact. 2003.

2.3.5 Identification of the BrkA signal peptide

It was previously reported that sequence analysis of the 1010 amino acid protein BrkA did not identify a conventional signal peptide (Henderson *et al.*, 1998) (Fernandez and Weiss, 1994). More recent analysis using SignalP V2.0 (Nielsen *et al.*, 1997) has predicted a signal peptide of 44 amino acids using the neural network prediction method, and a cleavage site at 43 amino acids using the hidden Markov model (HMM) method (Nielsen and Krogh, 1998). To experimentally determine the BrkA signal peptide, N-terminal sequencing was performed on the 73 kDa moiety of BrkA. The amount of BrkA seen in whole-cell lysates of *B. pertussis* represents a small fraction of the total amount of cellular protein. Furthermore, at 73 kDa, BrkA migrates to a similar position on SDS-PAGE gels as the 69 kDa protein pertactin, a protein with which it shares sequence identity (Fernandez and Weiss, 1994). To circumvent these issues, we introduced a second copy of the *brkA* gene into the chromosome of strain BBC9, a pertactin mutant of *B. pertussis* to create strain BBC9DO. Western blot analysis of this strain using antibodies to pertactin and BrkA confirmed the lack of expression of pertactin, and the increased expression of BrkA relative to wild type strains (data not shown). Whole cell lysates of strain BBC9DO were resolved by SDS-PAGE, transferred to an Immobilon-P membrane and a unique band migrating at approximately 73 kDa was excised and sequenced using Edman degradation. Six cycles of Edman degradation revealed a N-terminal sequence of QAPQA. This sequence corresponds to amino acids 43 through 47 of BrkA. Similar results were obtained with a recombinant *brkA* construct expressed in *E. coli* (data not shown). Thus, both in *B. pertussis* and in *E. coli*, BrkA is processed

between residues Ala^{42} and Gln^{43}. A signal peptide of this length is not unusual for autotransporters (Henderson *et al.*, 1998).

2.3.6 Identification of the minimal BrkA translocation unit necessary for surface expression.

The natural cleavage of three well-characterized autotransporters IgA protease (Klauser *et al.*, 1993), VirG/IcsA (Fukuda *et al.*, 1995), and AIDA-1 (Suhr *et al.*, 1996) results in β-domains of 45, 37, and 48 kDa, respectively. Using a series of protease susceptibility assays and experiments with heterologous proteins fused to N-terminally truncated β-domains, minimal regions necessary to display passenger proteins have been identified for these autotransporters. They have in common, a membrane-embedded β-core of ~25-30 kDa found at the extreme C-terminus, preceded by a so-called "linker" region (Klauser *et al.*, 1993) (Maurer *et al.*, 1999) (Suzuki *et al.*, 1995). In these autotransporters, the linker region has been shown to be necessary for the translocation of the passenger domain to the bacterial surface. The linker region together with the outer membrane-embedded β-core, make up what has been coined the translocation unit (Maurer *et al.*, 1999).

Having demonstrated that BrkA is targeted to the outer membrane of *E. coli*, we next developed a deletion-based strategy to define the boundaries of the minimal translocation unit of BrkA. N-terminal sequencing of proteins from outer membranes preparations of *B. pertussis,* has localized the processing of BrkA to between Asn^{731} and Ala^{732} (Passerini de Rossi *et al.*, 1999) resulting in a β-domain of 30 kDa (Shannon and Fernandez, 1999).

At 30 kDa, the BrkA β-domain is smaller than the β-domains for IgA protease, VirG/IcsA and AIDA-1, but it approaches the size of the outer membrane-embedded β-cores identified for these proteins (Klauser *et al.*, 1993) (Maurer *et al.*, 1999) (Suzuki *et al.*, 1995). We constructed a series of *brkA* deletion mutants using PCR mutagenesis. As shown in Figure 2A, mutant proteins consisted of the first 228 amino acids of BrkA (Met^{1}-Gly^{228}) fused in-frame to processive deletions of the C-terminal region of the BrkA α-domain leading into the BrkA β-domain. BrkA (Met^{1}-Gly^{228}) was chosen as a passenger since heterologous passengers such as cholera toxin β subunit (Klauser *et al.*, 1990) may be inefficiently translocated due to structural limitations (e.g. disulphide bond formation). In addition, it has been suggested that the extended signal sequences observed in many autotransporters may play a role in secretion (Henderson *et al.*, 1998). Therefore the inclusion of the native BrkA signal sequence within the passenger avoids any influence that a non-native signal sequence may have on secretion. All deletion strains were derivatives of pDO6935 thereby ensuring a common promoter for the wild type and mutant constructs (Table 2-1).

An attempt was made to target our deletions to regions that would not disrupt the core structure of the protein. Secondary structural analysis using PsiPred (McGuffin *et al.*, 2000) predicts that BrkA is predominantly composed of β-strands (data not shown). In addition, the closest relative to BrkA in the database is the *B. pertussis* autotransporter pertactin (Fernandez and Weiss, 1994). The structure of the pertactin passenger domain has been solved and shown to be a monomer folded into a single domain that is almost entirely made up of a right-handed cylindrical β-helix (Emsley *et al.*, 1996). Given that

BrkA and pertactin passenger domains share 27% sequence identity and 39% sequence similarity we refined our secondary structural prediction by overlaying the pertactin structural coordinates (1DABA) onto a BrkA-pertactin primary amino acid sequence alignment. The best alignment was between Arg^{175}-Pro^{572} in pertactin and Val^{301}-Gln^{707} in BrkA. Using this analysis we systematically targeted N-terminal deletions to regions intervening predicted β-strands (Fig. 2-6).

The effects of each deletion on BrkA expression and processing were assessed by immunoblots of whole cell lysates resolved by SDS-PAGE. As shown in Figure 2-7A, each mutant form of BrkA was expressed indicating that the specific deletions did not render the individual mutant protein products markedly unstable. In deletion mutants A through J, products corresponding to both the unprocessed precursor (region designated as "U") and the cleaved passenger (asterisk) were detected (Fig. 2-7A). In contrast, only the unprocessed precursor could be detected in deletion mutants K, L and M. Given our previous observation that the cleaved passenger domain represents a major fraction of the surface expressed (protease accessible) wild type BrkA (see Fig. 2-5), these data suggested that BrkA deletion mutants A through J were being exported to the bacterial surface but mutants K, L, and M were not. In support of this observation, trypsin accessibility assays and indirect immunofluorescence experiments were performed. As expected, exposure of whole cells to trypsin digestion resulted in the complete absence of the band corresponding to the processed passenger domain (Fig. 2-7A, lanes A-J) whereas a significant fraction of the unprocessed precursor remained stable (Fig. 2-7A, lanes A-M). Consistent with these data, surface expression of the passenger region was

detected via indirect immunofluorescence in mutants A through J but not in mutants K, L and M (Fig. 2-7B). The absence of immunofluorescence in mutants K, L, and M supports the tenet that the unprocessed, trypsin-resistant fraction of BrkA represents an intracellular form of BrkA, and not simply a trypsin-resistant surface molecule. It should be noted that an N-terminal deletion spanning residues Ala^{136}-Pro^{255} in the N-terminal reporter region did not affect surface expression of BrkA (data not shown). Collectively, these data show that the region spanning residues Ala^{136} to Glu^{693} of BrkA is not required for surface localization of passenger proteins in *E. coli* strain UT5600. Furthermore, since the processed form of the passenger is also evident in deletion constructs A-J (Fig. 2-7A) and in construct ΔAla^{136}-Pro^{255}, it argues against the BrkA passenger having autoproteolytic activity.

A

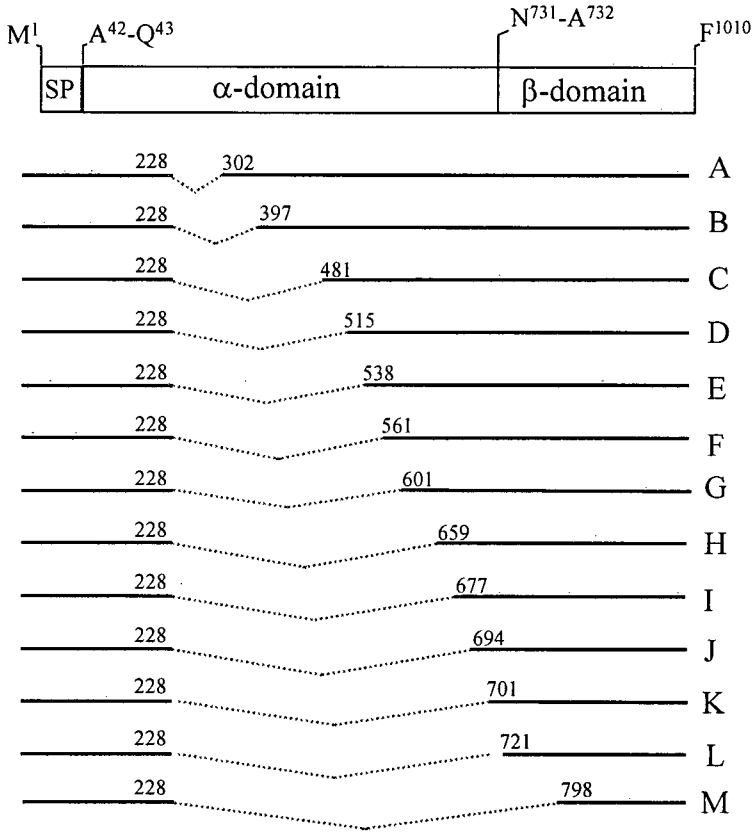

Figure 2-6. BrkA passenger deletion constructs

Diagram illustrating positions of BrkA in-frame deletions. Deleted regions are indicated by dotted lines and deletion boundaries correspond to wild type BrkA amino acid designation. BrkA domain structure is described in Fig. 1. Construction of mutations is described in the Materials and Methods. Plasmids are described in Table 1. A, pGD1; B, pGD2; C, pGD3; D, pGD4; E, pGD5; F, pGD6; G, pGD7; H, pGD8; I, pGD9; J, pGD10; K, pGD10.5; L, pGD11; M, pGD12. Figure from Oliver *et al.*, J. Bact. 2003.

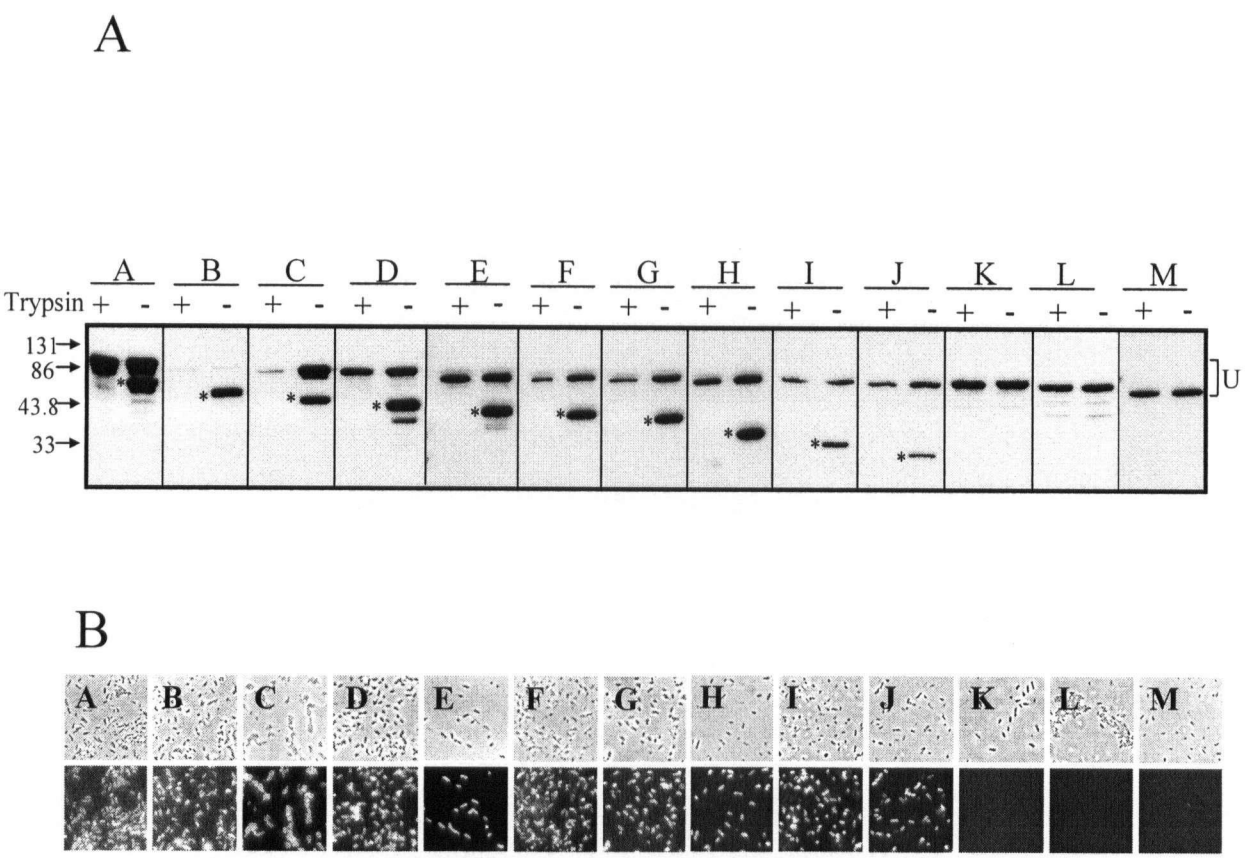

Figure 2-7 Expression of BrkA deletion constructs in *E. coli* UT5600.

A. *E. coli* UT5600 bacteria were transformed with BrkA deletion constructs (plasmids A-M) (see Fig. 3-2) and grown to approximately 0.7 optical density units. Bacteria were harvested and BrkA surface expression was assessed by immunoblot or indirect immunofluoresence. Immunoblot following resolution of whole cell lysates by SDS-PAGE. The band migrating within the region denoted as "U" in each lane corresponds to the unprocessed, precursor form of BrkA, and the band denoted with an asterisk (*) corresponds to the processed passenger domain of BrkA. Cells were processed in the presence (+) or absence (-) of trypsin as described in the Materials and Methods. Molecular mass markers in kDa are indicated on the left of the panel. **B.** BrkA expression in *E. coli* strain UT5600 detected by indirect immunofluorescence. Top panels: phase contrast images. Bottom panels: Epifluorescence images. Figure from Oliver *et al.*, J. Bact. 2003.

2.4 Discussion

Autotransporters are so-named since all of the information necessary for delivery to the cell surface is encoded within a single polypeptide. As originally demonstrated by Pohlner *et al* (1987), autotransporters can function in a foreign (Gram-negative) host without the addition of accessory genes. Consistent with this definition, BrkA can be expressed (and is processed) in *E. coli*, in a manner similar to what is observed in *B. pertussis*. In addition, BrkA bears the tripartite domain architecture characteristic of an autotransporter: an N-terminal signal peptide, a passenger domain to be delivered to the cell surface and a C-terminal translocation unit. Together the signal peptide and the translocation unit represent the BrkA secretion determinants. Features of these regions are discussed below.

2.4.1 The BrkA signal peptide

We have shown that in *B. pertussis* and in *E. coli*, BrkA is processed between residues Ala^{42} and Gln^{43}, suggesting that BrkA encodes a 42 amino acid signal peptide. A closer inspection of this region (1-42) reveals a non-conserved N-terminal extension (1-16) preceding a region (17-42) that bears the orthodox features of a Sec-dependent signal peptide (Pugsley, 1993). N-terminal extensions, some of which are conserved (Henderson *et al.*, 1998) (Sijbrandi *et al.*, 2003), have been observed in the signal peptides of other autotransporter proteins (Henderson *et al.*, 1998). The exact role of these extensions remains uncertain, although some evidence exists to suggest that they may influence the route of targeting to the inner membrane (Sijbrandi *et al.*, 2003) (Brandon *et al.*, 2003). In a subset of autotransporters these extensions are conserved,

consisting of a bipartite motif beginning with Met-Asn-Lys-Ile-Tyr-Leu-Lys-Tyr-(Ser/Cys/His) followed by a hydrophobic stretch of ~ 10 residues (i.e. Gly-Leu-Ile-Ala-Val-Ser-Glu-Leu-Ala-Arg) (Desvaux *et al.*, 2004). This motif is not present in the amino sequence of the N-terminal extension of the BrkA signal peptide, however it is worth noting that the BrkA signal peptide extension does bear (i) a similar net charge (+2), (*ii*) a Cys residue at position 9, and a (*iii*) series of hydrophobic residues preceding its N-domain.

2.4.2 The BrkA "translocation unit"

The data presented here indicate that the β-domain of BrkA is itself insufficient to translocate a passenger to the cell surface. The translocation unit for BrkA thus consists of the β-core plus a preceding linker region whose N-terminal boundary maps to within Glu^{693} to Ser^{701}. Historically, the β-domain has been defined as the C-terminal outer membrane resident fragment derived from proteolytic processing of the autotransporter protein. A comparison of diverse autotransporters reveals that while the β-domains can vary significantly in size, the sizes of the translocation units are remarkably similar (Fig. 2-8). Indeed, a comparison of experimentally defined linkers in diverse autotransporters, including BrkA, reveals a structurally conserved architecture which can be viewed as a signature for autotransporters. It consists of a 21-35 amino acid α-helical region that precedes a 255-294 amino acid transporter domain, a region rich in beta structure (Fig. 2-8). The common features of the translocation unit suggest that it, rather than 'β-domain' is a more appropriate operational definition for the transporter domain. The region upstream of the translocation unit would thus constitute the passenger moiety regardless

of the positioning of the proteolytic processing sites (Fig. 2-8). This definition is supported by the recently solved crystal structure of the translocator domain (Asp^{777}-Phe^{1084}) of the *Neisseria meningitidis* autotransporter NalP (Oomen *et al.*, 2004) (Turner *et al.*, 2002). NalP(Asp^{777}-Phe^{1084}) forms a monomeric 12-stranded β-barrel with a hydrophobic exterior, a hydrophilic interior, and a large extracellular region (Figure 1-2). The core of the β-barrel forms a 10 x 12.5 Å hydrophilic channel that is fully occupied by an N-terminal α-helix (Fig. 1-2). Thus the structure of NalP(Asp^{777}-Phe^{1084}) is consistent with the proposed architectural features of the "translocation unit".

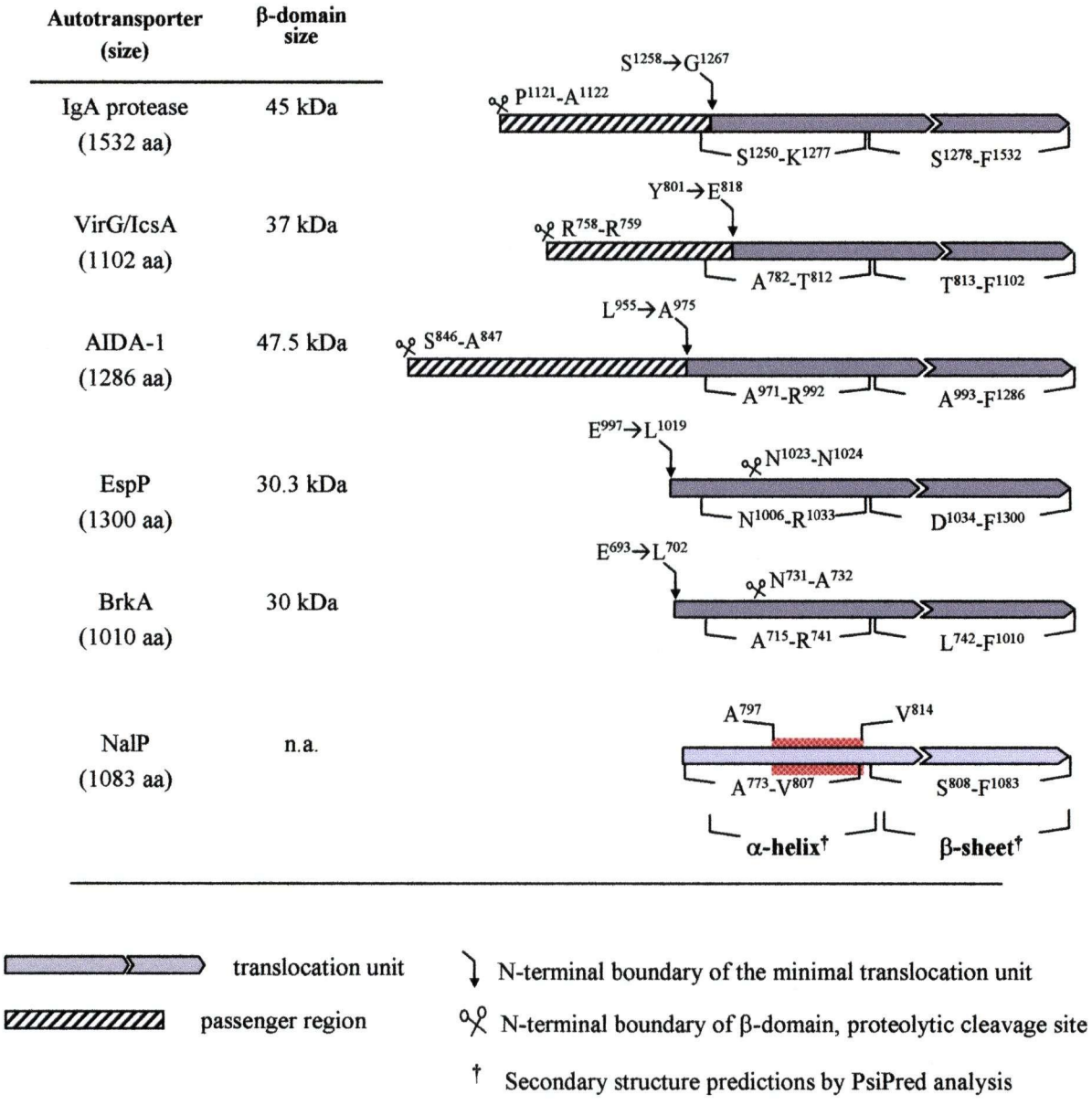

Figure 2-8. Comparison of the C-terminal regions of different autotransporters.
The C-terminal regions of 5 autotransporters are shown (not drawn to scale). See text for explanation. The N-terminal boundaries noted for each translocation unit have been defined experimentally: IgA protease (Klauser *et al.*, 1993), VirG/IcsA (Suzuki *et al.*, 1995), AIDA-1 (Mauer *et al.*, 1998), BrkA (Oliver *et al.* 2003), and EspP (Velarde and Nataro, 2004). The minimal translocation unit of NalP (Oomen *et al.*, 2004) has not been experimentally defined. The red hatched box demarked by residues A^{797}-V^{814} illustrates the region of the NalP(D^{777}-F^{1084}) linker (α-helical region) that resides within the membrane spanning region of the β-barrel. Figure modified from Oliver *et al.*, J. Bact. 2003.

2.4.3 What cleaves the BrkA precursor at Asn^{731}-Ala^{732} to yield the α- and β-domains?

The protease responsible for cleavage of BrkA precursor at Asn^{731}-Ala^{732} is not known. We have shown here that cleavage occurs (*i*) in *E. coli* strain UT5600, indicating that processing is not dependent on the outer membrane proteases OmpT or OmpP, and (*ii*) in the absence of residues 136 - 692 of the BrkA passenger, arguing against autoproteolysis mediated by the BrkA passenger. Theoretically, the protease responsible for cleaving BrkA could reside in the periplasmic compartment, in the outer membrane, in the extracellular milieu (as a surface associated product), or within the β-domain itself (i.e. autoproteolysis). The observation that BrkA is cleaved in both *E. coli* and *B. pertussis* argues for a conserved mechanism (e.g. a general protease) or for autoproteolysis.

Interestingly, comparison with the structure of the NalP translocator suggests that the BrkA cleavage site might be positioned on the cell surface or within the β-domain. Only residues Ala^{797}-Val^{814} of the NalP(Asp^{777}-Phe^{1084}) α-helix are located within the membrane embedded portion of the channel formed by the β-barrel structure (Fig. 2-8 and Fig. 1-2). Assuming that the BrkA translocation unit forms a structure similar to NalP(Asp^{777}-Phe^{1084}), positional alignment of their predicted α-helical regions suggests that residues Ala^{732}-Gly^{748} of the BrkA translocation unit would be located within the membrane embedded portion of its β-barrel (Figure 2-8). In this scenario, the BrkA cleavage site (Asn^{731}-Ala^{732}) would be positioned on the cell surface or possibly within the channel itself.

2.4.4 How does the BrkA α-domain remain anchored to the cell surface?

Unlike the passengers of IgA protease, VirG/IcsA, and AIDA-1 that can be released either naturally (Fukuda *et al.*, 1995) (Pohlner *et al.*, 1987), or induced to be released following heat treatment (Benz and Schmidt, 1992), BrkA remains steadfastly anchored to the surface of *B. pertussis* and is not detected in concentrated culture supernatants (Oliver and Fernandez, 2001). Further, the cleaved BrkA passenger remains associated with the cell surface of *E. coli* UT5600 and is not detected in culture supernatants, indicating that the primary mechanism of BrkA anchoring is not specific to *B. pertussis*. The notion that processing occurs on the cell surface or within the channel (see above) suggests that the BrkA linker might interact with extracellular regions of the β-barrel (e.g. loops) or within the channel itself. Interestingly, the cleaved BrkA β-domain can be "pulled-down" with the α-domain in co-immunoprecipitation experiments performed on solubilized *B. pertussis* extracts (D. Oliver and R. Fernandez, unpublished observations), thus providing support for the hypothesis that the BrkA α-domain and β-domain interact *in vivo*. It is likely that the region responsible for tethering BrkA to the cell surface is located in either the extreme N-terminus of the passenger (residues 43-51) or/and within the C-terminal linker region (residues 693-731) since overlapping deletions spanning residues 52-692 remain associated with the cell surface. The nature of this interaction and the mechanism of BrkA anchoring are currently under investigation.

2.5 References

Barnes, M.G., and Weiss, A.A. (2001) BrkA protein of *Bordetella pertussis* inhibits the classical pathway of complement after C1 deposition. *Infect Immun* **69**: 3067-3072.

Benz, I., and Schmidt, M.A. (1992) AIDA-I, the adhesin involved in diffuse adherence of the diarrhoeagenic *Escherichia coli* strain 2787 (O126:H27), is synthesized via a precursor molecule. *Mol Microbiol* **6**: 1539-1546.

Brandon, L.D., Goehring, N., Janakiraman, A., Yan, A.W., Wu, T., Beckwith, J., and Goldberg, M.B. (2003) IcsA, a polarly localized autotransporter with an atypical signal peptide, uses the Sec apparatus for secretion, although the Sec apparatus is circumferentially distributed. *Mol Microbiol* **50**: 45-60.

Charles, I., Rodgers, B., Musgrave, S., Peakman, T.C., Chubb, A., Fairweather, N., Dougan, G., and Roberts, M. (1993) Expression of P.69/pertactin from *Bordetella pertussis* in a baculovirus/insect cell expression system: protective properties of the recombinant protein. *Res Microbiol* **144**: 681-690.

Desvaux, M., Parham, N.J., and Henderson, I.R. (2004) The autotransporter secretion system. *Res Microbiol* **155**: 53-60.

Elish, M.E., Pierce, J.R., and Earhart, C.F. (1988) Biochemical analysis of spontaneous fepA mutants of *Escherichia coli*. *J Gen Microbiol* **134 (Pt 5)**: 1355-1364.

Emsley, P., Charles, I.G., Fairweather, N.F., and Isaacs, N.W. (1996) Structure of *Bordetella pertussis* virulence factor P.69 pertactin. *Nature* **381**: 90-92.

Ewanowich, C.A., Melton, A.R., Weiss, A.A., Sherburne, R.K., and Peppler, M.S. (1989) Invasion of HeLa 229 cells by virulent *Bordetella pertussis*. *Infect Immun* **57**: 2698-2704.

Fernandez, R.C., and Weiss, A.A. (1994) Cloning and sequencing of a *Bordetella pertussis* serum resistance locus. *Infect Immun* **62**: 4727-4738.

Fernandez, R.C., and Weiss, A.A. (1996) Susceptibilities of *Bordetella pertussis* strains to antimicrobial peptides. *Antimicrob Agents Chemother* **40**: 1041-1043.

Fernandez, R.C., and Weiss, A.A. (1998) Serum resistance in bvg-regulated mutants of *Bordetella pertussis*. *FEMS Microbiol Lett* **163**: 57-63.

Fukuda, I., Suzuki, T., Munakata, H., Hayashi, N., Katayama, E., Yoshikawa, M., and Sasakawa, C. (1995) Cleavage of *Shigella* surface protein VirG occurs at a specific site, but the secretion is not essential for intracellular spreading. *J Bacteriol* **177**: 1719-1726.

Gotto, J.W., Eckhardt, T., Reilly, P.A., Scott, J.V., Cowell, J.L., Metcalf, T.N., 3rd, Mountzouros, K., Gibbons, J.J., Jr., and Siegel, M. (1993) Biochemical and immunological properties of two forms of pertactin, the 69,000-molecular-weight outer membrane protein of *Bordetella pertussis*. *Infect Immun* **61**: 2211-2215.

Grodberg, J., and Dunn, J.J. (1988) ompT encodes the Escherichia coli outer membrane protease that cleaves T7 RNA polymerase during purification. *J Bacteriol* **170**: 1245-1253.

Henderson, I.R., Navarro-Garcia, F., and Nataro, J.P. (1998) The great escape: structure and function of the autotransporter proteins. *Trends Microbiol* **6**: 370-378.

Kerr, J.R., and Matthews, R.C. (2000) *Bordetella pertussis* infection: pathogenesis, diagnosis, management, and the role of protective immunity. *Eur J Clin Microbiol Infect Dis* **19**: 77-88.

Klauser, T., Pohlner, J., and Meyer, T.F. (1990) Extracellular transport of cholera toxin B subunit using *Neisseria* IgA protease beta-domain: conformation-dependent outer membrane translocation. *Embo J* **9**: 1991-1999.

Klauser, T., Pohlner, J., and Meyer, T.F. (1992) Selective extracellular release of cholera toxin B subunit by *Escherichia coli*: dissection of *Neisseria* Iga beta-mediated outer membrane transport. *Embo J* **11**: 2327-2335.

Klauser, T., Kramer, J., Otzelberger, K., Pohlner, J., and Meyer, T.F. (1993) Characterization of the *Neisseria* Iga beta-core. The essential unit for outer membrane targeting and extracellular protein secretion. *J Mol Biol* **234**: 579-593.

Laemmli, U.K. (1970) Cleavage of structural proteins during the assembly of the head of bacteriophage T4. *Nature* **227**: 680-685.

Li, L.J., Dougan, G., Novotny, P., and Charles, I.G. (1991) P.70 pertactin, an outer-membrane protein from *Bordetella parapertussis*: cloning, nucleotide sequence and surface expression in *Escherichia coli*. *Mol Microbiol* **5**: 409-417.

Locht, C., Antoine, R., and Jacob-Dubuisson, F. (2001) *Bordetella pertussis*, molecular pathogenesis under multiple aspects. *Curr Opin Microbiol* **4**: 82-89.

Locht, C., Antoine, R., Raze, D., Mielcarek, N., Hot, D., Lemoine, Y., and Mascart, F. (2004) *Bordetella pertussis* from functional genomics to intranasal vaccination. *Int J Med Microbiol* **293**: 583-588.

Loveless, B.J., and Saier, M.H., Jr. (1997) A novel family of channel-forming, autotransporting, bacterial virulence factors. *Mol Membr Biol* **14**: 113-123.

Maurer, J., Jose, J., and Meyer, T.F. (1997) Autodisplay: one-component system for efficient surface display and release of soluble recombinant proteins from *Escherichia coli*. *J Bacteriol* **179**: 794-804.

Maurer, J., Jose, J., and Meyer, T.F. (1999) Characterization of the essential transport function of the AIDA-I autotransporter and evidence supporting structural predictions. *J Bacteriol* **181**: 7014-7020.

McGuffin, L.J., Bryson, K., and Jones, D.T. (2000) The PSIPRED protein structure prediction server. *Bioinformatics* **16**: 404-405.

Miyazaki, H., Yanagida, N., Horinouchi, S., and Beppu, T. (1989) Characterization of the precursor of Serratia marcescens serine protease and COOH-terminal processing of the precursor during its excretion through the outer membrane of *Escherichia coli*. *J Bacteriol* **171**: 6566-6572.

Nielsen, H., Engelbrecht, J., Brunak, S., and von Heijne, G. (1997) Identification of prokaryotic and eukaryotic signal peptides and prediction of their cleavage sites. *Protein Eng* **10**: 1-6.

Nielsen, H., and Krogh, A. (1998) Prediction of signal peptides and signal anchors by a hidden Markov model. *Proc Int Conf Intell Syst Mol Biol* **6**: 122-130.

Oliver, D.C., and Fernandez, R.C. (2001) Antibodies to BrkA augment killing of *Bordetella pertussis*. *Vaccine* **20**: 235-241.

Oliver, D.C., Huang, G., and Fernandez, R.C. (2003) Identification of secretion determinants of the *Bordetella pertussis* BrkA autotransporter. *J Bacteriol* **185**: 489-495.

Oomen, C.J., Van Ulsen, P., Van Gelder, P., Feijen, M., Tommassen, J., and Gros, P. (2004) Structure of the translocator domain of a bacterial autotransporter. *Embo J* **23**: 1257-1266.

Parkhill, J., Sebaihia, M., Preston, A., Murphy, L.D., Thomson, N., Harris, D.E., Holden, M.T., Churcher, C.M., Bentley, S.D., Mungall, K.L., Cerdeno-Tarraga, A.M., Temple, L., James, K., Harris, B., Quail, M.A., Achtman, M., Atkin, R., Baker, S., Basham, D., Bason, N., Cherevach, I., Chillingworth, T., Collins, M., Cronin, A., Davis, P., Doggett, J., Feltwell, T., Goble, A., Hamlin, N., Hauser, H., Holroyd, S., Jagels, K., Leather, S., Moule, S., Norberczak, H., O'Neil, S., Ormond, D., Price, C., Rabbinowitsch, E., Rutter, S., Sanders, M., Saunders, D., Seeger, K., Sharp, S., Simmonds, M., Skelton, J., Squares, R., Squares, S., Stevens, K., Unwin, L., Whitehead, S., Barrell, B.G., and Maskell, D.J. (2003) Comparative analysis of the genome sequences of Bordetella pertussis, Bordetella parapertussis and Bordetella bronchiseptica. *Nat Genet* **35**: 32-40.

Passerini de Rossi, B.N., Friedman, L.E., Gonzalez Flecha, F.L., Castello, P.R., Franco, M.A., and Rossi, J.P. (1999) Identification of *Bordetella pertussis* virulence-associated outer membrane proteins. *FEMS Microbiol Lett* **172**: 9-13.

Pohlner, J., Halter, R., Beyreuther, K., and Meyer, T.F. (1987) Gene structure and extracellular secretion of *Neisseria gonorrhoeae* IgA protease. *Nature* **325**: 458-462.

Pugsley, A.P. (1993) The complete general secretory pathway in gram-negative bacteria. *Microbiol Rev* **57**: 50-108.

Sambrook, J., Fritsch, E.F., and Maniatis T. (1989) *Molecular Cloning: a Laboratory Manual, 2nd edn. Cold Spring Harbor Laboratory Press, Cold Springs Harbor, NY.*

Shannon, J.L., and Fernandez, R.C. (1999) The C-terminal domain of the *Bordetella pertussis* autotransporter BrkA forms a pore in lipid bilayer membranes. *J Bacteriol* **181**: 5838-5842.

Sijbrandi, R., Urbanus, M.L., ten Hagen-Jongman, C.M., Bernstein, H.D., Oudega, B., Otto, B.R., and Luirink, J. (2003) Signal recognition particle (SRP)-mediated targeting and Sec-dependent translocation of an extracellular *Escherichia coli* protein. *J Biol Chem* **278**: 4654-4659.

St Geme, J.W., 3rd, and Cutter, D. (2000) The *Haemophilus influenzae* Hia adhesin is an autotransporter protein that remains uncleaved at the C terminus and fully cell associated. *J Bacteriol* **182**: 6005-6013.

Suhr, M., Benz, I., and Schmidt, M.A. (1996) Processing of the AIDA-I precursor: removal of AIDAc and evidence for the outer membrane anchoring as a beta-barrel structure. *Mol Microbiol* **22**: 31-42.

Suzuki, T., Lett, M.C., and Sasakawa, C. (1995) Extracellular transport of VirG protein in *Shigella. J Biol Chem* **270**: 30874-30880.

Turner, D.P., Wooldridge, K.G., and Ala'Aldeen, D.A. (2002) Autotransported serine protease A of *Neisseria meningitidis*: an immunogenic, surface-exposed outer membrane, and secreted protein. *Infect Immun* **70**: 4447-4461.

Veiga, E., de Lorenzo, V., and Fernandez, L.A. (1999) Probing secretion and translocation of a beta-autotransporter using a reporter single-chain Fv as a cognate passenger domain. *Mol Microbiol* **33**: 1232-1243.

Veiga, E., Sugawara, E., Nikaido, H., de Lorenzo, V., and Fernandez, L.A. (2002) Export of autotransported proteins proceeds through an oligomeric ring shaped by C-terminal domains. *Embo J* **21**: 2122-2131.

Weiss, A.A., Hewlett, E.L., Myers, G.A., and Falkow, S. (1983) Tn5-induced mutations affecting virulence factors of *Bordetella pertussis*. *Infect Immun* **42**: 33-41.

Weiss, A.A., Melton, A.R., Walker, K.E., Andraos-Selim, C., and Meidl, J.J. (1989) Use of the promoter fusion transposon Tn5 lac to identify mutations in *Bordetella pertussis* vir-regulated genes. *Infect Immun* **57**: 2674-2682.

Weiss, A.A., Mobberley, P.S., Fernandez, R.C., and Mink, C.M. (1999) Characterization of human bactericidal antibodies to *Bordetella pertussis*. *Infect Immun* **67**: 1424-1431.

Chapter 3

Identification and initial characterization of a conserved domain required for folding of the BrkA passenger domain

3.1 Introduction

A fundamental aspect of any protein translocation system is the relationship between the folding state of the substrate and the nature of the channel through which it moves. Indeed, as noted by Desvaux *et al.*, for autotransporter proteins, the issues of substrate (passenger) folding, the formation and shape of the translocator, and secretion across the outer membrane are intimately linked (Desvaux *et al.*, 2004). Since the early studies describing the secretion of IgA protease (Pohlner *et al.*, 1987), the issue of whether autotransporter passengers are translocated across the outer membrane in an unfolded or a folded conformation has remained an open question that has garnered much debate (Klauser *et al.*, 1992) (Suzuki *et al.*, 1995) (Ohnishi *et al.*, 1994) (Brandon and Goldberg, 2001) (Veiga *et al.*, 1999) (Veiga *et al.*, 2004).

Studies of independent autotransporters have measured channels formed by the translocation unit to be between 1 nm for NalP (Oomen *et al.*, 2004) and 2 nm for IgA protease, PalA, and BrkA (Veiga *et al.*, 2002) (Shannon and Fernandez, 1999) (Lee and Byun, 2003). Veiga *et al.* (2004) have proposed that the secretion mechanism of IgA protease tolerates folded structures with a diameter of less than 2 nm, which appears consistent with biophysical measurements noted above. However, a 1 – 2 nm channel

Portions of this chapter have been published in Molecular Microbiology (Oliver *et al.*, 2003).

size would be incapable of secreting larger folded passenger domains. The β-helix structure formed by the passenger domain of pertactin (the only known structure of an autotransporter passenger) has an average width of 2.7 nm (and a maximum width of 3.8 nm) suggesting that it would be translocated in an unfolded or at most a partially folded ("translocation competent") conformation.

If autotransporter secretion involves a translocation competent folding state one would predict that mechanisms exist (i) to maintain the polypeptide in a translocation competent folding state within the periplasm (which would include providing protection from periplasmic proteases) and (ii) to promote proper and rapid folding of the passenger on the surface of the bacterium, ostensibly in the absence of chaperones. Consistent with the self-contained autotransporter theme, it is possible that the information required for folding of the passenger domain is encoded within the polypeptide itself. In this regard, a putative intramolecular chaperone region has previously been identified in PrtS, a *Serratia marcescens* autotransporter with protease activity (Ohnishi *et al.*, 1994). This region, termed the "junction", is found in the C-terminus of the passenger domain just upstream of the β domain and functional activity of the protease is dependent on the junction region being intact. Whether the proposed intramolecular chaperone function of the junction region is a general theme for all autotransporters, including non-proteases, remains to be determined.

Here the role of the C-terminal region of the passenger domain of BrkA is investigated, an autotransporter protein with no sequence or functional identity with PrtS. We identify

a region in the C-terminus of the BrkA passenger domain that is conserved in a large group of autotransporters having diverse functions suggesting that it serves an important function related to autotransporter secretion. Using a combination of genetic and biochemical approaches we show that this region of BrkA is required for folding of its passenger during secretion. Importantly, we show that the BrkA junction region mediates passenger folding when expressed in *trans* supporting the hypothesis that it can function as an intramolecular chaperone (Oliver *et al.*, 2003b). *In vitro* analyses indicate that the BrkA passenger does not adopt tertiary or secondary structure in the absence of the junction region, suggesting that this region serves to nucleate or initiate passenger folding. Further dissection has revealed a conserved region at the C-terminus the BrkA junction that is required for secretion of a "folding competent" form of the BrkA passenger. Based on these findings a working model of BrkA translocation across the outer membrane is presented.

3.2 Materials and methods

3.2.1 Bacterial strains, plasmids and growth conditions

Bacterial strains and plasmids used in this study are listed in Table 3-1. *E. coli* strains were cultured at 37 °C on Luria broth or Luria agar supplemented with the appropriate antibiotics. UT5600 and UT2300 were a gift from L. Fernandez and V. deLorenzo (Centro Nacional de Biotecnologia, Madrid, Spain). Kanamycin and chloramphenicol were added to the media at 50 μg/ml and 34 μg/ml, respectively. Ampicillin was added at 100 μg/ml for DH5α and 200 μg/ml for UT5600 and UT2300.

3.2.2 Recombinant DNA techniques

DNA manipulations and polymerase chain reactions (PCR) were carried out using standard techniques (Sambrook, 1989) and reagents, as described previously (Oliver *et al.*, 2003a). Primers used in this study were obtained from Alpha DNA (Montreal, PQ) or the University of British Columbia (UBC) Nucleic Acid and Protein Services (NAPS) Unit. DNA sequencing was done by the UBC NAPS Unit.

Construct pGH3-13 was made by digesting pDO6935 with *Eco*RV and *Bam*HI. The resulting 6.7 kilobase pair fragment was purified and the 5' *Bam*HI overhang was filled-in with the nucleotides dGTP, dATP, dTTP (Invitrogen, Burlington, ON) at 0.5 mM using Klenow large polymerase (Invitrogen). The remaining unpaired guanidine nucleotide was removed using mung bean endonuclease (Invitrogen) and the blunt-ended product was circularized by ligation to yield pGH3-13. Construct pDO-JB5 was made by digesting pGD7 with *Asc*I and *Xba*I. The resulting 5.0 kb product was purifed and the 5'

*Asc*I and *Xba*I overhangs were filled-in with the nucleotides dGTP and dCTP (Invitrogen, Burlington, ON) at 0.5 mM using Klenow large polymerase. The remaining unpaired nucleotides were removed using mung bean nuclease and the blunt-ended producted was circularized by ligation to yield pDO-JB5. Constructs pGH3-13K and pDO6935K were constructed by linearizing plasmids pGH3-13 and pDO6935 with *Xmn*I. A 1.4 kb *Sma*I cassette encoding resistance to kanamycin was excised from pUC4-KIXX and ligated into linearized plasmids pGH3-13 and pDO6935 to yield pGH3-13K and pDO-6935K, respectively.

Contructs pDO-PRN1 and pDO-PRN2 were constructed by PCR using forward primer PRN1550F (5' CCGGGCGGTTCAAGGTCC 3') and reverse primers PRN1820R (5' ACGGATCCGCGGCCAATCGATAGCG 3'), and PRN1961R (5' ACGGATCCGCGGCGGACAACTCC 3'), respectively. Amplified products were digested with *Bam*HI and ligated into a 4.7 kB *Stu*I – *Bam*HI fragment of pDO-JB5. Construct pDO-PRN3 was constructed by PCR using forward primer PRN1550F (sequence noted above) and reverse primer PRN-CR (5' CTGAAGCTTTAGACCCTCCTCGCTTTA 3'). The amplified product was digested with *Hind*III and ligated into a 3.8 kB *Stu*I – *Hind*III pDO-JB5 fragment. Construct pDO-PRN4 was constructed by PCR using forward primer PRN1823F (5' AAGGATCCGAATGGGCAGTGGAGC 3') and reverse primer PRN-CR (5' CTGAAGCTTTAGACCCTCCTCGCTTTA 3'). The amplified product was digested with *Bam*HI and *Hind*III and ligated into a 4.0 kB *Bam*HI – *Hind*III pDO-JB5 fragment. Plasmid pPRN-BS1 was used as template for PCR steps during the construction of pDO-PRN1, pDO-PRN2, pDO-PRN3, pDO-PRN4.

Expression construct pDO418 was made using primer pair G1NCO (5'-TCAGTCCATGGCGCAGGAAGGAGAGTTCGAC-3') and G2HIND (5'-CAGTGCAAGCTTCTGCAAGCTCCAGACATG-3') to amplify a 1.9 kb fragment representing the N-terminal passenger domain of BrkA. This product was cloned into pET30b using *Nco*I and *Hin*dIII to yield construct pDO418. Sequencing of pDO418 revealed a single base pair mutation that introduced a stop codon at the 3' terminus of the gene fusion resulting in a translated fusion protein lacking the C-terminal His-tag. Digesting plasmid pDO418 with *Eco*RV and *Not*I and filling-in the resulting 5' *Not*I extension using Klenow large polymerase generated a blunt ended product that was religated to yield plasmid pDO618. Digesting plasmid pDO418 with *Eco*RV and *Nco*I and filling-in the resulting 5' *Nco*I extension with Klenow large polymerase generated a blunt ended product that was re-ligated to yield plasmid pDO518. Plasmid pDO718 was made using primer pair BRK1975-NCOF (5'-TCAGTCCATGGCGCTCGATCGATCGCGTTGCC-3') and G2STOPR (5 - CAATTTAAGCTTTCACTGGCCCGCGCGCTGC-3') to amplify a 1.2 kB fragment of the BrkA passenger. The fragment was digested with *Nco*I and *Eco*RV and ligated into pDO418. Plasmids pBRK-H(61-605), pBRK-H(61-680), and pBRK-H(61-707) were constructed using forward primer G1NCO (sequence noted above) and reverse primers BRK3010-STOPR (5'- CAATTTAAGCTTTCACTTGTAAGAGGCCTC -3'), BRK3236-STOPR (5' TCACTTGCCGACGTTGGC '3), or G2STOPR (sequence noted above), respectively. Amplified products were digested with NcoI and HindIII and ligated into pET30b. Plasmid pRF1071 was made by excision of a 0.9 kB *Pst*I – *Eco*RI BrkA fragment from plasmid pRF1066, which was subsequently ligated into pRSETc (Rambow *et al.*, 1998). Plasmid pBRK-(601-707)H was constructed using primer pair BRK3025NdeIF (5'-

GGGGGGGCATATGGAGGCCTCTTACAAG -3') and G2STOPR (sequence noted above) to amplify an 0.3 kB fragment of BrkA, which was subsequently digested with *Nde*I and *Hind*III and ligated into pET30b. Plasmid pDO6935 was used as a template in all PCR steps involving *brk*A.

3.2.3 SDS-PAGE and immunoblot analysis

For detection of expressed BrkA via immunoblot, *E. coli* cultures were grown to 0.8 optical density (OD_{600}) units and sedimented by centrifugation. Washed pellets were resuspended finally in sample buffer and immediately boiled for 5 minutes prior to SDS-PAGE as previously described (Laemmli, 1970) (Fernandez and Weiss, 1994). Samples resolved by SDS-PAGE were transferred to Immobilon-P membranes (Millipore, Etobicoke, ON) as described (Oliver and Fernandez, 2001). Staining of the SDS-PAGE gels with Coomassie Blue verified that approximately equal amounts of lysates were loaded into each lane. Blots were probed using heat inactivated rabbit anti-BrkA antiserum and horseradish peroxidase-conjugated goat anti-rabbit secondary antibody (ICN Biomedicals, Costa Mesa, CA) diluted 1/50,000 and 1/10,000, respectively (Oliver and Fernandez, 2001). Kaleidoscope pre-stained markers (Bio-Rad, Hercules, CA) were used for estimation of molecular mass.

3.2.4 Immunofluorescence analysis

Indirect immunofluorescence was performed as previously described (Oliver *et al.*, 2003a) using a 1/200 dilution of heat inactivated rabbit anti-BrkA antiserum (Oliver and Fernandez, 2001) followed by a 1/100 dilution of FITC-conjugated goat anti-rabbit

antibody (Jackson ImmunoResearch Laboratories, West Grove, PA). Bacteria were visualized under epi-fluorescence using a Zeiss Axioscop-2 microscope. Phase contrast and fluorescent images were captured digitally.

3.2.5 Purification and refolding of BrkA fusion proteins

Recombinant His-tagged BrkA was expressed and purified using a protocol previously established in our laboratory (Shannon and Fernandez, 1999) (Oliver and Fernandez, 2001). *E. coli* strain BL21 (DE3) harboring expression constructs (Table 4-2) were grown to approximately 0.6 OD_{600} units and induced with 0.1 mM isopropyl-B-D-thiogalactopyranoside (IPTG). Purification was performed under denaturing conditions using nickel Ni^{2+}-nitrilotriacetic acid (NTA)-agarose following the protocol described in the Xpress System Protein Purification manual (Invitrogen). In brief, 50 ml of induced cell culture was pelleted by centrifugation and lysed using 6 M guanidinium hydrochloride, pH 7.8. Lysates were sonicated, centrifuged to remove insoluble material, and filtered through a 0.45 μm filter. Filtered lysates were bound to NTA-agarose and washed in 8 M urea at decreasing pH, and finally eluted in 8 M urea, pH 4.0. Eluted fractions were pooled, resolved by SDS-PAGE, and visualized by staining with Coomassie brilliant Blue-R250. Refolding of purified fusion proteins was performed as previously described (Oliver and Fernandez, 2001). Briefly, protein samples normalized to a concentration of 4.5 μM in 10 mM Tris buffer, pH 8.0, containing 0.1% Triton X-100 were dialysed against decreasing concentrations of urea. Samples were ultimately dialysed into 10 mM Tris, pH 8.0, and examined via SDS-PAGE. Solubility of dialysed

fusion proteins was assessed by centrifugation at 13,000 RPM for 30 minutes at 4 °C. Protein concentration was determined using the Bio-Rad Protein Assay.

3.2.6 Far-UV circular dichroism spectroscopy of BrkA fusion proteins

Circular dichroism (CD) analysis was performed on dialysed BrkA fusion protein using a Jasco J-810 CD spectropolarimeter (Jasco Inc, Easton, MD) at room temperature using a cell path length of 1 mm. Individual spectra were collected by averaging 10 scans made over a spectral window of 190 nm to 260 nm. Fusion proteins were analyzed at concentration of 0.3 μg/ml in 10 mM Tris buffer, pH 8.0.

3.2.7 *In vitro* limited proteolysis analysis

Limited proteolysis digestions were performed using 25 μl aliquots of each fusion protein (300 μg/ml) that had been dialysed into 10mM Tris buffer pH 8. 1 μl of trypsin (1 μg/ml) was added to each sample and digestion was allowed to proceed at room temperature. At time intervals of 1, 5, and 15 minutes, reactions were stopped by the addition of 2.5 μl of 100 mM phenyl methylsulfonyl fluoride (PMSF) and stored on ice. Each sample was precipitated using 30 μl of 20% trichloroacetic acid (TCA) and sendimented by centrifugation at 4 °C for 15 minutes. Prior to analysis by SDS-PAGE samples were washed with 300 μl ice-cold acetone and resuspended in 50 μl disruption buffer. Densitometry was performed using the Alpha Imager 1200 (Alpha Innotech Corporation, San Leandro, CA).

3.2.8 *In vivo* limited proteolysis analysis

E. coli UT5600 co-transformed with the indicated plasmids were grown to an OD_{600} of 0.8 in the presence of antibiotic selection. One ml of culture was harvested by centrifugation and resuspended in 150 µl of PBS. A 15 µl of aliquot was removed and added to 50 µl of SDS-PAGE disruption buffer and boiled for 5 minutes. Trypsin was then added to the remaining culture to a final concentration of 0.01 mg/ml. Following the addition of trypsin, 15 µl aliquots were removed at various time intervals (1, 5, 15 minutes) and added to 50 µl of disruption buffer and immediately boiled to stop digestion. Samples were resolved by SDS-PAGE, transferred to Immobilon-P membrane and probed for BrkA expression (as described above). Limited proteolysis experiments using α-chymotrypsin (Sigma) or proteinase K (Sigma) were performed as described above. Trypsin accessibility experiments were performed as previously described (Maurer *et al.*, 1997) (Oliver *et al.*, 2003a).

3.2.9 Cell surface refolding of DO(61-605)P fusion protein

E. coli UT5600 were transformed with pDO-JB5, pGH313, or a vector control and grown over night at 37 °C. Fresh transformants were grown to an optical density of ~ 0.8 and harvested by centrifugation. The supernatant was discarded and the pellet was resuspended in 140 µL of PBS. Ten microlitres of fusion protein DO(61-605)P (200 µg/ml) was added to each cell suspension, mixed, and incubated at room temperature for the indicated periods (5, 15, 60 minutes). At each time point, a 15 µl of aliquot was removed and added to 50 µl of SDS-PAGE disruption buffer and boiled for 5 minutes. Trypsin was then added to the remaining suspension to a final concentration of 0.01

mg/ml. Following the addition of trypsin, 15 µl aliquots were removed at various time intervals (1, 5, 15 minutes) and added to 50 µl of disruption buffer and immediately boiled to stop digestion. Samples were resolved by SDS-PAGE, transferred to Immobilon-P membrane and probed for BrkA (as described above).

3.2.10 Adherence assay

HeLa cells were maintained in complete minimal essential medium (MEM) supplemented with 10% heat-inactivated fetal bovine serum, 50 U of penicillin and 50 µg/ml streptomycin. All cell culture media were purchased from Invitrogen. The adherence assay was performed in triplicate in 96-well Falcon U-bottom plates (Becton Dickinson Labware, Franklin Lakes, NJ) essentially as described by van den Berg et al. (van den Berg *et al.*, 1999). Confluent monolayers were washed with PBS and the cells were detached with a 1 mM EDTA-0.25% trypsin solution (Invitrogen). A buffer control or 0.2 µg of fusion protein in 100 µl of PBS containing 0.5% BSA (PBS-BSA) were added to 100 µl of PBS-BSA containing 10^6 detached HeLa cells that had been previously fixed for 10 minutes with 1% formaldehyde in PBS. After incubating for 30 minutes at 37 °C, the cells were washed twice in PBS-BSA and incubated for 30 minutes at room temperature with a 1:400 dilution of the rabbit anti-BrkA antiserum (Oliver and Fernandez, 2001). The cells were washed again, and incubated with a 1:200 dilution of a FITC-conjugated goat anti-rabbit antibody (Jackson ImmunoResearch Laboratories). Washed cells were then subjected to flow cytometry using a FACScan (Becton Dickinson, San Jose, CA) and the data from 10,000 cells were analyzed using the CellQuest program.

Table 3-1. Strains and plasmids.

Strain/Plasmid	Relevant Characteristics[a]	Reference/Source
Strains		
E. coli		
UT2300	F⁻ *ara-14 leuB6 azi-6 lacYI proC14 tsx-67 entA403 trpE38 rfbD1 rpsL109 xyl-5 mtl-1 thi1*	Elish *et al.*, 1988
UT5600	UT2300 derivative, Δ*ompT-fepC266*	Elish *et al.*, 1988
DH5αF'	K–12 cloning strain	Invitrogen
Plasmids		
pET30b	Kan^r; Expression vector	Novagen
pBluescriptII SK^-	Amp^r; cloning vector	Stratagene
pUC4-KIXX	pUC4 vector carrying a Kan^r cassette	Barany, 1985
pBBRMCS-1	Cm^r; broad host range, medium copy vector	Kovach, 1994
pDO6935	Amp^r, *brk*A	Oliver *et al.*, 2003
pDO244	Amp^r, *brk*A mutant; $\Delta(A^{136}\text{-}P^{255})$	Oliver *et al.*, 2003
pGD7	Amp^r, *brk*A mutant; $\Delta(S^{229}\text{-}P^{600})$	Oliver *et al.*, 2003
pGH3-13	Amp^r, *brk*A mutant; $\Delta(E^{601}\text{-}A^{692})$, derived from pDO6935	Oliver *et al.*, 2003
pGH3-13BBR	Cm^r, *brk*A mutant; $\Delta(E^{601}\text{-}A^{692})$, derived from pGH313	this study
pDO-JB5	Amp^r, *brk*A mutant; $\Delta(A^{52}\text{-}P^{600})$, derived from pGD7	Oliver *et al.*, 2003
pGH3-13K	Kan^r, pGH3-13 derivative carrying a 1.4 kb *Sma*I Kan^r cassette derived from pUC4-KIXX	Oliver *et al.*, 2003
pDO-6935K	Kan^r, pDO-6935 derivative carrying a 1.4 kb *Sma*I Kan^r cassette derived from pUC4-KIXX	Oliver *et al.*, 2003
pDO418	Kan^r, pET30b fusion construct; $BrkA(E^{61}\text{-}V^{699})$	Oliver *et al.*, 2003

pDO518	Kan^r, pDO418 derivative, fusion construct; BrkA(I^{535}-V^{699})	Oliver *et al.*, 2003
pDO618	Kan^r, pDO418 derivative, fusion construct; BrkA(E^{61}-D^{534})	Oliver *et al.*, 2003
pDO718	Kan^r, pET30b fusion construct; BrkA(L^{257}-V^{699})	this study
pBRK-H(61-707)	Kan^r, pET30b fusion construct; BrkA(E^{61}- Q^{707})	this study
pBRK-H(61-680)	Kan^r, pET30b fusion construct; BrkA(E^{61}-K^{680})	this study
pBRK-H(61-605)	Kan^r, pET30b fusion construct; BrkA(E^{61}-V^{605})	this study
pBRK-(601-707)H	Kan^r, pRSETb fusion construct; BrkA(E^{61}-Q^{707})	this study
pRF1071	Amp^r, pRSETb fusion construct; BrkA(E^{298}-V^{595})	this study
pDO-PRN1	Amp^r, pertactin junction / BrkA TU chimera;	this study
pDO-PRN1BBR	Chl^r, pertactin junction / BrkA TU chimera; gene sub-cloned from pDO-PRN1	this study
pDO-PRN2	Amp^r, pertactin junction / BrkA TU chimera;	this study
pDO-PRN2BBR	Cm^r, pertactin junction / BrkA TU chimera; gene sub-cloned from pDO-PRN1	this study
pDO-PRN3	Amp^r, pertactin junction / BrkA TU chimera;	this study
pDO-PRN3BBR	Cm^r, pertactin junction / BrkA TU chimera; gene sub-cloned from pDO-PRN1	this study
pDO-PRN4	Amp^r, pertactin junction / BrkA TU chimera;	this study
pDO-PRN4BBR	Cm^r, pertactin junction / BrkA TU chimera; gene sub-cloned from pDO-PRN1	this study
pDO-313PrnTUBBR	Cm^r, BrkA passenger/pertactin TU chimera	this study
pDO-313-IPTU1124 BBR	Cm^r, BrkA passenger/IgA protease (V^{1124}-F^{1532}) TU chimera	this study
pDO313-IPTU1225 BBR	Cm^r, BrkA passenger/IgA protease (G^{1225}-F^{1532}) TU chimera	this study

Kan^r, Cm^r and Amp^r refer to resistance to kanamycin, chloramphenicol and ampicillin, respectively.

3.3 Results

3.3.1 BrkA Glu^{601}-Ala^{692} is necessary for passenger stability in the presence of endogenous outer membrane proteases

In an effort to dissect the mechanism of BrkA secretion I have made several in-frame deletions within the BrkA passenger domain. Interestingly, mutations within the C-terminus of the passenger domain rendered the secreted form of the protein unstable in *E. coli* strain DH5α (data not shown). Based on these observations we postulated that the BrkA passenger might encode a region important for folding of its passenger domain similar to the PrtS protease junction region (Ohnishi *et al.*, 1994). Ohnishi *et al.* observed that when a junction-deleted PrtS was expressed in *E. coli*, neither the mature PrtS protein nor enzymatic activity could be detected. On the other hand, a processed form of the β-core was found in the outer membrane. They proposed that the mature protease was being degraded at the cell surface because it could not fold into an active and stable conformation. We wondered whether a similar region might exist to promote folding of BrkA thereby conferring stability to the exported protein. We hypothesized that a properly folded BrkA passenger would be stable in the presence of proteases, but if the BrkA passenger were unable to fold properly, it would be unstable and subject to degradation during secretion. To test this hypothesis, we developed an assay to compare the surface expression of wildtype and mutant constructs of BrkA in *E. coli* strains UT2300 and UT5600. As previously mentioned, these strains have been used routinely to study secretion of autotransporters from different bacterial species (Klauser *et al.*, 1993a) (Suzuki *et al.*, 1995) (Maurer *et al.*, 1997) (Maurer *et al.*, 1999) (Veiga *et al.*, 1999) including BrkA (Oliver *et al.*, 2003a). UT2300 has an $OmpT^+$ and $OmpP^+$ phenotype,

whereas UT5600 lacks these outer membrane proteases (Elish *et al.*, 1988). We thus compared wildtype BrkA with mutant constructs (Fig. 3-1A) bearing deletions in either the amino (ΔAla^{136}-Pro^{255}) or carboxy (ΔGlu^{601}-Ala^{692}) termini of the BrkA passenger α–domain; this carboxy terminus deletion would effectively represent the junction region in PrtS protease, despite a lack of sequence identity.

Expression of wild type BrkA in both *E. coli* UT5600 and in UT2300 was detected by immunoblot (Fig. 3-1B, lanes 1a and 1b). Recall, the upper band migrating at approximately 103 kDa corresponds to the unprocessed BrkA precursor and the lower band migrating at 73 kDa corresponds to the cleaved BrkA passenger region. The intensity of the precursor band is variable and its nature and cellular location are not known. It has been noted that IPTG-induction of the PrtS autotransporter in *E. coli* resulted in a fraction of the PrtS precursor forming insoluble periplasmic species (Miyazaki *et al.*, 1989) (Shikata *et al.*, 1993). It is possible that a proportion of the BrkA precursor may undergo a similar fate when expressed in *E. coli.* As shown in Chapter 2 (Fig. 2-5), the lower band represents the surface exposed fraction of BrkA in UT5600 (Oliver *et al.*, 2003a); a corresponding band is seen in the UT2300 background. Surface expression of BrkA was also detected via indirect immunofluorescence on both *E. coli* UT2300 and UT5600 (Fig. 3-1C, panels 1a and 1b). Taken together these data indicate that the BrkA passenger domain is surface expressed in a stable manner in *E. coli* strains UT2300 and UT5600.

When BrkA (ΔGlu^{601}-Ala^{692}) was expressed in UT5600 both the unprocessed precursor and the processed passenger were detected by immunoblot (Fig. 3-1B, lane 3a). In contrast, when BrkA (ΔGlu^{601}-Ala^{692}) was expressed in *E. coli* strain UT2300 only the unprocessed BrkA (ΔGlu^{601}-Ala^{692}) precursor was observed (Fig. 3-1B, lane 3b), suggesting that deletion of residues 601-692 rendered the processed BrkA passenger susceptible to proteolysis by the outer membrane proteases OmpT and OmpP. Consistent with this observation, immunofluorescence data showed that BrkA (ΔGlu^{601}-Ala^{692}) was detected on the surface of *E. coli* strain UT5600 but not on *E. coli* strain UT2300 (Fig. 3-1C, panels 3a and 3b), despite the precursor (upper band) being made. Deletions within the N-terminal region of BrkA had a different outcome. BrkA (ΔAla^{136}-Pro^{255}) was surface expressed in a stable manner in both *E. coli* strain UT5600 and UT2300 (Figs. 3-1B and C, panels 2a and 2b) suggesting that the deletion of amino acids 136-255 did not influence the stability of the BrkA passenger.

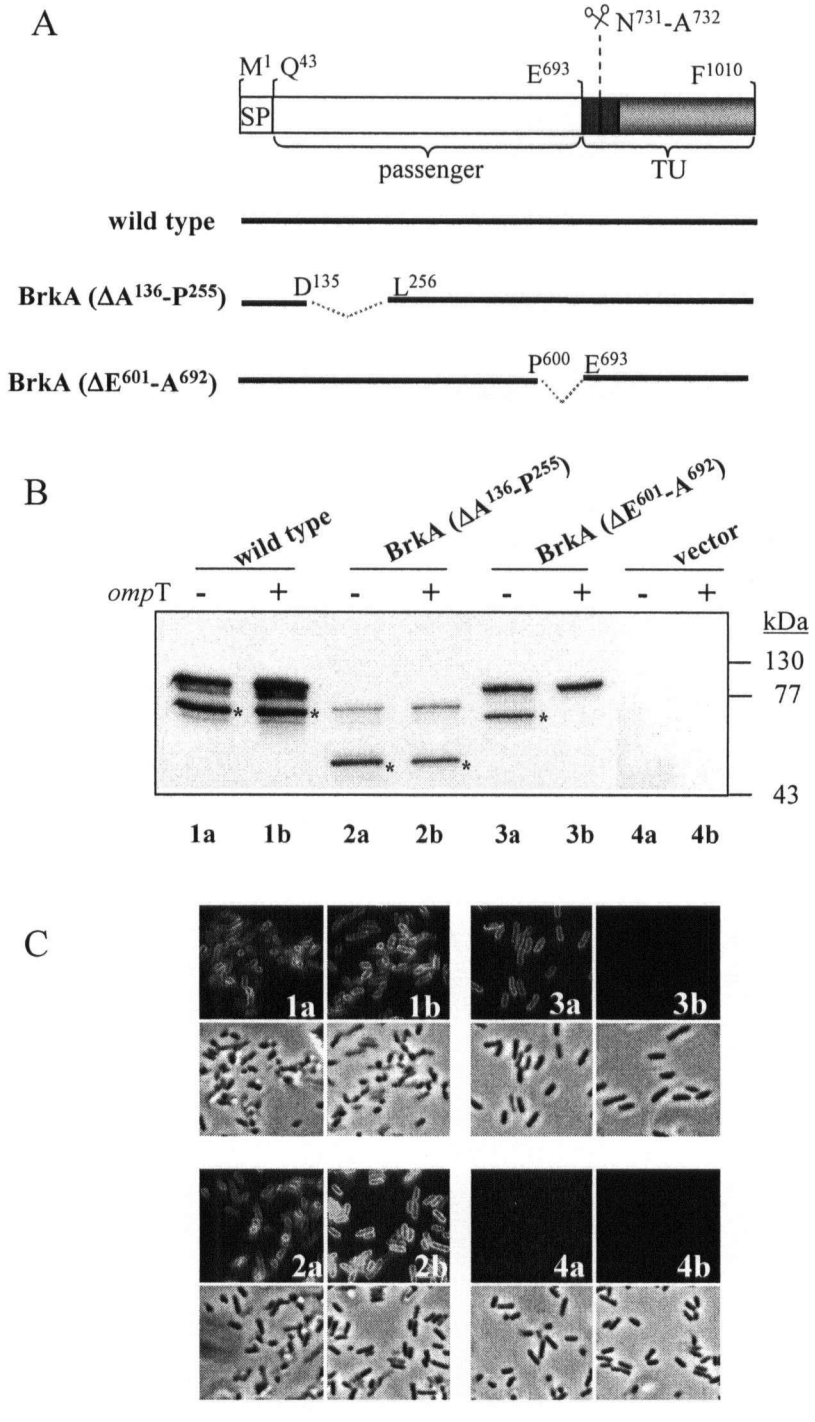

Fig. 3-1. Expression of mutant forms of BrkA.

A. BrkA domain organization. SP, signal peptide (residues 1-42); passenger domain (residues 43-692); shaded boxes represent the BrkA linker region (dark grey) and β-core (light grey) which form the translocation unit (TU; residues 693-1010) (Oliver *et al.* 2003a). Wild type BrkA was expressed from pDO6935; BrkA (ΔA^{136}-P^{255}) was expressed from pDO244; and BrkA (ΔE^{601}-A^{692}) was expressed from pGH3-13. **B.** Analysis of BrkA expression. Plasmids were transformed into isogenic *E. coli* strains UT2300 (*ompT*$^+$) and UT5600 (*ompT*$^-$). Bacteria were grown to 0.8 optical density units and harvested for analysis of BrkA expression by immunoblot and indirect immunofluorescence. Whole cell lysates were resolved by SDS-PAGE and blots were probed with anti-BrkA antiserum. (a) *E. coli* strain UT5600 and (b) *E. coli* strain UT2300. Band denoted by an asterisk (*), corresponds to the passenger processed between residues N^{731} and A^{732}. Plasmid pBluescript served as a vector control. **C.** Indirect immunofluorecence was used to evaluate surface expression of each of the mutants. Figure from Oliver *et al.*, Molec. Micro. 2003.

3.3.2 A conserved domain is found within the passenger region of several autotransporters

The observations that deletion of Glu^{601}-Ala^{692} renders the BrkA passenger unstable in the presence of outer membrane proteases are consistent with the results presented by Ohnishi *et al* characterizing the PrtS protease junction region (Ohnishi *et al.*, 1994). The functional parallels with this junction region suggest that the role of region Glu^{601}-Ala^{692} may be common to other autotransporter proteins. Therefore, to further our analysis we queried the ProDom database with the BrkA sequence (http://protein.toulouse.inra.fr/prodom/doc/prodom.html) to look for proteins in the database that might have sequence identity with region Glu^{601}-Ala^{692} of BrkA. We reasoned that such an analysis might identify regions of weak homology that would provide an evolutionarily conserved function. The ProDom database (Corpet *et al.*, 2000) consists of an automatic compilation of homologous domains compiled using recursive position specific iterative BLAST (PSI-BLAST) searches of non-fragmentary sequences from SWISS-PROT 39, TREMBL and TREMBL update databases. ProDom (release 2001.3) analysis of the BrkA primary amino acid sequence identified a conserved domain (PD002475) at the C-terminus of the BrkA passenger spanning residues Asn^{578} – Asp^{702} (Fig. 3-3A). BrkA (ΔGlu^{601}-Ala^{692}) is found within this region. Domain PD002475 was found in at least 55 proteins, all of which are known to be or predicted to be autotransporters. Fig. 3-2 depicts a subset of autotransporters bearing domain PD002475. Interestingly, domain PD002475 is consistently located near the C-terminus of the passenger domain upstream of the predicted β-domain, although the distance between domain PD002475 and the predicted β-domain varies. The observation that domain

PD002475 is conserved amongst autotransporter proteins having diverse functions from multiple Gram negative species suggests that the region may play a general role in autotransporter secretion.

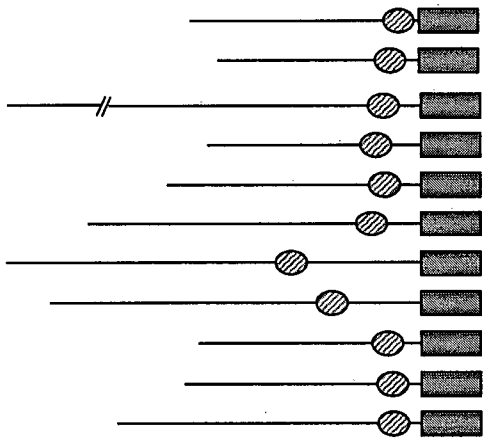

Domain architecture	Protein	Function	Organism	Accession number
	BrkA	serum^R / adherence	*B. pertussis*	U12276
	Prn	adherence	*B. pertussis*	AJ006158
	ShdA	shedding	*Salmonella sp.*	AF140550
	MisL	unknown	*S. typhimurium*	AF106566
	IcsA*	intracellular spread	*S. flexneri*	M22802
	Hap	protease	*H. influenzae*	U11024
	IgA prot.	protease	*H. influenzae*	X59800
	IgA prot.	protease	*N. gonorrhoeae*	X04835
	TibA	unknown	*E. coli*	AF109215
	Ag43	aggregation	*E. coli*	P39180
	AIDA-I	diffuse adherence	*E. coli*	X65022

Fig. 3-2. Identification of a conserved domain within the passenger region of several autotransporter proteins. Domain architecture of selected autotransporters. The ProDom database (version 2001.3) was searched using the BrkA primary amino acid sequence (Met^1-Phe^{1010}) and narrowed by querying domain PD002475. Ovals represent the relative position of domain PD002475 within each peptide sequence and the rectangular boxes represent the conserved β-domain (ProDom assignment PD002217). Protein name, function, bacterial host, and the GenBank accession number are noted. ShdA does not match amino acid scale, denoted by (//). *IcsA is also known as VirG. Figure from Oliver *et al.*, Molec. Micro. 2003.

Due to the automatic compilation of the ProDom database, the boundaries of the ProDom domains can vary with each release of the database as more entries are added to it. Thus, to refine our analysis of domain PD002475, a ClustalW (Thompson *et al.*, 1994) alignment of domain PD002475 from the autotransporter proteins depicted in Fig. 3-2 was performed. As shown in Fig. 3-3A the highest degree of sequence conservation occurs over a region corresponding to residues Thr^{606} – Leu^{702} of BrkA. The predicted secondary structure for this region in these proteins was also highly conserved (Fig. 3-3A).

The list of proteins bearing ProDom PD002475 includes pertactin (Prn). The structure of the pertactin passenger domain has been solved (accession number 1DAB) and shown to be a monomer folded into a single domain that is almost entirely made up of a right-handed cylindrical β-helix (Fig. 3-3B) (Emsley *et al.*, 1996). Given the remarkable degree of primary and secondary structural conservation within ProDom domain PD002475 we decided to examine the known structure of the pertactin passenger domain to gain insights into the tertiary structure of domain PD002475. Residues Val^{472} – Leu^{566} of the pertactin passenger, which correspond to residues Thr^{606} –Leu^{702} of BrkA, are located at the base of the β-helical structure (Fig. 3-3B). Interestingly, residues Glu^{463}-Phe^{470} comprise a loop located at the N-terminus of the conserved region (Fig. 3-3B, denoted by an arrow). This loop region corresponds to residues Ala^{597} – Tyr^{604} of BrkA (Fig. 3-3A).

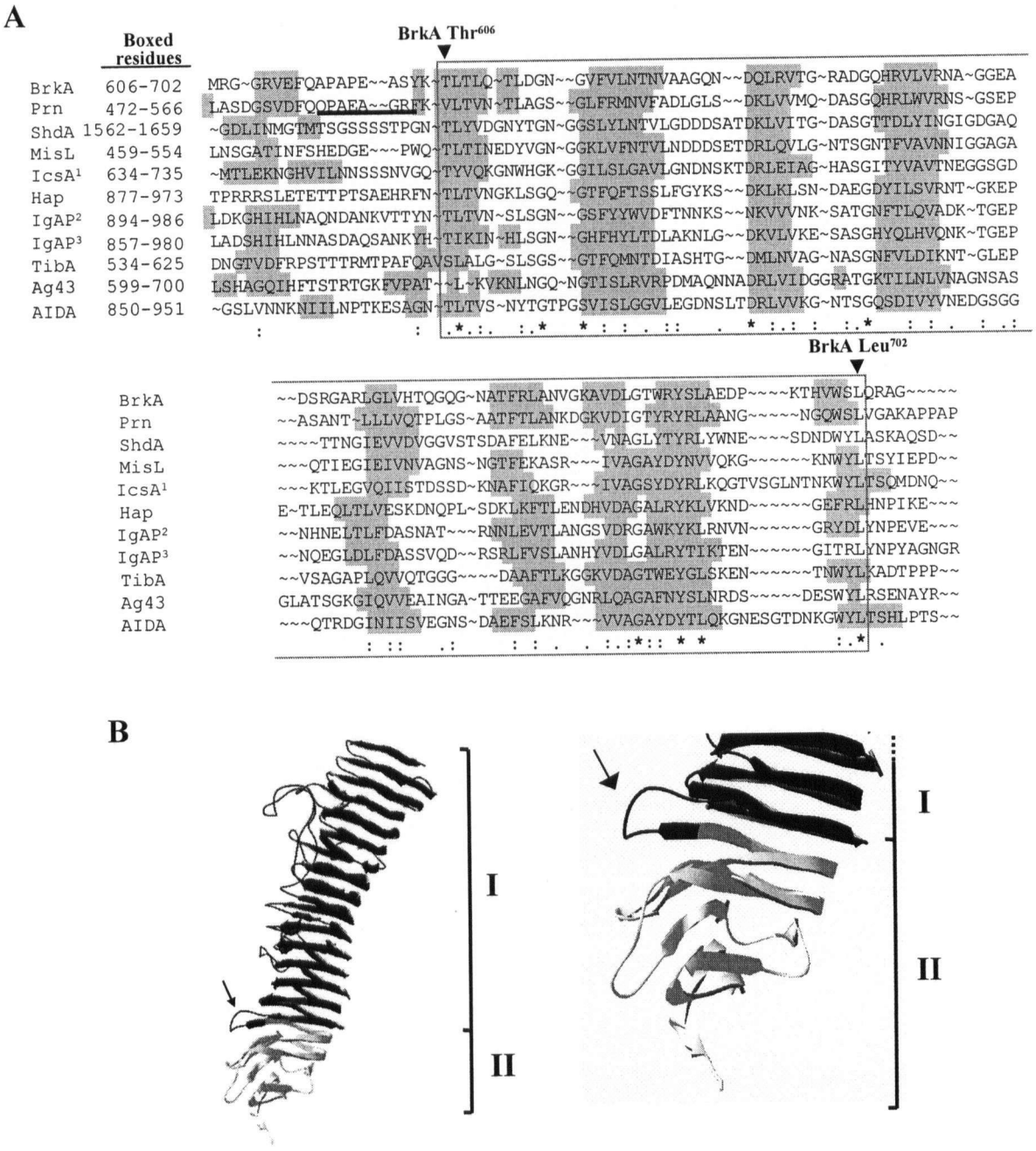

Fig. 3-3. Comparative analysis of the junction region found within several autotransporters.
A. ClustalW alignment of autotransporters depicted in Fig. 2. The position of the amino acids within the boxed region is noted for each protein. Only regions of significant amino acid conservation are shown. (*), >80% identity; (.), >40% identity; (:), >60% similarity. Grey shading denotes regions predicted to form β-sheet structure by the secondary structural prediction program PsiPred. Unshaded regions are predicted to have coil structure. PsiPred scores were assigned at a confidence level of >2. Underlined region of Prn denotes a loop region comprised of residues Gln^{463}-Phe^{470}. [1]Also known as VirG; [2]From *H. influenzae*; [3]From *N. gonorrhoeae*. **B**. Ribbon representation of the 3D structure of pertactin (1DAB) illustrating the relative location and architecture of residues Asp^{35}-Pro^{573}. (I) demarks residues Asp^{35}-Arg^{452}; and (II) demarks residues Leu^{453}- Pro^{573}. Residues Val^{472}-Pro^{573} are shaded grey. Arrow denotes a loop region comprised of residues Gln^{463}-Phe^{470} of Prn. Note, amino acid numbers correspond to GenBank Accession number CAA06900 for pertactin. Left: complete 1DAB structure. Right: Close-up view of regions I and II. Figure from Oliver *et al.*, Molec. Micro. 2003.

3.3.3 *In vivo trans* complementation of BrkA folding

The data indicating that residues Glu^{601}-Ala^{692} are required for stability of the BrkA passenger domain suggested that this region might either serve to prevent unfolding of the passenger, or it might facilitate folding of the passenger domain during secretion. Domain PD002475 is naturally cleaved away from the mature form of the *E. coli* autotransporter AIDA-1 (Benz and Schmidt, 1992), arguing against the notion that it functions to prevent unfolding of the passenger. We thus hypothesized that residues Glu^{601}-Ala^{692} are involved in promoting folding of BrkA. To test this hypothesis we developed an *in vivo* system to assess whether residues Glu^{601}-Ala^{692} are able to restore stability to BrkA (ΔGlu^{601}-Ala^{692}) when expressed in *trans*. Plasmid pDO-JB5 was constructed bearing an in-frame deletion of residues Ala^{52}-Pro^{600} of BrkA. The product expressed from pDO-JB5 includes the BrkA signal peptide (Met^{1}-Ala^{42}) and the BrkA translocation unit (Glu^{693}-Phe^{1010}) (Oliver *et al.*, 2003a) thus enabling export of residues Glu^{601}-Ala^{692} (the putative BrkA junction region) to the bacterial surface. Glu^{601} was chosen as the N-terminal boundary of the BrkA junction region since (i) the level of sequence conservation decreases markedly N-terminal to Thr^{606} (Fig. 3-3A) and (ii) because residues Ala^{597} – Tyr^{604} may represent an exposed loop (Fig. 3-3B) which could serve as a practical linker to construct a fusion that would avoid disrupting the core structure of the protein. Plasmid pDO-JB5 was introduced into *E. coli* strain UT5600. Immunoblot analysis of an over-exposed blot using an antibody that recognizes residues 1-693 of BrkA revealed that BrkA (ΔAla^{52}-Pro^{600}) was expressed (Fig. 3-4B). Several forms of BrkA (ΔAla^{52}-Pro^{600}) were detected that correspond to unprocessed and processed forms of the precursor. Having demonstrated that BrkA (ΔAla^{52}-Pro^{600}) is

expressed, we next asked whether co-expression of BrkA (ΔAla^{52}-Pro^{600}) could rescue the instability of BrkA (ΔGlu^{601}-Ala^{692}) (Fig. 3-1). We first co-transformed *E. coli* strains UT5600 and UT2300 with plasmids pDO-JB5 and pDO6935K representing BrkA (ΔAla^{52}-Pro^{600}) and wildtype BrkA, respectively. Co-transformed clones were grown to an OD_{600} of ~0.8 and whole cell lysates were resolved by SDS-PAGE. BrkA expression was probed by immunoblot. As shown in Fig. 3-4C, processing and expression of wild type BrkA was not affected in either *E. coli* UT5600 or UT2300 strains that were co-transformed with pDO-JB5 and pDO6935K, indicating that BrkA (ΔAla^{52}-Pro^{600}) does not interfere with the expression of wild type BrkA.

We next co-transformed *E. coli* strains UT5600 and UT2300 with plasmids pDO-JB5 and pGH3-13K; the latter encoding the junction-deleted BrkA species. As a negative control, *E. coli* UT5600 and UT2300 were co-transformed with plasmids pBluescript (vector control) and pGH3-13K. In *E. coli* co-transformed with pDO-JB5 and pGH3-13K, a band migrating at approximately 65 kDa corresponding to the cleaved passenger region of BrkA (ΔGlu^{601}-Ala^{692}) was detected in strains UT5600 and UT2300 (Fig. 3-4C). In contrast, in *E. coli* co-transformed with plasmids pBluescript and pGH3-13K the band migrating at approximately 65 kDa was detected in strain UT5600 but not in UT2300. These results indicate that expression of BrkA (ΔAla^{52}-Pro^{600}) is sufficient to produce a stable form of the BrkA (ΔGlu^{601}-Ala^{692}) passenger in *E. coli* strain UT2300, although the level of complementation is not 100%, a result possibility reflecting BrkA (ΔGlu^{601}-Ala^{692}) passenger proteolysis mediated by OmpT occurring concurrently with BrkA (ΔGlu^{601}-Ala^{692}) passenger folding mediated by BrkA (ΔAla^{52}-Pro^{600}). Similar results

were obtained using a co-expression system where the genes coding for BrkA (ΔGlu^{601}-Ala^{692}) and BrkA (ΔAla^{52}-Pro^{600}) were carried on a single plasmid, arguing against the notion that complementation efficiency reflected a difference in plasmid copy number (not shown).

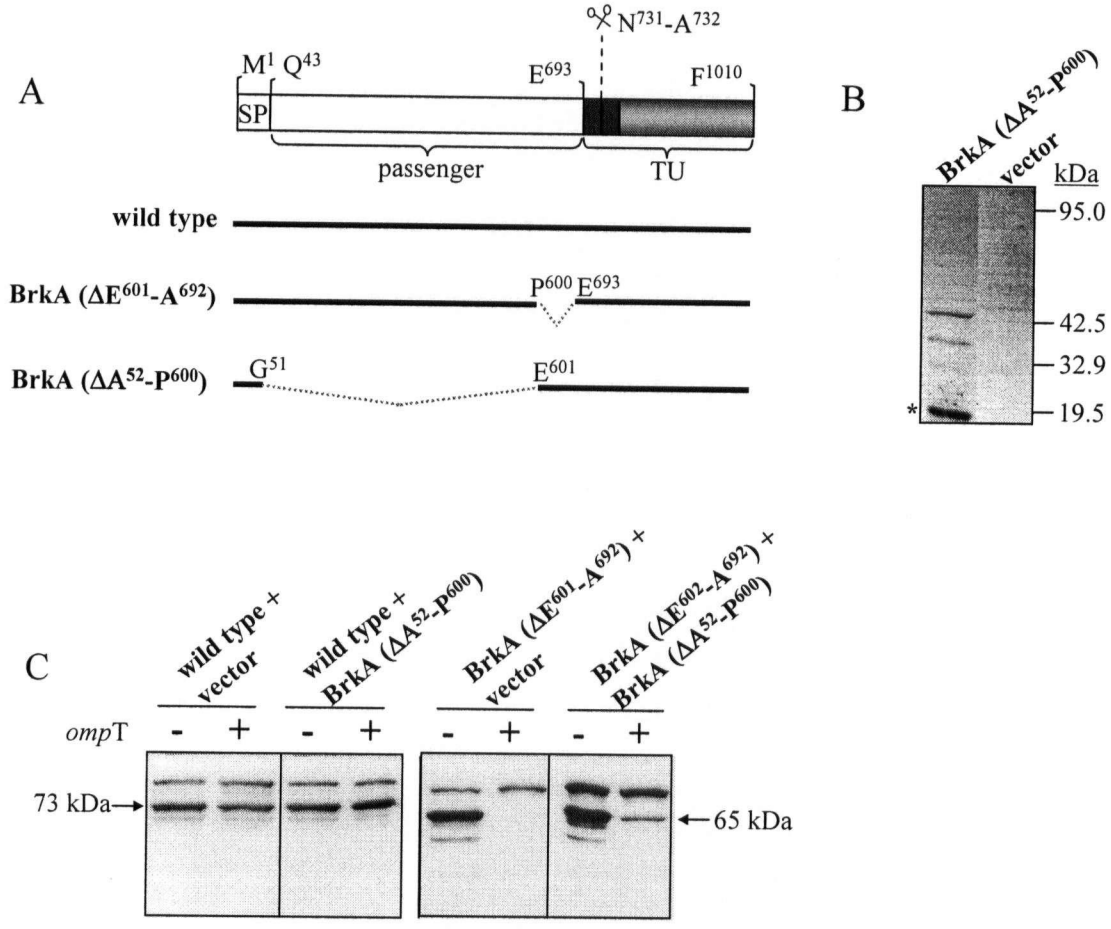

Fig. 3-4. *In vivo trans* complementation of BrkA stability.
A. BrkA domain organization as described in Fig. 3-1A. **B**. Detection of BrkA (ΔA^{52}-P^{600}) expression in *E. coli* strain UT5600. *E. coli* strain UT5600 harboring plasmid pDO-JB5 was grown to 0.8 OD units and harvested by centrifugation. Whole cell lysates were resolved by SDS-PAGE and BrkA expression was probed by immunoblot. The asterisk denotes the band corresponding to the processed passenger domain and the lowest band represents a further cleavage of the passenger. Blots were over-exposed since the deleted clone has only a small fraction of the residues recognized by the antiserum. **C.** Evaluating the effect of BrkA (ΔA^{52}-P^{600}) expression on the stability of wild type BrkA and BrkA (ΔE^{601}-A^{692}) in *E. coli* strains UT5600 (*ompT*$^-$) and UT2300 (*ompT*$^+$). *E. coli* were co-transformed with individual plasmids encoding BrkA variants depicted in Fig. 3-4A. Cells were grown to an OD of 0.8 and harvested by centrifugation. Whole cell lysates were resolved by SDS-PAGE and probed by immunoblot. When present the co-expression of BrkA (ΔA^{52}-P^{600}) was observed in over-exposed blots (data not shown). Experiments were performed 3 times and a representative experiment is shown. Wild type BrkA, BrkA (ΔE^{601}-A^{692}) and BrkA (ΔA^{52}-P^{600}) were expressed from plasmids pDO6935K, pGH3-13K and pDO-JB5, respectively. Plasmid pBluescript was employed as a vector control. Figure from Oliver *et al.*, Molec. Micro. 2003.

3.3.4 *In vivo* evidence demonstrating that residues Glu^{601}-Ala^{692} of BrkA are required for folding of the BrkA passenger

The observation that the stability of the BrkA (ΔGlu^{601}-Ala^{692}) passenger region in *E. coli* strain UT2300 can be rescued by expressing BrkA (ΔAla^{52}-Pro^{600}) as a separate polypeptide within the same cell suggests that the BrkA junction region plays a role in folding of the BrkA passenger domain. To further investigate the role of the BrkA junction region we performed trypsin analyses of BrkA expressed on the surface of *E. coli* strain UT5600 (i.e. in the absence of OmpT). We first performed trypsin accessibility assays to confirm that the 73 kDa and 65 kDa passengers were indeed surface expressed. Cells were exposed to trypsin, washed and whole cell lysates were analysed by immunoblot. Exposure of each clone to trypsin resulted in the removal of the band corresponding to the processed passenger domain indicating that the passenger was exported to the surface (Fig. 3-5A). It is worth noting that co-expression of BrkA (ΔAla^{52}-Pro^{600}) did not affect the surface expression of either wild type BrkA or BrkA (ΔGlu^{601}-Ala^{692}) (Fig. 3-5A).

Having shown that each passenger was accessible to trypsin we performed trypsin susceptibility assays on each of the clones to probe the tertiary structure of surface expressed BrkA. Trypsin susceptibility was assayed by limited proteolysis experiments where cells were exposed to low concentrations (0.01 mg/ml) of trypsin and the stability of each passenger was monitored over time. As shown in Fig. 3-5B, the band corresponding to the 73 kDa processed form of the wild type BrkA passenger domain remained stable following exposure to trypsin indicating that the protein had adopted a

conformation that was resistant to low concentrations of trypsin. Similarly, when BrkA (ΔGlu^{601}-Ala^{692}) was co-expressed with BrkA (ΔAla^{52}-Pro^{600}) a band corresponding to the 65 kDa passenger was also detected after 15 minutes. In marked contrast, when BrkA (ΔGlu^{601}-Ala^{692}) was expressed in the absence of BrkA (ΔAla^{52}-Pro^{600}), the band corresponding to the 65 kDa passenger was not detected following exposure to trypsin. The rapid disappearance of the 65 kDa band indicates that the passenger existed in a conformation exposing multiple trypsin sensitive cleavage sites suggesting BrkA (ΔGlu^{601}-Ala^{692}) had not assumed a folded conformation. It is also worth noting that BrkA (ΔGlu^{601}-Ala^{692}) passenger stability was not complemented in clones co-expressing BrkA mutants lacking residues Glu^{601}-Ala^{692} including BrkA(ΔSer^{229}-Ala^{658}), BrkA(ΔSer^{229}-Ala^{676}), BrkA(ΔSer^{229}-Glu^{693}), from plasmids pGD8, pGD9, pGD10, respectively (not shown).

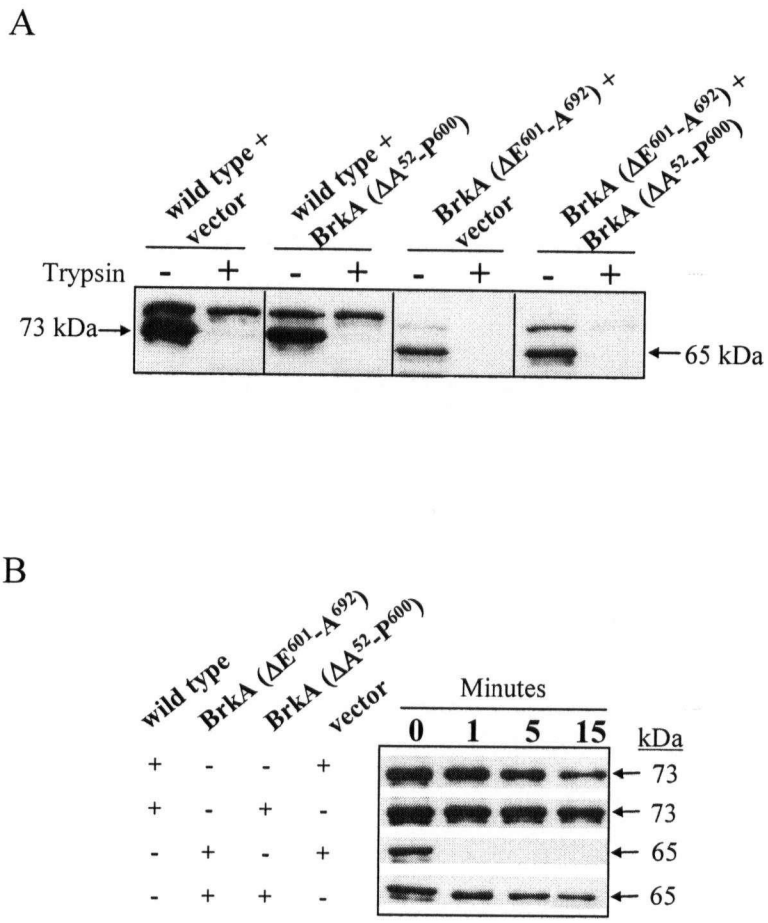

Fig. 3-5. Characterization of surface expressed forms of BrkA by trypsin analysis.
A. Trypsin accessibility analysis of BrkA expression. *E. coli* UT5600 was co-transformed with plasmids encoding the indicated BrkA variants. Cells were grown to an OD of 0.8 and harvested by centrifugation. Surface expressed BrkA was digested with 0.1 mg/ml trypsin and washed as described in the Experimental Procedures. Whole cell lysates were resolved by SDS-PAGE and BrkA expression was assessed by immunoblot. Arrows denote the surface exposed passenger domain of BrkA (wild type) and BrkA (ΔE^{601}-A^{692}), migrating at approximately 73kDa and 65 kDa, respectively. **B.** Trypsin susceptibility analysis of surface exposed BrkA. *E. coli* UT5600 were co-transformed with plasmids encoding BrkA variants indicated on the right. (+) indicates presence of plasmids and (-) indicates absence of plasmid. Cells were grown to an OD of 0.8 and harvested by centrifugation. Cells were exposed to 0.01 mg/ml trypsin and digestion was stopped at various time points (minutes) as described in the Experimental Procedures. BrkA expression was detected by immunoblot. Arrows denote the surface exposed passenger domain of BrkA (wild type) and BrkA (ΔE^{601}-A^{692}), migrating at approximately 73kDa and 65 kDa, respectively. Experiments were performed 3 times and a representative experiment is shown. Wild type BrkA, BrkA (ΔE^{601}-A^{692}) and BrkA (ΔA^{52}-P^{600}) were expressed from plasmids pDO6935K, pGH3-13K and pDO-JB5, respectively. Plasmid pBluescript was employed as a vector control. Figure from Oliver *et al.*, Molec. Micro. 2003.

3.3.5 BrkA (ΔGlu^{601}-Ala^{692}) *trans* complemented *in vivo* yields a proteolytic profile similar to wild type BrkA expressed in *E. coli* and *B. pertussis*

In order to assess the conformation of the *trans*-complemented (trypsin resistant) form of BrkA (ΔGlu^{601}-Ala^{692}) we used immunoblots to compare proteolytic profiles of surface expressed forms of the BrkA passenger following digestion with trypsin, α-chymotrypsin II, or proteinase K. Consistent with our earlier results, BrkA (ΔGlu^{601}-Ala^{692}) was not detected after 5-minutes in the presence of trypsin, α-chymotrypsin II, or proteinase K (Fig. 3-6, lane 1-D). In contrast, digestion of BrkA (ΔGlu^{601}-Ala^{692}) co-expressed with BrkA (ΔAla^{52}-Pro^{600}) resulted in the production of protease specific patterns detected in overexposed immunoblots (Fig. 3-6, lane 2-E, -H and -K). Significantly, the digestion profile of *trans* complemented BrkA (ΔGlu^{601}-Ala^{692}) was similar to the profile of full-length (wild type) BrkA expressed in *E. coli* UT5600 (Fig. 3-6, lane 3 F, I, and L) and in *B. pertussis* (Fig. 3-7A, lane 4). These data indicate that the *trans* complemented BrkA (ΔGlu^{601}-Ala^{692}) passenger adopted a folded conformation similar to the native full-length BrkA passenger.

It is worth noting that a predominant species migrating at approximately 50-55 kDa was observed following digestion with each protease (Figure 3-7A). Given that (i) the BrkA passenger is naturally cleaved between residues Ala^{42}-Gln^{43} and Asn^{731}-Ala^{732} during secretion, and that (ii) the 50-55 kDa species is apparent following digestion of the *trans*-complemented BrkA (ΔGlu^{601}-Ala^{692}) passenger, the existence of an exposed protease sensitive loop region in close proximately to Glu^{600} of the BrkA passenger is probable (Figure 3-7B).

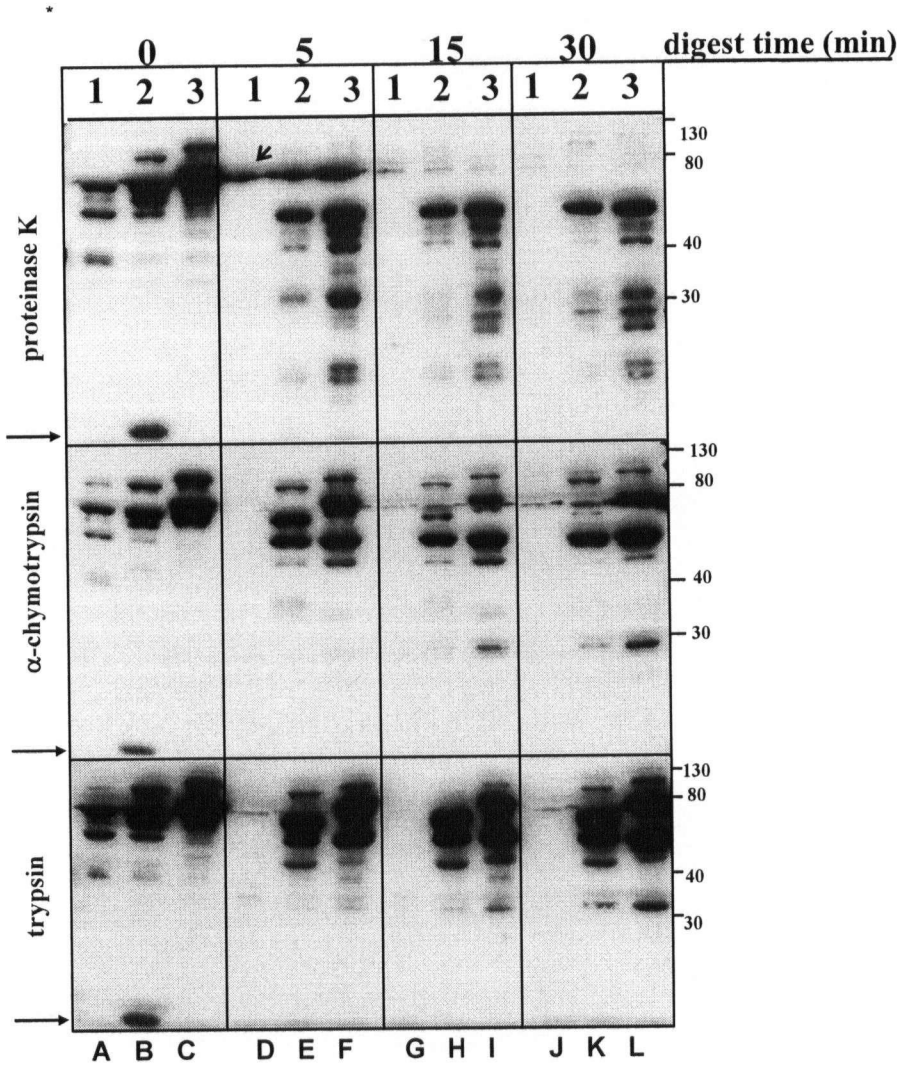

Fig. 3-6. Over exposed immunoblot depicting proteolytic profiles of surface expressed forms of BrkA.
Cells were grown to an OD of 0.8 and harvested by centrifugation. Cells were exposed to 0.1 mg/ml trypsin, α-chymotrypsin or proteinase K and digestion was stopped at the indicated time points (0, 5, 15, 30 minutes). Whole cell lysates were resolved by SDS-PAGE and BrkA expression was detected by immunoblots (15 hour exposure). Lane numbers correspond to cells expressing BrkA (ΔE^{601}-A^{692}) (lane 1), BrkA (ΔE^{601}-A^{692}) and BrkA (ΔA^{52}-P^{600}) (lane 2), and wild type BrkA (lane 3). Notes: Closed arrows denote the processed form of the BrkA (ΔA^{52}-P^{600}). Open arrow (lane D, proteinase K digest) denotes a contaminating band resulting from spillover from lane C. Plasmid pBluescript was employed as a vector control. Molecular weight markers are approximate.

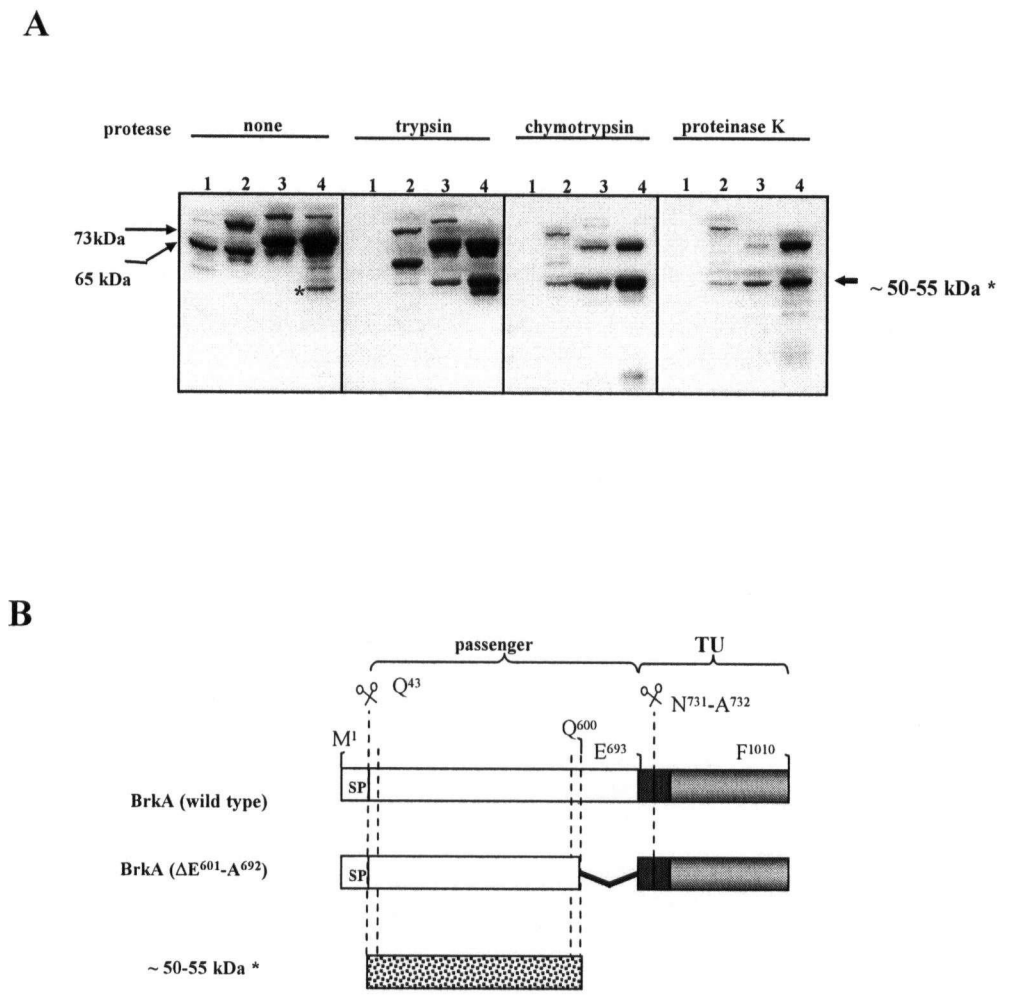

Fig. 3-7. Limited proteolysis of surface exposed BrkA yields a stable 50-55 kDa fragment. A. Proteolytic profiles of surface exposed forms of BrkA expressed in *E. coli* UT5600 and *B. pertussis* strain BP338. Overnight *E. coli* UT5600 clones were grown to an OD of 0.8 and harvested by centrifugation. *B. pertussis* were grown at 37C for 2 days in Bordet-Gengou agar, harvested to an OD of 0.5, and centrifuged. Samples were digested with 0.1 mg/ml trypsin, α-chymotrypsin or proteinase K. Digestion stopped after 30 minutes for samples treated with trypsin and α-chymotrypsin and 5 minutes for samples treated with proteinase K. Whole cell lysates were resolved by SDS-PAGE and BrkA expression was detected by immunoblot. Lane numbers 1, 2, and 3 correspond to *E. coli* UT5600 expressing BrkA (ΔE^{601}-A^{692}) (lane 1), BrkA (ΔE^{601}-A^{692}) and BrkA (ΔA^{52}-P^{600}) (lane 2), wild type BrkA (lane 3). Lane number 4 corresponds to *B. pertussis* strain BP338. Arrows with numbers denote the surface exposed passenger domain of BrkA (wild type) and BrkA (ΔE^{601}-A^{692}), migrating at approximately 73kDa (lane 3 and 4) and 65 kDa (lanes 1 and 2), respectively. 50-55 kDa fragment denoted by arrow/asterisk on right. **B.** Diagram comparing the domain structure and proteolytic cleavage sites of wild type BrkA and BrkA(ΔE^{601}-A^{692}). Black and grey boxes represent the BrkA translocation unit, white box represents the BrkA passenger, and box labeled SP represents the signal peptide. Scissors denote known BrkA cleavage sites between residues A^{42}-Q^{43} and N^{731}-A^{732}. Dotted lines indicate possible cleavage sites. Speckled box denotes putative region corresponding to the ~ 50-55 kDa BrkA proteolytic fragment (asterisk) described in A.

3.3.6 *In vitro* evidence demonstrating that residues Thr^{606}-Val^{699} of BrkA are required for folding of the BrkA passenger

To further investigate the role of the BrkA junction in folding of the passenger domain, we performed *in vitro* structural and functional analyses on refolded, purified recombinant forms of the protein. Expression constructs pDO418, pDO-BRK-H(61-605), and pDO-BRK-(601-707)H were used to over express His-tagged fusion proteins DO418P, BRK-H(61-605)P and BRK-(601-707)HP containing residues (Glu^{61}-Val^{699}), (Glu^{61}-Lys^{605}), (Glu^{601}-Gln^{702}) corresponding to the wild type BrkA passenger, a junction-deleted BrkA passenger, and the BrkA junction region, respectively (Fig. 3-8A). Fusion proteins DO418P and BRK-H(61-605)P include N-terminal 6XHis tags and BRK-(601-707)HP has a C-terminal 6XHis tag (see Table 3-1). Each fusion protein was purified from inclusion bodies under denaturing conditions (8M urea) using nickel affinity chromatography, as previously described (Shannon and Fernandez, 1999) (Oliver *et al.*, 2003a). Purified proteins were renatured by dialyzing them simultaneously against decreasing concentrations of urea in the presence of 0.1% Triton X-100, followed by a final dialysis against 10 mM Tris, pH 8 (Shannon and Fernandez, 1999) (Oliver *et al.*, 2003a). Following dialysis, fusion proteins DO418P and BRK-H(61-605)P remained soluble whereas fusion BRK-(601-707)HP formed a visible precipitate indicative of protein aggregation (Fig. 3-8B, lane 3). Since it was insoluble, BRK-(601-707)HP was excluded from further analyses.

Fusion proteins DO418P and BRK-H(61-605)P were assayed for function. BrkA contributes to *B. pertussis* adherence to both HeLa epithelial cells (Ewanowich *et al.*,

1989) and MRC5 lung fibroblasts (Fernandez and Weiss, 1994), in addition to mediating serum resistance. To determine whether the dialyzed fusion proteins were able to bind host cells we incubated each peptide with HeLa cells and measured binding via flow cytometry analysis using an antibody to the BrkA passenger domain. This antibody recognizes both native and denatured BrkA (Oliver and Fernandez, 2001). As shown in Fig. 3-8C, treatment of HeLa cells with DO418P resulted in a significant increase in fluorescence over the untreated control. In contrast, treatment with BRK-H(61-605)P resulted in a signal that was only slightly above the background levels seen with the untreated control. These results indicate that renatured DO418P bound to HeLa cells well, whereas renatured BRK-H(61-605)P bound poorly. Thus, the information encoded within the region bounded by residues Thr^{606}-Val^{699}, which spans the junction region, is necessary for the production of functional recombinant BrkA.

To gain insights into the structure of dialysed DO418P and BRK-H(61-605)P we used limited proteolysis as a probe of tertiary structure. Exposure to trypsin resulted in a significant and rapid reduction in the band corresponding to BRK-H(61-605)P over time (Fig. 3-8D). In contrast, DO418P remained stable in the presence of trypsin suggesting that the protein had adopted a folded conformation. To characterize the secondary structure of the soluble fusion proteins we employed far-UV circular dichroism spectroscopy. Fusion protein DO418P was shown to have a far-UV CD profile indicative of a protein rich in beta-structure with a minimum at 218 nm (Fig. 3-8E). This far-UV CD profile is consistent with PsiPred secondary structural analysis (McGuffin *et al.*, 2000) that predicts that the BrkA passenger domain is primarily composed of β-sheet. In

contrast, fusion protein BRK-H(61-605)P had a non-structured far-UV CD profile with a minimum at 202 nm (Fig. 3-8E). These data indicate that residues Thr^{606}-Val^{699} of the BrkA passenger are required for folding of the BrkA passenger.

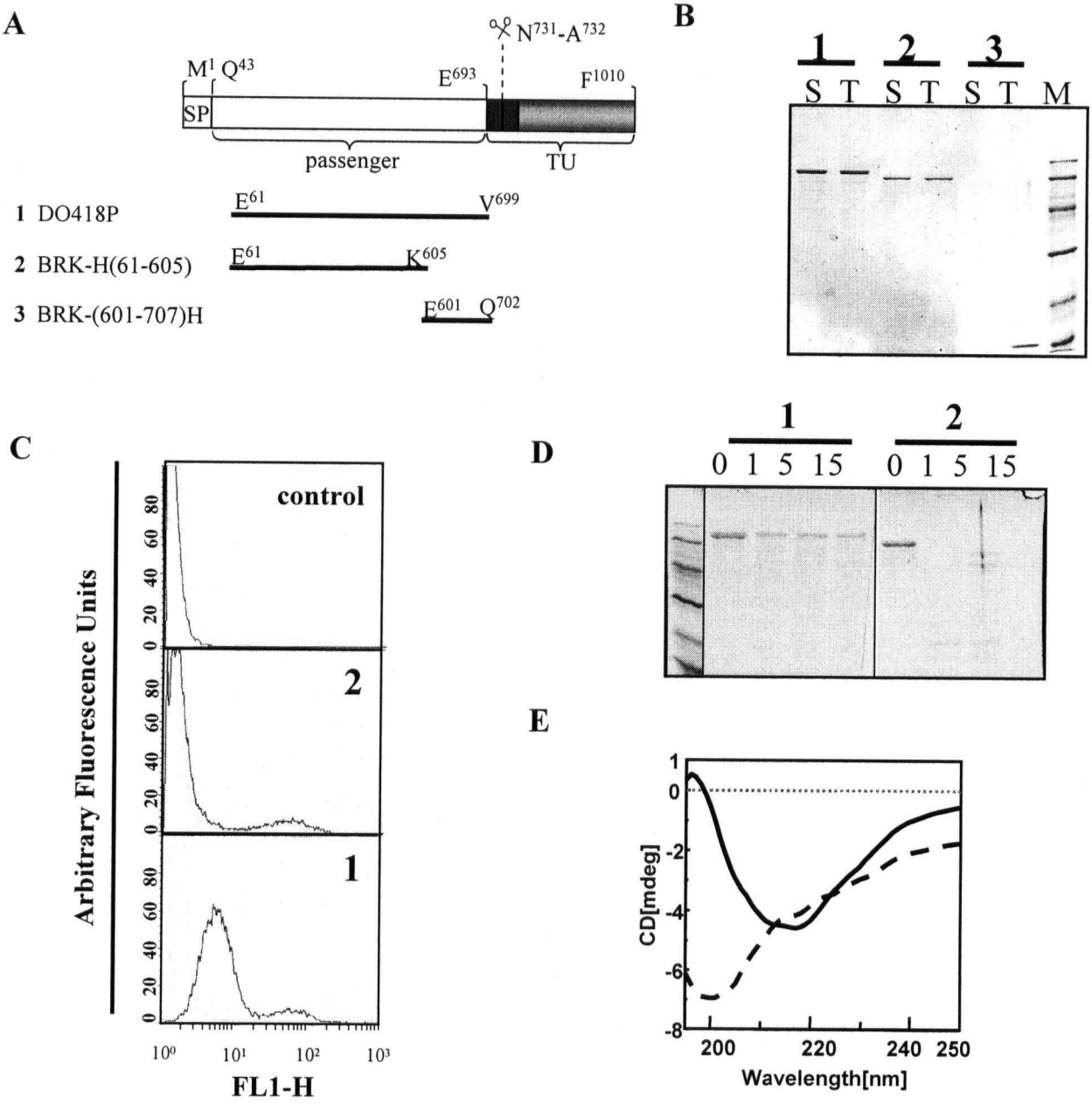

Fig. 3-8. Characterization of refolded BrkA fusion peptides. A. Diagram illustrating positions of fusion constructs compared to primary BrkA sequence. BrkA domain structure is described in Fig. 4-1. **B.** Post-dialysis solubility analysis of fusion proteins. Following dialysis, samples were vortexed and aliquots representing total (insoluble and soluble) protein were removed (lane T). Remaining samples were centrifuged at 4 °C for 30 minutes and an aliquot of the soluble fraction was removed (lane S). Samples were resolved by SDS-PAGE and stained with Coomassie brilliant Blue. **C.** Binding assays for DO418P and rBRK-H(61-605). Equimolar concentrations of fusion proteins DO418P and rBRK-H(61-605) were added to HeLa cells and binding was assessed via flow cytometry. Binding assays were performed as described in the Experimental Procedures. **D.** Protease sensitivity analysis comparing the relative stability of renatured DO418P and rBRK-H(61-605). 7.5ug of dialysed DO418P or rBRK-H(61-605) was digested with trypsin at room temperature. Digestion was stopped at various time points and samples were resolved by SDS-PAGE and visualized by staining with Coomassie brilliant blue (top panel). Densitometry was performed on each lane at positions corresponding to the migration of undigested fusion protein. Density of each band was recorded as arbitrary units and percent recovered was calculated based on arbitrary densitometry units measured for each time point (minutes) relative to time zero. **E.** Far-UV circular dichroism (CD) profiles of DO418P and DO618P. Equimolar amounts of purified DO418P and rBRK-H(61-605) were dialysed against decreasing concentrations of urea into a final buffer of 10 mM Tris, pH 8, and submitted to 10 scans between 195 nm and 250 nm. Solid line, DO418P; dashed line, rBRK-H(61-605).

3.3.7 Purified junction-deleted BRK-H(61-605)P passenger adopts a protease resistant conformation when added exogenously to *E. coli* UT5600 expressing the BrkA "junction" region

Having shown genetically that BrkA(ΔGlu^{601}-Ala^{692}) passenger folding can be complemented when BrkA(ΔAla^{52}-Pro^{600}) is co-expressed in the same cell, we wondered whether folding of a recombinant form of a junction-deleted BrkA passenger could be complemented *in trans*. Since fusion protein BRK-(601-707)HP (encompassing the junction) was prone to aggregation *in vitro*, we employed *E. coli* UT5600 as a vehicle to display the "junction" region at its surface. As shown in Fig. 3-9, the addition of the unfolded BRK-H(61-605)P polypeptide to *E. coli* UT5600 expressing BrkA(ΔAla^{52}-Pro^{600}) resulted in the production of a trypsin resistant moiety migrating at approximately 60 kDa. Significantly, the intensity of the trypsin resistant band increased as the refolding period increased (5 < 15 < 60 minutes) (Figure 3-9, left panel). In contrast, when fusion BRK-H(61-605)P was incubated with *E. coli* UT5600 transformed with the vector control (Fig. 3-9, right panel) or pGH313 (BrkA(Δ601-692)) (not shown) a trypsin resistant band was not detected, even after a 60 minute incubation period. These data provide additional evidence to support the hypothesis that the junction region of BrkA is required for folding of the BrkA passenger. Moreover, this experiment demonstrates that BrkA passenger folding *can* occur at the cell surface.

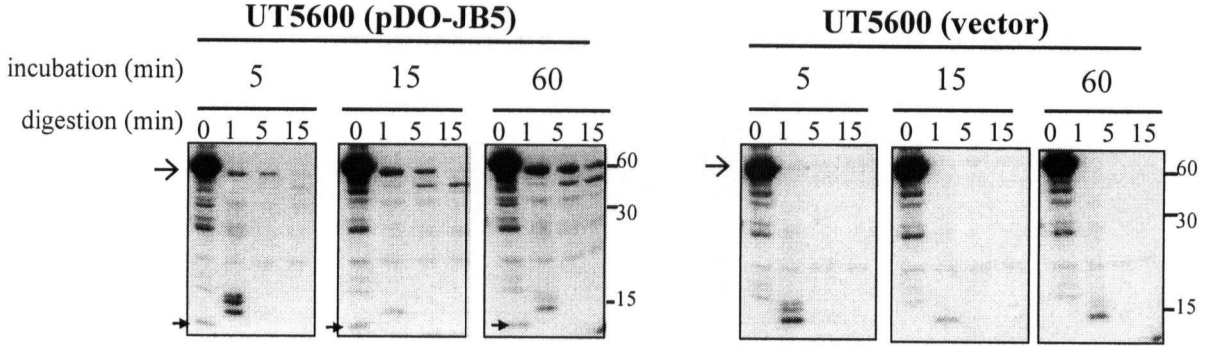

Fig. 3-9 Exogenous addition of recombinant junction-deleted BrkA passenger to *E. coli* UT5600. Recombinant BrkA fusion protein rBrkA-H(61-605) (see Fig. 3-8) was purified under denaturing conditions and dialyzed into 10mM Tris buffer at pH 8.0 (as described in Materials and Methods). Ten microlitres of rBrkA-H(61-605) (200ug/ml) was added to 140ul of *E. coli* UT5600 that had been transformed with either pDO-JB5 (see Fig. 3-4A) or pBluescript vector (control). One millilitre of *E. coli* UT5600 culture (~ 1.0 OD) that were harvested by centrifugation and resuspended in 140uL PBS. rBrkA-H(61-605) folding was assessed by limited trypsin digestion at the indicated time points (5, 15 and 60 minutes) as described in Material and Methods. Closed arrows denote the band corresponding to the junction region in clones transformed with pDO-JB5. Open arrows denote the band corresponding to rBrkA-H(61-605).

3.3.8 Summary of BrkA fusion protein refolding studies

Over the course of these studies a number of BrkA fusion protein variants bearing truncations of the N- or C-terminus of the passenger were constructed, purified, refolded and analysed. The results of these analyses are summarized in Table 3-2. First, following dialysis BrkA fusion proteins bearing C-terminal deletions of the passenger (A, B, C, D, and E) remained soluble whereas fusion proteins bearing N-terminal deletions (G, H, and I) precipitated from solution over time. Notably, fusion protein F, truncated at both the N- and C-termini, remained soluble following dialysis. We examined the structure and function of each of the soluble fusion proteins (A, B, C, D, E, F). Fusion proteins A, B, and C: (*i*) were resistant to limited trypsin digestion, (*ii*) had far-UV CD profiles indicative of a peptide rich in β-structure (minimum at 218 nm), and (*iii*) bound HeLa cells. In contrast, fusion proteins D, E, and F: (*i*) were sensitive to limited trypsin digestion, (*ii*) had far-UV CD profiles indicative of an unstructured peptide (minimum at 200 nm), and (*iii*) did not bind HeLa cells. Taken together these data demonstrate that information encoded within residues Lys^{608}-Lys^{680} is required for folding of the BrkA passenger. The observation that fusion proteins bearing N-terminal truncations (G, H, I) precipitate following dialysis suggests that information encoded within the N-terminus of the passenger is required for *in vitro* solubility under the conditions tested. Significantly, the observation that fusion protein I (Leu^{298}-Phe^{595}), which is truncated at both the C- and N-terminus, remained soluble and unfolded suggests that initiation of folding mediated by the C-terminal region (Lys^{608}-Lys^{680}) is required for aggregation. Taken together these data support a model where (i) BrkA (Lys^{608}-Lys^{680}) encodes information required

to initiate passenger folding and (ii) that information encoded with the N-terminus of the passenger is required to prevent off-pathway aggregation, once folding has been initiated.

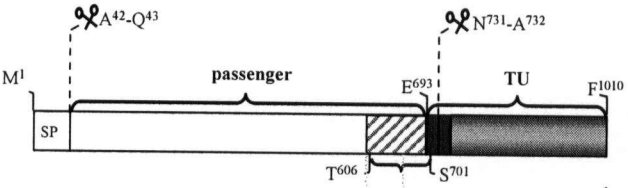

Code		residues	MW (kDa)	solubility (10mM Tris pH 8.0)	trypsin^R	CD minimum (nm)	Tm (Δ_{218nm})	function (binding)
A	(6XH)-	E^{61}-Q^{707}	69.6	+	+	218	62.8	+
B	(6XH)-	E^{61}-V^{699}	68.0	+	+	218	62.8	+
C	(6XH)-	E^{61}-K^{680}	66.6	+	+	218	62.8	+
D	(6XH)-	E^{61}-K^{605}	58.1	+	-	200	na	-
E	(6XH)-	E^{61}-D^{534}	51.6	+	-	200	na	-
F	(6XH)-	L^{298}-F^{595}	38.8	+	-	200	na	-
G	(6XH)-	L^{257}-V^{699}	48.6	-	na	na	na	na
H	(6XH)-	I^{534}-V^{699}	22.0	-	na	na	na	na
I	(M)- -(6XH*)	E^{601}-Q^{707}	13.0	-	na	na	na	na

Table 3-2. Summary of characterization studies of dialyzed BrkA fusion proteins. Each fusion protein was expressed, purified, refolded and analyzed as described in Figure 3-8 and in Material and Methods. Top: BrkA domain structure as described in Figure 3-1. Grey dotted lines demark the boundaries of the region required for BrkA passenger folding. 6XHis denotes an 46 residue tag included in fusion proteins A-H (MHHHHHHSSGLVPRGSGMKETAAAKFERQHMDSPDLGTDDDDKAMA--). 6XHis* denotes a 13 residue tag included in fusion protein I (--KLAAALEHHHHHH). Fusion proteins corresponding to codes A, B, C, D, E, F, G, H, and I were expressed from plasmids pBRK-H(61-707), pDO418, pBRK-H(61-680), pBRK-H(61-605), pDO618, pRF1071, pDO718, pDO518, and pBRK-(601-707)H, respectively. Notably, since the completion of these experiments, Dr. Lily Zhao (Fernandez laboratory) has produced a number of BrkA passenger fusion proteins lacking His-tags that have the same characteristics as the His-tag fusion proteins described in this study. (na) not available

3.3.9 Residues Ala^{681}-Gln^{707} are not required for BrkA passenger folding or stability

Despite being highly conserved in many autotransporters (see Fig. 3-3), residues Ala^{681}-Gln^{707}, corresponding to the C-terminus of the BrkA junction, were not required for folding or function of the BrkA passenger *in vitro* (Table 3-2). Moreover, deletion of residues Ala^{681}-Gln^{707} did not influence the melting profile and transition midpoint (62.8C) of refolded BrkA passenger (Table 3-2) (Figure 3-11A and B) suggesting that this region does not comprise an integral part of the BrkA passenger structure. Consistent with this notion, examination of the crystal structure of pertactin (1DAB) and a structural model of BrkA(Leu^{485}-Leu^{702}) (Appendix, Fig A-1 and A-2), reveals that residues Ala^{681}-Gln^{707} form what appears to be a sub-domain extending from the C-terminus of the β-helix. A possible role for this conserved region is discussed below in Section 3.5.3.

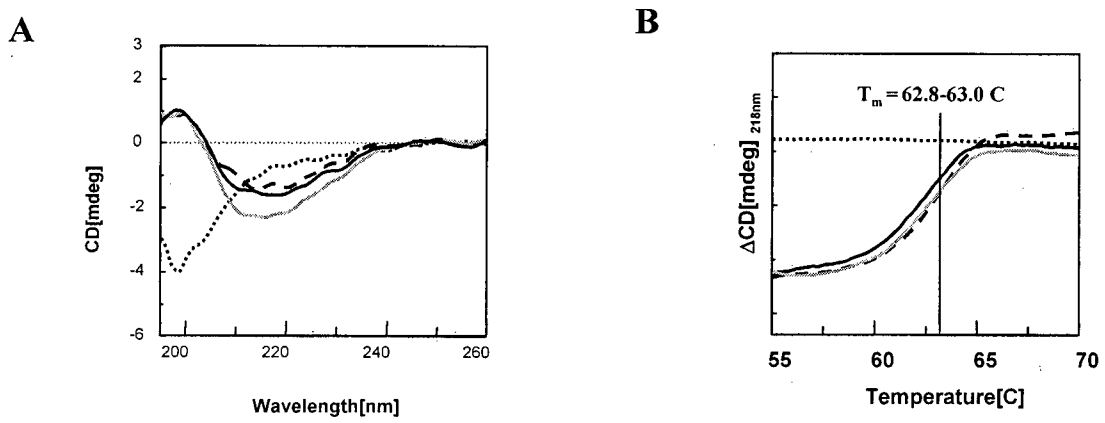

Figure 3-10. Residues K^{680}-Q^{707} are not required for BrkA passenger folding or stability.
A. Far-UV circular dichroism analysis of fusion proteins BrkA-H(E^{61}-Q^{707}), BrkA-H(E^{61}-V^{693}), BrkA-H(E^{61}-K^{680}) and BrkA-H(E^{61}-D^{534}) (see Fig. 3-9) that were expressed from plasmids pBRK-H(61-707), pDO418, pBRK-H(61-680), pDO618, respectively. B. Thermal denaturation profiles of proteins described in (A) measured as a shift in elipticity at 218 nm over 20 °C to 80 °C at a ramp rate of 1 °C per minute. The transition midpoints (T_m) was determined using the Jascow 810 spectrum analysis software. Grey line, BrkA-H(E^{61}-Q^{707}); black line, rBrkA-H(E^{61}-V^{693}); dashed black line, BrkA-H(E^{61}-K^{680}); and dotted black line, BrkA-H(E^{61}-D^{534}). Fusion proteins were expressed and purified as described in Material and Methods.

3.3.10 Co-expression of the pertactin junction (Phe^{470}-Ser^{607}) complements BrkA(ΔGlu^{601}-Ala^{692}) passenger folding

The observation that folding of a junction-deleted BrkA passenger is complemented when co-expressed in, or when added exogenously to, cells surface expressing BrkA(ΔAla^{52}-Pro^{600}) is strong evidence to support the hypothesis that information encoded within Glu^{601}-Ala^{692} of BrkA (domain PD002475) is required for passenger folding. The presence of domain PD002475 in other autotransporters suggests that the function of this region is conserved. To test whether passenger folding is a conserved function of this domain, we asked whether the corresponding region of pertactin would *trans* complement BrkA (ΔGlu^{601}-Ala^{692}) passenger folding. As shown in Figure 3-12B, pertactin and BrkA share 45% identity, 55% similarity over residues Phe^{461}-Asn^{631} and Phe^{595}-Asn^{731}, respectively. Chimeras were constructed in which the region corresponding to the BrkA junction in construct pJB5 (BrkA (ΔAla^{52}-Pro^{600})) was replaced with the corresponding region of pertactin (Fig. 3-12, A and B). As shown in Figure 3-11, two variants were generated that differ at the C-terminus of the pertactin insert; construct pDO-Prn-J2 encodes an additional 51 amino acid proline-rich region whereas pDO-Prn-J1 does not. *E.coli* UT5600 was co-transformed with pBrkA (ΔGlu^{601}-Ala^{692})BBR and either pDO-Prn-J1, pDO-Prn-J2, pDO-JB5 or pBluescript; the latter two constructs serving as positive and negative controls, respectively (Fig. 3-12A). For each clone, the stability of the 65 kDa BrkA(ΔGlu^{601}-Ala^{692}) passenger was assessed by limited digestion with trypsin and detected by immunoblot. It is worth noting that BrkA (ΔGlu^{601}-Ala^{692}) was expressed from pBrkA (ΔGlu^{601}-Ala^{692})BBR which was constructed using pBBR1MCS (Kovach *et al.*, 1994), a medium-copy, broad host-range plasmid that

is compatible with plasmids bearing a colE1 origin of replication. This vector was employed to create a more versatile (e.g. broad host range, replication compatible) expression system for future studies.

As shown in Fig. 3-12C, transformation with plasmid pDO-Prn-J1, pDO-Prn-J2, or BrkA(ΔAla^{52}-Pro^{600}) resulted in the production of a trypsin resistant 65kDa form of BrkA(ΔGlu^{601}-Ala^{692}). In contrast, the 65-kDa BrkA(ΔGlu^{601}-Ala^{692}) passenger was completely digested after 1-minute in clones transformed with a vector control (Fig. 3-12C). Thus, the region of pertactin bounded by Phe^{470}-Ser^{607} (fused to the BrkA translocation unit) is able to *trans* complement folding of the BrkA(ΔGlu^{601}-Ala^{692}) passenger, supporting the hypothesis that passenger folding mediated by this region is conserved, at least between closely related autotransporters. It is also worth noting that the inclusion of the polyproline region located at the C-terminus of the pertactin junction region (residues Val^{567}-Pro^{601}) did not influence passenger folding, indicating that the location of the junction (within the primary sequence) relative to the α-helical linker region is not critical for BrkA(ΔGlu^{601}-Ala^{692}) passenger folding.

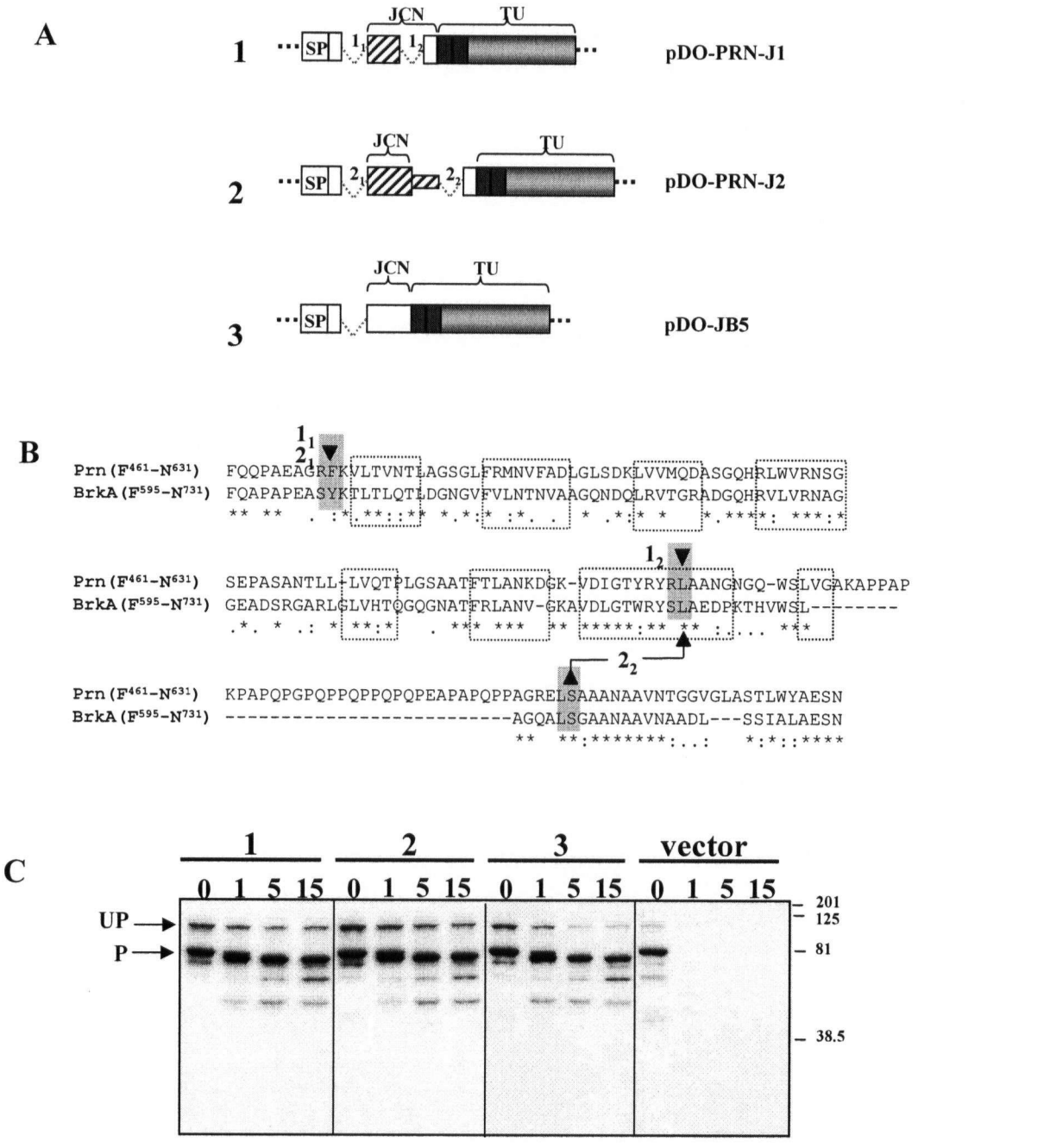

Fig. 3-11 Expression of the pertactin junction region fused to the BrkA translocation unit complements BrkA(ΔE^{601}-A^{692}) passenger folding *in trans*.

A. Diagram of constructs encoding the BrkA or pertactin junction regions. Black and gray boxes denote BrkA linker and β-core regions, respectively; white box denotes BrkA passenger sequence; hatched box denotes pertactin passenger sequence; white box labeled SP denotes BrkA signal peptide. JCN indicates region corresponding to junction region (PD002475) and TU denotes boundaries of BrkA translocation unit. Fusion boundaries denoted 1_1, 1_2, 2_1, 2_2 correspond to alignment boundaries shown in B. **B.** Pairwise sequence alignment of Prn(F^{461}-N^{631})and BrkA(F^{595}-N^{731}) : sequences share 45% identity and 55% similarity. Asterisks (*) denote identical residues and (.) and (:) denote conserved residues. Dotted boxes indicate β-strands corresponding to the pertactin structure 1DAB and predicted by PsiPred. Construct fusion region are denoted by 1_1, 1_2, 2_1, 2_2(compare to A). **C.** Trypsin susceptibility analysis of surface exposed BrkA. *E. coli* UT5600 was co-transformed with pGH3-13K and pDO-JB5 (3), pDO-PRN-J1 (1), pDO-PRN-J2 (2), or pBluescript. Surface exposed BrkA was probed using limited trypsin digestion and detected by immunoblot of whole cell lysates that had been resolved by SDS-PAGE. Unprocessed full-length and processed forms of BrkA(Δ601-692) are denoted (UP) and (P), respectively. Molecular weight markers are approximate.

3.4 Discussion

Here we identify a conserved domain located at the C-terminus of the BrkA passenger region. This junction region is found in a functionally diverse group of proteins known or predicted to be autotransporter proteins suggesting that it performs a general role in secretion.

3.4.1 The BrkA junction region mediates folding of the BrkA passenger domain

We have shown that the BrkA junction, defined as residues Glu^{601}-Ala^{692}, confers stability to the BrkA passenger domain. Deletion of residues Glu^{601}-Ala^{692} rendered the protein susceptible to proteolysis by the outer membrane proteases OmpP and OmpT, and by trypsin. Consistent with this *in vivo* data, BrkA passenger domain fusion proteins bearing a deletion comprising the BrkA junction were non-functional in an adherence assay and were also highly susceptible to proteolysis by trypsin. Furthermore, we demonstrated that BrkA fusions that lacked the junction region had a far-UV CD profile indicative of an unfolded protein. Collectively, these data suggest that the BrkA junction is important for folding of the BrkA passenger domain.

An indication as to how the junction region might effect folding has come from an analysis of the folding behaviour of fusion proteins encompassing or lacking the junction region. Fusion protein BRK-H(61-605)P, representing a junction-deleted passenger (Glu^{61}-Lys^{605}), remained soluble and unfolded following dialysis; however fusion protein BRK-(601-707)HP (Glu^{601}-Gln^{707}) which encompasses the junction precipitated following dialysis, suggesting that folding of the protein had been initiated but resulted in

an off-pathway (misfolded) aggregate. This interpretation is further supported by the observation that (*i*) fusion proteins bearing N-terminal deletions up to residue Ala^{600} were prone to aggregation, (*ii*) fusion proteins bearing C-terminal deletions up to residue Ala^{681} remained soluble and folded and (*iii*) a fusion protein truncated at both termini (including the junction) remained soluble and unfolded. Taken together these data support the hypothesis that information encoded within residues Thr^{606}-Lys^{680} is necessary to initiate or trigger folding of the BrkA passenger. Moreover, these data indicate that residues Thr^{606}-Lys^{680} are sufficient for passenger folding (i.e. the β-domain is not essential). However, this does not rule out the possibility that the BrkA β-domain or other factors within or associated with the outer membrane (e.g. lipopolysacharride, Omp85) might participate in the folding process *in vivo*.

The fact that the junction region engineered to be surface expressed, could rescue the instability of (*i*) a mutant lacking Glu^{601}-Ala^{692}, when provided in *trans* via co-transformation (Fig. 3-5), and (*ii*) a fusion protein encoding residues Glu^{61}-Lys^{605}, that was added exogenously to the cell surface (Fig. 3-9), is strong evidence that the junction region serves an intramolecular chaperone-like role to catalyze folding of the BrkA passenger. Although *in vitro* attempts to refold fusion protein BRK-(601-707)HP resulted in the formation of insoluble aggregates, possibly by exposing reactive β-strands (Richardson and Richardson, 2002), anchoring of the junction region on the bacterial surface via the translocation unit may have served to circumvent aggregation between junction regions thereby allowing *trans* complementation to occur.

The observation that co-expression of the pertactin junction region (Phe^{470}-Ser^{607}) *trans* complemented folding of the BrkA passenger provides experimental evidence to support the hypothesis that folding mediated by this region is conserved, at least between closely related autotransporters. Further, structural modeling of the BrkA passenger domain implies a β-helix fold (see Appendix Section A-1) similar to pertactin suggesting that the mechanism of folding would be similar between these two proteins. Inspection of the BrkA(Leu^{475}-Leu^{702}) model and the pertactin(Ala^{349}-Lys^{570}) structure (1DABA), indicates that the experimentally defined folding region BrkA(Thr^{606}-Lys^{680}) includes four β-strands that form two-rungs at the C-terminus of the β-helix. Interestingly, many of the conserved residues within this region (BrkA Thr^{606}-Lys^{680}) are oriented toward the interior of the structure forming a hydrophobic core or are located in turns (e.g. Gly^{616}, Asp^{630}, Gly^{640}) suggesting that the overall fold may be important. Given these observation, it is tempting to speculate that the "junction" region might represent a folding nucleus that undergoes local hydrophobic collapse to produce a structural scaffold (i.e. two rungs) upon which the N-terminal polypeptide folds vectorially from C- to N-terminus. Assuming the final structure is a β-helix (discussed below), a network of inter-rung hydrogen bonds and an elongated hydrophobic core of stacked or aligned residues would stabilize the final structure (Emsley *et al.*, 1996) (Jenkins *et al.*, 1998). From a structural perspective, initiating folding from a terminal nucleation point may ensure proper in-register folding of the β-helix. In this regard, other rod-like proteins, such as collagen (Frank *et al.*, 2003) and T4 fibritin (Letarov *et al.*, 1999), have been shown to employ nucleation domains to initiate folding and assembly. From a more

biological perspective, the presence of a local folding nucleus could be important for regulating passenger folding during secretion (discussed below).

3.4.2 The role of the junction in BrkA secretion

Figure 3-13 depicts a model of BrkA secretion, taking into account previous models (Henderson *et al.*, 1998) (Klauser *et al.*, 1993b) (Ohnishi and Horinouchi, 1996) and incorporating the data presented here. Using the mechanism of porin biogenesis as an analogy (Tamm *et al.*, 2001) (Kleinschmidt, 2003), it is proposed that following the Sec-dependent transit of BrkA through the inner membrane, the β-domain folds into a β-barrel conformation in the outer membrane. The passenger domain remains unfolded as it transits through the channel (Shannon and Fernandez, 1999) and folding, using the junction region as a scaffold, begins vectorially in a C- to N-terminal direction on the bacterial surface as the passenger emerges from the β-domain channel. Although we depict the passenger domain of BrkA as an unfolded intermediate, and the transporter domain as a monomer, the possibility that BrkA could adopt a partially-folded conformation within the periplasm, and that the channel could itself be a multimer (Veiga *et al.*, 2002) or even formed by another protein (Oomen *et al.*, 2004), should not be excluded. In any case, two key questions in this model are: does protein folding occur on the bacterial surface, and if so, how does the protein maintain an unfolded or partially-folded state in the periplasm?

We have shown that the junction region is necessary for folding of the BrkA passenger (Figs. 3-5 and 3-10) and that surface expression can occur in its absence (Fig. 3-1B and 1C). The fact that we can detect an unfolded BrkA passenger on the surface of an OmpT deficient strain (UT5600) (Fig. 3-1) indicates that folding is not a prerequisite for translocation, and that the unfolded BrkA passenger survived its stay in the periplasm.

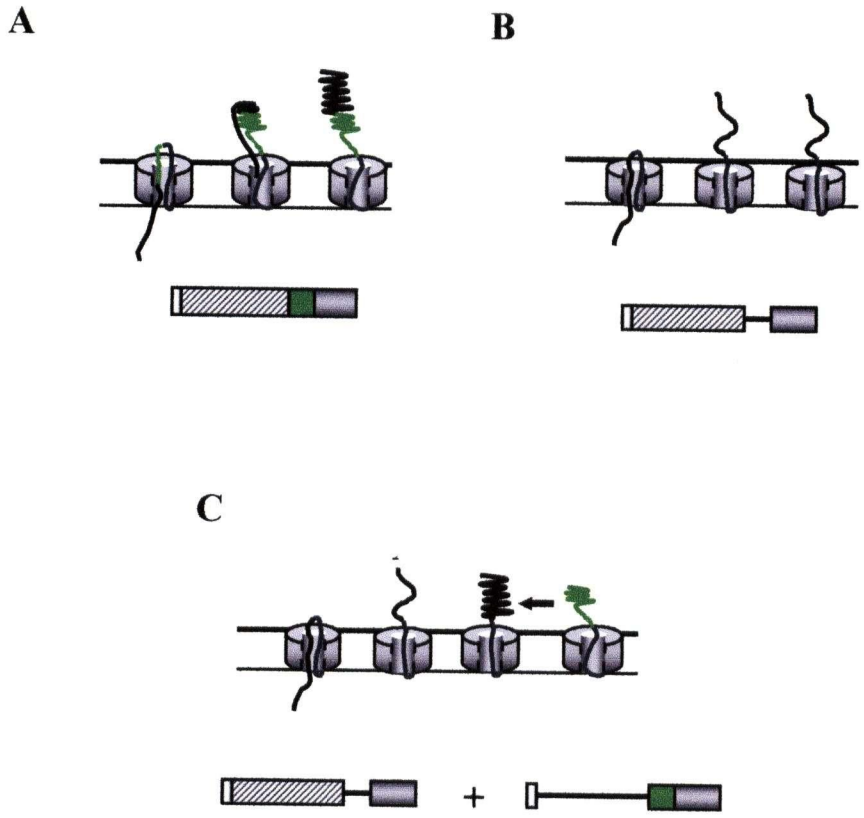

Fig. 3-12. Model of BrkA secretion: the role of the "junction" region in promoting BrkA passenger folding concurrent with or following translocation across the outer membrane.
Translocation unit (linker + β-core) (grey); junction (green); passenger (dark blue); signal peptide (white). Note: folded passenger represented by scribbled line. **A.** Wild type BrkA secretion. (*i*) Following export into the periplasm and cleavage of the N-terminal signal peptide, the 30 kDa β-domain folds into the outer membrane forming an amphipathic β-barrel. (*ii*) The alpha helical linker region initiates translocation of the passenger domain across the outer membrane. Although depicted as an unfolded intermediate, it is possible that the passenger domain may exist in a partially-folded conformation in the periplasm. (*iii*) The passenger domain is translocated across the outer membrane in an unfolded or 'translocation-competent' state. (*iv*) Following export, or possibly concurrent with translocation onto the cell surface, the junction region acts as a scaffold to trigger folding of the passenger domain. Cleavage of the BrkA passenger is mediated by an unknown protease (in an OmpT independent manner) and the passenger remains non-covalently associated with the bacterial surface. A monomeric channel is shown but it is possible that the channel may be oligomeric. **B.** Secretion of a junction deleted (unfolded) BrkA passenger. **C.** Hypothetical interpretation of *trans* complementation of BrkA passenger folding mediated by the BrkA junction region.

Based on the proposed channel size (1 - 2 nm) (Veiga *et al.*, 2002) (Oomen *et al.*, 2004) (Shannon and Fernandez, 1999) (Lee and Byun, 2003), the translocation-competent state of the passenger domain is likely to comprise an unfolded or partially folded intermediate (Jacob-Dubuisson *et al.*, 1999; Klauser *et al.*, 1992; Konninger *et al.*, 1999; Paschen *et al.*, 2003; Pohlner *et al.*, 1987; Schleiff *et al.*, 2003; Thanassi *et al.*, 1998). If the assumption that the BrkA passenger transits through the channel in an unfolded conformation is correct (Shannon and Fernandez, 1999), the fact that the junction is not necessary for transit implies that the junction may be responsible for initiating folding of the BrkA passenger following translocation across the outer membrane. Indeed, the susceptibility of unfolded proteins (Fig. 3-1) to outer membrane proteases such as OmpT (Grodberg and Dunn, 1988) makes it essential that the nascent passenger domain adopts a folded conformation while or shortly after it emerges from the channel. The observation that a purified BrkA passenger lacking the junction region folds when added exogenously to the surface of cells expressing the junction region supports this hypothesis (Figure 3-9). Further, Ohnishi *et al* reported that in the absence of the PrtS junction region, passengers could be surface expressed using the PrtS translocation unit but limited (*i.e.* 4-25%) functional activity was only evident when the junction region was supplied as an outer membrane protein extract in *trans* (Ohnishi *et al.*, 1994). Our *in vivo* complementation experiments corroborate these data. In these experiments, both the junction region itself and the junction-deleted passenger were engineered to be surface expressed using the BrkA signal peptide and translocation unit. Using this system we show that the junction-deleted species is capable of being exported albeit in a protease-

sensitive unfolded conformation. A surface-exposed, protease-resistant species would arise if complementation by the junction region occurred on the surface. In order for complementation to occur, it is reasonable to assume that the junction region and the junction-deleted proteins were in close proximity on the bacterial surface (Fig 3-13C). The model put forth by Veiga *et al* depicting the IgA protease β domain as forming a channel made of multimers (Veiga *et al.*, 2002) seems to support such a scenario, this point is revisited in the next chapter.

3.4.3 Other functions of the junction

We have argued that one function of the BrkA junction region (PD002475) is to promote passenger following (or possibly concurrent with) translocation onto the cell surface. *In vitro* analyses indicate that the folding activity (since coined "autochaperone" activity (Desvaux *et al.*, 2004)) resides near the N-terminus of the junction within a region bounded by residues Thr^{606}-Lys^{680}. However, we have not directly addressed other possible functions *or* regions (i.e. residues 681-702) of the junction during secretion. Recently Velarde and Nataro (2004) have performed a detailed structure-function analysis focusing on the role of the C-terminal region of the *E. coli* autotransporter EspP α-domain. This study revealed two functions of the EspP junction region (residues 880-955) that are related to secretion.

The junction region promotes secretion efficiency

Using a dual epitope (Myc and 6XHis) reporter as a passenger, it was shown that N-terminal deletions into the EspP junction region result in a graded decrease in the level of

secreted reporter. These deletions however, did not result in a decrease in the level of cleaved EspP β domain in outer membrane fractions suggesting that the secretion defect is independent of β domain insertion. We see a similar effect on BrkA expression in constructs bearing deletions of its junction region. Although we cannot accurately compare expression levels of different deletion mutants using a polyclonal antibody, we estimate the level of BrkA(Δ600-693) expression to be about 50-70% that of wild type BrkA. Further, we have qualitatively observed a decrease in passenger expression levels when residues 1-229 of BrkA were fused to processive deletions of the BrkA junction (Chapter 2, Fig. 2-7). Maurer *et al.* reported a similar trend when deletions of the AIDA-I junction region were made (Maurer *et al.*, 1999). Thus, although the junction region is not essential for passenger surface expression, it appears to have a role in facilitating efficient secretion. How does the junction region facilitate efficient secretion? Deletion of the EspP or BrkA junction regions does not affect β domain insertion suggesting that the secretion defect reflects passenger proteolysis occurring during transit through the periplasm or translocation across the outer membrane (following insertion of the β barrel), which could be a function of (i) the folding state of the passenger (i.e. an unfolded passenger would be protease susceptible), and/or (ii) the rate at which the protein passes through this compartment (i.e. slower secretion would increase exposure time to proteases). Velarde and Nataro (2004) observed a decrease in secretion efficiency using a small heterologous epitope passenger fused to EspP, suggesting that role of the junction in promoting secretion efficiency is probably not linked to the folding state of the passenger itself. Further, Brandon and Goldberg (2001) have measured the kinetics of IcsA secretion and shown the soluble periplasmic step is short-lived whereas the outer

membrane translocation step is rate limiting. Given these observations it is probable that the junction region increases secretion efficiency by facilitating translocation across the outer membrane. (This point is discussed further below.)

The C-terminal region of the junction is required for efficient secretion full-length "folding competent" native passengers

A region at the C-terminus of the autotransporter EspP was identified that is necessary for efficient secretion of its full-length passenger, but not of a heterologous reporter (Velarde and Nataro, 2004). Closer analysis, using site directed mutants, revealed a number of hydrophobic residues between amino acids 933 and 955 of the EspP junction that are critical for efficient secretion of the full-length EspP passenger. This region of EspP was coined the "hydrophobic secretion facilitator" (HSF) domain (Velarde and Nataro, 2004).

Again, these findings are consistent with our current understanding of BrkA secretion. Interestingly however, we have arrived at a similar result via an independent path, which may shed additional light on the function of this region. As mentioned, we have localized the region required for BrkA passenger folding to residues Thr^{606}-Lys^{680}, located at the N-terminus of domain PD002475. However, despite being highly conserved, we found that the C-terminal region of domain PD002475 (residues Ala^{681}-Glu^{707}) is not required for folding or stability of the BrkA passenger *in vitro* (Fig. 3-10). On the other hand, the conservation of this region (BrkA Ala^{681}-Glu^{707}) in a wide variety of autotransporters suggests that it plays a role in secretion (Fig. 3-3).

We hypothesized that information encoded within region Ala^{681}-Gln^{707} might be important for secretion of a "folding competent" passenger (as opposed to an unfolded passenger). This hypothesis was based on the following rationale. First, although this region overlaps slightly with the experimentally defined boundary of the BrkA translocation unit, studies of other autotransporters have shown that it is not required for surface expression of heterologous passengers (Maurer *et al.*, 1999) (Velarde and Nataro, 2004) (Klauser *et al.*, 1993a) (Suzuki *et al.*, 1995) suggesting that its main role is not related to the activity of the translocator itself. Second, this region is not required to surface express unfolded BrkA passengers (i.e. bearing a deletion of region Glu^{601}-Ala^{692}). And third, the location of this region, directly adjacent to the region required for passenger folding, suggests that the functions of these regions might be related.

To test whether region Ala^{681}-Gln^{707} is required for secretion of a "folding competent" passenger, we constructed a mutant bearing a deletion of residues Ala^{681}-Glu^{693}. This construct includes the information required for passenger folding (The^{606}-Lys^{680}) and for surface expression (Glu^{693}-Phe^{1010}) (i.e. the translocation unit). Interestingly, unlike BrkA mutants bearing deletions of the folding region (ΔGlu^{601}-Ala^{692} or ΔArg^{603}-Ala^{676}) that are surface expressed, the mutant bearing a deletion of residues Ala^{681}-Ala^{692} showed a significant decrease in surface expression (similar to the vector control) as detected by immunofluorescence (Yue J., Oliver D., and Fernandez R., poster presentation, American Society for Microbiology General Meeting 2004, New Orleans). These data indicate that region Ala^{681}-Ala^{692} of BrkA is required for efficient secretion of a "folding competent" passenger, however it is not required for secretion of an unfolded passenger.

Significantly, the EspP HSF domain and Ala^{681}-Ala^{692} of BrkA share sequence identity. Figure 3-13B shows an alignment of the conserved region of BrkA and EspP corresponding to the junction (PD002475 / PF0312). The C-terminal boundary of the BrkA autochaperone region and the N-terminal boundary of the EspP HSF region overlap. It is possible that this overlap reflects a functional relationship between these regions, however it should be noted that the autochaperone and HSF domain boundaries have yet to be systematically defined. Comparison with the BrkA(Leu^{485}-Leu^{702}) model and the pertactin structure (1DAB) reveals that the region corresponding the to the EspP HSF domain forms an extended fold at C-terminus of the β-helix (Fig. 3-13C). Interestingly, the hydrophobic residues that were shown to be important for secretion of the EspP passenger appear to cluster on one face of the fold forming a hydrophobic groove or pocket (Fig. 3-13C).

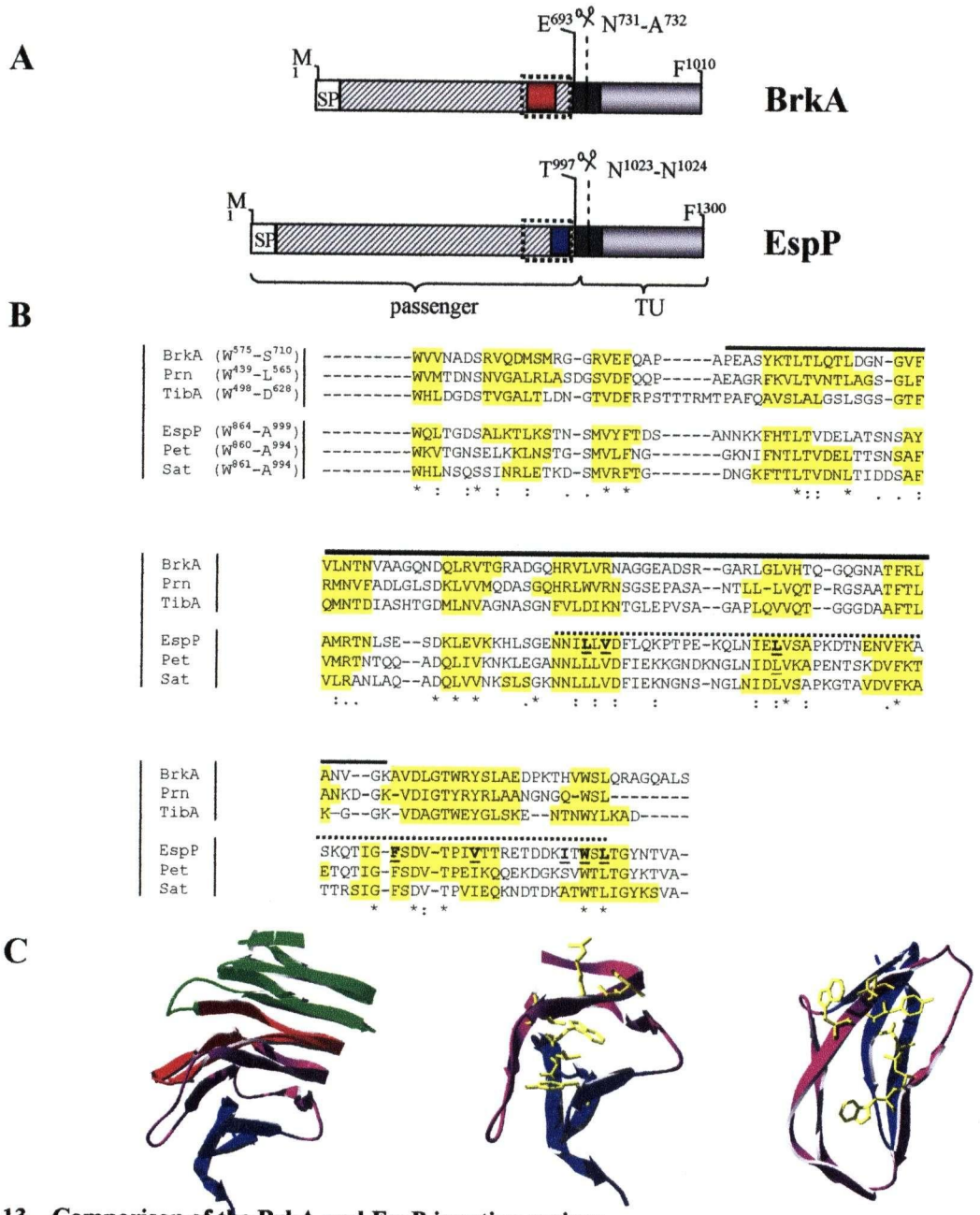

Fig. 3-13. Comparison of the BrkA and EspP junction regions.

A. Domain architecture of BrkA and EspP. Shaded boxes, translocation unit (TU), which is made up of the linker region (dark grey) and the β-core (light grey); passenger region (hatched box); signal peptide (SP). Dotted box demarks relative position of junction region in BrkA and EspP. Red box represents the region necessary for folding of the BrkA passenger (autochaperone). Blue box represents the region of EspP shown to be required for efficient translocation of the full-length EspP passenger (HSF domain). **B.** ClustalW alignment of junction regions of autotransporters closely related to BrkA (pertactin, TibA) and EspP (Pet, Sat). ((*) identity, (:) and (.) similarity) The yellow highlights denote regions of sequence predicted (PsiPred) to form β-strands. The solid black line denotes the region of BrkA shown to be required for passenger folding. The dotted black line denotes the region of EspP shown to be required for efficient translocation. Hydophobic residues shown to be important for efficient translocation of the EspP passenger are underlined (Velarde and Nataro, 2004). **C.** Structure of the C-terminal region (residues of the pertactin passenger (1DABA). Right: depicts residues G^{425}-P^{573}, region corresponding to the autochaperone region (red, pertactin E^{466}-K^{546}) corresponding to the HSF domain (blue, pertactin H^{508}-L^{566}), region overlapping between the autochaperone and the HSF domain (purple); N-terminal region of pertactin passenger (green). Middle: side view of pertactin H^{508}-L^{566} showing side chains (yellow) of residues shown to be important for efficient EspP passenger secretion. Right: top view of the pertactin H^{508}-L^{566} (N-terminus extending out of page). Yellow side chains correspond to conserved hydrophobic residues shown be important for EspP secretion (compare to underlined residues in B).

How might the HSF region facilitate secretion of a "folding competent" passenger?

The observation that the HSF region is required for surface expression of a folding competent full-length "folding competent" native passenger but not of an unfolded passenger suggests that it might regulate passenger folding in the periplasm. Such a mechanism could involve an interaction with a *trans* acting factor (e.g.. a periplasmic chaperone) that would bind to the hydrophobic groove/face of the HSF fold. Further, since the HSF domain and the autochaperone domain are juxtaposed (if not overlapping), it is conceivable that a protein-protein interaction involving the HSF domain could inhibit the activity of the autochaperone domain (i.e. passenger folding). Based on this model predictions can be made about the secretion of native autotransporter passengers. First, as shown in Figure 3-14A, the HSF domain prevents autochaperone activity (i.e. passenger folding) in the periplasm via an interaction with a periplasmic factor. Conversely, on the cell surface, in the absence of the periplasmic factor, the inhibitory role of the HSF domain has been removed and passenger folding, triggered by the autochaperone, proceeds. Second, native passengers bearing deletions of the autochaperone region (i.e. that are unable to fold) do not require the HSF domain for efficient secretion (Fig. 3-14C and D) whereas native (full-length) passengers bearing a deletion of the HSF domain fold prematurely (or irreversibly) in the periplasm and are not translocated efficiently to the surface (Fig. 3-14B). These predictions are consistent with the current data; however, significant experimentation is required to test this model further.

Alternatively, secretion might involve a folded periplasmic intermediate that partially or completely unfolds prior to translocation, and then refolds on the cell surface. Although this scenario seems energetically unfavorable, evidence does exist to suggest that some degree of passenger folding *can* happen in the periplasm. Brandon and Goldberg have shown that a protease resistant form of IcsA can be detected in periplasmic extracts, which seems to support this scenario (Brandon and Goldberg, 2001). Importantly, the protease-resistant profile of the periplasmic form was similar to the surface expressed form, suggesting that the IcsA passenger adopts its native conformation in the periplasm. However, as the authors note, whether this protease resistant species represents the folding state of a translocation competent form of the IcsA passenger is not certain (Brandon and Goldberg, 2001). In this regard, it is conceivable that an intermolecular or intramolecular mechanism that prevents passenger folding in the periplasm could be sensitive to perturbations in environmental conditions (e.g. osmotic shock, proteolysis), thus making it difficult to directly assess the periplasmic ("translocation competent") folding state *in vivo*.

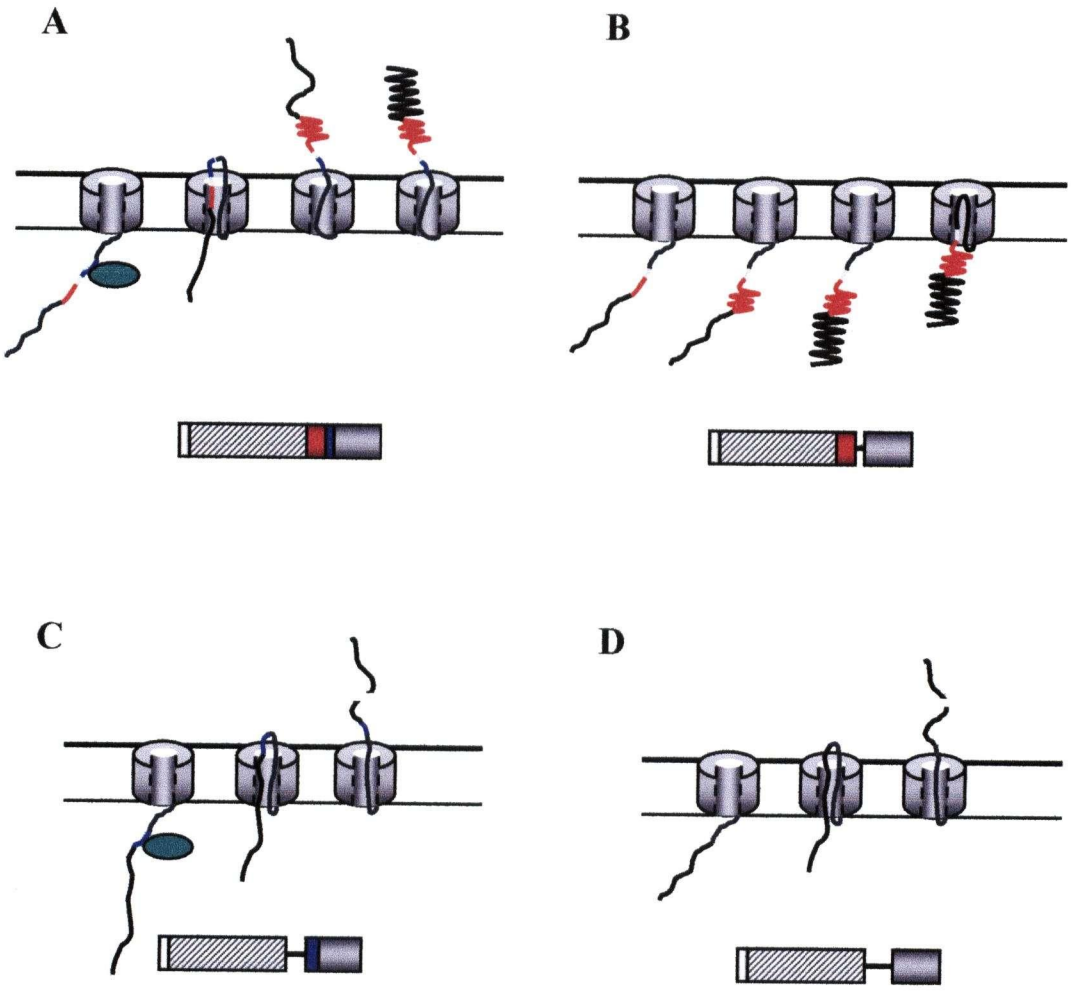

3-14. Model of BrkA secretion: the role of residues Ala^{681}-Glu^{707} - the hydrophobic secretion facilitator (HSF) domain).

For explanation of each model see text. Translocation unit (grey); HSF domain (blue); autochaperone (red); passenger (black); signal peptide (white). **A.** Wild type BrkA. **B.** BrkA bearing a deletion of the HSF domain. **C.** BrkA bearing a delteion of the autochaperone region. **D.** BrkA bearing a deletion of the autochaperone region and the HSF domain. Note: folded passenger represented by scribbled line.

Is secretion efficiency related to the function of the autochaperone or the HSF domain?

The model presented above suggests that the functions of the autochaperone and the HSF domain are localized to the cell surface and the periplasm, respectively. However, whether secretion efficiency (discussed above) is related to the function of the autochaperone or the HSF domain has not yet been deciphered. The observation of a step-wise decrease in secretion efficiency when deletions of the EspP junction region are made suggests that the contributions of the autochaperone (~ 50-75% wild type) and HSF domain (~ 20-30% wild type) might be separable (Velarde and Nataro, 2004). Assuming that translocation proceeds in an unfolded or partially folded conformation, it is conceivable that folding of the autochaperone domain on the cell surface would contribute free energy to draw the reaction forward, thereby minimizing the duration of time that the passenger is exposed to periplasmic proteases. In the periplasm, the HSF domain might facilitate translocation via an interaction with the β-domain or by harnessing energy to drive translocation via an interaction with a periplasmic chaperone. In any case, while the autochaperone and HSF regions might contribute energy to drive translocation, neither is required since unfolded (Oliver *et al.*, 2003b) and folded passengers (Veiga *et al.*, 2004) can be translocated in their absence. In this regard, it is important to note that the expression level of BrkA (ΔGlu^{601}-Ala^{692}) passenger did not increase when co-expressed with BrkA (ΔAla^{52}-Pro^{600}) suggesting that the junction region cannot rescue a defect in secretion efficiency *in trans* (Fig. 3-5B, compare at time 0). Furthermore, given the assumption that a folded passenger cannot (efficiently) traverse the outer membrane in the absence of the HSF region, this observation supports

the hypothesis that *trans* complementation of BrkA (ΔGlu^{601}-Ala^{692}) passenger folding mediated by BrkA (ΔAla^{52}-Pro^{600}) occurs on the cell surface.

3.4.4 Do all autotransporters encode a "junction" region, and are the "autochaperone" and "HSF" functions conserved?

The data and models reviewed here pertain to experiments performed with BrkA and EspP. However, the notion that the junction region plays an important role in autotransporter secretion raises two questions: (*i*) are "junction" domains are present in all autotransporters, and (*ii*) are the functions ascribed to this region (passenger folding and translocation) conserved?

(*i*) Are "junction" domains are present in all autotransporters?

Conserved domains for the junction region can be detected in most of the predicted autotransporters in the database. In this regard the PFAM (Bateman *et al.*, 2004) protein family database assigns domains PF0312, Pfam-B_3005, and PF07548 to the junction regions of proteins related to BrkA/EspP (Oliver *et al.*, 2003b) (Velarde and Nataro, 2004), PrtS of *Serratia marcescens* (Ohnishi *et al.*, 1994), and a large family of *Chlamydial* autotransporters dubbed the "POMPS" (Henderson and Lam, 2001), respectively. There are some exceptions where a junction region is not detected such as TcfA from *B. pertussis* (Finn and Stevens, 1995) and VacA of *Helicobacter pylori* (Reyrat *et al.*, 2000). It is possible that the passenger domains of these proteins have a different structure and so may not need folding/translocation assistance, or that the presence of such a domain escapes detection by sequence analysis.

(ii) **Are the autochaperone and HSF functions conserved?**

We have shown here that the junction region of pertactin can complement folding of the BrkA passenger. To our knowledge this is the only experiment that has directly tested whether passenger folding mediated by this region is conserved. However, as previously noted, the hypothesis that the BrkA passenger adopts a β-helix structure similar to pertactin suggests this region may have evolved to mediate folding of a common structure (i.e. a β-helix). Interestingly, repetitive sequences consistent with a β-helix fold have been predicted (Bradley *et al.*, 2001) in many autotransporters (Yen *et al.*, 2002)), including AIDA-I (Kajava *et al.*, 2001) and Ag43 (Kajava *et al.*, 2001) (Klemm *et al.*, 2004), as well as members of the *Chlamydial* POMPS (Vandahl *et al.*, 2002) which encode putative junction domains PF0312 and PF07548, respectively. Thus, suggesting that the autochaperone or HSF activities of some autotransporters might be related to folding (and possibly translocation) of β-helical structures. To our knowledge, the role of the HSF domain in mediating translocation of full-length (folding competent) passenger has not been tested for other autotransporters.

How about the junction region of PrtS? As previously noted, despite a lack of sequence identity with the BrkA junction, PrtS also has a similarly positioned junction region that mediates folding of its passenger domain as evidence by complementation of protease activity (discussed above) (Ohnishi *et al.*, 1994). Whether the PrtS junction (Pfam-B_3005) and the BrkA junctions (PF0312) are mechanistically similar awaits further elucidation. The junction region is cleaved from PrtS but not from BrkA suggesting that the folding mechanism may vary depending on the autotransporter. Incidentally, the

junction region identified in PrtS is conserved in two well-characterized autotransporters with serine protease activities that are currently being studied: the *B. pertussis* protein SphB1 (Coutte *et al.*, 2001) and the *Neisseria meningitidis* protein NalP (Turner *et al.*, 2002) (van Ulsen *et al.*, 2003). Perhaps these model proteins will provide future insights into the role of the PrtS-related junction/linker domains.

3.4.5 Terminology: "junction" vs. "linker"

Before moving on it is worth taking a moment to clarify the terminology, as it will be used here at least, to describe the domain features associated with C-terminus of the passenger (α-domain) and/or the N-terminus of the translocation unit (β-domain). The conserved region corresponding to PFAM domain PF03212 will be termed the "junction" (Oliver *et al.*, 2003b) and the functional attributes associated within this region will be termed the "autochaperone" domain (passenger folding) (Oliver *et al.*, 2003b) (Desvaux *et al.*, 2004) and the "hydrophobic secretion facilitor" (HSF) domain (translocation of "folding competent" native passengers) (Velarde and Nataro, 2004). The translocation unit will be divided into the "linker" region and the "β-core" corresponding to the N-terminal α-helical region and the C-terminal region that is predicted to form an amphipathic β-barrel, respectively. For several autotransporters the junction domain and the translocation unit are separated by stretch of sequence of variable length (eg. see Fig. 3-2); this region will be termed the "spacer". Notably, the spacer region is often predicted to be unstructured and can contain proteolytic cleavage sites, as is the case for IgA protease (Klauser *et al.*, 1992). In the case of BrkA a spacer region separating the junction region and the translocation unit appears to be absent (Fig. 3-2). In this regard,

it is worth noting that the N-terminal boundary of the BrkA translocation unit (residues 693-702) overlaps with the C-terminus of the BrkA HSF region (bounded by residue 702). Experiments are underway to fully resolve the boundaries of these domains. Finally, it should be stressed that experimental testing is required before these attributes are formally ascribed to homologous proteins.

3.5 References

Bateman, A., Coin, L., Durbin, R., Finn, R.D., Hollich, V., Griffiths-Jones, S., Khanna, A., Marshall, M., Moxon, S., Sonnhammer, E.L., Studholme, D.J., Yeats, C., and Eddy, S.R. (2004) The Pfam protein families database. *Nucleic Acids Res* **32 Database issue**: D138-141.

Benz, I., and Schmidt, M.A. (1992) AIDA-I, the adhesin involved in diffuse adherence of the diarrhoeagenic *Escherichia coli* strain 2787 (O126:H27), is synthesized via a precursor molecule. *Mol Microbiol* **6**: 1539-1546.

Bradley, P., Cowen, L., Menke, M., King, J., and Berger, B. (2001) BETAWRAP: successful prediction of parallel beta -helices from primary sequence reveals an association with many microbial pathogens. *Proc Natl Acad Sci U S A* **98**: 14819-14824.

Brandon, L.D., and Goldberg, M.B. (2001) Periplasmic transit and disulfide bond formation of the autotransported *Shigella* protein IcsA. *J Bacteriol* **183**: 951-958.

Corpet, F., Servant, F., Gouzy, J., and Kahn, D. (2000) ProDom and ProDom-CG: tools for protein domain analysis and whole genome comparisons. *Nucleic Acids Res* **28**: 267-269.

Coutte, L., Antoine, R., Drobecq, H., Locht, C., and Jacob-Dubuisson, F. (2001) Subtilisin-like autotransporter serves as maturation protease in a bacterial secretion pathway. *Embo J* **20**: 5040-5048.

Desvaux, M., Parham, N.J., and Henderson, I.R. (2004) The autotransporter secretion system. *Res Microbiol* **155**: 53-60.

Elish, M.E., Pierce, J.R., and Earhart, C.F. (1988) Biochemical analysis of spontaneous fepA mutants of *Escherichia coli*. *J Gen Microbiol* **134 (Pt 5)**: 1355-1364.

Emsley, P., Charles, I.G., Fairweather, N.F., and Isaacs, N.W. (1996) Structure of *Bordetella pertussis* virulence factor P.69 pertactin. *Nature* **381**: 90-92.

Ewanowich, C.A., Melton, A.R., Weiss, A.A., Sherburne, R.K., and Peppler, M.S. (1989) Invasion of HeLa 229 cells by virulent *Bordetella pertussis*. *Infect Immun* **57**: 2698-2704.

Fernandez, R.C., and Weiss, A.A. (1994) Cloning and sequencing of a *Bordetella pertussis* serum resistance locus. *Infect Immun* **62**: 4727-4738.

Fernandez, R.C., and Weiss, A.A. (1996) Susceptibilities of Bordetella pertussis strains to antimicrobial peptides. *Antimicrob Agents Chemother* **40**: 1041-1043.

Finn, T.M., and Stevens, L.A. (1995) Tracheal colonization factor: a *Bordetella pertussis* secreted virulence determinant. *Mol Microbiol* **16**: 625-634.

Frank, S., Boudko, S., Mizuno, K., Schulthess, T., Engel, J., and Bachinger, H.P. (2003) Collagen triple helix formation can be nucleated at either end. *J Biol Chem* **278**: 7747-7750.

Grodberg, J., and Dunn, J.J. (1988) ompT encodes the *Escherichia coli* outer membrane protease that cleaves T7 RNA polymerase during purification. *J Bacteriol* **170**: 1245-1253.

Henderson, I.R., Navarro-Garcia, F., and Nataro, J.P. (1998) The great escape: structure and function of the autotransporter proteins. *Trends Microbiol* **6**: 370-378.

Henderson, I.R., and Lam, A.C. (2001) Polymorphic proteins of *Chlamydia* spp.--autotransporters beyond the Proteobacteria. *Trends Microbiol* **9**: 573-578.

Jacob-Dubuisson, F., El-Hamel, C., Saint, N., Guedin, S., Willery, E., Molle, G., and Locht, C. (1999) Channel formation by FhaC, the outer membrane protein involved in the secretion of the *Bordetella pertussis* filamentous hemagglutinin. *J Biol Chem* **274**: 37731-37735.

Jenkins, J., Mayans, O., and Pickersgill, R. (1998) Structure and evolution of parallel beta-helix proteins. *J Struct Biol* **122**: 236-246.

Kajava, A.V., Cheng, N., Cleaver, R., Kessel, M., Simon, M.N., Willery, E., Jacob-Dubuisson, F., Locht, C., and Steven, A.C. (2001) Beta-helix model for the filamentous haemagglutinin adhesin of *Bordetella pertussis* and related bacterial secretory proteins. *Mol Microbiol* **42**: 279-292.

Klauser, T., Pohlner, J., and Meyer, T.F. (1992) Selective extracellular release of cholera toxin B subunit by Escherichia coli: dissection of *Neisseria* Iga beta-mediated outer membrane transport. *Embo J* **11**: 2327-2335.

Klauser, T., Kramer, J., Otzelberger, K., Pohlner, J., and Meyer, T.F. (1993a) Characterization of the *Neisseria* Iga beta-core. The essential unit for outer membrane targeting and extracellular protein secretion. *J Mol Biol* **234**: 579-593.

Klauser, T., Pohlner, J., and Meyer, T.F. (1993b) The secretion pathway of IgA protease-type proteins in gram-negative bacteria. *Bioessays* **15**: 799-805.

Kleinschmidt, J.H. (2003) Membrane protein folding on the example of outer membrane protein A of *Escherichia coli*. *Cell Mol Life Sci* **60**: 1547-1558.

Klemm, P., Hjerrild, L., Gjermansen, M., and Schembri, M.A. (2004) Structure-function analysis of the self-recognizing Antigen 43 autotransporter protein from *Escherichia coli*. *Mol Microbiol* **51**: 283-296.

Konninger, U.W., Hobbie, S., Benz, R., and Braun, V. (1999) The haemolysin-secreting ShlB protein of the outer membrane of *Serratia marcescens*: determination of surface-exposed residues and formation of ion-permeable pores by ShlB mutants in artificial lipid bilayer membranes. *Mol Microbiol* **32**: 1212-1225.

Kovach, M.E., Phillips, R.W., Elzer, P.H., Roop, R.M., 2nd, and Peterson, K.M. (1994) pBBR1MCS: a broad-host-range cloning vector. *Biotechniques* **16**: 800-802.

Laemmli, U.K. (1970) Cleavage of structural proteins during the assembly of the head of bacteriophage T4. *Nature* **227**: 680-685.

Lee, H.W., and Byun, S.M. (2003) The pore size of the autotransporter domain is critical for the active translocation of the passenger domain. *Biochem Biophys Res Commun* **307**: 820-825.

Letarov, A.V., Londer, Y.Y., Boudko, S.P., and Mesyanzhinov, V.V. (1999) The carboxy-terminal domain initiates trimerization of bacteriophage T4 fibritin. *Biochemistry (Mosc)* **64**: 817-823.

Maurer, J., Jose, J., and Meyer, T.F. (1997) Autodisplay: one-component system for efficient surface display and release of soluble recombinant proteins from *Escherichia coli*. *J Bacteriol* **179**: 794-804.

Maurer, J., Jose, J., and Meyer, T.F. (1999) Characterization of the essential transport function of the AIDA-I autotransporter and evidence supporting structural predictions. *J Bacteriol* **181**: 7014-7020.

Miyazaki, H., Yanagida, N., Horinouchi, S., and Beppu, T. (1989) Characterization of the precursor of Serratia marcescens serine protease and COOH-terminal processing

of the precursor during its excretion through the outer membrane of *Escherichia coli*. *J Bacteriol* **171**: 6566-6572.

Ohnishi, Y., Nishiyama, M., Horinouchi, S., and Beppu, T. (1994) Involvement of the COOH-terminal pro-sequence of *Serratia marcescens* serine protease in the folding of the mature enzyme. *J Biol Chem* **269**: 32800-32806.

Ohnishi, Y., and Horinouchi, S. (1996) Extracellular production of a *Serratia marcescens* serine protease in Escherichia coli. *Biosci Biotechnol Biochem* **60**: 1551-1558.

Oliver, D.C., and Fernandez, R.C. (2001) Antibodies to BrkA augment killing of *Bordetella pertussis*. *Vaccine* **20**: 235-241.

Oliver, D.C., Huang, G., and Fernandez, R.C. (2003a) Identification of secretion determinants of the *Bordetella pertussis* BrkA autotransporter. *J Bacteriol* **185**: 489-495.

Oliver, D.C., Huang, G., Nodel, E., Pleasance, S., and Fernandez, R.C. (2003b) A conserved region within the *Bordetella pertussis* autotransporter BrkA is necessary for folding of its passenger domain. *Mol Microbiol* **47**: 1367-1383.

Oomen, C.J., Van Ulsen, P., Van Gelder, P., Feijen, M., Tommassen, J., and Gros, P. (2004) Structure of the translocator domain of a bacterial autotransporter. *Embo J* **23**: 1257-1266.

Paschen, S.A., Waizenegger, T., Stan, T., Preuss, M., Cyrklaff, M., Hell, K., Rapaport, D., and Neupert, W. (2003) Evolutionary conservation of biogenesis of beta-barrel membrane proteins. *Nature* **426**: 862-866.

Pohlner, J., Halter, R., Beyreuther, K., and Meyer, T.F. (1987) Gene structure and extracellular secretion of *Neisseria gonorrhoeae* IgA protease. *Nature* **325**: 458-462.

Rambow, A.A., Fernandez, R.C., and Weiss, A.A. (1998) Characterization of BrkA expression in *Bordetella bronchiseptica*. *Infect Immun* **66**: 3978-3980.

Reyrat, J.M., Rappuoli, R., and Telford, J.L. (2000) A structural overview of the Helicobacter cytotoxin. *Int J Med Microbiol* **290**: 375-379.

Richardson, J.S., and Richardson, D.C. (2002) Natural beta-sheet proteins use negative design to avoid edge-to-edge aggregation. *Proc Natl Acad Sci U S A* **99**: 2754-2759.

Schleiff, E., Soll, J., Kuchler, M., Kuhlbrandt, W., and Harrer, R. (2003) Characterization of the translocon of the outer envelope of chloroplasts. *J Cell Biol* **160**: 541-551.

Shannon, J.L., and Fernandez, R.C. (1999) The C-terminal domain of the *Bordetella pertussis* autotransporter BrkA forms a pore in lipid bilayer membranes. *J Bacteriol* **181**: 5838-5842.

Shikata, S., Shimada, K., Ohnishi, Y., Horinouchi, S., and Beppu, T. (1993) Characterization of secretory intermediates of *Serratia marcescens* serine protease produced during its extracellular secretion from Escherichia coli cells. *J Biochem (Tokyo)* **114**: 723-731.

Suzuki, T., Lett, M.C., and Sasakawa, C. (1995) Extracellular transport of VirG protein in *Shigella*. *J Biol Chem* **270**: 30874-30880.

Tamm, L.K., Arora, A., and Kleinschmidt, J.H. (2001) Structure and assembly of beta-barrel membrane proteins. *J Biol Chem* **276**: 32399-32402.

Thanassi, D.G., Saulino, E.T., Lombardo, M.J., Roth, R., Heuser, J., and Hultgren, S.J. (1998) The PapC usher forms an oligomeric channel: implications for pilus biogenesis across the outer membrane. *Proc Natl Acad Sci U S A* **95**: 3146-3151.

Thompson, J.D., Higgins, D.G., and Gibson, T.J. (1994) CLUSTAL W: improving the sensitivity of progressive multiple sequence alignment through sequence weighting, position-specific gap penalties and weight matrix choice. *Nucleic Acids Res* **22**: 4673-4680.

Turner, D.P., Wooldridge, K.G., and Ala'Aldeen, D.A. (2002) Autotransported serine protease A of *Neisseria meningitidis*: an immunogenic, surface-exposed outer membrane, and secreted protein. *Infect Immun* **70**: 4447-4461.

van den Berg, B.M., Beekhuizen, H., Mooi, F.R., and van Furth, R. (1999) Role of antibodies against *Bordetella pertussis* virulence factors in adherence of *Bordetella pertussis* and *Bordetella parapertussis* to human bronchial epithelial cells. *Infect Immun* **67**: 1050-1055.

van Ulsen, P., van Alphen, L., ten Hove, J., Fransen, F., van der Ley, P., and Tommassen, J. (2003) A *Neisserial* autotransporter NalP modulating the processing of other autotransporters. *Mol Microbiol* **50**: 1017-1030.

Vandahl, B.B., Pedersen, A.S., Gevaert, K., Holm, A., Vandekerckhove, J., Christiansen, G., and Birkelund, S. (2002) The expression, processing and localization of polymorphic membrane proteins in *Chlamydia pneumoniae* strain CWL029. *BMC Microbiol* **2**: 36.

Veiga, E., de Lorenzo, V., and Fernandez, L.A. (1999) Probing secretion and translocation of a beta-autotransporter using a reporter single-chain Fv as a cognate passenger domain. *Mol Microbiol* **33**: 1232-1243.

Veiga, E., Sugawara, E., Nikaido, H., de Lorenzo, V., and Fernandez, L.A. (2002) Export of autotransported proteins proceeds through an oligomeric ring shaped by C-terminal domains. *Embo J* **21**: 2122-2131.

Veiga, E., de Lorenzo, V., and Fernandez, L.A. (2004) Structural tolerance of bacterial autotransporters for folded passenger protein domains. *Mol Microbiol* **52**: 1069-1080.

Velarde, J.J., and Nataro, J.P. (2004) Hydrophobic residues of the autotransporter EspP linker domain are important for outer membrane translocation of its passenger. *J Biol Chem* **279**: 31495-31504.

Yen, M.R., Peabody, C.R., Partovi, S.M., Zhai, Y., Tseng, Y.H., and Saier, M.H. (2002) Protein-translocating outer membrane porins of Gram-negative bacteria. *Biochim Biophys Acta* **1562**: 6-31.

Chapter 4

Homologous translocation units are not required for *trans* complementation of BrkA passenger folding

4.1 Introduction

The observation that folding of a junction-deleted form of the BrkA passenger can be rescued by co-expressing the BrkA junction region *in trans* in the same cell suggests that these polypeptides interact at some point along the secretion pathway. However, the nature of this interaction (e.g. transient, stable) and its sub-cellular location (e.g. periplasm, outer membrane) are not known. Interestingly, the observation of a multi-subunit complex formed by the β-domain of IgA protease (Fig. 4-1A) (Veiga *et al.*, 2002) suggested that a similar structure formed by the BrkA β-domain might have assembled to facilitate co-localization of the junction-deleted BrkA passenger and the junction region during secretion (Fig 4-1B). We decided to test whether these two phenomena (*trans* complementation of passenger folding *and* the formation of a multimeric secretion complex) are linked. We hypothesised that *trans* complementation of BrkA(ΔGlu^{601}-Ala^{692}) passenger folding mediated by BrkA(ΔAla^{52}-Pro^{600}), is facilitated by specific interactions between homologous translocation units in the outer membrane, an interaction perhaps related to the formation of a multimeric translocation complex (Fig. 4-1C). To test this, we used the translocation units of BrkA, pertactin and IgA protease to surface express a junction-deleted form of the BrkA passenger (a reporter). Using these reporter constructs, we asked whether passenger folding is *trans*

complemented by the BrkA or pertactin junction regions fused to their cognate translocation units. We determine that homologous translocation units are *not* required for *trans* complementation of BrkA passenger folding mediated by the junction regions of BrkA or pertactin. However, these data do not rule out the possibility that passenger translocation could involve the formation of a homo- or even a hetero-oligomeric secretion complex. The tools developed in this study are currently be used to investigate these possibilities.

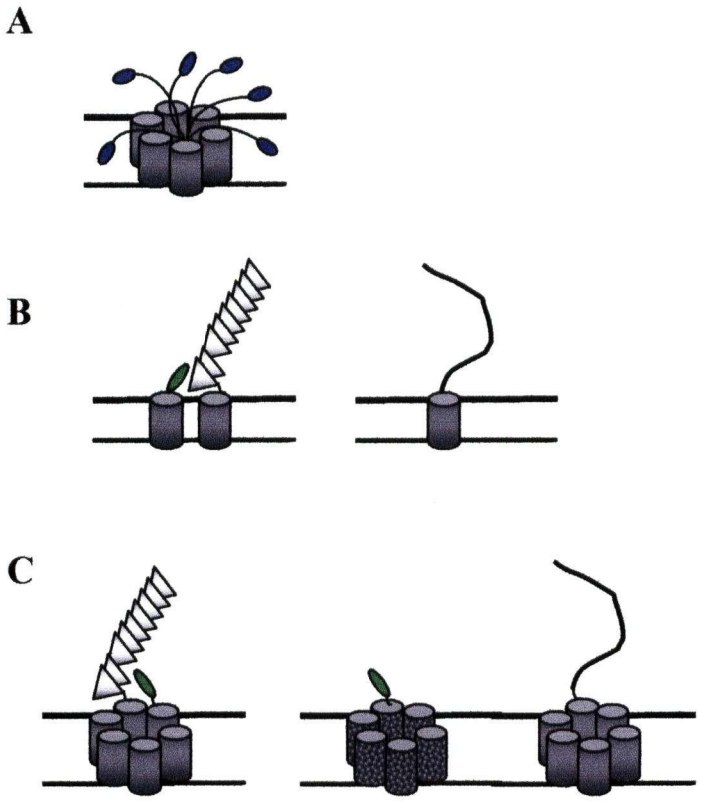

Fig. 4-1. Experimental concepts.

A. The "central pore" model of autotransporter secretion (Veiga *et al.* 2002). Depicted is a 6-subunit complex formed by individual β-domains (cylinders). The space between the β-domains forms the 2 nm channel through which passengers (line with blue ball) are translocated. **B.** Model of *trans* complementation of BrkA passenger folding experiment. Left: Co-expression of the BrkA junction region (green oval) rescues folding of a junction-deleted BrkA passenger (grey triangles). Right: Junction-deleted BrkA passenger remains unfolded at the cell surface (curved black line) in the absence of the BrkA junction. C. Experimental hypothesis. Left: Co-expression of the BrkA junction and the junction-deleted BrkA passenger using *homologous* translocation units results in *trans* complementation of BrkA passenger folding due to the formation of a homo-oligomeric translocation complex. Right. Co-expression of the BrkA junction and the junction-deleted BrkA passenger using *heterologous* translocation units *does not* result in *trans* complementation of BrkA passenger folding.

4.2 Methods and Materials

4.2.1 Bacterial Strains, plasmids and growth conditions

Bacterial strains and plasmids used in this study are listed in Table 3-1 (Chapter 3). *E. coli* strains were cultured at 37 °C on Luria broth or Luria agar supplemented with the appropriate antibiotics. Chloramphenicol was added to the media at 34 μg/ml. Ampicillin was added at 100 μg/ml for DH5α and 200 μg/ml for UT5600 and UT2300.

4.2.2 Recombinant DNA techniques

DNA manipulations and polymerase chain reactions (PCR) were carried out using standard techniques (Sambrook, 1989) and reagents, as described previously (Oliver *et al.*, 2003). Primers used in this study were obtained from Alpha DNA (Montreal, PQ) or the University of British Columbia (UBC) Nucleic Acid and Protein Services (NAPS) Unit. DNA sequencing was done by the UBC NAPS Unit.

Plasmid pDO-313PrnTU was made by subcloning a 1.0 kB *Bam*HI – *Hind*III fragment of pDO-PRN4 into a 5.4 kB *Bam*HI – *Hind*III fragment of pGH313. Constructs pDO-313-IPTU1124 and pDO-313-IPTU1225 were constructed by PCR using reverse primer IGASTOPR (5' CTGAAGCTTTTAGAAACGAATCTG 3') and forward primers IGA1124F (5' AAGGATCCGGTATTTTCATTGGATG 3') or IGA1225F (5' AAGGATCCGGGTTTACAACAAAGAG 3'), respectively. Plasmid pIGAP-MS11 (a gift from Emil Pai, University of Toronto), which carries the *iga* gene from *Neisseria gonorrhea* strain MS11, was used as a template. Amplified products were digested with *Bam*HI and *Hind*III and ligated into a 5.4 kB *Bam*HI – *Hind*III pGH313 fragment. Constructs pDO-313BBR, pDO-313PrnTU-

BBR, pDO-313IPTU1-BBR and pDO-313IPTU2-BBR were constructed by ligation of *Nru*I – *Hind*III fragments excised from plasmids pGH313, pDO-PRN3, pDO-313-IPTU1 and pDO-313-IPTU2 into a 4.7 kB *Sma*I – *Hind*III fragment of pBBR1MCS (Kovach *et al.*, 1994).

4.2.3 SDS-PAGE and immunoblot analysis

For detection of expressed BrkA via immunoblot, *E. coli* cultures were grown to 0.8 optical density (OD_{600}) units and sedimented by centrifugation. Washed pellets were resuspended finally in sample buffer and immediately boiled for 5 minutes prior to SDS-PAGE as previously described (Laemmli, 1970) (Fernandez and Weiss, 1994). Samples resolved by SDS-PAGE were transferred to Immobilon-P membranes (Millipore, Etobicoke, ON) as described (Oliver and Fernandez, 2001). Staining of the SDS-PAGE gels with Coomassie Blue verified that approximately equal amounts of lysates were loaded into each lane. Blots were probed using heat inactivated rabbit anti-BrkA antiserum and horseradish peroxidase-conjugated goat anti-rabbit secondary antibody (ICN Biomedicals, Costa Mesa, CA) diluted 1/50,000 and 1/10,000, respectively (Oliver and Fernandez, 2001). Kaleidoscope pre-stained markers (Bio-Rad, Hercules, CA) were used for estimation of molecular mass.

4.2.4 *In vivo* limited proteolysis analysis

E. coli UT5600 co-transformed with the indicated plasmids were grown to an OD_{600} of 0.8 in the presence of antibiotic selection. One ml of culture was harvested by centrifugation and resuspended in 150 µl of PBS. A 15 µl of aliquot was removed and

added to 50 µl of SDS-PAGE disruption buffer and boiled for 5 minutes. Trypsin was then added to the remaining culture to a final concentration of 0.01 mg/ml. Following the addition of trypsin, 15 µl aliquots were removed at various time intervals (1, 5, 15 minutes) and added to 50 µl of disruption buffer and immediately boiled to stop digestion. Samples were resolved by SDS-PAGE, transferred to Immobilon-P membrane and probed for BrkA expression (as described above).

4.3 Results

4.3.1 Construction of BrkA, pertactin, IgA protease chimeras

To test the hypothesis that homologous translocation units are required for *trans* complementation of BrkA(ΔGlu^{601}-Ala^{692}) passenger folding we developed a genetic system consisting of (*i*) a construct encoding either the BrkA junction and translocation unit or the pertactin junction and translocation unit, and (*ii*) a reporter construct encoding a junction-deleted form of the BrkA passenger (Met^{1}-Ala^{600}) fused to the translocation unit of either BrkA, pertactin or IgA protease. The translocation units of BrkA and pertactin share 43% identity and 55% similarity whereas the IgA protease translocation unit shares less than 10% sequence similarity with either BrkA or pertactin. As shown in Figure 4-2, the BrkA(Met^{1}-Ala^{600}) reporter was fused to Leu^{566} of pertactin which is located at the N-terminus of a 51 residue polyproline rich spacer region that precedes its translocation unit. The BrkA(Met^{1}-Ala^{600}) reporter was fused at residues Val^{1124} and Gly^{1225} of IgA protease: Val^{1124} is C-terminal to the β-domain cleavage site (Pro^{1123}-Val^{1124}) and includes a spacer region of 100 residues (additionally, this site has been used previously to fuse heterologous polypeptides for surface presentation (Klauser *et al.*, 1990)), and Val^{1225} lies N-terminal to the experimentally defined minimal translocation unit (Klauser *et al.*, 1993). The reporter constructs used in this experiment were constructed using pBBR1MCS (Kovach *et al.*, 1994), a medium-copy number plasmid with broad host range, including *B. pertussis*.

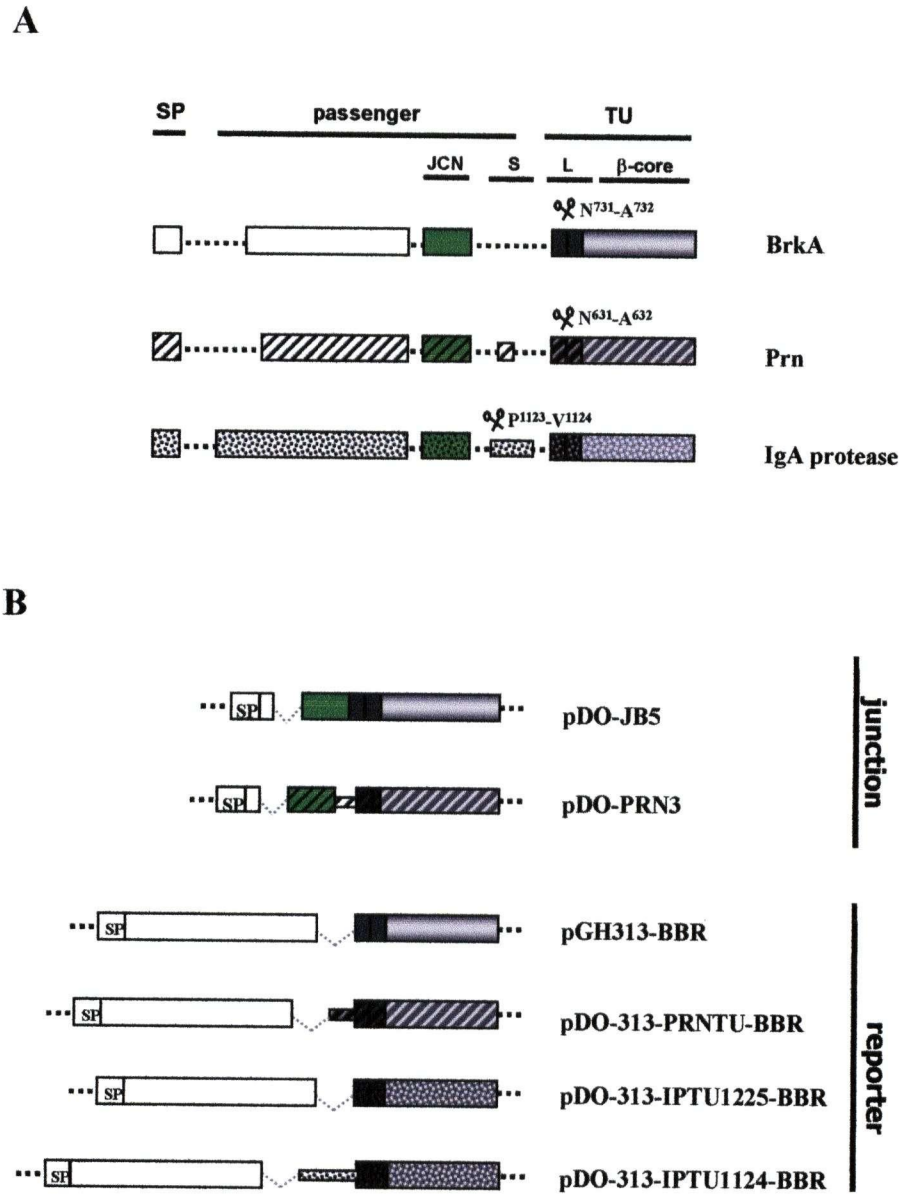

Fig. 4-2. Autotransporter chimeras.

A. Domain architecture of BrkA, Prn and IgA protease. Domains and sub-domains are separated by dotted line. Signal peptide (SP), passenger and translocation unit (TU) are denoted across top line. Lower line denotes junction (JCN, green), spacer region (S, narrow box), linker region (L, dark grey) and β-core (light grey). β-domain cleavage sites are denoted by scissors. Open boxes denote BrkA sequence, hatched boxes denote pertactin sequence, and speckled boxes denote IgA protease sequence. Light grey denotes β-core region, dark grey denotes linker region, white and green denotes passenger region. **B.** Junction constructs pDO-JB5 and pDO-PRN3 encode residues M^{1}-G^{51} of the BrkA passenger fused in-frame with residues E^{601}-F^{1010} of BrkA or Y^{604}-W^{910} of pertactin, respectively. Reporter constructs pGH313-BBR, pDO-313-PRNTU-BBR, pDO-313-IPTU1225-BBR and pDO-313-IPTU1124-BBR encode residues M^{1}-P^{600} of the BrkA passenger fused in-frame with residues E^{693}-F^{1010} of BrkA, L^{566}-W^{910} of pertactin, G^{1225}-F^{1532} of IgA protease and V^{1124}-F^{1532} of IgA protease, respectively. Domains are not drawn to scale.

4.3.2 Homologous translocation units are not required for *trans* complementation of BrkA(Gln^{43}-Ala^{600}) folding

We first asked whether *trans* complementation of BrkA(ΔGlu^{601}-Ala^{692}) passenger folding would occur when the closely related BrkA and pertactin translocation units were employed. Junction and reporter constructs were co-transformed into *E. coli* UT5600 and BrkA((ΔGlu^{601}-Ala^{692}) passenger folding was probed by limited proteolysis using trypsin and detected by immunoblot. As expected, when pGH313-BBR and pDO-JB5 were introduced into *E. coli* UT5600 a trypsin resistant 65 kDa band corresponding to the BrkA(ΔGlu^{601}-Ala^{692}) passenger was observed (Fig. 4-3A). By contrast, co-transformation with pGH313-BBR and the vector control resulted in a trypsin-sensitive 65 kDa band corresponding to the BrkA(ΔGlu^{601}-Ala^{692}) passenger (Fig. 4-3A). Similarly, co-transformation of pDO-313-PRNTU-BBR and pDO-Prn-J3 resulted in the production of a band migrating at approximately 68 kDa corresponding to the cleaved α-domain which encompasses the BrkA(Met^{1}-Ala^{600}) reporter (Fig. 4-3B). The appearance of the lower band following exposure to trypsin is presumably due to cleavage of the C-terminal polyproline region. Identical results were observed when pGH-313BBR and pDO-313-PRNTU-BBR were co-transformed with pDO-Prn-J3 and pDO-JB5, respectively (Fig. 4-3B). Thus, it can be concluded that homologous translocation units are *not* required for *trans* complementation of BrkA(Gln^{43}-Ala^{600}) folding.

Although the translocation units of BrkA and pertactin were shown to be functionally interchangeable in terms of their ability to *trans* complement folding of the BrkA(Met^{1}–Ala^{600}) reporter, we considered the possibility that closely related

translocation units (i.e. BrkA and pertactin) might have the capacity to interact with each other whereas translocation units sharing less sequence identity might not (i.e. BrkA and IgA protease). To address this possibility, we asked whether folding of the BrkA(Met^{1}–Ala^{600}) reporter fused to the IgA protease translocation unit could be complemented when co-expressed with junction constructs bearing the BrkA or pertactin translocation units. As shown in Fig. 5-3 C and D, immunoblots of *E. coli* UT5600 co-transformed with pDO-313-IPTU1124-BBR or pDO-313-IPTU1225-BBR and the vector control revealed bands migrating at approximately 100 kDa and 90 kDa corresponding to the unprocessed forms of each construct, respectively. Following exposure to trypsin, the 100 kDa and 90 kDa bands were completely removed confirming that the BrkA(Met^{1}-Ala^{600}) reporter was (*i*) expressed at the cell surface and (*ii*) presented in a protease sensitive (unfolded) conformation. Co-transformation with plasmids pDO-JB5 or pDO-Prn-J3 did not alter the expression level or processing (i.e. remains uncleaved) of the 100 kDa and 90 kDa species. However, upon exposure to trypsin, the unprocessed bands (100 kDa and 90 kDa) disappeared and a trypsin-resistant band migrating at approximately 65 kDa resulted (Fig. 4-3 C and D). The 65 kDa product corresponds to the predicted size of the BrkA reporter region (Met^{1}–Ala^{600}), (presumably *sans* signal peptide). Taken together these data indicate that *trans* complementation of BrkA passenger folding (mediated by the junction region) occurs when co-expression studies are performed with translocation units sharing less than 10% sequence identity.

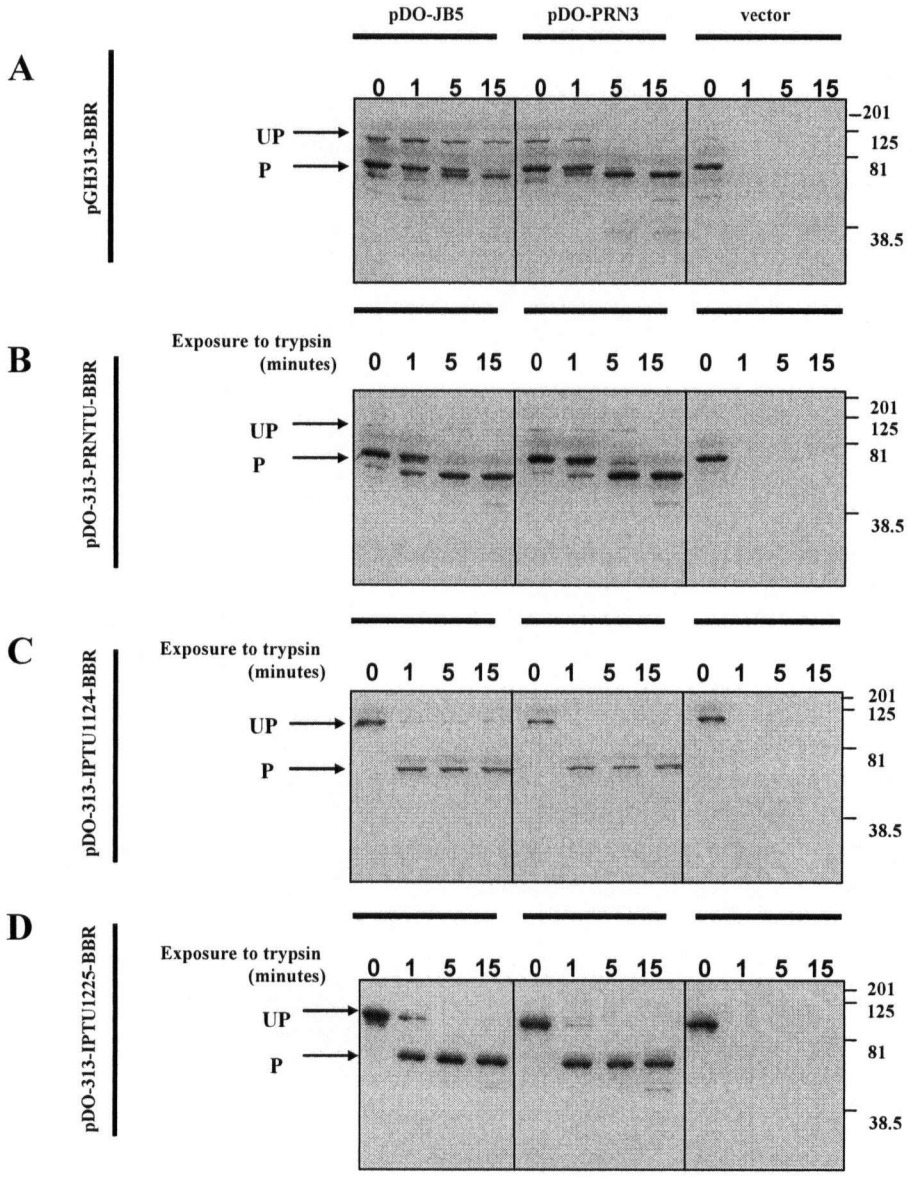

Fig. 4-3. Homologous translocation units are not required for *trans* complementation of BrkA passenger folding.

(A-D) Reporter constructs were co-transformed into *E. coli* UT5600 with junction constructs or a pBBRMCS1 vector control. Reporter and junction constructs are depicted in Figure 5-2. Cells were grown to 0.8 OD units and harvested by centrifugation. Stability of surface expressed BrkA was assessed by limited trypsin digestion as described in Materials and Methods. Whole cell lysates were resolved by SDS-PAGE and BrkA was detected by immunoblot. UP denotes the unprocessed full-length form of the protein. P denotes the processed form of the BrkA passenger. Notes: bands corresponding to the junction constructs are not visible. Molecular weight markers in kDa denoted on right are approximate.

4.3 Discussion

The fact the folding of a junction-deleted form of the BrkA passenger can be rescued by co-expressing the junction region fused to the BrkA translocation unit suggests that these polypeptides interact at some point along the secretion pathway. The observation of a high molecular weight complex formed by several β domain subunits of IgA protease suggested that the junction-deleted BrkA passenger and BrkA junction were perhaps being co-localized via intermolecular interactions between two or more BrkA translocation units involved in the formation of a secretion complex in the outer membrane. We hypothesized that the formation of an oligomeric secretion complex would involve specific interactions between homologous translocation units. To test this hypothesis we asked whether homologous translocation units are required to *trans* complement folding of a junction-deleted form of the BrkA passenger folding (residues Met^{1}-Ala^{600}).

We show that a surface expressed protease resistant species is produced when the BrkA(Met^{1}-Ala^{600}) reporter is fused to the translocation unit of pertactin (43% identity with BrkA) or two variants of IgA protease (< 10% identity with BrkA or pertactin) encompassing the β-domain and translocation unit, respectively. These data indicate that the formation of a homo-oligomeric complex comprised of multiple translocation units is not required for *trans* complementation of BrkA passenger folding. We favour the idea that *trans* complementation of BrkA passenger folding is occurring at the cell surface (post-translocation) via transient interactions occurring between autotransporters moving about laterally in the plane of the membrane. However, we cannot rule out the possibility

that *trans* complementation of BrkA passenger folding involves the formation of a hetero-oligomeric complex, an interaction between homo-oligomeric complexes, or even co-localization via a polar secretion mechanism, perhaps analogous to secretion of the autotransporter IcsA (Charles *et al.*, 2001).

The notion that functional interactions can occur between autotransporter passengers presents an interesting option for engineering surface display strategies. In this regard, Jose *et al.* (2002) have shown that a bovine adrenodoxin subunit is secreted as a monomer and assembled as a functional dimer on the surface of *E. coli* when fused to the translocation unit of AIDA-I. Further, it has been shown that intermolecular cleavage of autotransporter passengers can be mediated by homologous (Fink *et al.*, 2001) and heterologous autotransporters (van Ulsen *et al.*, 2003). Thus, functional intermolecular interactions between autotransporters include, proteolysis, the formation of ternary complexes, and as shown here, protein folding.

4.5 References

Charles, M., Perez, M., Kobil, J.H., and Goldberg, M.B. (2001) Polar targeting of *Shigella* virulence factor IcsA in *Enterobacteriacae* and *Vibrio*. *Proc Natl Acad Sci U S A* **98**: 9871-9876.

Fernandez, R.C., and Weiss, A.A. (1994) Cloning and sequencing of a *Bordetella pertussis* serum resistance locus. *Infect Immun* **62**: 4727-4738.

Fink, D.L., Cope, L.D., Hansen, E.J., and Geme, J.W., 3rd (2001) The *Hemophilus influenzae* Hap autotransporter is a chymotrypsin clan serine protease and undergoes autoproteolysis via an intermolecular mechanism. *J Biol Chem* **276**: 39492-39500.

Jose, J., Bernhardt, R., and Hannemann, F. (2002) Cellular surface display of dimeric Adx and whole cell P450-mediated steroid synthesis on *E. coli*. *J Biotechnol* **95**: 257-268.

Klauser, T., Pohlner, J., and Meyer, T.F. (1990) Extracellular transport of cholera toxin B subunit using *Neisseria* IgA protease beta-domain: conformation-dependent outer membrane translocation. *Embo J* **9**: 1991-1999.

Klauser, T., Kramer, J., Otzelberger, K., Pohlner, J., and Meyer, T.F. (1993) Characterization of the *Neisseria* Iga beta-core. The essential unit for outer membrane targeting and extracellular protein secretion. *J Mol Biol* **234**: 579-593.

Kovach, M.E., Phillips, R.W., Elzer, P.H., Roop, R.M., 2nd, and Peterson, K.M. (1994) pBBR1MCS: a broad-host-range cloning vector. *Biotechniques* **16**: 800-802.

Laemmli, U.K. (1970) Cleavage of structural proteins during the assembly of the head of bacteriophage T4. *Nature* **227**: 680-685.

Maurer, J., Jose, J., and Meyer, T.F. (1997) Autodisplay: one-component system for efficient surface display and release of soluble recombinant proteins from *Escherichia coli*. *J Bacteriol* **179**: 794-804.

Oliver, D.C., and Fernandez, R.C. (2001) Antibodies to BrkA augment killing of *Bordetella pertussis*. *Vaccine* **20**: 235-241.

Oliver, D.C., Huang, G., and Fernandez, R.C. (2003) Identification of secretion determinants of the *Bordetella pertussis* BrkA autotransporter. *J Bacteriol* **185**: 489-495.

van Ulsen, P., van Alphen, L., ten Hove, J., Fransen, F., van der Ley, P., and Tommassen, J. (2003) A *Neisserial* autotransporter NalP modulating the processing of other autotransporters. *Mol Microbiol* **50**: 1017-1030.

Veiga, E., Sugawara, E., Nikaido, H., de Lorenzo, V., and Fernandez, L.A. (2002) Export of autotransported proteins proceeds through an oligomeric ring shaped by C-terminal domains. *Embo J* **21**: 2122-2131.

Chapter 5

General Discussion

The studies presented herein focus primarily on defining structural and functional attributes of BrkA related to its secretion (summarized in Fig. 5-1), and more specifically with respect to the expression and folding state of the BrkA passenger domain at the cell surface. Aspects of each study have been discussed in Chapters 2 through 4. To conclude, our current knowledge of BrkA secretion will be placed in the context of our current understanding of autotransporter secretion. Work performed by several labs in recent years has begun to reveal details of the autotransporter secretion mechanism that have begun to shape (and shift) the way we view this seemingly simple protein secretion strategy. In turn, these discoveries have led to many new questions that now need to be addressed. These issues and areas of future research are discussed.

5.1 Autotransporter secretion: simply biochemistry

Autotransporter secretion can be viewed as a stepwise process where the polypeptide transits through the cytoplasm, across the inner membrane, through the periplasm, and across the outer membrane on the way to the cell surface (Fig 1-1). Each of these steps can be broken into discrete biochemical processes some of which have been, and many of which remain to be, experimentally dissected. Understanding how this biochemistry comes together to create a functional protein secretion pathway is the ultimate goal of research in the autotransporter secretion field.

Portions of this chapter have been submitted for publication in the journal Molecular Microbiology.

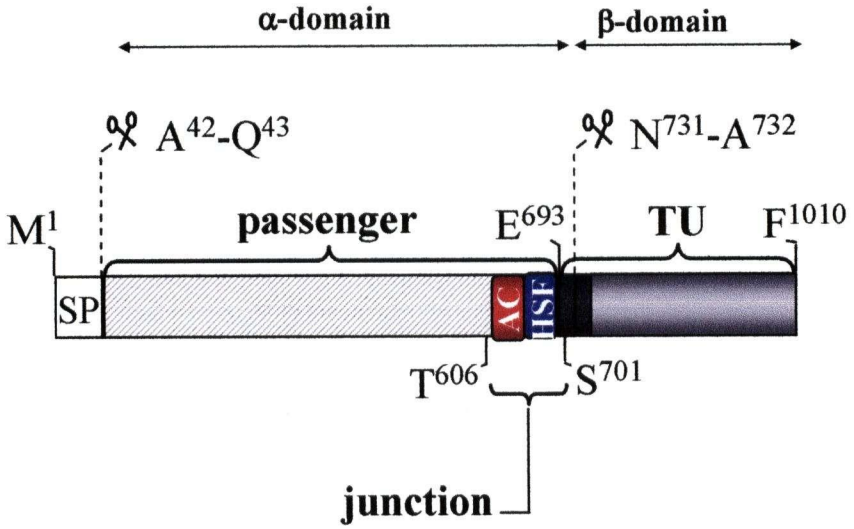

Fig. 5-2. Overview of BrkA structure.
BrkA is expressed as a 103 kDa (1010 amino acid) polypeptide that encodes three functional domains: an N-terminal signal peptide, a passenger domain to be delivered to the bacterial surface, and a C-terminal translocation unit. The signal peptide (white, SP) and translocation unit (solid grey, TU) represent the minimal secretion determinants. Overlapping deletion analysis has shown that residues 52-693 of the BrkA passenger (hatched grey) are not required for secretion. The **signal peptide** is 42 amino acids long and encodes the orthodox information required for export via the Sec translocon (N-, H-, and C-domain) as well as a 16 residue long N-terminal extension whose function is currently unknown. Signal peptide cleavage between residues 42 and 43 is presumed to be mediated by signal peptidase I. Using residues 1-229 of the BrkA passenger as a reporter of surface display (and hence translocator activity), the N-terminal boundary of the BrkA **translocation unit** has been experimentally mapped to a region bounded by residues 693-702 (Oliver et al., 2003). The translocation unit consists of 2 structurally distinct (yet conserved) sub-domains: the linker region and the β-core. The linker region (dark grey) is predicted to adopt an α-helical conformation whereas the β-core (light grey) is predicted (based on primary and secondary sequence alignments with related autotransporters) to form a 12-stranded β-barrel structure. The BrkA translocation unit has been shown to form 3.2 nanoSiemen channels in artificial membranes (Shannon and Fernandez, 1999). Whether the BrkA translocation unit forms high molecular complexes similar to IgA protease (Veiga et al. 2002) is not known. During secretion, the translocation unit undergoes cleavage between residues 731 and 732 located within the linker region to yield the α-domain and β-domain. Following cleavage, the α-domain remains steadfastly anchored to the cell surface by an unknown mechanism. The BrkA **passenger** (grey hatched box + red + blue) is predicted to form a 19-24 rung β-helix structure similar to pertactin (1DAB). Efforts to solve the crystal structure of the BrkA passenger domain are currently underway (Lily Zhao, Fernandez lab). The passenger domain mediates the two known functions of BrkA: serum resistance and adherence. The mechanism by which BrkA mediates these functions is currently under investigation. A conserved region located at the C-terminus of the BrkA passenger has been termed the junction (red and blue). Although this region is not required for the activity of the translocation unit itself, it appears to play an important role in the secretion and folding of the native BrkA passenger. Two sub-domains with distinct, but probably interrelated, functions have been identified: the autochaperone domain (red, located at the N-terminus) and the hydrophobic secretion facilitator (HSF) domain (blue, located at the C-terminus). The autochaperone domain is thought to promote passenger folding as it emerges on the cell surface. The HSF domain is required for efficient secretion of a folding competent passenger. A model describing the functions of the the autochaperone and HSF domains during BrkA secretion is presented in Fig 3-15. Scissors denote cleavage sites. The BrkA accession number is AAA51646

5.1.1 Targeting to the inner membrane

All known autotransporters encode an N-terminal signal peptide that contains the orthodox information required for targeting to the Sec translocon (an N-, H- and C-domain). In addition to these features, many (but not all) autotransporters bear signal peptides with an N-terminal extension. It has long been proposed that this extension might influence the route of targeting to the inner membrane, possibly by engaging signal recognition particle (SRP) to facilitate co-translational translocation via the Sec translocase (which accommodates only unfolded protein substrates) (Henderson *et al.*, 1998). The alternative route for inner membrane targeting involves the cytosolic chaperone SecB that pilots proteins to the inner membrane in an unfolded conformation. Arguably, targeting via SRP could be an efficient mechanism for exporting very large passenger proteins that could potentially exceed the chaperone capacity of SecB and thus be prone to aggregation, proteolysis, and/or premature folding in the cytoplasm (Sijbrandi *et al.*, 2003). Although a reasonable hypothesis, SRP targeting had been demonstrated only for integral inner membrane proteins (Driessen *et al.*, 2001). Recently, Sijbrandi *et al.* have shown that secretion of the *E. coli* autotransporter Hbp involves SRP, thus becoming the first example of a secreted protein to this cytosolic targeting pathway (Sijbrandi *et al.*, 2003). The observation that Hbp encodes an N-terminal extension that is conserved in a number of autotransporter proteins led to the suggestion that this feature might be important for engaging SRP (Sijbrandi *et al.*, 2003). More recently however, Peterson *et al.* (2003) have dissected the signal peptide of EspP and shown that the hydrophobicity of its H-domain, rather than the presence of the N-terminal extension, is the primary determinant for targeting via SRP. These authors suggest, however, that the

presence of the N-terminal extension may play a role in cytosolic targeting, perhaps by "fine-tuning" the interaction with SRP (e.g. by increasing its affinity for SRP relative to SecB) (Peterson *et al.*, 2003). Further, Brandon *et al.* (2003) have shown that the *Shigella* autotransporter IcsA is targeted to the inner membrane via SecB, presumably in a post-translational manner. IcsA encodes a 52 amino acid signal peptide with a non-conserved N-terminal extension. N-terminal extensions seen in other secreted proteins have been proposed either to slow cytoplasmic protein folding by an as yet uncharacterized mechanism (Liu *et al.*, 1989). Perhaps the N-terminal extensions observed in autotransporter proteins that use SecB (such as IcsA) function in this manner. The role of the non-conserved N-terminal extension in the BrkA signal peptide has not yet been investigated (Fig. 5-1). In this regard, it is worth noting that experiments to distinguish between SRP and SecB targeting routes are non-trivial since these systems display a remarkable degree of functional flexibility (Froderberg *et al.*, 2003). For example, while SRP-mediated and SecB-mediated targeting are favoured for Hbp (Sijbrandi *et al.*, 2003) and IcsA (Brandon *et al.*, 2003), respectively, neither study could rule out the possibility that the other pathway could be utilized. Thus, the exact role of the N-terminal extensions observed in the signal peptides of many autotransporter proteins remains to be determined. Finally, it is also worth mentioning that no examples exist of autotransporters exported via the twin arginine translocase (Tat). It would be interesting to determine whether autotransporters engineered with Tat-dependent (i.e. Sec avoidance) signal peptides can be surface expressed, especially since the Tat system is thought to only recognize and translocate folded proteins (DeLisa *et al.*, 2003) (Berks *et al.*, 2000).

5.1.2 Translocation across the inner membrane and transit through the periplasm

Translocation of unfolded proteins across the inner membrane via the ATP-dependent Sec translocon proceeds in an N-terminal to C-terminal orientation. The function of the Sec translocon represents an area of vigorous and detailed study (Economou, 2002; Van den Berg *et al.*, 2004) and will not be discussed in detail here. However, with respect to autotransporter secretion, it is worth noting that release from the Sec translocon into the periplasm can be mediated by either signal peptidase I or by lipoprotein signal peptidase (Lsp), the latter depending on the presence of a lipoprotein modification signal within the C-domain of the signal peptide (Fig 1-2). Most autotransporter proteins studied to date (including BrkA) do not encode lipoprotein modification signals and are thus presumed to be released into the periplasm following cleavage by signal peptidase I. Autotransporters that encode lipoprotein modification motifs include NalP of *Neisseria meningitides* (van Ulsen *et al.*, 2003), SphB1 of *B. pertussis* (Coutte *et al.*, 2003b) and AlpA of *Helicobacter pylori* (Odenbreit *et al.*, 1999). In order to preserve the continuity of this discussion, aspects of lipoprotein modification relating to autotransporter secretion are presented in Appendix A.2. It is worth bearing in mind however, that processing and modification of autotransporters containing lipoprotein modification signals could influence (i) the route of trafficking though the periplasm, (ii) β-domain assembly in the outer membrane, (iii) the mechanism of translocation across the outer membrane, and (iv) passenger anchoring to the inner leaflet of the outer membrane (Appendix A.2).

Proteins entering the periplasm are presumably protected from misfolding, aggregation and proteolysis by resident chaperones (e.g. Skp, SurA, DegP) that interact with the incoming polypeptide as it emerges from the Sec translocon. The multidomain nature of autotransporter proteins suggests that distinct chaperones might be required for efficient secretion of individual functional modules (e.g. β-domain vs. passenger domain).

It is conceivable that the autotransporter β-domain is routed through the periplasm in a manner similar to what has been proposed for outer membrane protein biogenesis. The current model of outer membrane protein biogenesis (Kleinschmidt, 2003; Voulhoux and Tommassen, 2004) suggests that (i) in the periplasm, the chaperone Skp interacts with incoming polypeptides to maintain a soluble "folding competent" conformation, (ii) during transit through the periplasm, the polypeptide interacts with soluble lipopolysaccharide to enhance folding and (iii) an interaction with the conserved outer membrane protein Omp85 facilitates β-barrel assembly and folding into the outer membrane. Whether autotransporters follow a similar pathway for β-domain insertion and assembly remains to be determined. In this regard, it has been shown that depletion of Omp85 in *Neisseria meningitides* abrogates processing of the IgA protease β-domain (Voulhoux *et al.*, 2003), although its exact role in autotransporter secretion remains to be elucidated.

The hypothesis that folding of native autotransporter passengers involves the junction domain (located at its C-terminus) (Oliver *et al.*, 2003b) suggests that the N-terminus of the passenger would be unfolded and thus susceptible to proteolysis in the periplasm, at

least until the junction region (autochaperone) and the β-domain emerge from the Sec translocon. Moreover, the fact that an unfolded BrkA passenger can be surface expressed indicates that passenger folding is not a prerequisite for secretion (Oliver *et al.*, 2003b). This implies that mechanisms probably exist to protect the passenger domain from proteolysis in the periplasm. Intriguingly, an unfolded β-helix structure would have a similar amphipathic character as an unfolded outer membrane protein (OMP) (i.e. alternating hydrophobic / hydrophilic residues). Thus, it is tempting to speculate that autotransporter passengers predicted (e.g. BrkA, AIDA-I (Kajava *et al.*, 2001), Ag43 (Kajava *et al.*, 2001; Klemm *et al.*, 2004)) or known (e.g. pertactin (Emsley *et al.*, 1996)) to form β-helices might engage general periplasmic chaperones in a manner similar to OMP's. It has been demonstrated that both folding and secretion of native (Brandon and Goldberg, 2001) (Purdy *et al.*, 2002) and non-native (Veiga *et al.*, 2004) (Klauser *et al.*, 1990) passengers can be mediated by periplasmic chaperones. Exactly how (or whether) each of these chaperones influences the autotransporter secretion process remains to be determined. It is worth noting that, similar to the problem of inner membrane targeting, experimentally unraveling protein folding in the periplasm is complicated by the existence of parallel chaperone pathways that display a degree of functional redundancy (Rizzitello *et al.*, 2001). It is also possible that autotransporter passengers protect themselves from proteolysis by adopting a folded or at least partially folded conformation within the periplasm (possibly in conjunction with a periplasmic chaperone). As mentioned previously, Brandon and Goldberg have observed a proteinase K resistant form of IcsA in periplasmic extracts (Brandon and Goldberg, 2001). However, whether this structure represents the translocation competent form of IcsA was not determined. In

this regard, the model of BrkA secretion presented in Chapter 3 (Fig. 3-15) proposes that the hydrophobic secretion facilitator (HSF) domain (Velarde and Nataro, 2004) plays a critical role in the secretion of a folding competent autotransporter passenger. The model suggests that a *trans* acting periplasmic factor could interact with the HSF domain to either (i) prevent premature passenger folding in the periplasm mediated by the autochaperone domain, or (ii) permitting passenger unfolding as translocation across the membrane occurs (discussed further below). It is also conceivable that the HSF domain could act in an intramolecular manner, perhaps in concert with the translocation unit, to promote passenger unfolding prior to (or concurrent with) translocation across the outer membrane. Clearly, more research is required to elucidate the folding state of autotransporters during transit through the periplasm.

5.1.3 Outer Membrane Translocation: Working Models

A defining feature of the autotransporter secretion system is the self-mediated process of passenger translocation across the outer membrane. Two primary models have been proposed that attempt to take into account several lines of experimental evidence: (i) the hairpin model (Klauser *et al.*, 1993) and (ii) the central pore model (Veiga *et al.*, 2002). Recently, a third model of autotransporter secretion has been proposed suggesting that the conserved outer membrane protein Omp85 might serve as the channel for passenger translocation (rather than the autotransporter translocation unit) (Oomen *et al.*, 2004). However, to date, no compelling experimental evidence has been provided to directly support or test the "Omp85 autotransporter secretion" model so it will be left for another discussion.

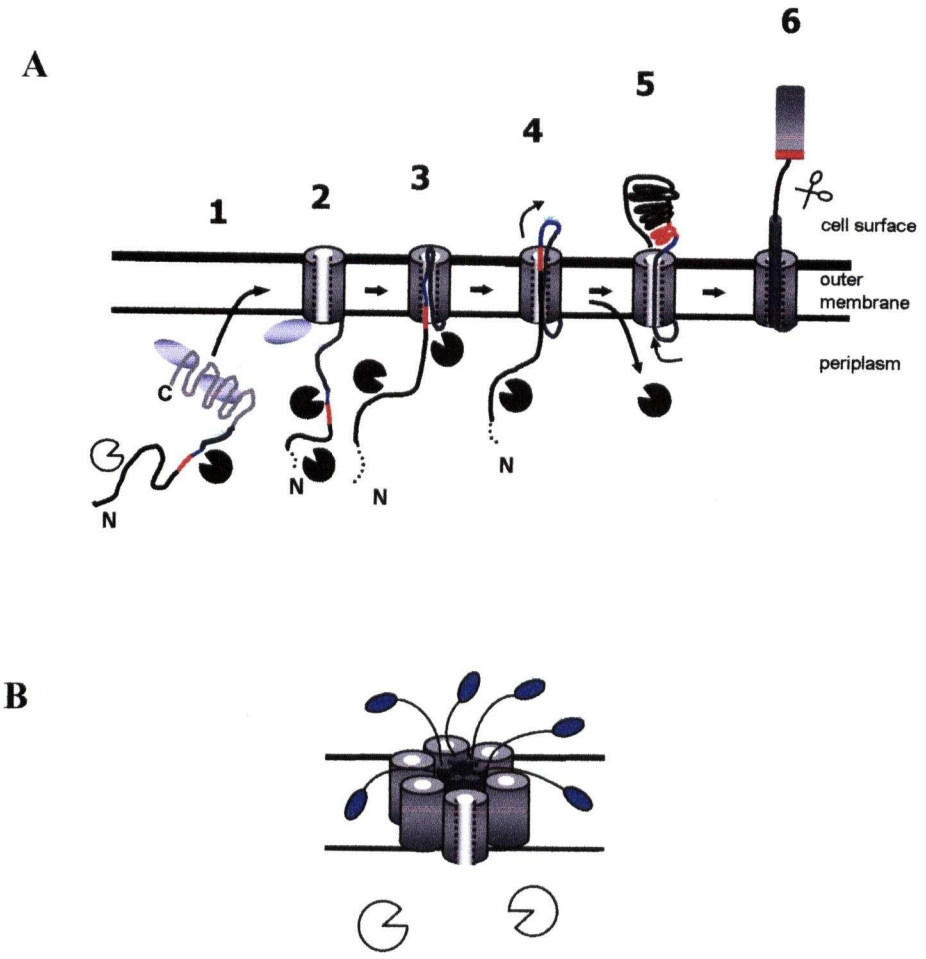

Fig. 5-2. Models of autotransporter secretion.
A. The hairpin model: described in main text. Translocation unit (β-core + linker) shown as a grey cylinder and line. Junction region comprised of autochaperone (red) and hydrophobic secretion facilitator (blue). Passenger (black line). Putative periplasmic chaperones are shown as white and black pies and grey ovals. Although the linker is shown to insert into membrane bound β-core (step 2), it is also conceivable that the linker region could fold into the β-core (as depicted in step 3) prior to, or concurrent with, membrane insertion (i.e. omit step 2). **B.** The central pore model: described in main text. Individual translocation units shown as a grey cylinders. As depicted, central secretion channel formed by 6 translocation units. Folded passengers are depicted as blue ovals. Putative periplasmic chaperones depicted as white pies.

(i) The hairpin model represents an adaptation (Ohnishi and Horinouchi, 1996) (Oliver *et al.*, 2003b) (Oomen *et al.*, 2004) of the original two-step model of IgA protease secretion (Klauser *et al.*, 1992) (Pohlner *et al.*, 1987). As depicted in Fig. 5-2A, following export into the periplasm (step 1), the β-core inserts into the outer membrane forming a β-barrel structure (step 2). The core of the β-barrel forms a hydrophilic conduit through which the passenger is extruded. The α-helical linker region inserts into the channel forming a temporary hairpin structure that facilitates movement of the passenger region across the outer membrane (step 3). Translocation of the unfolded or partially folded passenger proceeds vectorially in a C-terminal to N-terminal direction. Passenger folding occurs after or concurrent with translocation across the outer membrane (steps 4 and 5). Finally, the linker region adopts an α-helical conformation to close the channel (step 6). This is proposed to happen after passenger transit, since the channel size (1 nm based on the structure of NalP Asp^{777}-Phe^{1084}) would accommodate a maximum of only two unfolded polypeptide strands or a single folded α-helix segment (see Fig. 1-2) (Oomen *et al.*, 2004).

The proposed functions of the BrkA junction region can be incorporated into this model. As discussed above (and in Fig. 3-15), the HSF domain might prevent premature passenger folding in the periplasm (or facilitate unfolding prior to translocation) perhaps via interaction with a periplasmic chaperone or with the β-domain itself. At the cell surface, the autochaperone would initiate passenger folding as the nascent chain emerges from the channel (Fig. 3-13) (Ohnishi *et al.*, 1994) (Oliver *et al.*, 2003b).

While this model appears to be consistent with the structure of NalP (Asp^{777}-Phe^{1084}) depicting the α-helical linker region embedded within the channel formed by the β-domain, its obvious weakness is that it does not explain how folded proteins are secreted. How could a non-native folded structure with a diameter of 2 nm (e.g. an immunoglobulin domain) be translocated through a 1 nm pore (e.g. NalP Asp^{777}-Phe^{1084})? A possible explanation is that diameter of the channels vary between autotransporters. In this scenario, the channel formed by the NalP (Asp^{777}-Phe^{1084}) translocator would simply be smaller than the channel formed by the translocator of an autotransporter that can secrete folded structures (e.g. IgA protease (Veiga *et al.*, 2004), Ag43 (Kjaergaard *et al.*, 2000)). The biophysical measurements of channels formed by BrkA, IgA protease and PalA (~ 2nm) and NalP (~ 1 nm) are consistent with this theory. The size of the channel formed by the β-barrel would increase if (ι) additional β-strands (e.g. 12 vs. 14) were incorporated, or (ii) by increasing the shear number (i.e. the angle of the β-strands relative to the plane of the membrane) (Schulz, 2003). It is also worth noting that NalP does not share sequence identity with BrkA, IgA protease and PalA, and clusters phylogenetically with a separate group of autotransporters (that includes PrtS and SphB1) (Yen *et al.*, 2002), supporting the idea that the structures of these autotransporters could be different. Further, the fact that NalP and SphB1 are N-terminally lipidated during secretion may influence the route of targeting and sorting in the periplasm as well as the mechanism of translocation across the outer membrane (discussed in Appendix A.2). On the other hand, the hypothesis that autotransporter β-domains form different sized channels can be challenged by the observation the α-helical linker region is a conserved structural feature of the translocation unit (Oliver *et al.*, 2003a) (Desvaux *et al.*, 2004).

Thus, it is conceivable that this feature inserts into the β-barrel of other autotransporters (e.g. BrkA, IgA protease and PalA) in a similar manner to what is observed for NalP(Asp^{777}-Phe^{1084}). It seems unlikely that an α-helix with a diameter of approximately 1 nm would "plug" a 2 nm channel, however the participation of extracellular loops or bulky side chains should not be ruled out. Additional structures of autotransporter translocator domains are required to resolve this issue.

(ii) The central pore model accommodates the translocation of folded structures (Veiga *et al.*, 2002). In this model (Fig. 5-2B), the β-cores insert into the outer membrane to form a ring-shaped structure of six or more β-domains with a central channel of ~ 2 nm that allows the secretion of each passenger domain in a pre-folded conformation segment (see Fig. 1-2).

The central pore model is supported by the observation of high molecular weight complexes formed by the β-domain of IgA protease. Gel filtration analysis of the BrkA passenger domain indicates a monomer, however the quaternary structure of the BrkA β-domain has not yet be addressed. The availability of a recombinant form of the BrkA β-domain that has the capacity to form 3.2 nanoSieman (~2 nm) channels in artificial membranes (Shannon and Fernandez, 1999) presents an obvious resource to address this question. The notion of a homo-oligomeric secretion complex formed by several autotransporter β-domain subunits presents a possible explanation for the observation that BrkA(ΔGlu^{601}-Ala^{692}) passenger folding can occur in *trans* by co-expressing BrkA(ΔAla^{52}-Pro^{600}) as a separate polypeptide (Fig. 3-13C). Using a set of chimeras, we

have shown that homologous β-domains are not required for *trans* complementation of BrkA passenger folding (Chapter 4). These data do not rule out the possibliliy that a homo-oligomeric, or even a hetero-oligomeric, secretion complex could exist. The chimera constructs described in Chapter 4 represent valuable tools to compare the properties of the IgA protease, BrkA and pertactin β-domains both *in vivo* and *in vitro*. However, the fact that the BrkA and pertactin passengers are cleaved from the β-domain (whereas IgA protease is not) complicates side-by-side comparisons. This issue could be overcome by inserting an epitope tag at the extreme C-terminus of the β-domain of each construct. It has been shown that a 6xHis tag preceded by a glycine linker region does not affect BrkA (M. Kramar and R. Fernandez, unpublished observations) or IgA protease (Strauss *et al.*, 1995) β-domain insertion.

While the idea of a common 2 nm channel formed by several translocation units provides a possible solution to the problem of exporting folded structures, this model raises several questions. What is the nature of channel? If several translocation units form the channel then how are lipids displaced and how is a hydrophilic conduit created. One possibility is that each of the linker regions positions itself into the central cavity to create a hydrophilic channel (as shown in Fig. 5-2B), however this scenario appears to be inconsistent with the NalP (Asp^{777}-Phe^{1084}) structure depicting the linker region within the β-barrel (Fig. 1-2). Further, (as discussed above) if passenger folding occurs in the periplasm prior to translocation then it seems unlikely that folding would be initiated from the its C-terminus via the junction, especially since translocation across the inner membrane into the periplasm (via Sec) proceeds in an N- to C-terminal orientation. One

also wonders how translocation of multiple passengers through a common pore would be coordinated – or as Lee and Byun have put it "how is thronging of the pore avoided?" (Lee and Byun, 2003). In this regard, it is possible that translocation could proceed through the central pore in sequential fashion. In this scenario, one could envision the existence of periplasmic or outer membrane chaperones that orchestrate the assembly and translocation processes. In this regard, information encoded with the junction region (e.g. the HSF domain) could perhaps participate in this process by preventing (or permitting unfolding) of native passengers prior to translocation and promote passenger folding on the cell surface (eg. the autochaperone domain) similar to what has been proposed for the hairpin model.

5.1.5 What is the driving force for translocation across the outer membrane?

An open (and fundamental) question that remains to be addressed is the source of free energy driving passenger translocation across the outer membrane. The absence of (known) ATP dependent processes in the periplasm and the presence of opens channels (porins) in the outer membrane make it seem unlikely that this process is driven by ATP or by a proton motive force. Based on the assumption that translocation occurs in an unfolded conformation, it has been suggested that passenger folding and hydration on the cell surface may yield free energy to drive translocation. However, the observation that an unfolded BrkA passenger can be surface expressed in a protease sensitive (unfolded) conformation argues against passenger folding as the primary source of free energy in this reaction. On the other hand, the observation that secretion efficiency is linked to the presence of the junction domain (Velarde and Nataro, 2004) suggests that passenger

folding mediated by the autochaperone and/or a function or interaction of the HSF domain could contribute free energy to drive translocation. Further, Velarde and Nataro have also suggested that folding of the β-barrel domain into the outer membrane might provide free energy required to drive passenger translocation across the outer membrane (Velarde and Nataro, 2004).

Another possible mechanism that has not yet been discussed in the literature is the possibility that passenger translocation may be driven by Brownian motion, similar to what has been proposed for the mitochondrial import system (Neupert and Brunner, 2002). In this system, polypeptides are translocated from the cytocol in the mitochondial matrix via the Tom and Tim complexes that are embedded within the outer and inner membranes, respectively. Incoming polypeptides engage the Tom complex via self-encoded presequences and local (rather than global) unfolding of the incoming protein is mediated by cytosolic chaperones and by the Tom40 β-barrel channel (Esaki *et al.*, 2003; Voos, 2003). Polypeptides are translocated in an unfolded or partially folded conformation and energy for this process is derived from the random molecular motion of the polypeptide within the channel. The chaperone Hsp70 (SSC1) applies a directional force by trapping the incoming polypeptide on the *trans* side of the membrane to prevent "backsliding" into the cytoplasmic compartment (Liu *et al.*, 2003). Notably, this system has been shown to translocate both unfolded and folded structures (folded structures unfold prior to translocation) (Matouschek *et al.*, 1997) (Okamoto *et al.*, 2002).

By analogy, for autotransporter secretion it is conceivable that positioning of the linker region with the channel formed by the β-barrel could orient the C-terminus of the passenger towards the cell surface such that random molecular motion associated with the incoming polypeptide is rendered directional (i.e. toward the cell surface). It is worth noting that (i) insertion of the linker region could occur concomitantly with folding of the β-barrel into the outer membrane (Fig. 5-2, step 3), rather that following insertion of the β-barrel into the outer membrane (Fig. 5-2, step 2), and (ii) that the channel could be formed by a monomer or multimer, as has been proposed for the hairpin and central pore models, respectively (Fig 5-2 A and B). Local unfolding of the folded (or partially folded) passenger could be facilitated by an interaction with a periplasmic chaperone (perhaps in conjunction with the HSF domain) and/or possibly by the β-barrel itself (similar to Tom40 (Voos, 2003)). In the model of mitochondrial protein import, the distinction between local protein unfolding and global protein unfolding is critical. It is thought that unfolding of a small region of a passenger (or "breathing") is sufficient to trigger a cascade of local unfolding events as translocation proceeds (Matouschek, 2003) – perhaps a working definition of the elusive "translocation competent" folding state. Interestingly, it has been shown that folded structures, including tightly folded immunoglobulin domains (Okamoto *et al.*, 2002) and polypeptides containing disulphide bonds (Schwartz *et al.*, 1999), can be translocated by the mitochondrial import system due to local unfolding events. Comparatively, it is tempting to speculate that the folded immunoglobulin domains employed by Veiga *et al.* to probe the structural constraints of the IgA protease secretion process might also be capable of adopting a locally unfolded or "translocation competent" conformation (Veiga *et al.*, 2004). It is also worth

mentioning that local unfolding of mitochondrial preproteins prior to translocation is initiated from the N-terminus and that the overall stability of the protein is dependent on the nature of the N-terminal sequence since this serves as the initiating point for unfolding during import (Huang *et al.*, 1999). In this regard, Huang *et al.* have suggested that even the most stable proteins could be unfolded by the mitochondrial translocase if the N-terminus is positioned appropriately (i.e. exposed at the surface of the protein). Similarily, the autotransporter HSF domain might act as a C-terminal motif to interact with the translocation unit to facilitate unfolding of the passenger domain. In this scenario, deletion of the HSF domain would prevent passenger unfolding and translocation would arrest; a prediction consistent with our current data and working model (Fig. 3-15). Lastly, at the cell surface, folding of the passenger (triggered by the autochaperone region) might contribute additional free energy to drive the reaction forward, while forming a stable "plug" to prevent "backsliding" of the polypeptide into the periplasm.

While this model provides a possible explanation for the source of free energy to drive translocation, as well as an explanation of how both folded and unfolded structures are translocated, it is somewhat difficult to test using *in vivo* systems. In the field of mitochondrial protein import, significant advances have been made using *in organellar* systems where protein translocation can be manipulated biochemically and studied kinetically from an outside-in perspective. By contrast, bacterial secretion presents an inside-out problem where the periplasmic environment is less easy to manipulate. Thus, it is likely that testing of this and other models of autotransporter secretion will require the

establishment of *in vitro* membrane systems that enable researchers to elucidate critical translocation intermediates, such as protein folding/unfolding events.

5.1.6 At the surface: the final station and destinations beyond...

Following translocation across the outer membrane the fate of the passenger domains diverge (Section 1.1.5). While most autotransporters undergo cleavage to yield the α- and β-domains, the significance of this event (if any) with respect to the secretion process remains to be determined. As illustrated in Chapter 4, cleavage is not essential for surface expression and folding (*in trans*) of a junction-deleted BrkA passenger fused to the IgA protease translocation unit. For native BrkA secretion, the observation that (i) following cleavage the α-domain remains tightly associated with the cell surface when expressed in *B. pertussis* and *E. coli* and (ii) that the BrkA α-domain can be co-immunoprecipitated with the β-domain, strongly suggests that these species interact *in vivo*. Overlapping deletion analysis suggests that the region responsible for anchoring the BrkA passenger to the cell surface resides within the extreme N-terminus (residues 43-51) or within the C-terminal linker region (residues 693-731). Experiments using heterologous passengers are currently underway to define the BrkA anchoring mechanism. In this regard, it is tempting to speculate that BrkA passenger anchoring to the cell surface may be required to observe *trans* complementation of BrkA passenger folding mediated by the junction domain. By comparison, for autotransporters that are released from the cell surface, it may be difficult to observe *trans* complementation of passenger folding mediated by the junction region since the polypeptides are not anchored (or co-localized) at the outer membrane.

Like many other autotransporters, the protease activity responsible for releasing the BrkA passenger from the β-domain is not yet known. Once the protease mediating BrkA cleavage has been identified, it would be interesting to determine whether this is the mechanism common to other autotransporters. Finally, the thrifty and versatile nature of the autotransporter secretion system could be viewed as an effective strategy for delivering a variety of proteins to the cell surface that could potentially engage in intermolecular interactions with other proteins (including other autotransporters). These interactions might facilitate processes such as protein maturation and macromolecular assembly. Indeed, examples currently exist of autotransporters that mediate processing of proteins at the cell surface (Coutte *et al.*, 2001; Coutte *et al.*, 2003a; Fink *et al.*, 2001; van Ulsen *et al.*, 2003). The biological significance and the regulation of these interactions with respect to the biogenesis of the "outer membrane proteome" and virulence of bacterial pathogens will be an area of interesting study. As discussed briefly in Chapter 4, a better understanding of these interactions could be useful in engineering novel surface display strategies for biotechnological purposes.

5.2 Future directions in BrkA secretion

Research in the autotransporter field is now well underway and interest in this remarkable family of proteins has increased significantly in recent years. New insights have raised many questions that represent intriguing avenues for future studies. BrkA is now well established as a model system to contribute to the next phase of discovery and can now be viewed as a multidomain protein. Many of the questions associated with the function of its modules (e.g. signal peptide, passenger, autochaperone, HSF domain, linker region and β-core) have been described in the preceding sections. A key advance that has come out of these studies is the discovery and initial characterization of the BrkA "junction" domain. Indeed, understanding how BrkA passenger folding is coordinated with secretion will certainly be an area of important and stimulating research. The model (Fig. 3-13 and 3-15) of native autotransporter passenger secretion involving the autochaperone and HSF domain represents an attractive hypothesis that now needs to be tested. The hypothesis that the HSF domain is required for secretion of a folding-competent native BrkA passenger suggests that passenger translocation occurs in an unfolded or partially folded conformation. Working within the context of this model, determining how the HSF domain prevents passenger folding (or permits unfolding) in the periplasm would represent a significant advance. Further, the availability of a passenger that is inefficiently translocated in the absence of the HSF domain provides a useful tool, a "molecular stopper" if you will, that could be used in conjunction with flexible linker regions and epitope tags to probe the orientation of translocation. In addition, this type of approach may yield translocation intermediates that could shed light on the nature of the channel through which the passenger transits, especially if coupled with three-

dimensional structural data. A better understanding of the mechanism by which the autochaperone initiates BrkA passenger folding could provide a useful model to understand autotransporter secretion as well as protein folding in general. Kinetic analyses of folding intermediates using stopped flow methods could be used to test the hypothesis that BrkA passenger folding occurs in a C- to N-terminal direction. *In vitro* refolding experiments and *in vivo trans* complementation of folding experiments could be used in tandem to identify (and distinguish between) key residues within the BrkA junction region involved in (i) passenger folding, (ii) passenger surface expression and (iii) interactions between the junction region and the passenger. It would also be interesting to determine whether folding of all (or other) autotransporter passengers occurs via an autochaperone domain. Finally, the nature of the autotransporter secretion system suggests that the functional evolution of the substrate (passenger) and the secretion system (translocation unit) are linked. In this regard, it would be interesting to test whether domain modules are interchangeable between different autotransporters.

5.3 Practical potential

Autotransporters have been touted as promising systems for surface displaying heterologous proteins (Jose *et al.*, 2001; Kjaergaard *et al.*, 2000; Lattemann *et al.*, 2000; Maurer *et al.*, 1997; Shimada *et al.*, 1994; Valls *et al.*, 2000). The native passengers have evolved to be efficiently expressed using this mechanism and it stands to reason that a better understanding of the process of secretion of native passengers including the mechanism by which the junction folds passengers will allow the better design of surface display strategies for producing functional heterologous proteins. The surface location

of autotransporters has made some of them attractive candidates for vaccines (Hadi *et al.*, 2001; Oliver and Fernandez, 2001; Roberts *et al.*, 1992; van Ulsen *et al.*, 2001). We have shown that the BrkA passenger domain can be refolded *in vitro* from inclusion bodies. The conservation of the junction suggests that it may be possible to produce other autotransporters in a similar manner, at minimal cost. Finally, many autotransporters are known or proposed to be virulence factors. Inhibitors of the folding mechanism may provide a possible therapeutic approach to block colonization by limiting the ability of the autotransporter to express functional virulence factors.

5.4 References

Berks, B.C., Sargent, F., and Palmer, T. (2000) The Tat protein export pathway. *Mol Microbiol* **35**: 260-274.

Brandon, L.D., and Goldberg, M.B. (2001) Periplasmic transit and disulfide bond formation of the autotransported *Shigella* protein IcsA. *J Bacteriol* **183**: 951-958.

Brandon, L.D., Goehring, N., Janakiraman, A., Yan, A.W., Wu, T., Beckwith, J., and Goldberg, M.B. (2003) IcsA, a polarly localized autotransporter with an atypical signal peptide, uses the Sec apparatus for secretion, although the Sec apparatus is circumferentially distributed. *Mol Microbiol* **50**: 45-60.

Coutte, L., Antoine, R., Drobecq, H., Locht, C., and Jacob-Dubuisson, F. (2001) Subtilisin-like autotransporter serves as maturation protease in a bacterial secretion pathway. *Embo J* **20**: 5040-5048.

Coutte, L., Alonso, S., Reveneau, N., Willery, E., Quatannens, B., Locht, C., and Jacob-Dubuisson, F. (2003a) Role of adhesin release for mucosal colonization by a bacterial pathogen. *J Exp Med* **197**: 735-742.

Coutte, L., Willery, E., Antoine, R., Drobecq, H., Locht, C., and Jacob-Dubuisson, F. (2003b) Surface anchoring of bacterial subtilisin important for maturation function. *Mol Microbiol* **49**: 529-539.

DeLisa, M.P., Tullman, D., and Georgiou, G. (2003) Folding quality control in the export of proteins by the bacterial twin-arginine translocation pathway. *Proc Natl Acad Sci U S A* **100**: 6115-6120.

Desvaux, M., Parham, N.J., and Henderson, I.R. (2004) The autotransporter secretion system. *Res Microbiol* **155**: 53-60.

Driessen, A.J., Manting, E.H., and van der Does, C. (2001) The structural basis of protein targeting and translocation in bacteria. *Nat Struct Biol* **8**: 492-498.

Economou, A. (2002) Bacterial secretome: the assembly manual and operating instructions (Review). *Mol Membr Biol* **19**: 159-169.

Emsley, P., Charles, I.G., Fairweather, N.F., and Isaacs, N.W. (1996) Structure of *Bordetella pertussis* virulence factor P.69 pertactin. *Nature* **381**: 90-92.

Esaki, M., Kanamori, T., Nishikawa, S., Shin, I., Schultz, P.G., and Endo, T. (2003) Tom40 protein import channel binds to non-native proteins and prevents their aggregation. *Nat Struct Biol* **10**: 988-994.

Fink, D.L., Cope, L.D., Hansen, E.J., and Geme, J.W., 3rd (2001) The *Hemophilus influenzae* Hap autotransporter is a chymotrypsin clan serine protease and undergoes autoproteolysis via an intermolecular mechanism. *J Biol Chem* **276**: 39492-39500.

Froderberg, L., Houben, E., Samuelson, J.C., Chen, M., Park, S.K., Phillips, G.J., Dalbey, R., Luirink, J., and De Gier, J.W. (2003) Versatility of inner membrane protein biogenesis in *Escherichia coli*. *Mol Microbiol* **47**: 1015-1027.

Hadi, H.A., Wooldridge, K.G., Robinson, K., and Ala'Aldeen, D.A. (2001) Identification and characterization of App: an immunogenic autotransporter protein of Neisseria meningitidis. *Mol Microbiol* **41**: 611-623.

Henderson, I.R., Navarro-Garcia, F., and Nataro, J.P. (1998) The great escape: structure and function of the autotransporter proteins. *Trends Microbiol* **6**: 370-378.

Huang, S., Ratliff, K.S., Schwartz, M.P., Spenner, J.M., and Matouschek, A. (1999) Mitochondria unfold precursor proteins by unraveling them from their N-termini. *Nat Struct Biol* **6**: 1132-1138.

Jose, J., Bernhardt, R., and Hannemann, F. (2001) Functional display of active bovine adrenodoxin on the surface of E. coli by chemical incorporation of the [2Fe-2S] cluster. *Chembiochem* **2**: 695-701.

Kajava, A.V., Cheng, N., Cleaver, R., Kessel, M., Simon, M.N., Willery, E., Jacob-Dubuisson, F., Locht, C., and Steven, A.C. (2001) Beta-helix model for the filamentous haemagglutinin adhesin of Bordetella pertussis and related bacterial secretory proteins. *Mol Microbiol* **42**: 279-292.

Kjaergaard, K., Schembri, M.A., Hasman, H., and Klemm, P. (2000) Antigen 43 from Escherichia coli induces inter- and intraspecies cell aggregation and changes in colony morphology of *Pseudomonas fluorescens*. *J Bacteriol* **182**: 4789-4796.

Klauser, T., Pohlner, J., and Meyer, T.F. (1990) Extracellular transport of cholera toxin B subunit using *Neisseria* IgA protease beta-domain: conformation-dependent outer membrane translocation. *Embo J* **9**: 1991-1999.

Klauser, T., Pohlner, J., and Meyer, T.F. (1992) Selective extracellular release of cholera toxin B subunit by *Escherichia coli*: dissection of *Neisseria* Iga beta-mediated outer membrane transport. *Embo J* **11**: 2327-2335.

Klauser, T., Pohlner, J., and Meyer, T.F. (1993) The secretion pathway of IgA protease-type proteins in gram-negative bacteria. *Bioessays* **15**: 799-805.

Kleinschmidt, J.H. (2003) Membrane protein folding on the example of outer membrane protein A of Escherichia coli. *Cell Mol Life Sci* **60**: 1547-1558.

Klemm, P., Hjerrild, L., Gjermansen, M., and Schembri, M.A. (2004) Structure-function analysis of the self-recognizing Antigen 43 autotransporter protein from *Escherichia coli*. *Mol Microbiol* **51**: 283-296.

Lattemann, C.T., Maurer, J., Gerland, E., and Meyer, T.F. (2000) Autodisplay: functional display of active beta-lactamase on the surface of Escherichia coli by the AIDA-I autotransporter. *J Bacteriol* **182**: 3726-3733.

Lee, H.W., and Byun, S.M. (2003) The pore size of the autotransporter domain is critical for the active translocation of the passenger domain. *Biochem Biophys Res Commun* **307**: 820-825.

Liu, G., Topping, T.B., and Randall, L.L. (1989) Physiological role during export for the retardation of folding by the leader peptide of maltose-binding protein. *Proc Natl Acad Sci U S A* **86**: 9213-9217.

Liu, Q., D'Silva, P., Walter, W., Marszalek, J., and Craig, E.A. (2003) Regulated cycling of mitochondrial Hsp70 at the protein import channel. *Science* **300**: 139-141.

Maurer, J., Jose, J., and Meyer, T.F. (1997) Autodisplay: one-component system for efficient surface display and release of soluble recombinant proteins from Escherichia coli. *J Bacteriol* **179**: 794-804.

Matouschek, A., Azem, A., Ratliff, K., Glick, B.S., Schmid, K., and Schatz, G. (1997) Active unfolding of precursor proteins during mitochondrial protein import. *Embo J* **16**: 6727-6736.

Matouschek, A. (2003) Protein unfolding--an important process in vivo? *Curr Opin Struct Biol* **13**: 98-109.

Neupert, W., and Brunner, M. (2002) The protein import motor of mitochondria. *Nat Rev Mol Cell Biol* **3**: 555-565.

Odenbreit, S., Till, M., Hofreuter, D., Faller, G., and Haas, R. (1999) Genetic and functional characterization of the alpAB gene locus essential for the adhesion of Helicobacter pylori to human gastric tissue. *Mol Microbiol* **31**: 1537-1548.

Ohnishi, Y., Nishiyama, M., Horinouchi, S., and Beppu, T. (1994) Involvement of the COOH-terminal pro-sequence of *Serratia marcescens* serine protease in the folding of the mature enzyme. *J Biol Chem* **269**: 32800-32806.

Ohnishi, Y., and Horinouchi, S. (1996) Extracellular production of a *Serratia marcescens* serine protease in Escherichia coli. *Biosci Biotechnol Biochem* **60**: 1551-1558.

Okamoto, K., Brinker, A., Paschen, S.A., Moarefi, I., Hayer-Hartl, M., Neupert, W., and Brunner, M. (2002) The protein import motor of mitochondria: a targeted molecular ratchet driving unfolding and translocation. *Embo J* **21**: 3659-3671.

Oliver, D.C., and Fernandez, R.C. (2001) Antibodies to BrkA augment killing of Bordetella pertussis. *Vaccine* **20**: 235-241.

Oliver, D.C., Huang, G., and Fernandez, R.C. (2003a) Identification of secretion determinants of the *Bordetella pertussis* BrkA autotransporter. *J Bacteriol* **185**: 489-495.

Oliver, D.C., Huang, G., Nodel, E., Pleasance, S., and Fernandez, R.C. (2003b) A conserved region within the *Bordetella pertussis* autotransporter BrkA is necessary for folding of its passenger domain. *Mol Microbiol* **47**: 1367-1383.

Oomen, C.J., Van Ulsen, P., Van Gelder, P., Feijen, M., Tommassen, J., and Gros, P. (2004) Structure of the translocator domain of a bacterial autotransporter. *Embo J* **23**: 1257-1266.

Peterson, J.H., Woolhead, C.A., and Bernstein, H.D. (2003) Basic amino acids in a distinct subset of signal peptides promote interaction with the signal recognition particle. *J Biol Chem* **278**: 46155-46162.

Pohlner, J., Halter, R., Beyreuther, K., and Meyer, T.F. (1987) Gene structure and extracellular secretion of *Neisseria gonorrhoeae* IgA protease. *Nature* **325**: 458-462.

Purdy, G.E., Hong, M., and Payne, S.M. (2002) *Shigella flexneri* DegP facilitates IcsA surface expression and is required for efficient intercellular spread. *Infect Immun* **70**: 6355-6364.

Rizzitello, A.E., Harper, J.R., and Silhavy, T.J. (2001) Genetic evidence for parallel pathways of chaperone activity in the periplasm of *Escherichia coli*. *J Bacteriol* **183**: 6794-6800.

Roberts, M., Tite, J.P., Fairweather, N.F., Dougan, G., and Charles, I.G. (1992) Recombinant P.69/pertactin: immunogenicity and protection of mice against Bordetella pertussis infection. *Vaccine* **10**: 43-48.

Schulz, G.E. (2003) Transmembrane beta-barrel proteins. *Adv Protein Chem* **63**: 47-70.

Schwartz, M.P., Huang, S., and Matouschek, A. (1999) The structure of precursor proteins during import into mitochondria. *J Biol Chem* **274**: 12759-12764.

Shannon, J.L., and Fernandez, R.C. (1999) The C-terminal domain of the *Bordetella pertussis* autotransporter BrkA forms a pore in lipid bilayer membranes. *J Bacteriol* **181**: 5838-5842.

Shimada, K., Ohnishi, Y., Horinouchi, S., and Beppu, T. (1994) Extracellular transport of pseudoazurin of Alcaligenes faecalis in Escherichia coli using the COOH-terminal domain of Serratia marcescens serine protease. *J Biochem (Tokyo)* **116**: 327-334.

Sijbrandi, R., Urbanus, M.L., ten Hagen-Jongman, C.M., Bernstein, H.D., Oudega, B., Otto, B.R., and Luirink, J. (2003) Signal recognition particle (SRP)-mediated targeting and Sec-dependent translocation of an extracellular *Escherichia coli* protein. *J Biol Chem* **278**: 4654-4659.

Strauss, A., Pohlner, J., Klauser, T., and Meyer, T.F. (1995) C-terminal glycine-histidine tagging of the outer membrane protein Iga beta of *Neisseria gonorrhoeae*. *FEMS Microbiol Lett* **127**: 249-254.

Valls, M., Atrian, S., de Lorenzo, V., and Fernandez, L.A. (2000) Engineering a mouse metallothionein on the cell surface of Ralstonia eutropha CH34 for immobilization of heavy metals in soil. *Nat Biotechnol* **18**: 661-665.

Van den Berg, B., Clemons, W.M., Jr., Collinson, I., Modis, Y., Hartmann, E., Harrison, S.C., and Rapoport, T.A. (2004) X-ray structure of a protein-conducting channel. *Nature* **427**: 36-44.

van Ulsen, P., van Alphen, L., Hopman, C.T., van der Ende, A., and Tommassen, J. (2001) In vivo expression of Neisseria meningitidis proteins homologous to the Haemophilus influenzae Hap and Hia autotransporters. *FEMS Immunol Med Microbiol* **32**: 53-64.

van Ulsen, P., van Alphen, L., ten Hove, J., Fransen, F., van der Ley, P., and Tommassen, J. (2003) A *Neisserial* autotransporter NalP modulating the processing of other autotransporters. *Mol Microbiol* **50**: 1017-1030.

Veiga, E., Sugawara, E., Nikaido, H., de Lorenzo, V., and Fernandez, L.A. (2002) Export of autotransported proteins proceeds through an oligomeric ring shaped by C-terminal domains. *Embo J* **21**: 2122-2131.

Veiga, E., de Lorenzo, V., and Fernandez, L.A. (2004) Structural tolerance of bacterial autotransporters for folded passenger protein domains. *Mol Microbiol* **52**: 1069-1080.

Velarde, J.J., and Nataro, J.P. (2004) Hydrophobic residues of the autotransporter EspP linker domain are important for outer membrane translocation of its passenger. *J Biol Chem* **279**: 31495-31504.

Voos, W. (2003) Tom40: more than just a channel. *Nat Struct Biol* **10**: 981-982.

Voulhoux, R., Bos, M.P., Geurtsen, J., Mols, M., and Tommassen, J. (2003) Role of a highly conserved bacterial protein in outer membrane protein assembly. *Science* **299**: 262-265.

Voulhoux, R., and Tommassen, J. (2004) Omp85, an evolutionarily conserved bacterial protein involved in outer-membrane-protein assembly. *Res Microbiol* **155**: 129-135.

Yen, M.R., Peabody, C.R., Partovi, S.M., Zhai, Y., Tseng, Y.H., and Saier, M.H. (2002) Protein-translocating outer membrane porins of Gram-negative bacteria. *Biochim Biophys Acta* **1562**: 6-31.

Appendix A.1

Structural modeling of the BrkA passenger domain

The observation that (*i*) the BrkA and Prn passengers regions are 27% identical at the amino acid level and 39% similar at the chemical level, and (*ii*) the pertactin junction (Phe^{470}-Ser^{607}) *trans* complements folding of the BrkA passenger (Fig. 3-12C), suggests that the BrkA passenger might adopt a β-helical fold similar to pertactin (depicted in Fig. 3-3) (Emsley *et al.*, 1996). The parallel β-helix represents a repetitive fold where each repeat (termed a rung or coil) consists of three β-strands (termed S1, S2, S3) and three turns (termed T1, T2, T3). Rungs stack in a parallel orientation forming a solenoid with three β-sheet faces. β-helices do not often display direct sequence repeats, but rather the core of each rung is packed primarily with aliphatic side chains that contribute to the stability of the structure by aligning or stacking with similar residues in flanking rungs, a hallmark feature observed in all known parallel β-helices (Jenkins *et al.*, 1998). Consistent with these features, secondary structural prediction using PsiPred (McGuffin *et al.*, 2000) indicates that the BrkA passenger (Glu^{60}-Asn^{714}) is composed entirely of short β-strands (48%) and coil (52%), and far-UV CD analysis reveals that a purified form of the BrkA passenger is rich in β-structure (Fig. 3-8). Further, Beta-Wrap (http://betawrap.lcs.mit.edu/), a computer based algorithm that scores sequences for features compatible with a right-handed parallel β-helix fold (Bradley *et al.*, 2001), predicts two series of 5 rungs spanning residues 99-226 and 227-383 of BrkA (Fig. A-1, B1 and B2). Taken together these observations support the notion that the BrkA passenger might form a β-helix.

Since pertactin and BrkA share sequence identity, an attempt was made to identify putative rungs in the BrkA primary sequence by comparison with the pertactin structure (1DAB). This analysis was carried out in three steps: (*i*) First, the three-dimensional structure of pertactin (1DAB) (Fig. 3-3, page 99) was inspected for the features of a β-helix fold and a topological representation describing the core structure of the pertactin β-helix was generated (not shown). (*ii*) Next, putative rungs within the BrkA passenger were identified by pairwise alignment with pertactin. BLAST analysis of BrkA (Met^{1}-Asn^{731}) and Prn (Met^{1}-Asn^{606}) generated an alignment spanning BrkA(Gly^{268}-Leu^{702}) and Prn(Gly^{60}-Leu^{566}) with 27% identity, 39% similarity, with 20% attributed to gaps. Comparison of this alignment with the 1DAB coordinates revealed that the gapped regions correspond roughly with loops in the pertactin three-dimensional structure. We therefore re-aligned the sequence corresponding to the core structure of Prn (Gly^{60}-Leu^{566} core) with BrkA(Gly^{268}-Leu^{702}) to obtain an alignment showing 31% identity, 45% similarity and only 10% gaps (iii) Finally, the BrkA/pertactin alignment was superimposed onto the map of the pertactin core structure to produce a two-dimensional schematic of the BrkA passenger domain (Fig. A-1). Significantly, 106 of 126 amino acids corresponding to inward oriented side chains are Val, Leu or Ile, and of the remaining 20, 10 are identical with respect to pertactin and the rest are hydrophobic. The absence of extended loops within turn T1 is consistent with the structure of a β-helix (Jenkins *et al.*, 1998). Further, the BrkA secondary structural prediction (PsiPred; underlined regions in Fig. A-1) and the β-helix rung prediction (Fig. A-1, B2) (BetaWrap) are consistent with this model.

An attempt was made to develop a three-dimensional model of the BrkA passenger using the structural modeling program MOE (Chemical Computing Group, Cambridge MA). Based on the BrkA/pertactin sequence alignment described above (Fig. A-1), a model of the BrkA passenger spanning residues Leu^{485}-Leu^{702} was generated and energy minimized. The model suggests that the structures of BrkA(Leu^{485}-Leu^{702}) and pertactin(Ala^{349}-Ala^{571}) are remarkably similar (Fig. A-2). Structural models of possible rungs could also be generated for regions in the N-terminus of the BrkA passenger corresponding to β-helix predictions B1 and B2 (Fig. A-1), although at lower confidence levels (i.e. based on energy minimization) suggesting that structural adjustments or sequence re-alignment might be necessary.

From these analyses a crude structural model of the BrkA passenger domain can be fashioned (Fig. A-1). The model suggests that the BrkA passenger forms a β-helix fold consisting of 19 to 23 rungs. The difference of 4 rungs is based on the uncertainly in defining rungs in the region spanning residues Gln^{384} – Asn^{458}; it is possible that a loop structure exists within this region. Importantly, three-dimensional modeling of the C-terminal region of the BrkA passenger spanning residues Leu^{485}-Leu^{702}, which encompasses the junction region, is strongly predicted to adopt a structural fold similar to pertactin (Fig. A-2).

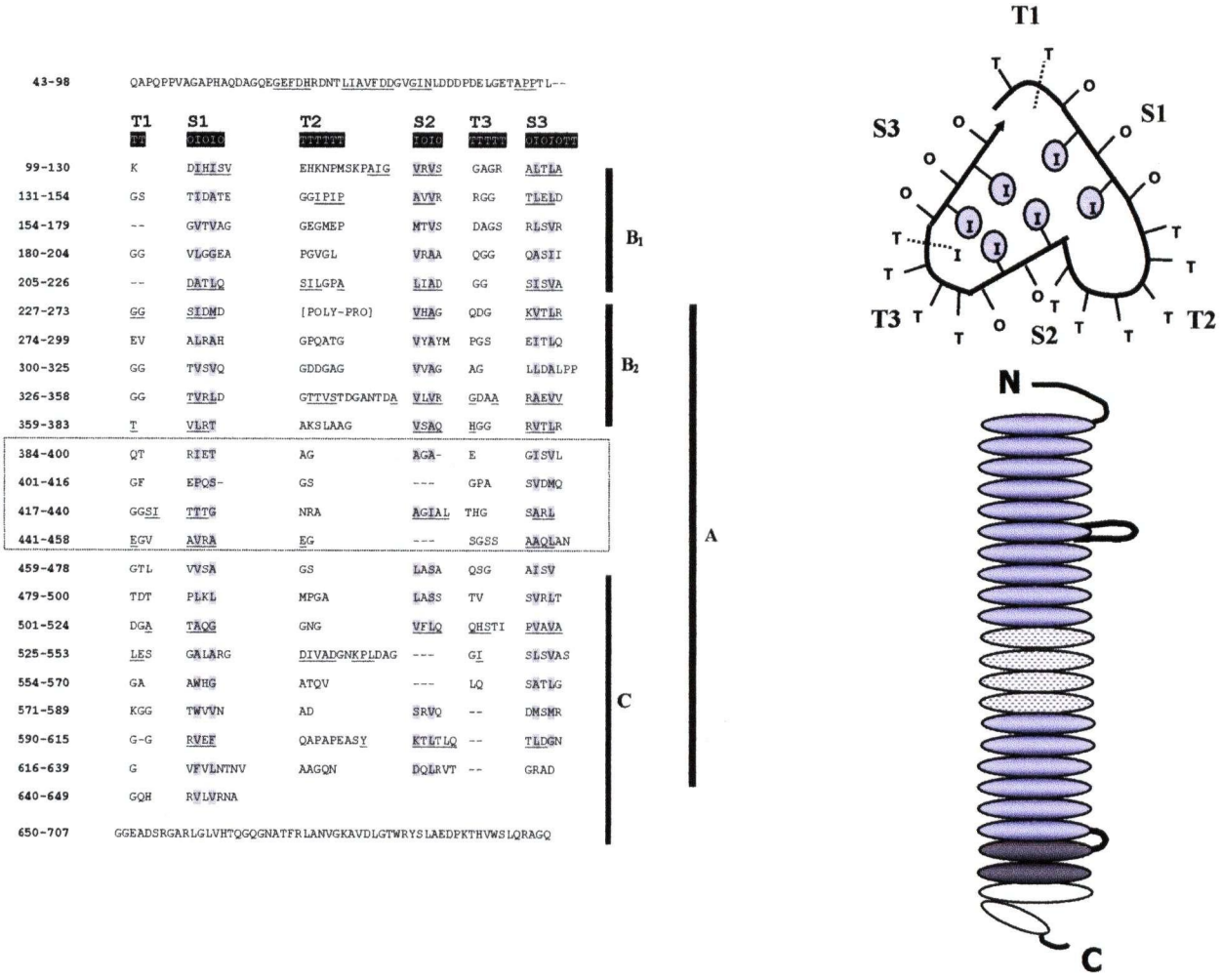

Fig. A-1 A model of the BrkA passenger domain.

Left: two-dimensional β-helix model of the BrkA passenger domain. Each line represents a putative rung in the β-helix. Each rung consists of three turns (T1, T2, T3) and three β-strands (S1, S2, S3). Side chain orientation are noted as I (inward) or O (outward). Grey boxes highlight residues proposed to be oriented toward the core of the β-helix. Region A denotes the region of BrkA aligned with the core structural features of the pertactin β-helix (1DAB) (described in main text). Regions B1 and B2 denote regions of the BrkA passenger predicted by BetaWrap (Hidden Markov Model option) (Bradley *et al.*, 2001) to form a β-helix. BetaWrap assigns this prediction an E-Value score of 4.6e-08. Underlined regions are predicted by PsiPred to form β-strands. Dotted line encompassing residues 384-458 denotes a region of uncertainty (i.e. a region that might not form a β-helix fold). Residues 43-98 and 650-707 are not predicted to form part of the core β-helix structure. Also, a region denoted [POLY-PRO] that is predicted to form a proline rich loop spanning residues M^{234}-A^{261} was omitted from the diagram. The sequence of the [POLY-PRO] region is (MGPGFPPPPPPPLPGAPLAAHPPLDRVAA). **Top right:** Schematic representation of a single rung within the BrkA β-helix. **Bottom right:** Cartoon model of the BrkA passenger domain. Ovals represent rungs in the β-helix. Dark grey ovals correspond to the BrkA folding region identified in this study (T^{606}-K^{680}). Hatched ovals represent poorly defined rung predictions (see above). White ovals at the extreme C-terminus represents the conserved region of the BrkA junction (A^{681}-L^{702}) that is not required for passenger folding. Putative loop regions extend to the right of the structure.

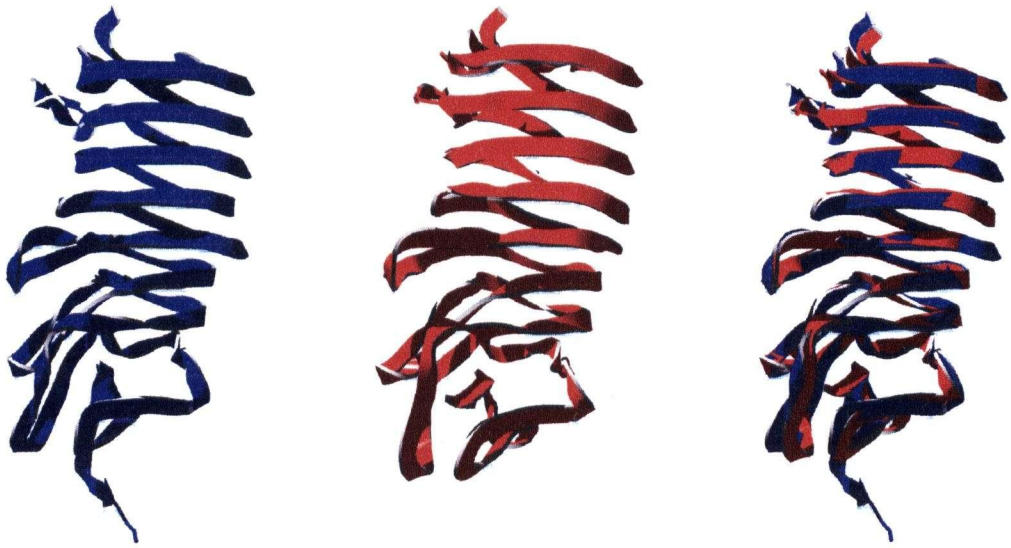

Fig. A-2 Three dimensional structural model of the BrkA(L^{485}-L^{702}) passenger domain.
A. BrkA(L^{485}-L^{702}) was constructed by homology modeling using the pertactin structural coordinates (1DAB). Modeling was performed using Molecular Operating Environment evaluation software version 2004.03 (Chemical Computing Group) and energy minimized using the AMBER 89 energy force field. The structure on the left depicts the structure of pertactin as determined by crystallography (1DAB), the middle structure depicts the model of BrkA(L^{485}-L^{702}), and the figure on the right shows an overlay of the BrkA(L^{485}-L^{702}) model and the pertactin(A^{349}-A^{571}) structure.

Appendix A.2

Lipidation of autotransporters

Autotransporter signal peptides that include a consensus lipoprotein modification signal (Fig. 6-2B) undergo modification and presumably trafficking by the Lol system (Juncker *et al.*, 2003). The LOL system consists of the LolCDE ABC transporter, the LolA periplasmic chaperone, and the LolB outer membrane protein (Takeda *et al.*, 2003). Subsequent to translocation across the inner membrane via the Sec pathway, proteins encoding signal peptides with the motif (LA(G,A)↓C) are sequentially modified at the Cys residue by addition of a diacylglyceride cleaved by lipoprotein signal peptidase (Lsp) (rather than signal peptidase I) and then N-acylated on the Cys residue. Fatty acylation enables anchoring to the periplasmic leaflet of the inner or outer membranes. Lipoproteins destined for the outer membrane are shuttled across the periplasmic compartment via the LolA chaperone to the outer membrane protein LolB. Proteins encoding an aspartate residue immediately following the modified Cys do not associate with LolA and remain anchored to the inner membrane (Hara *et al.*, 2003), although it should be noted that amino acids other aspartate can achieve a similar affect (Seydel *et al.*, 1999).

The adhesin AlpA from *Helicobacter pylori* (Odenbreit *et al.*, 1999), and two proteases, NalP (AspA) which is secreted from *Neisseria meningitides* (Turner *et al.*, 2002) (van Ulsen *et al.*, 2003), and SphB1 which is anchored to *Bordetella pertussis* via its N-terminus (Coutte *et al.*, 2001), are examples of autotransporter proteins with the

LA(G,A)↓C motif. There is evidence that all 3 proteins undergo lipid modification (Coutte *et al.*, 2003) (Odenbreit *et al.*, 1999) (van Ulsen *et al.*, 2003). Interestingly, in AlpA (which is a *Helicobacter* variant of the AT1 proteins) and NalP the consensus cysteine residue is positioned at amino acids 15 and 28 respectively, however, N-terminal sequencing of the mature proteins reveals that they are further cleaved following amino acids 21 (AlpA) and 64 (NalP). With AlpA however, Odenbreit *et al.* (1999) have proposed that it is cleaved at Cys15 by Lsp and remains tethered to the periplasmic face of the inner membrane until its C-terminus inserts itself into the outer membrane, after which point its N terminus is cleaved by signal peptidase I (after Ala21) to free the passenger to transit across the outer membrane. This 2 step processing of AlpA might obviate the need for the Lol system, and if so, it raises questions of whether or how the Lol pathway is avoided since AlpA does not have the requisite Lol avoidance residue following the modified cysteine; and, why the protein undergoes lipid modification if the modification is ultimately removed by proteolysis.

Appendix References (Sections A.1 and A.2)

Bradley, P., Cowen, L., Menke, M., King, J., and Berger, B. (2001) BETAWRAP: successful prediction of parallel beta -helices from primary sequence reveals an association with many microbial pathogens. *Proc Natl Acad Sci U S A* 98: 14819-14824.

Coutte, L., Antoine, R., Drobecq, H., Locht, C., and Jacob-Dubuisson, F. (2001) Subtilisin-like autotransporter serves as maturation protease in a bacterial secretion pathway. *Embo J* 20: 5040-5048.

Coutte, L., Willery, E., Antoine, R., Drobecq, H., Locht, C., and Jacob-Dubuisson, F. (2003) Surface anchoring of bacterial subtilisin important for maturation function. *Mol Microbiol* 49: 529-539.

Emsley, P., Charles, I.G., Fairweather, N.F., and Isaacs, N.W. (1996) Structure of *Bordetella pertussis* virulence factor P.69 pertactin. *Nature* 381: 90-92.

Hara, T., Matsuyama, S., and Tokuda, H. (2003) Mechanism underlying the inner membrane retention of *Escherichia coli* lipoproteins caused by Lol avoidance signals. *J Biol Chem* 278: 40408-40414.

Jenkins, J., Mayans, O., and Pickersgill, R. (1998) Structure and evolution of parallel beta-helix proteins. *J Struct Biol* 122: 236-246.

Juncker, A.S., Willenbrock, H., Von Heijne, G., Brunak, S., Nielsen, H., and Krogh, A. (2003) Prediction of lipoprotein signal peptides in Gram-negative bacteria. *Protein Sci* 12: 1652-1662.

McGuffin, L.J., Bryson, K., and Jones, D.T. (2000) The PSIPRED protein structure prediction server. *Bioinformatics* 16: 404-405.

Odenbreit, S., Till, M., Hofreuter, D., Faller, G., and Haas, R. (1999) Genetic and functional characterization of the alpAB gene locus essential for the adhesion of *Helicobacter pylori* to human gastric tissue. *Mol Microbiol* 31: 1537-1548.

Seydel, A., Gounon, P., and Pugsley, A.P. (1999) Testing the '+2 rule' for lipoprotein sorting in the *Escherichia coli* cell envelope with a new genetic selection. *Mol Microbiol* 34: 810-821.

Takeda, K., Miyatake, H., Yokota, N., Matsuyama, S., Tokuda, H., and Miki, K. (2003) Crystal structures of bacterial lipoprotein localization factors, LolA and LolB. *Embo J* 22: 3199-3209.

Turner, D.P., Wooldridge, K.G., and Ala'Aldeen, D.A. (2002) Autotransported serine protease A of *Neisseria meningitidis*: an immunogenic, surface-exposed outer membrane, and secreted protein. *Infect Immun* 70: 4447-4461.

van Ulsen, P., van Alphen, L., ten Hove, J., Fransen, F., van der Ley, P., and Tommassen, J. (2003) A *Neisserial* autotransporter NalP modulating the processing of other autotransporters. *Mol Microbiol* 50: 1017-1030.

Appendix A.3

Antibodies to BrkA augment killing of *Bordetella pertussis*

Vaccine. 2001 Oct 12;20(1-2):235-41.

Oliver DC, Fernandez RC.

2. Materials and methods

2.1. Bacterial strains and growth media

The *B. pertussis* strains used in this study are the wild-type Tohama1 derivative BP338 [9], BrkA mutant strains BPM2041 which has a transposon insertion within *brkA* [2,10] and RFBP2152 which has a gentamicin cassette disrupting *brkA* [6], and the *Bvg* mutant strain BP347 [9]. *E. coli* strains RF1066 [6] and DO218 [11] have been described previously. In brief, RF1066 contains the *brk* locus cloned into pBluescript SKII (Stratagene, La Jolla, CA) and transformed into DH5a (Canadian Life Technologies, Burlington, Ont.). DO218 was constructed by cloning a fragment of the *brkA* gene from the *Afl*III site to the *Bam*HI site into pET30b (Novagen, Madison, WI), and transforming the resulting plasmid into BL21 (DE3) pLysS (Novagen). *B. pertussis* strains were maintained on Bordet-Gengou agar (Becton Dickinson Microbiology Systems, Franklin Lakes, NJ) supplemented with 15% sheep blood (RA Media, Calgary, Alta.) as described [2]. Cultures (48 h old) were used for the serum assays. Antibiotic concentrations were as follows: naladixic acid, 30 μg/ml; kanamycin, 50 μg/ml; ampicillin, 100 μg/ml; gentamicin, 30 μg/ml; and chloramphenicol, 34 μg/ml.

2.2. Purification of rBrkA$^{1-693}$

The recombinant fusion protein produced by DO218 consists of the first 693 amino acids of BrkA flanked by N- and C-terminal histidine tags and is designated as rBrkA$^{1-693}$. DO218 was grown to an OD_{600} of approximately 0.6 and induced with 1 mM isopropyl-β-D-thiogalactopyranoside (IPTG) for 2 h. Recombinant BrkA$^{1-693}$ was purified under denaturing conditions using the protocol in the Xpress System Protein Purification manual (Invitrogen, Carlsbad, CA) as described [11]. In brief, the bacteria were lysed in 6 M guanidine hydrochloride, and the lysate was applied to Ni^{2+}-nitrilotriacetic acid (NTA) agarose (Qiagen Inc., Mississauga, Ont.). After successive washes in 8 M urea of decreasing pH, purified rBrkA$^{1-693}$ was eluted at pH 4 and the fractions were pooled. The urea was removed by slow dialysis at 4°C against 10 mM Tris, pH 8.0 in the presence of 0.1% Triton X-100 [11]. The final dialysis was either against 10 mM Tris, pH 8 or phosphate-buffered saline. Protein concentrations were determined by the bicinchoninic acid (BCA) method following protocol TPRO-562 (Sigma Chemical Company, St. Louis, MO).

2.3. Generation of polyclonal antibodies to rBrkA$^{1-693}$

Polyclonal antibodies to rBrkA$^{1-693}$ were generated at Harlan Bioproducts for Science (Indianapolis, IN) in a pathogen-free, barrier-raised New Zealand white rabbit. Harlan's standard 112-day production protocol was followed using 1 mg antigen per rabbit and four immunisations in total.

2.4. SDS-PAGE and immunoblot analysis

SDS-PAGE was performed as described [2,12] and the separated proteins were visualised after staining with Coomassie brilliant blue. The low molecular weight markers were purchased from Amersham Pharmacia Biotech (Baie d'Urfé, Que., Canada). For immunoblot analysis, whole-cell lysates of the *B. pertussis* strains were separated by SDS-PAGE and transferred to Immobilon-P membranes (Millipore, Bedford, MA) as described [11]. The dilutions for the rabbit anti-rBrkA antiserum and the horseradish peroxidase-conjugated goat anti-rabbit secondary antibody (Cappel, ICN Biomedicals, Costa Mesa, CA) were 1:50 000 and 1:10 000, respectively. The blots were developed with the Renaissance chemiluminescence reagent (NEN Life Science Products, Boston, MA). Kaleidoscope pre-stained molecular weight markers were obtained from Bio-Rad (Hercules, CA).

2.5. Immunofluorescence

B. pertussis strains were incubated with a 1:200 dilution of the rabbit anti-rBrkA antiserum in phosphate-buffered saline (PBS) containing 1% bovine serum albumin (BSA) for 30 min at 37°C. The bacteria were subsequently washed three times prior to incubating them with a 1:100 dilution of a FITC-conjugated goat anti-rabbit antibody (Jackson ImmunoResearch Laboratories, WestGrove, PA). After washing, the bacteria were immobilised on a glass slide that had been previously treated with 0.1% poly-L-lysine (Sigma). The bacteria were viewed under epi-fluorescence using a Zeiss Axioskop-2 microscope. Phase-contrast and fluorescent images were captured digitally. For UV microscopy, a constant exposure time of 18 s was used.

2.6. Radial diffusion serum killing assay

The sera used in this study came from adults who had no re-collection of exposure to *B. pertussis*. The bactericidal capacity of each of these samples was similar to previously published values from other individuals with "no re-collection of disease" [8]. The radial diffusion serum killing assay was performed essentially as described [6–8] with two notable modifications, described below. In general, the radial diffusion serum assay consists of adding 200 μl of bacteria (OD_{600} = 0.2) to 10 ml of Stainer Scholte (SS) broth containing 1% molten agarose and pouring the mixture into an Integrid square Petri dish. The agarose is allowed to harden. Wells (3 mm in diameter) are formed using an aspirator punch and 5 μl of serum is added to each well. After the serum is allowed to diffuse, an overlay of SS-agarose (lacking bacteria) is added and the plates are incubated for 24–48 h at 37°C. Zones of clearing are noted and the size of the zones, which is proportional to the killing capacity of the serum, is measured. For some experiments, 200 μl of strain BPM2041 were pelleted, and re-suspended in 100 μl of PBS

containing rBrkA$^{1-693}$ at a concentration of 2 mg/ml prior to the addition of the molten agarose. For other experiments, the conventional radial diffusion assay was done, except in this case, various concentrations of rabbit anti-rBrkA antiserum (diluted in RPMI medium) were mixed with a constant amount of the human serum prior to adding the serum mix to the wells. The concentration of rabbit antiserum in the mix ranged from 20% to none. The control antiserum used in these experiments came from a rabbit that was immunised with an irrelevant antigen; in this case, a non-native form of the C-terminal (amino acids 694–1010) of BrkA. Unless otherwise stated, the experiments were repeated at least three times. Student's *t*-test was used for statistical analysis of the data.

3. Results and discussion

3.1. Expression and purification of functional recombinant rBrkA$^{1-693}$

BrkA is a member of the autotransporter family of outer-membrane proteins [13]. It is synthesised as a 103 kDa precursor which is processed to yield a 73 kDa N-terminal passenger and a 30 kDa C-terminal porin-like transporter region [11]. When full-length BrkA is expressed in *B. pertussis* or in *E. coli*, it represents only a small fraction of the total protein in whole-cell lysates. Unlike many autotransported proteins whose N-terminal passenger domains are released into the culture media, the BrkA passenger domain remains tightly associated with the bacterium despite being processed. Over-expression of the full-length BrkA protein in *E. coli* is lethal. Thus, in order to obtain sufficient quantities of BrkA for functional studies, it was necessary to uncouple the N-terminal passenger portion of BrkA from its outer-membrane embedded transporter moiety. BrkA comprising the first 693 amino acids was cloned with both amino and carboxy terminal histidine tags. Induction of this clone (DO218) with IPTG resulted in the production of approximately 2 mg of recombinant protein (rBrkA$^{1-693}$) per ml of culture (Fig. 1A). Most of the recombinant protein was insoluble; therefore, all purification steps were performed under denaturing conditions. Purified rBrkA$^{1-693}$ was eluted from a nickel column in 8 M urea at pH 4.0 (Fig. 1A), and re-folded by diluting the urea in a drop-wise manner during dialysis [11].

To determine whether the re-folded rBrkA$^{1-693}$ was functional, we bathed *B. pertussis* strain BPM2041, a *brkA* mutant, with rBrkA$^{1-693}$ and assessed whether the protein could rescue the serum sensitive phenotype of this mutant. The effective concentration of rBrkA$^{1-693}$ was 20 μg/ml for the course of the assay. As shown in Fig. 1B, whereas the zone surrounding the well in BPM2041 panel is completely clear due to bacterial lysis, the bathing of BPM2041 with rBrkA$^{1-693}$ resulted in a significant restoration of serum resistance as indicated by a turbid zone, similar to what is seen

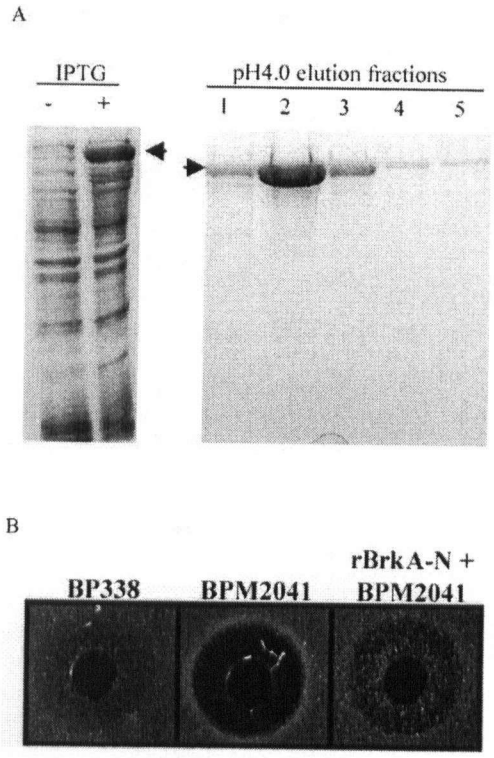

Fig. 1. Purification and demonstration of functional activity of recombinant BrkA. BrkA comprising the first 693 amino acids (BrkA$^{1-693}$) was expressed as a histidine-tagged fusion protein and purified under denaturing conditions. The left side of Panel A shows the SDS-PAGE (11% gel) and Coomassie Blue staining of whole-cell lysates of strain DO218 before and after a 1 h induction with IPTG. The right side of Panel A shows the SDS-PAGE and Coomassie Blue staining of the pH 4 elution profile of BrkA$^{1-693}$ following Ni-NTA chromatography. The arrowheads show the histidine-tagged recombinant BrkA$^{1-693}$. In Panel B, purified recombinant BrkA$^{1-693}$ was added to *B. pertussis* strain BPM2041 (*brkA*) for 30 min prior to performing the radial diffusion serum assay with 5 μl of undiluted human serum. For comparison, the wild-type strain BP338 and BPM2041 to which no rBrkA$^{1-693}$ was added are also shown. The dark area surrounding the well to which serum was added represents a zone of bacterial lysis. The light area represents the surviving bacteria.

with the wild-type, serum-resistant strain, BP338. While it is clear that the addition of the recombinant protein to BPM2041 mimics what is seen in the wild-type strain, it is not known how or whether rBrkA$^{1-693}$ physically associates with *B. pertussis* to protect it from serum killing since the mechanism of BrkA has not been deciphered. Restoration of serum resistance in BPM2041 was also observed when a wild-type copy of the *brkA* gene was recombined into its chromosome (data not shown).

3.2. Antibodies to rBrkA$^{1-693}$ recognise surface-expressed BrkA

Antibodies to rBrkA$^{1-693}$ were made in a barrier-raised, pathogen-free rabbit. Immunoblot analysis showed that the antiserum recognises the N-terminal portion of BrkA in its unprocessed (103 kDa) and processed (73 kDa) forms. Other

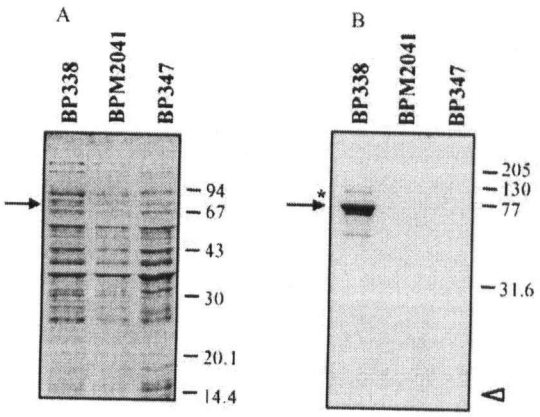

Fig. 2. Immunoblot analysis of the rBrkA$^{1-693}$ antiserum. Panel A shows whole-cell lysates of *B. pertussis* strains characterised by SDS-PAGE (11% gel) and stained with Coomassie Blue. Panel B shows an immunoblot of a duplicate gel visualised by chemiluminescence. BP338 is the wild-type strain, BPM2041 is the BrkA mutant, and BP347 is the *Bvg* mutant. The arrow shows the 73 kDa N-terminal portion of BrkA. The single asterisk is the 103 kDa full-length form of BrkA. The open arrowhead shows the dye-front. Molecular sizes are in kDa.

processed forms of BrkA are also evident. The antiserum is specific for BrkA as no cross-reactivity to any other *B. pertussis* antigens is evident (Fig. 2).

To assess whether the rabbit anti-rBrkA$^{1-693}$ antiserum was capable of recognising native BrkA, we performed an indirect immunofluorescence assay for surface-expressed BrkA. For this assay, bacteria were first stained and then immobilised on poly-L-lysine coated glass slides. Fig. 3 demonstrates that the rBrkA$^{1-693}$ antiserum is indeed capable of recognising native, surface-expressed BrkA on *B. pertussis*. This figure also shows that even at high concentrations of antiserum, there is no cross-reactivity with other *B. pertussis* antigens.

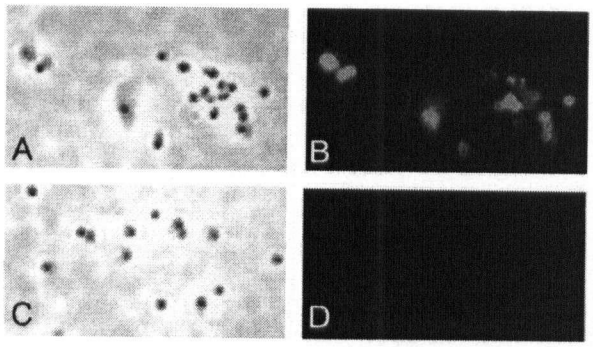

Fig. 3. The rBrkA$^{1-693}$ antiserum recognises surface-expressed BrkA. *B. pertussis* strains were incubated with the rBrkA$^{1-693}$ antiserum followed by incubation with a FITC-conjugated goat anti-rabbit secondary antibody. The stained bacteria were immobilised on poly-L-lysine coated slides and visualised by phase-contrast (Panels A and C) and fluorescence (Panels B and D) microscopy. The exposure times for Panels B and D were identical. Panels A and B show strain BP338, Panels C and D show strain BPM2041.

3.3. Antibodies to rBrkA$^{1-693}$ neutralise serum resistance

Because the rBrkA$^{1-693}$ antiserum was shown to recognise native BrkA, we asked whether it could neutralise serum resistance in wild-type *B. pertussis*. Radial diffusion serum killing assays were performed rather than the traditional killing assays (where the numbers of surviving bacteria are determined by colony counts) to circumvent potential agglutination of *B. pertussis* cells via the anti-BrkA antibodies; agglutinated bacteria would influence the colony counts. Various concentrations of the rBrkA$^{1-693}$ antiserum were added to a constant amount of an individual human serum sample and 5 μl of these mixtures were then dispensed into the wells of the radial diffusion serum assay that was seeded with either wild-type *B. pertussis*, or RFBP2152 another independent BrkA mutant [6]. In the absence of the rBrkA$^{1-693}$ antiserum, the wild-type strain was found to be resistant to killing by the human serum sample, whereas the same human serum killed the BrkA mutant strain very well (Fig. 4A and B, 4th column in the top panels; Fig. 4C). When the human serum spiked with the rBrkA$^{1-693}$ antiserum was added to wild-type *B. pertussis*, there was a dose-dependent neutralisation of serum resistance (Fig. 4A (top panel) and C). Virtually maximum neutralisation was achieved when the total concentration of the rBrkA$^{1-693}$ antiserum was 20% ($P < 0.00000001$), whereas little neutralisation was seen at 2% ($P < 0.04$), and no neutralisation whatsoever was seen at 0.2%. The abrogation of serum resistance was specifically due to the neutralisation of BrkA, since a control rabbit antiserum which was raised against an irrelevant antigen (i.e. a non-native form of the C-terminal transporter moiety of BrkA) did not have any effect (Fig. 4A, bottom panel; Fig. 4C); the rBrkA$^{1-693}$ antiserum was itself not bacteriolytic (data not shown); and there was no increased killing of the BrkA mutant strain (Fig. 4B, top panel; Fig. 4C). The augmentation of bactericidal activity mediated by BrkA neutralisation was not unique to this sample. Similar results were seen using sera from other individuals (Fig. 5).

The serum samples that we used in this study were obtained from adults with no re-collection or history of exposure to pertussis. In terms of killing capacity, these samples have the same profile as others that fit this category [8]. The *B. pertussis*-specific bactericidal antibodies in our samples may have arisen from vaccination with the whole-cell pertussis vaccine and/or from a previously unrecognised infection with *B. pertussis*. It is also possible that they represent cross-reacting antibodies. Although, we have not characterised these bactericidal antibodies, immunoblot analysis of the sera at a 1:1000 dilution showed a heterogeneous response. Two bands, however were common to all samples; one at approximately 40 kDa which may represent the *B. pertussis* porin and the other a low molecular mass band corresponding to the lipo-oligosaccharide of *B. pertussis*. It is well established that anti-LPS antibodies are the major antibodies responsible for bactericidal

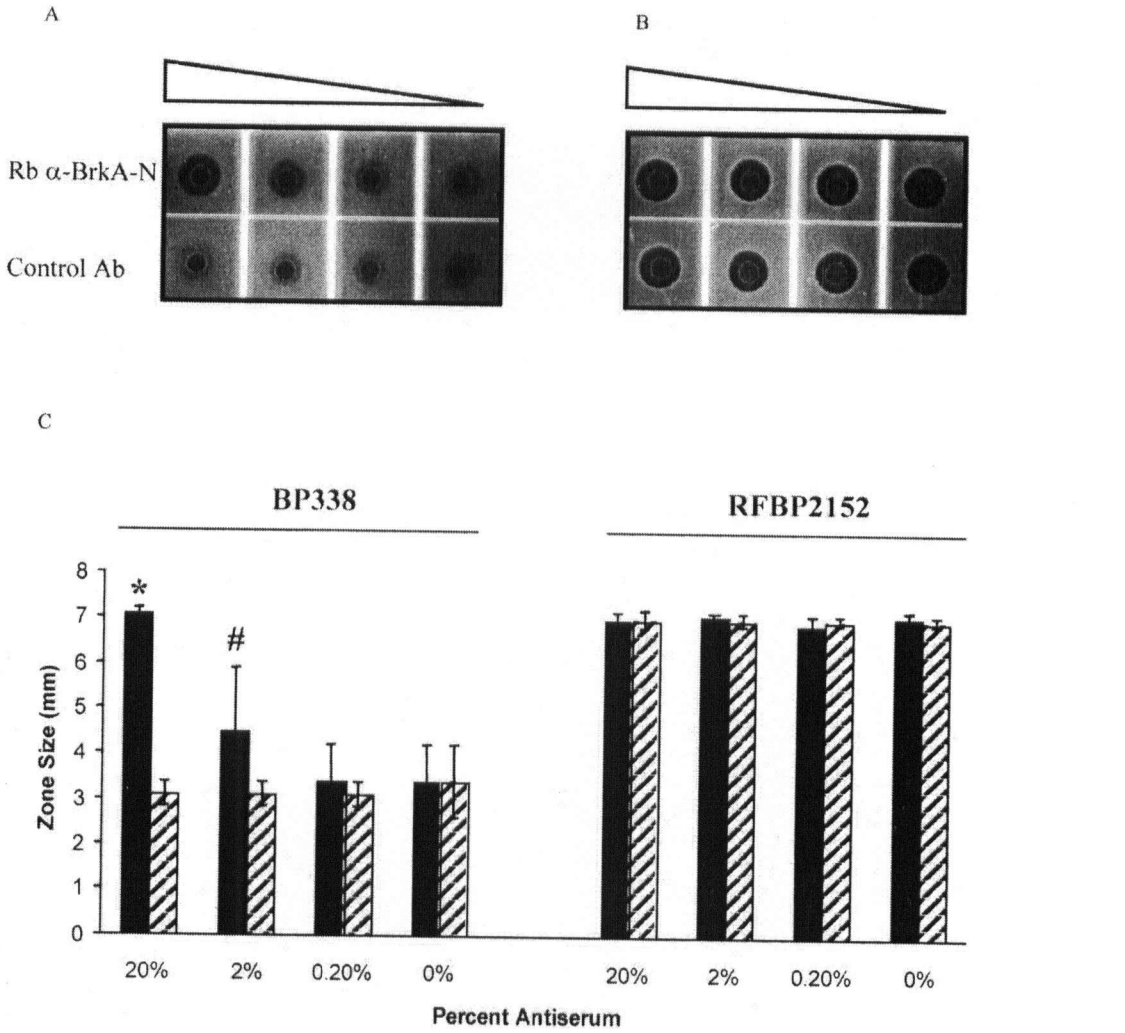

Fig. 4. The rBrkA$^{1-693}$ antiserum neutralises serum resistance in wild-type *B. pertussis*. Panels A and B show a representative radial diffusion killing assay. The radial diffusion serum killing assay was done in the presence or absence of the rabbit rBrkA$^{1-693}$ antiserum (designated as Rb α-BrkA-N), or a control rabbit serum. The rBrkA$^{1-693}$ antiserum (or control) in decreasing concentrations (20, 2, 0.2, 0%), was added to 100% human serum. Each mixture of 5 μl was added to the wells. Panel A shows the radial diffusion killing assay with wild-type strain BP338. Panel B shows the radial diffusion killing assay with strain BPRF2152, a *brkA* mutant. The control antibody is a rabbit antiserum which recognises a denatured (but not native) form of the C-terminal moiety of BrkA. Panel C shows the quantitation of the radial diffusion assay from five experiments using the same serum that was used in Panels A and B. Solid bars represent treatment with rBrkA$^{1-693}$ antiserum. Hatched bars represent treatment with control rabbit serum. $P < 0.00000001$ (*) and $P < 0.04$ (#) when the rBrkA$^{1-693}$ antiserum treatment is compared to control serum treatment at 20 and 2% serum, respectively.

activity against *B. pertussis* [8,14–20], though bactericidal antibodies to other *B. pertussis* antigens have also been found [8,21].

Infection with *B. pertussis* generates a type of humoral and cell-mediated immunity that is largely influenced by a polarised Th1 response [22,23]. The cytokines produced by Th1 cells are involved in recruiting phagocytic cells to the site of infection [24]. They can also stimulate the production of opsonising antibody and complement-fixing IgG antibody subtypes. The presence of a Th1 response arising from infection with *B. pertussis*, or from vaccination with the whole-cell pertussis vaccine has been shown to correlate with increased clearance of *B. pertussis* [23]. Antibodies play a significant role in this process; for example, they can block adherence and neutralise toxins. Antibodies can also participate directly in the clearance of *B. pertussis*. For instance, passive immunisation of mice with monoclonal antibodies to LOS that were bactericidal has resulted in increased clearance of *B. pertussis* from the lungs following aerosol challenge [25]. In addition, immunisation of mice with pertactin was found to reduce colonisation and the resulting polyclonal antibodies were shown to be bactericidal [21]. Generally speaking, bacterial clearance can also be achieved by phagocytosis of antibody-opsonised bacteria. Despite these potent defences, we continue to be re-infected with pertussis, in part because immunity to pertussis wanes

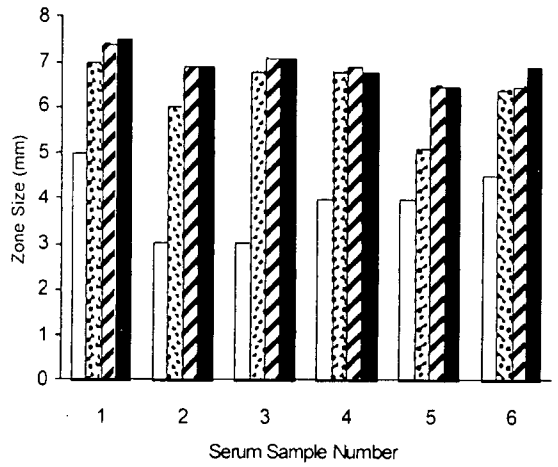

Fig. 5. The rBrkA$^{1-693}$ antiserum augments killing of wild-type *B. pertussis* in different human serum samples. The experiment was performed as described in the legend to Fig. 4. Six different donors were used. The experiment was repeated twice with similar results. Open bars, BP338 with control rabbit serum; stippled bars, BP338 with rBrkA$^{1-693}$ antiserum; hatched bars, RFBP2152 with control rabbit serum; solid bar, RFBP2152 with rBrkA$^{1-693}$ antiserum.

with time [26–31], and in part because virulence factors of *B. pertussis* can circumvent host bactericidal mechanisms. In this context, the BrkA protein protects against complement lysis, and adenylate cyclase toxin can prevent phagocytosis of opsonised bacteria by neutrophils [32,33]. Interestingly, both BrkA (shown in this report) and the anti-phagocytic properties of adenylate cyclase toxin [34] can be neutralised by their cognate antibodies.

Current vaccine strategies against *B. pertussis* protect against disease, but do not prevent mild infection or colonisation [35–38]. This may be so because vaccination with acellular vaccines triggers a Th2 or mixed Th1/Th2 [22,39,40] response and consequently does not appear to augment either phagocytic or complement-dependent bacteriolytic mechanisms [24,41]. Since humans are the natural target of *B. pertussis*, it has been suggested that adolescents and adults in whom immunity to pertussis has waned are the reservoirs for the disease. The ability to generate or boost existing bactericidal mechanisms, perhaps by neutralising BrkA or adenylate cyclase toxin, would arguably eliminate this reservoir.

Acknowledgements

This work was supported by grants from the British Columbia Health Research Foundation and the Natural Sciences and Engineering Research Council of Canada. D.O. was a recipient of a University of British Columbia University Graduate Fellowship award. We thank Mike Barnes and Alison Weiss for sharing their unpublished data and Carrie Mathewson for technical assistance on this project.

References

[1] Kerr JR, Matthews RC. *Bordetella pertussis* infection: pathogenesis, diagnosis, management, and the role of protective immunity. Eur J Clin Microbiol Infect Dis 2000;19:77–88.
[2] Fernandez RC, Weiss AA. Cloning and sequencing of a *Bordetella pertussis* serum resistance locus. Infect Immun 1994;62:4727–37.
[3] Weiss AA, Goodwin MSM. Lethal infection by *Bordetella pertussis* mutants in the infant mouse model. Infect Immun 1989;57:3757–64.
[4] Ewanowich CA, Melton AR, Weiss AA, Sherburne RK, Peppler MS. Invasion of He–La cells by virulent *Bordetella pertussis*. Infect Immun 1989;57:2698–704.
[5] Persson CGA, Erjefalt I, Alkner U, et al. Plasma exudation as a first line respiratory mucosal defence. Clin Exp Allergy 1991;21:17–24.
[6] Fernandez RC, Weiss AA. Serum resistance in bvg-regulated mutants of *Bordetella pertussis*. FEMS Microbiol Lett 1998;163:57–63.
[7] Fernandez RC, Weiss AA. Susceptibilities of *Bordetella pertussis* strains to anti-microbial peptides. Antimicrobiol Agents Chemother 1996;40:1041–3.
[8] Weiss AA, Mobberley P, Fernandez RC, Mink CM. Characterization of human bactericidal antibodies to *Bordetella pertussis*. Infect Immun 1999;67:1424–31.
[9] Weiss AA, Hewlett EL, Myers GA, Falkow S. *Tn5*-induced mutations affecting virulence factors of *Bordetella pertussis*. Infect Immun 1983;42:33–41.
[10] Weiss AA, Melton AR, Walker KE, Andraos-Selim C, Meidl JJ. Use of the promotor fusion transposon *Tn5 lac* to identify mutations in *Bordetella pertussis vir*-regulated genes. Infect Immun 1989;57:2674–82.
[11] Shannon JL, Fernandez RC. The C-terminal domain of the *Bordetella pertussis* autotransporter BrkA forms a pore in lipid bilayer membranes. J Bacteriol 1999;181:5838–42.
[12] Laemmli UK. Cleavage of structural proteins during the assembly of the head of bacteriophage T4. Nature 1970;227:680–5.
[13] Henderson IR, Navarro-Garcia F, Nataro JP. The great escape: structure and function of the autotransporter proteins. Trends Microbiol 1998;6:370–8.
[14] Ackers JP, Dolby JM. The antigen of *Bordetella pertussis* that induces bactericidal antibody and its relationship to protection of mice. J Gen Microbiol 1972;70:371–82.
[15] Aftandelians R, Connor JD. Bactericidal antibody in serum during infection with *Bordetella pertussis*. J Infect Dis 1973;128:555–8.
[16] Archambault D, Rondeau P, Martin D, Brodeur BR. Characterization and comparative bactericidal activity of monoclonal antibodies to *Bordetella pertussis* lipo-oligosaccharide A. J Gen Microbiol 1991;137:905–11.
[17] Brighton WD, Lampard J, Sheffield F, Perkins FT. Variation of killing power of human sera against *Bordetella pertussis*. Clin Exp Immunol 1969;5:541–8.
[18] Brodeur BR, Hamel J, Martin D, Rondeau P. Biological activity of a human monoclonal antibody to *Bordetella pertussis* lipo-oligosaccharide. Hum Antibodies Hybridomas 1991;2:194–9.
[19] Dolby JM, Vincent WA. Characterization of the antibodies responsible for the bactericidal activity patterns of antisera to *Bordetella pertussis*. Immunology 1965;8:499–510.
[20] Dolby JM, Ackers JP. Taxonomic distribution of the antigen eliciting bactericidal antibody for *Bordetella pertussis*. J Gen Microbiol 1975;87:239–44.
[21] Gotto JW, Eckhardt T, Reilly PA, et al. Biochemical and immunological properties of two forms of pertactin, the 69 000-molecular-weight outer-membrane protein of *Bordetella pertussis*. Infect Immun 1993;61:2211–5.
[22] Ryan M, Gothefors L, Storsaeter J, Mills KH. *Bordetella pertussis*-specific Th1/Th2 cells generated following respiratory infection or immunization with an acellular vaccine: comparison of the T-cell cytokine profiles in infants and mice. Dev Biol Stand 1997;89:297–305.

[23] Mills KH, Ryan M, Ryan E, Mahon BP. A murine model in which protection correlates with pertussis vaccine efficacy in children reveals complementary roles for humoral and cell-mediated immunity in protection against *Bordetella pertussis*. Infect Immun 1998;66:594–602.

[24] McGuirk P, Mills KH. A regulatory role for interleukin-4 in differential inflammatory responses in the lung following infection of mice primed with Th1- or Th2-inducing pertussis vaccines. Infect Immun 2000;68:1383–90.

[25] Mountzouras KT, Kimura A, Cowell JL. A bactericidal monoclonal antibody specific for the lipo-oligosaccharide of *Bordetella pertussis* reduces colonization of the respiratory tract of mice after aerosol infection with *B. pertussis*. Infect Immun1992;60: 5316–8.

[26] Cattaneo LA, Reed GW, Haase DH, Wills MJ, Edwards KM. The seroepidemiology of *Bordetella pertussis* infections: a study of persons ages 1–65 years. J Infect Dis 1996;173:1256–9.

[27] Cherry JD. Epidemiological, clinical, and laboratory aspects of pertussis in adults. Clin Infect Dis 1999;28(Suppl 2):S112–7.

[28] Deen JL, Mink CM, Cherry JD, et al. Household contact study of *Bordetella pertussis* infections. Clin Infect Dis 1995;21:1211–9.

[29] Long SS, Welkon CJ, Clark JL. Widespread silent transmission of pertussis in families: antibody correlates of infection and symptomatology. J Infect Dis 1990;161:480–6.

[30] Mortimer EA. Pertussis and its prevention: a family affair. J Infect Dis 1990;161:473–9.

[31] van Boven M, de Melker HE, Schellekens JF, Kretzschmar M. Waning immunity and sub-clinical infection in an epidemic model: implications for pertussis in The Netherlands. Math Biosci 2000;164:161–82.

[32] Weingart CL, Weiss AA. *Bordetella pertussis* virulence factors affect phagocytosis by human neutrophils. Infect Immun 2000;68:1735–9.

[33] Weiss AA. Mucosal immune defenses and the response of *Bordetella pertussis*. ASM News 1997;63:22–8.

[34] Weingart CL, Mobberley-Schuman PS, Hewlett EL, Gray MC, Weiss AA. Neutralizing antibodies to adenylate cyclase toxin promote phagocytosis of *Bordetella pertussis* by human neutrophils. Infect Immun 2000;68:7152–5.

[35] Cherry JD, Gornbein J, Heininger U, Stehr K. A search for serologic correlates of immunity to *Bordetella pertussis* cough illnesses. Vaccine 1998;16:1901–6.

[36] Hewlett EL, Halperin SA. Serological correlates of immunity to *Bordetella pertussis*. Vaccine 1998;16:1899–900.

[37] Plotkin SA, Cadoz M. The acellular pertussis vaccine trials: an interpretation. Pediatr Infect Dis J 1997;16:508–17.

[38] Storsaeter J, Hallander HO, Gustafsson L, Olin P. Levels of anti-pertussis antibodies related to protection after household exposure to *Bordetella pertussis*. Vaccine 1998;16:1907–16.

[39] Ausiello CM, Urbani F, la Sala A, Lande R, Cassone A. Vaccine- and antigen-dependent types 1 and 2 cytokine induction after primary vaccination of infants with whole-cell or acellular pertussis vaccines. Infect Immun 1997;65:2168–74.

[40] Barnard A, Mahon BP, Watkins J, Redhead K, Mills KHG. Th1/Th2 cell dichotomy in acquired immunity to *Bordetella pertussis*: variables in the in vivo priming and in vitro cytokine detection techniques affect the classification of T-cell subsets as Th1, Th2 or Th0. Immunology 1996;87:372–80.

[41] Weingart CL, Keitel WA, Edwards KM, Weiss AA. Characterization of bactericidal immune responses following vaccination with acellular pertussis vaccines in adults. Infect Immun 2000;68:7175–9.

Appendix A.4

Identification of secretion determinants of the *Bordetella pertussis* BrkA autotransporter.

J Bacteriol. 2003 Jan;185(2):489-95.

Oliver DC, Huang G, Fernandez RC.

TABLE 1. Strains and plasmids used in this study

Strain or plasmid	Relevant characteristics	Source or reference
Strains		
B. pertussis		
BP338	Wild type, Tohama background, Nal^r	36
RFBP2152	BP338 *brkA*::*gen* Nal^r Gen^r	5
BBC9	W28 *prn*::*kan* Kan^r	4
BBC9DO	BBC9::pUW2171 *brkA*$^+$ *brkB*$^+$ duplication, Nal^r Gen^r Amp^r	This study
E. coli		
UT5600	F$^-$*ara-14 leuB6 azi-6 lacY1 proC14 tsx-67 entA403 trpE38 rfbD1 rpsL109 xyl-5 mtl-1 thi1 ΔompT-fepC266*	2
DH5αF′	K-12 cloning strain	Invitrogen
Plasmids		
pBluescriptII SK$^-$	Amp^r, cloning vector	Stratagene
pRF1066	Amp^r, 4.5-kb *brk* locus	5
pUW2171	pRF1066 + Gen^r *oriT* cassette	5
pDO6935	Amp^r, pRF1066 derivative, 476-bp *Aat*II fragment excised resulting Δ*brkB*	This study
pDO181	Amp^r, pDO6935 derivative, BrkA Δ(A136-Q562), *Xba*I linker	This study
pDO182	Amp^r, pDO6935 derivative, BrkA Δ(S229-Q562), *Xba*I linker	This study
pDO244	Amp^r, pDO181 derivative, BrkA Δ(A136-P255), *Xba*I linker	This study
pDO246	Amp^r, pDO182 derivative, BrkA Δ(S229-P255), *Xba*I linker	This study
pGD1	Amp^r, pDO246 derivative, BrkA Δ(S229-G301), *Xba*I linker	This study
pGD2	Amp^r, pDO246 derivative, BrkA Δ(S229-G396), *Xba*I linker	This study
pGD3	Amp^r, pDO246 derivative, BrkA Δ(S229-D480), *Xba*I linker	This study
pGD4	Amp^r, pDO246 derivative, BrkA Δ(S229-Q514), *Xba*I linker	This study
pGD5	Amp^r, pDO246 derivative, BrkA Δ(S229-A537), *Xba*I linker	This study
pGD6	Amp^r, pDO246 derivative, BrkA Δ(S229-A560), *Xba*I linker	This study
pGD7	Amp^r, pDO246 derivative, BrkA Δ(S229-P600), *Xba*I linker	This study
pGD8	Amp^r, pDO246 derivative, BrkA Δ(S229-A658), *Xba*I linker	This study
pGD9	Amp^r, pDO246 derivative, BrkA Δ(S229-A676), *Xba*I linker	This study
pGD10	Amp^r, pDO246 derivative, BrkA Δ(S229-E693), *Xba*I linker	This study
pGD10.5	Amp^r, pDO246 derivative, BrkA Δ(S229-W700), *Xba*I linker	This study
pGD11	Amp^r, pDO246 derivative, BrkA Δ(S229-A720), *Xba*I linker	This study
pGD12	Amp^r, pDO246 derivative, BrkA Δ(S229-G797), *Xba*I linker	This study

acid, 30 μg/ml; kanamycin, 50 μg/ml; ampicillin, 100 μg/ml; and gentamicin, 10 μg/ml.

Recombinant DNA techniques. All DNA manipulations were carried out by standard techniques (27). Restriction enzymes were purchased from New England Biolabs (Beverly, Mass.). The primers used in this study were purchased either from the University of British Columbia (UBC) Nucleic Acid Protein Services Unit (Vancouver), Sigma-Genosys (The Woodlands, Tex.), or Alpha DNA (Montreal, Quebec, Canada) (Table 2). DNA sequencing was done with an ABI Prism 377 DNA sequencer (Applied Biosystems, Foster City, Calif.) at the UBC Nucleic Acid Protein Services Unit.

The *B. pertussis* strain BBC9DO was made by introducing a second copy of the *brkA* gene (on plasmid pUW2171) into the chromosome of strain BBC9, a pertactin mutant of *B. pertussis*, as described previously (5).

Construct pDO6935, which constitutively expresses low levels of BrkA in *E. coli*, was derived by excision of a 476-bp *Aat*II fragment of pRF0166. Plasmid pDO6935 was used as a template in all subsequent PCRs described in this study. All PCRs were performed with Vent polymerase (New England BioLabs) with the following cycles: an initial denaturation step of 2 min at 94°C followed by 30 cycles of 45 s at 94°C, 30 s at 60°C, and 1 min/kb at 72°C. The last cycle was followed by an additional 10 min at 72°C. Amplified PCR products were separated on an agarose gel, and a band of the expected size was extracted and cloned as described below. The primers used in this study are listed in Table 2.

Construct pDO181 was made by PCR with primer pairs DO1210F and DO1614R and DO2894F and BRK-CR. The resulting products were digested with restriction enzyme pairs *Asc*I and *Xba*I and *Xba*I and *Bam*HI, respectively. In a triple-ligation reaction, these products were ligated into a 5-kb *Asc*I- to *Bam*HI-digested fragment of pDO6935 to yield pDO181. Construct pDO182 was generated via the same strategy with primer sets DO1210F and DO1893R and DO2894F and BRK-CR. Constructs pDO244 and pDO246 were made with primer pair DO1975F and BRK-CR to generate a PCR product that was subsequently digested with *Asc*I and *Bam*HI. The resulting 1.3-kb product was then ligated into either a 5.3-kb *Xba*I- to *Bam*HI-digested fragment of pDO181 or a 5.5-kb *Xba*I- to *Bam*HI-digested fragment of pDO182 to yield pDO244 and pDO246, respectively.

Constructs pGD1, pGD2, pGD3, pGD4, pGD5, pGD6, pGD7, pGD8, pGD9, pGD10, pGD10.5, pGD11, and pGD12 were made by PCR with forward primers BRK-2113F, BRK-2398F, BRK-2650F, BRK-2752F, BRK-2821F, BRK-2890F, BRK-3010F, BRK-3184F, BRK-3238F, BRK-3289F, BRK-3310F, BRK-3370F, and BRK-3601F, respectively. BRK-CR was used as the reverse primer in each of the reactions. The amplified products were purified, digested with *Xba*I and *Hin*dIII, and ligated into a 4.3-kb *Xba*I- to *Bam*HI-digested fragment of pDO246.

SDS-PAGE and immunoblot analysis. For detection of expressed BrkA via sodium dodecyl sulfate-polyacrylamide gel electrophoresis (SDS-PAGE) or immunoblotting, *E. coli* cultures were grown to an optical density at 600 nm (OD_{600}) of 0.7 and pelleted. Trypsin accessibility experiments were performed according to a previously described protocol (18) with slight modifications. In brief, cell pellets were resuspended in 0.2 ml of phosphate-buffered saline (PBS) to an OD_{600} of ~10. To 0.1 ml of cells, 2 μl of 10-mg/ml trypsin was added to yield a final trypsin concentration of 200 μg/ml. Cells were incubated in the presence of protease for 10 min at 37°C, pelleted by centrifugation, and washed three times with PBS containing 10% fetal calf serum to stop digestion and once in PBS alone. As a control, cell pellets were simultaneously processed in the same manner in the absence of trypsin. Washed pellets were finally resuspended in sample buffer and immediately boiled for 5 min prior to SDS-PAGE.

For immunoblot analysis, samples were resolved by SDS-PAGE (4, 15) and transferred to Immobilon-P membranes (Millipore, Etobicoke, Ontario, Canada) as described previously (24). Blots were probed with heat-inactivated rabbit anti-BrkA antiserum and horseradish peroxidase-conjugated goat anti-rabbit secondary antibody (ICN Biomedicals, Costa Mesa, Calif.) diluted 1/50,000 and 1/10,000, respectively (24). Renaissance chemiluminescent reagent (NEN Life Science Products, Boston, Mass.) was used to develop immunoblots. The rabbit anti-BrkA antiserum is specific for residues Met^1 to Glu^{693} of BrkA (24). Mo-

TABLE 2. Primers used in this study

Primer	Sequence (5′ → 3′)[a]
BRK-CR	TATAAGCTTCGCTCAGAAGCTGTAGCG
DO2894F	ATTTCTAGATG-GGTGCTCCAGTCG
DO1614R	CATCTAGAAAT-ATCGATGGTCGAG
DO1893R	CATCTAGAAAT-ACCGCCGGCGACG
DO2374R	CATCTAGAAAT-GATGCGGGTCTGC
DO1210F	TAGTCCATGGCG-ATGTATCTCGATAG
DO1975F	ATTTCTAGAGTT-CTCGATCGCGTTGCC
BRK-2113F	ATTTCTAGA-ACAGTCAGCGTGCAGGGC
BRK-2398F	ATTTCTAGA-ATCTCCGTGCTGGGCTTC
BRK-2650F	ATTTCTAGA-ACGCCGCTGAAGCTGATG
BRK-2752F	ATTTCTAGA-CAGCATTCCACCATTCCG
BRK-2821F	ATTTCTAGA-GACGGCAACAAGCCCCTC
BRK-2890F	ATTTCTAGA-ACCCAGGTGCTCCAGTCG
BRK-3010F	ATTTCTAGA-GAGGCCTCTTACAAGACC
BRK-3184F	ATTTCTAGA-CGCCTGGGCCTGGTGCAT
BRK-3238F	ATTTCTAGA-AACGTCGGCAAGGCGGTT
BRK-3289F	ATTTCTAGA-GATCCGAAGACGCATGTC
BRK-3310F	ATTTCTAGA-AGCTTGCAGCGCGCG
BRK-3370F	ATTTCTAGA-GATCTTTCCAGCATCGCC
BRK-3610F	ATTTCTAGA-TACACCTATGCCGACCGC

[a] The *Hin*dIII and *Xba*I sites are underlined.

lecular masses were determined with Kaleidoscope prestained markers purchased from Bio-Rad (Hercules, Calif.).

N-terminal sequencing. Whole-cell lysates of strains BBC9DO (a pertactin [*prn*] mutant with two copies of *brkA*), and BBC9BrkA (a *prn brkA* double mutant) (4) were resolved by SDS-PAGE and transferred to an Immobilon-P membrane (Millipore). A unique band migrating at approximately 73 kDa in the BBC9DO lane was excised from the membrane and sequenced by Edman degradation by the UBC Nucleic Acid and Protein Services core facility.

Immunofluorescence analysis. *E. coli* cells were grown to an OD_{600} of 0.7, pelleted by centrifugation, and resuspended in PBS. Resuspended cells were immobilized on a glass slide that had been previously treated with 0.1% poly-L-lysine (Sigma). Slides were washed three times with PBS to remove unbound bacteria and subsequently probed with a 1/200 dilution of heat-inactivated rabbit anti-BrkA antiserum (24) and a 1/100 dilution of fluorescein isothiocyanate (FITC)-conjugated goat anti-rabbit antibody (Jackson ImmunoResearch Laboratories, West Grove, Pa.), respectively. Slides were washed three times with PBS containing 1% bovine serum albumin between each step to remove unbound material. Bacteria were visualized under epifluorescence with a Zeiss Axioscop-2 microscope. Phase-contrast and fluorescent images were captured digitally.

RESULTS AND DISCUSSION

Identification of the BrkA signal peptide. It was previously reported that sequence analysis of the 1,010-amino-acid protein BrkA did not identify a conventional signal peptide (4). More recent analysis with SignalP V2.0 (22) has predicted a signal peptide of 44 amino acids by the neural network prediction method and a cleavage site at 43 amino acids by the hidden Markov model method (23). To experimentally determine the BrkA signal peptide, N-terminal sequencing was performed with the 73-kDa moiety of BrkA. The amount of BrkA seen in whole-cell lysates of *B. pertussis* represents a small fraction of the total amount of cellular protein. Furthermore, at 73 kDa, BrkA migrates to a similar position on SDS-PAGE gels as the 69-kDa protein pertactin, a protein with which it shares sequence identity (4). To circumvent these issues, we introduced a second copy of the *brkA* gene into the chromosome of strain BBC9, a pertactin mutant of *B. pertussis*, to create strain BBC9DO. Western blot analysis of this strain with antibodies to pertactin and BrkA confirmed the lack of expression of pertactin and the increased expression of BrkA relative to that in wild-type strains (data not shown). Whole-cell lysates of strain BBC9DO were resolved by SDS-PAGE and transferred to an Immobilon-P membrane, and a unique band migrating at approximately 73 kDa was excised and sequenced by Edman degradation. Six cycles of Edman degradation revealed an N-terminal sequence of QAPQA. This sequence corresponds to amino acids 43 through 47 of BrkA. Similar results were obtained with a recombinant *brkA* construct expressed in *E. coli* (data not shown). Thus, both in *B. pertussis* and in *E. coli*, BrkA is processed between residues Ala^{42} and Gln^{43}. A signal peptide of this length is not unusual for autotransporters (9).

Expression of BrkA in *E. coli*. We chose to study BrkA secretion in *E. coli*, since it has been used as a host to study secretion of a variety of autotransporters (11–13, 18, 21, 29, 31, 34, 35), thus allowing comparisons to be made between different autotransporters and because mutational analysis of BrkA is greatly facilitated in *E. coli*. Plasmid pDO6935 was derived from pRF1066 (4), which carries the entire *brk* locus encoding the divergently transcribed *brkA* and *brkB* genes (Table 1). pDO6935 was generated by excision of a 476-bp *Aat*II fragment from pRF1066, resulting in a deletion of the 5′ region of the *brkB* gene. pDO6935 was transformed into *E. coli* strain UT5600, which is deficient for the outer membrane proteases OmpT and OmpP (7). UT5600 has been used in the past to study secretion of the *Neisseria* immunoglobulin A (IgA) protease (11, 34, 35), the *E. coli* AIDA-1 adhesin (18, 19), and the *Shigella* VirG (IcsA) autotransporters (31). BrkA expression was assessed by a previously described anti-BrkA polyclonal antiserum (24) that specifically recognizes both denatured and native forms of the 73-kDa BrkA α-domain. Immunoblots of whole-cell lysates resolved by SDS-PAGE show that BrkA was expressed to yield two major species migrating at approximately 103 and 73 kDa. The 103-kDa product corresponds to the unprocessed full-length precursor and the species migrating at 73 kDa corresponds to the cleaved α-domain (Fig. 1A and B, lane 1). Although BrkA is Bvg regulated in *B. pertussis*, the promoter region responsible for driving BrkA expression from pDO6935 in *E. coli* is not known. We previously reported that the overexpression of full-length BrkA in *E. coli* is toxic (24); however, in the absence of IPTG induction, the levels of BrkA expression in *E. coli* with this construct are similar to those seen in *B. pertussis* (4, 24).

To determine whether BrkA is translocated to the surface of *E. coli*, trypsin accessibility and immunofluorescence experiments were performed with whole cells. When cells were incubated with trypsin, a marked decrease in the 73-kDa moiety was observed, and two products of approximately 40 and 45 kDa were detected by Western immunoblotting (Fig. 1B, lane 2). The cleavage sites producing the 40- and 45-kDa species are unknown, and over time, both species are lost. The intensity of the 103-kDa product remained constant following trypsin digestion, suggesting that the 103-kDa band represents an intracellular form of the protein inaccessible to trypsin. Concomitant with this result, BrkA was detected on the surface of *E. coli* (Fig. 1C) and appeared evenly distributed, as shown by indirect immunofluorescence staining. Secreted BrkA could not be detected in concentrated culture supernatants, suggesting that the cleaved passenger remains noncovalently associated with the bacterium (data not shown). Taken together,

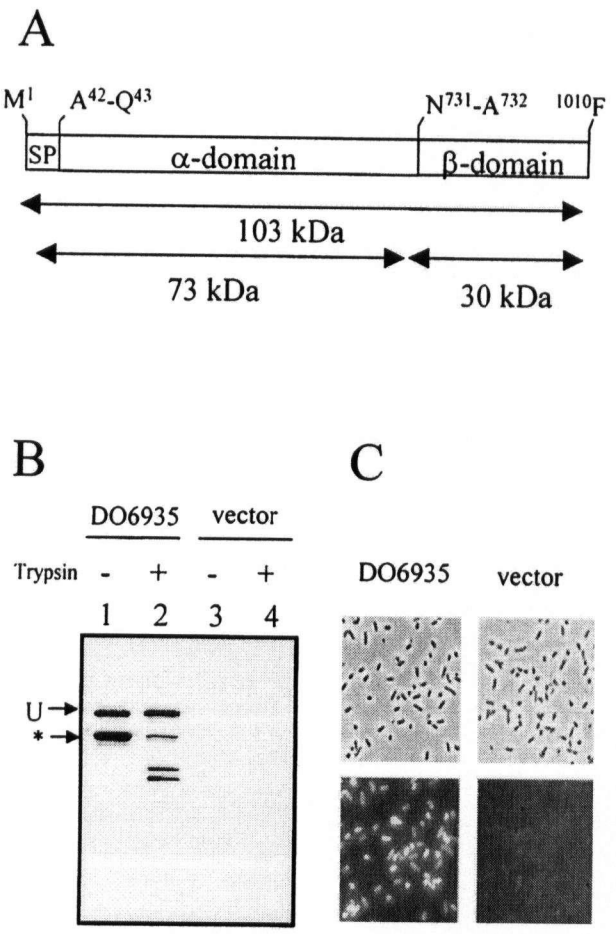

FIG. 1. BrkA expression in *E. coli* strain UT5600. (A) BrkA domain organization: signal peptide (SP [residues 1 to 42]), passenger or α-domain (residues 43 to 731), and β-domain (residues 732 to 1010). (B) Western immunoblot of *E. coli* UT5600 whole-cell lysates resolved by SDS-PAGE (11% polyacrylamide), probed with anti BrkA antiserum, and detected with goat anti-rabbit antiserum conjugated to horseradish peroxidase. Lanes: 1 and 2, pDO6935 (wild-type copy of *brkA* gene); 3 and 4, pBluescript (vector control). Specific BrkA bands are indicated. U, unprocessed 103-kDa precursor protein; *, 73-kDa processed passenger moiety. Cells were processed in the presence (+) or absence (−) of trypsin as described in Materials and Methods. (C) Surface expression of BrkA in *E. coli* UT5600 detected via indirect immunofluorescence. The top panels show phase-contrast images, and the bottom panels show epifluorescence images.

these data indicate that BrkA is exported to the surface of *E. coli* strain UT5600 and is processed (independently of proteases OmpT or OmpP) in a manner similar to that observed in *B. pertussis* (24).

Identification of the minimal BrkA translocation unit necessary for surface expression. The natural cleavage of three well-characterized autotransporters, IgA protease (11), VirG/IcsA (6), and AIDA-1 (30), results in β-domains of 45, 37, and 48 kDa, respectively. By using a series of protease susceptibility assays and experiments with heterologous proteins fused to N-terminally-truncated β-domains, minimal regions necessary to display passenger proteins have been identified for these autotransporters. They have in common, a membrane-embedded β-core of ~25 to 30 kDa found at the extreme C terminus, preceded by a so-called "linker" region (11, 19, 31). In these autotransporters, the linker region has been shown to be necessary for the translocation of the passenger domain to the bacterial surface. The linker region together with the outer membrane-embedded β-core make up what has been coined the "translocation unit" (19).

Having demonstrated that BrkA is targeted to the outer membrane of *E. coli*, we next developed a deletion-based strategy to define the boundaries of the minimal translocation unit of BrkA. N-terminal sequencing of proteins from outer membrane preparations of *B. pertussis* has localized the processing of BrkA to between Asn^{731} and Ala^{732} (25), resulting in a β-domain of 30 kDa (28). At 30 kDa, the BrkA β-domain is smaller than the β-domains for IgA protease, VirG/IcsA, and AIDA-1, but it approaches the size of the outer membrane-embedded β-cores identified for these proteins (11, 19, 31). We constructed a series of *brkA* deletion mutants by using PCR mutagenesis. As shown in Fig. 2A, mutant proteins consisted of the first 228 amino acids of BrkA (Met^1 to Gly^{228}) fused in frame to processive deletions of the C-terminal region of the BrkA α-domain leading into the BrkA β-domain. BrkA (Met^1 to Gly^{228}) was chosen as a passenger, since heterologous passengers such as cholera toxin B subunit (12) may be inefficiently translocated due to structural limitations (i.e., disulfide bond formation). In addition, it has been suggested that the extended signal sequences observed in many autotransporters may play a role in secretion (9). Therefore, the inclusion of the native BrkA signal sequence within the passenger avoids any influence that a nonnative signal sequence may have on secretion. All deletion strains were derivatives of pDO6935, thereby ensuring a common promoter for the wild-type and mutant constructs (Table 1).

An attempt was made to target our deletions to regions that would not disrupt the core structure of the protein. Secondary structural analysis with PsiPred (20) predicts that BrkA is predominantly composed of β-strands (data not shown). In addition, the closest relative to BrkA in the database is the *B. pertussis* autotransporter pertactin (4). The structure of the pertactin passenger domain has been solved and was shown to be a monomer folded into a single domain that is almost entirely made up of a right-handed cylindrical β-helix (3). Given that BrkA and pertactin passenger domains share 27% sequence identity and 39% sequence similarity, we refined our secondary structural prediction by overlaying the pertactin structural coordinates (1DABA) onto a BrkA-pertactin primary amino acid sequence alignment. The best alignment was between Arg^{175} to Pro^{572} in pertactin and Val^{301} to Gln^{707} in BrkA. Using this analysis, we systematically targeted N-terminal deletions to intervening regions with the predicted β-strands.

The effects of each deletion on BrkA expression and processing were assessed by immunoblotting of whole-cell lysates resolved by SDS-PAGE. As shown in Fig. 2B, each mutant form of BrkA was expressed, indicating that the specific deletions did not render the individual mutant protein products markedly unstable. In deletion mutants A through J, products corresponding to both the unprocessed precursor (region designated as "U") and the cleaved passenger (asterisk) were detected (Fig. 2B). In contrast, only the unprocessed precursor could be detected in deletion mutants K, L, and M. Given our

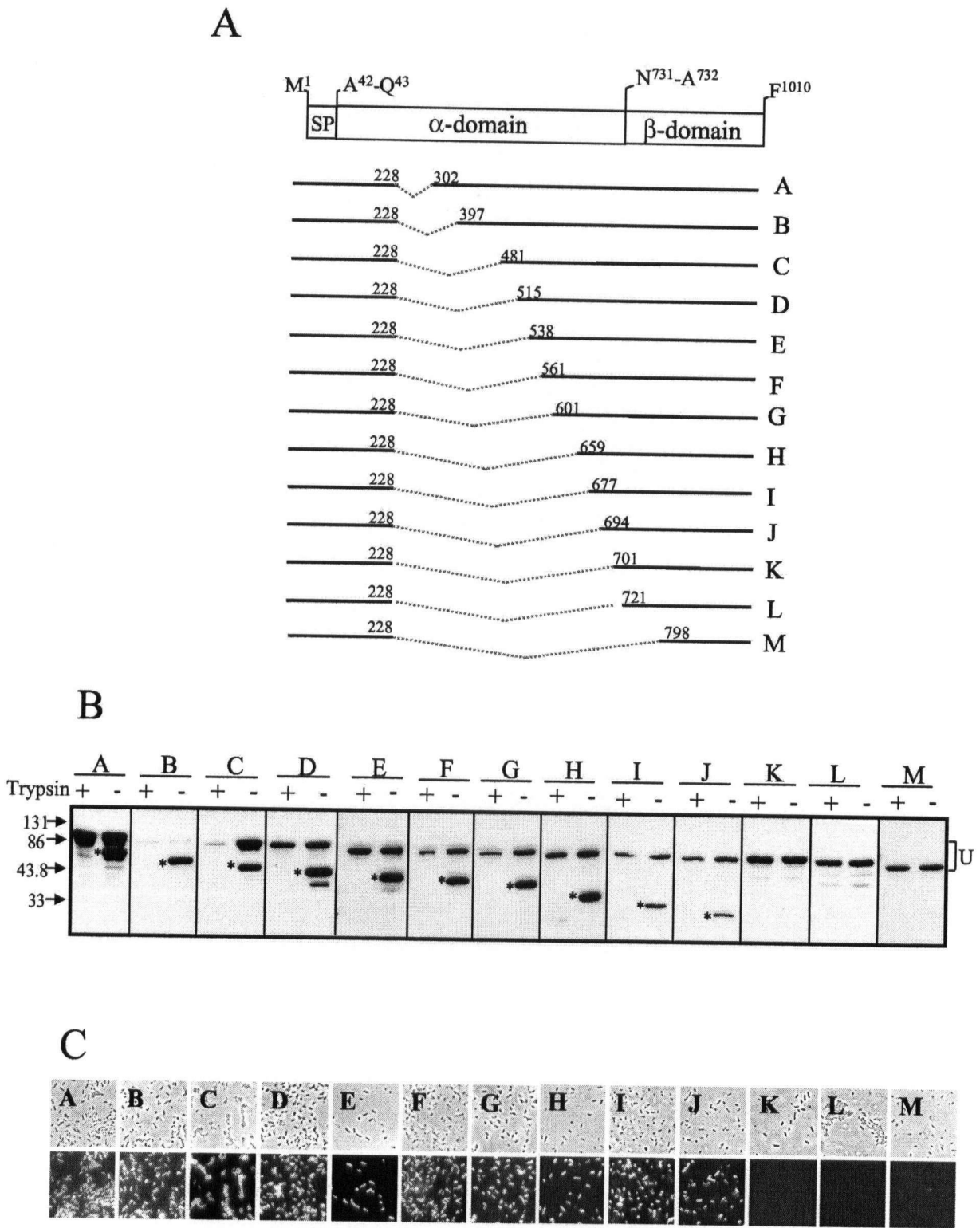

FIG. 2. Expression of BrkA deletion constructs in *E. coli* UT5600. (A) Diagram illustrating positions of BrkA in-frame deletions. Deleted regions are indicated by dotted lines, and deletion boundaries correspond to the wild-type BrkA amino acid designation. The BrkA domain structure is described in Fig. 1. Construction of mutations is described in the Materials and Methods. Plasmids are described in Table 1. (A) pGD1. (B) pGD2. (C) pGD3. (D) pGD4. (E) pGD5. (F) pGD6. (G) pGD7. (H) pGD8. (I) pGD9. (J) pGD10. (K) pGD10.5. (L) pGD11. (M) pGD12. *E. coli* UT5600 bacteria were transformed with BrkA deletion constructs (plasmids A to M) and grown to an OD_{600} of approximately 0.7. Bacteria were harvested, and BrkA surface expression was assessed by immunoblotting or indirect immunofluorescence. (B) Immunoblotting following resolution of whole-cell lysates by SDS-PAGE. The band migrating within the region denoted as "U" in each lane corresponds to the unprocessed, precursor form of BrkA, and the band denoted with an asterisk (*) corresponds to the processed passenger domain of BrkA. Cells were processed in the presence (+) or absence (−) of trypsin as described in Materials and Methods. Molecular mass markers (in kilodaltons) are indicated to the left of the panel. (C) BrkA expression in *E. coli* strain UT5600 detected by indirect immunofluorescence. The top panels show phase-contrast images, and the bottom panels show epifluorescence images.

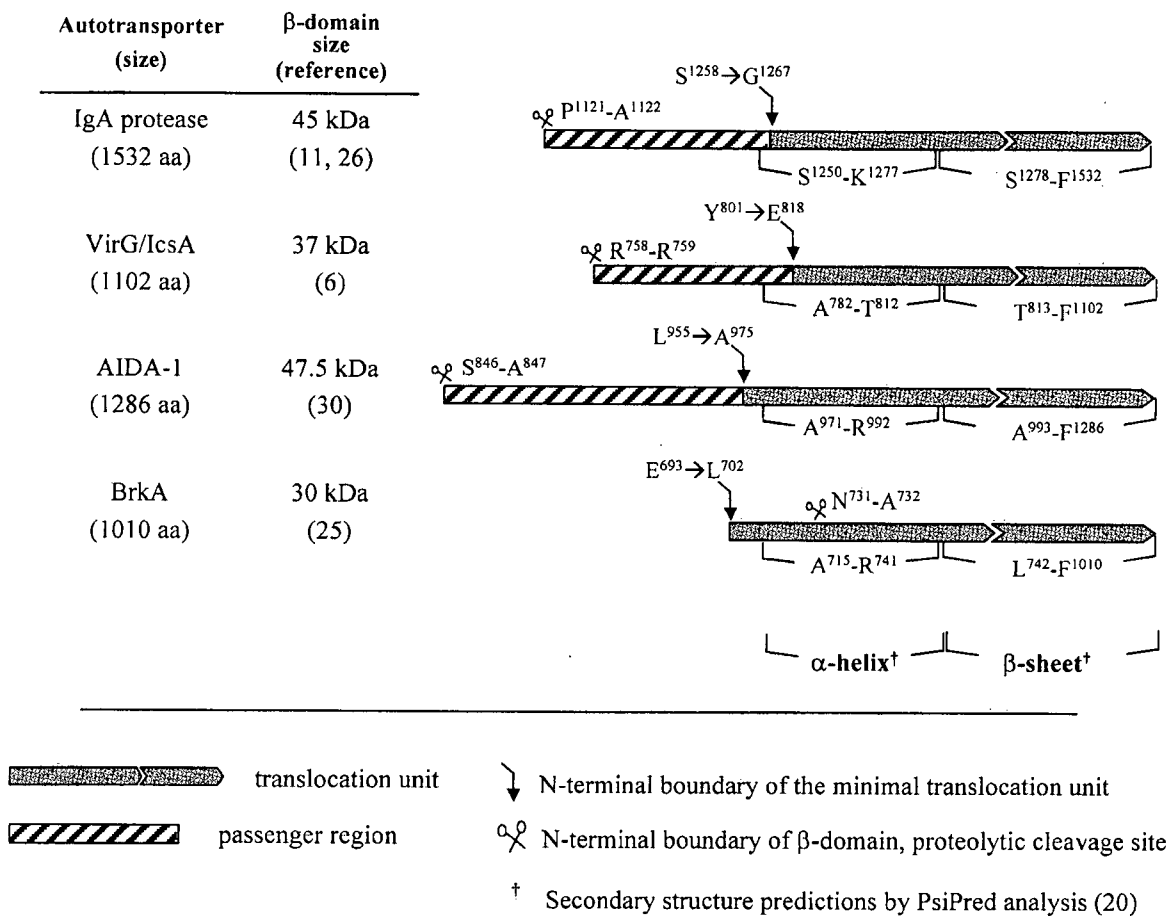

FIG. 3. Comparison of the translocation units of different autotransporters. The C-terminal regions of four autotransporters are shown (not drawn to scale). See the text for explanation. The N-terminal boundaries noted for each translocation unit have been defined experimentally in references 11 (IgA protease), 31 (VirG/IcsA), and 19 (AIDA-1), as well as in this paper (BrkA).

previous observation that the cleaved passenger domain represents a major fraction of the surface-expressed wild-type BrkA (Fig. 1), these data suggested that BrkA deletion mutants A through J were being exported to the bacterial surface, but mutants K, L, and M were not. In support of this observation, trypsin accessibility assays and indirect immunofluorescence experiments were performed. As expected, exposure of whole cells to trypsin digestion resulted in the complete absence of the band corresponding to the processed passenger domain (Fig. 2B, lanes A to J), whereas a significant fraction of the unprocessed precursor remained stable (Fig. 2B, lanes A to M). Consistent with these data, surface expression of the passenger region was detected via indirect immunofluorescence in mutants A through J, but not in mutants K, L, and M (Fig. 2C). The absence of immunofluorescence in mutants K, L, and M supports the tenet that the unprocessed, trypsin-resistant fraction of BrkA represents an intracellular form of BrkA, and not simply a trypsin-resistant surface molecule. It should be noted that a deletion (ΔAla^{136}–Pro^{255}) within the BrkA passenger (Met^{1} to Gly^{228}) construct used for mutants A to M did not affect surface expression of BrkA (data not shown). Collectively, these data show that the region spanning residues Ala^{136} to Glu^{693} of BrkA is not required for surface localization of passenger proteins in *E. coli* strain UT5600. Furthermore, since the processed form of the passenger is also evident in deletion constructs A to J (Fig. 2) as well as construct ΔAla^{136}–Pro^{255}, it argues against BrkA having autoproteolytic activity.

Our data indicate that the β-domain of BrkA is itself insufficient to translocate a passenger to the cell surface. The minimal translocation unit for BrkA thus consists of the β-core plus a preceding linker region, the N-terminal boundary of which maps within Glu^{693} to Ser^{701}. Historically, the β-domain has been defined as the C-terminal outer membrane resident fragment derived from proteolytic processing of the autotransporter protein. Although the β-domains of IgA protease (11), VirG/IcsA (31), and AIDA-1 (19) are larger than the β-domain of BrkA, the sizes of their minimal translocation units are remarkably similar. Indeed, a comparison of experimentally defined linkers in four diverse autotransporters including BrkA reveals a structurally conserved architecture that can be viewed as a signature for autotransporters. It consists of a 21- to 30-amino-acid α-helical region that precedes a 255- to 294-amino-acid transporter domain, a region rich in β structure (Fig. 3). It has been proposed that the linker region is involved in forming a hairpin-like structure that leads secretion of the passenger domain through the channel formed by the β-core

(9). The common features of the translocation unit suggest that it, rather than the β-domain, is a more appropriate operational definition for the transporter domain. The region upstream of the translocation unit would thus constitute the passenger moiety regardless of the positioning of the proteolytic processing sites (Fig. 3).

IgA protease, VirG/IcsA, and AIDA-1 are naturally cleaved well upstream of the predicted α-helical region (Fig. 3) and either can be released naturally (6, 26) or can be induced to be released following heat treatment (1). Unlike these proteins, BrkA is steadfastly associated with the bacterial outer membrane both in *B. pertussis* and in *E. coli* and cannot be released by heat treatment (G. Huang and R. Fernandez, unpublished data). Cleavage of BrkA occurs within the predicted α-helical region. Thus, it is possible that the linker region also acts as the anchor (11) for BrkA, since none of the deletion mutant proteins spanning Ala^{136} to Glu^{693} was detected in immunoblots of concentrated culture supernatants (data not shown).

In summary, we have shown that the *B. pertussis* autotransporter BrkA can be surface expressed in *E. coli*, enabling dissection of autotransporter secretion mechanisms in a host more amenable to genetic manipulation. Adding to our previous studies on the BrkA β-domain (28), which we demonstrated has the capacity to form a channel, we have identified two additional secretion determinants of BrkA: a 42-amino-acid signal peptide and a 30- to 39-amino-acid region preceding the β-domain that, together with the β-domain, defines the BrkA translocation unit (Fig. 3). The data presented provide further experimental support for the importance of the predicted α-helical region in autotransporter secretion of both native and heterologous passengers (12, 19, 31).

ACKNOWLEDGMENTS

We thank V. deLorenzo and L. Fernandez for the gift of UT5600 and UT2300. D.C.O. was a recipient of a University of British Columbia graduate student fellowship.

This work was funded by a grant from the Natural Sciences and Engineering Research Council of Canada.

REFERENCES

1. **Benz, I., and M. A. Schmidt.** 1992. Isolation and serologic characterization of AIDA-I, the adhesin mediating the diffuse adherence phenotype of the diarrhea-associated *Escherichia coli* strain 2787 (O126:H27). Infect. Immun. **60**:13–18.
2. **Elish, M. E., J. R. Pierce, and C. F. Earhart.** 1988. Biochemical analysis of spontaneous *fepA* mutants of *Escherichia coli*. J. Gen. Microbiol. **134**:1355–1364.
3. **Emsley, P., I. G. Charles, N. F. Fairweather, and N. W. Isaacs.** 1996. Structure of *Bordetella pertussis* virulence factor P.69 pertactin. Nature **381**:90–92.
4. **Fernandez, R. C., and A. A. Weiss.** 1994. Cloning and sequencing of a *Bordetella pertussis* serum resistance locus. Infect. Immun. **62**:4727–4738.
5. **Fernandez, R. C., and A. A. Weiss.** 1998. Serum resistance in bvg-regulated mutants of *Bordetella pertussis*. FEMS Microbiol. Lett. **163**:57–63.
6. **Fukuda, I., T. Suzuki, H. Munakata, N. Hayashi, E. Katayama, M. Yoshikawa, and C. Sasakawa.** 1995. Cleavage of *Shigella* surface protein VirG occurs at a specific site, but the secretion is not essential for intracellular spreading. J. Bacteriol. **177**:1719–1726.
7. **Grodberg, J., and J. J. Dunn.** 1988. *ompT* encodes the *Escherichia coli* outer membrane protease that cleaves T7 RNA polymerase during purification. J. Bacteriol. **170**:1245–1253.
8. **Henderson, I. R., and J. P. Nataro.** 2001. Virulence functions of autotransporter proteins. Infect. Immun. **69**:1231–1243.
9. **Henderson, I. R., F. Navarro-Garcia, and J. P. Nataro.** 1998. The great escape: structure and function of the autotransporter proteins. Trends Microbiol. **6**:370–378.
10. **Jose, J., R. Bernhardt, and F. Hannemann.** 2002. Cellular surface display of dimeric Adx and whole cell P450-mediated steroid synthesis on *E. coli*. J. Biotechnol. **95**:257–268.
11. **Klauser, T., J. Kramer, K. Otzelberger, J. Pohlner, and T. F. Meyer.** 1993. Characterization of the *Neisseria* IgA beta-core. The essential unit for outer membrane targeting and extracellular protein secretion. J. Mol. Biol. **234**: 579–593.
12. **Klauser, T., J. Pohlner, and T. F. Meyer.** 1990. Extracellular transport of cholera toxin B subunit using *Neisseria* IgA protease beta-domain: conformation-dependent outer membrane translocation. EMBO J. **9**:1991–1999.
13. **Klauser, T., J. Pohlner, and T. F. Meyer.** 1992. Selective extracellular release of cholera toxin B subunit by *Escherichia coli*: dissection of *Neisseria* IgA beta-mediated outer membrane transport. EMBO J. **11**:2327–2335.
14. **Konieczny, M. P., M. Suhr, A. Noll, I. B. Autenrieth, and M. Alexander Schmidt.** 2000. Cell surface presentation of recombinant (poly-) peptides including functional T-cell epitopes by the AIDA autotransporter system. FEMS Immunol. Med. Microbiol. **27**:321–332.
15. **Laemmli, U. K.** 1970. Cleavage of structural proteins during the assembly of the head of bacteriophage T4. Nature **227**:680–685.
16. **Lattemann, C. T., J. Maurer, E. Gerland, and T. F. Meyer.** 2000. Autodisplay: functional display of active β-lactamase on the surface of *Escherichia coli* by the AIDA-I autotransporter. J. Bacteriol. **182**:3726–3733.
17. **Locht, C., R. Antoine, and F. Jacob-Dubuisson.** 2001. *Bordetella pertussis*, molecular pathogenesis under multiple aspects. Curr. Opin. Microbiol. **4**:82–89.
18. **Maurer, J., J. Jose, and T. F. Meyer.** 1997. Autodisplay: one-component system for efficient surface display and release of soluble recombinant proteins from *Escherichia coli*. J. Bacteriol. **179**:794–804.
19. **Maurer, J., J. Jose, and T. F. Meyer.** 1999. Characterization of the essential transport function of the AIDA-I autotransporter and evidence supporting structural predictions. J. Bacteriol. **181**:7014–7020.
20. **McGuffin, L. J., K. Bryson, and D. T. Jones.** 2000. The PSIPRED protein structure prediction server. Bioinformatics **16**:404–405.
21. **Miyazaki, H., N. Yanagida, S. Horinouchi, and T. Beppu.** 1989. Characterization of the precursor of *Serratia marcescens* serine protease and COOH-terminal processing of the precursor during its excretion through the outer membrane of *Escherichia coli*. J. Bacteriol. **171**:6566–6572.
22. **Nielsen, H., J. Engelbrecht, S. Brunak, and G. von Heijne.** 1997. Identification of prokaryotic and eukaryotic signal peptides and prediction of their cleavage sites. Protein Eng. **10**:1–6.
23. **Nielsen, H., and A. Krogh.** 1998. Prediction of signal peptides and signal anchors by a hidden Markov model. Proc. Int. Conf. Intell. Syst. Mol. Biol. **6**:122–130.
24. **Oliver, D. C., and R. C. Fernandez.** 2001. Antibodies to BrkA augment killing of *Bordetella pertussis*. Vaccine **20**:235–241.
25. **Passerini de Rossi, B. N., L. E. Friedman, F. L. Gonzalez Flecha, P. R. Castello, M. A. Franco, and J. P. Rossi.** 1999. Identification of *Bordetella pertussis* virulence-associated outer membrane proteins. FEMS Microbiol. Lett. **172**:9–13.
26. **Pohlner, J., R. Halter, K. Beyreuther, and T. F. Meyer.** 1987. Gene structure and extracellular secretion of *Neisseria gonorrhoeae* IgA protease. Nature **325**:458–462.
27. **Sambrook, J., E. F. Fritsch, and T. Maniatis.** 1989. Molecular cloning: a laboratory manual, 2nd ed. Cold Spring Harbor Laboratory Press, Cold Spring Harbor, N.Y.
28. **Shannon, J. L., and R. C. Fernandez.** 1999. The C-terminal domain of the *Bordetella pertussis* autotransporter BrkA forms a pore in lipid bilayer membranes. J. Bacteriol. **181**:5838–5842.
29. **St. Geme, J. W., III, and D. Cutter.** 2000. The *Haemophilus influenzae* Hia adhesin is an autotransporter protein that remains uncleaved at the C terminus and fully cell associated. J. Bacteriol. **182**:6005–6013.
30. **Suhr, M., I. Benz, and M. A. Schmidt.** 1996. Processing of the AIDA-I precursor: removal of $AIDA^c$ and evidence for the outer membrane anchoring as a beta-barrel structure. Mol. Microbiol. **22**:31–42.
31. **Suzuki, T., M. C. Lett, and C. Sasakawa.** 1995. Extracellular transport of VirG protein in *Shigella*. J. Biol. Chem. **270**:30874–30880.
32. **Valls, M., S. Atrian, V. de Lorenzo, and L. A. Fernandez.** 2000. Engineering a mouse metallothionein on the cell surface of *Ralstonia eutropha* CH34 for immobilization of heavy metals in soil. Nat. Biotechnol. **18**:661–665.
33. **van Ulsen, P., L. van Alphen, C. T. Hopman, A. van der Ende, and J. Tommassen.** 2001. In vivo expression of *Neisseria meningitidis* proteins homologous to the *Haemophilus influenzae* Hap and Hia autotransporters. FEMS Immunol. Med. Microbiol. **32**:53–64.
34. **Veiga, E., V. de Lorenzo, and L. A. Fernandez.** 1999. Probing secretion and translocation of a beta-autotransporter using a reporter single-chain Fv as a cognate passenger domain. Mol. Microbiol. **33**:1232–1243.
35. **Veiga, E., E. Sugawara, H. Nikaido, V. de Lorenzo, and L. A. Fernandez.** 2002. Export of autotransported proteins proceeds through an oligomeric ring shaped by C-terminal domains. EMBO J. **21**:2122–2131.
36. **Weiss, A. A., E. L. Hewlett, G. A. Myers, and S. Falkow.** 1983. Tn*5*-induced mutations affecting virulence factors of *Bordetella pertussis*. Infect. Immun. **42**:33–41.
37. **Weiss, A. A., A. R. Melton, K. E. Walker, C. Andraos-Selim, and J. J. Meidl.** 1989. Use of the promoter fusion transposon Tn*5 lac* to identify mutations in *Bordetella pertussis vir*-regulated genes. Infect. Immun. **57**:2674–2682.

Appendix A.5

A conserved region within the *Bordetella pertussis* autotransporter BrkA is necessary for folding of its passenger domain.

Mol Microbiol. 2003 Mar;47(5):1367-83.

Oliver DC, Huang G, Nodel E, Pleasance S, Fernandez RC.

that directs the translocation of passengers through the channel. On the surface, passengers may be cleaved from the translocation unit and remain non-covalently associated with the bacterial surface, or released into the extracellular milieu. Cleavage of the passenger from the translocation unit can occur via an autoproteolytic mechanism (for example if the passenger domain is a protease) or it can be mediated by endogenous outer membrane proteases.

The recent results by Veiga *et al.* (2002) have shown that the IgA protease β-domain is capable of forming channels with an inner diameter of 2 nm. The size of the channel is 2.5–5 times smaller than other characterized type II and type III secretion system secretins that translocate folded proteins (Thanassi, 2002). Veiga *et al.* (1999) point out that such a channel would be sufficient for secreting small folded proteins or protein domains. However, a channel of this size would be incapable of secreting larger folded passenger domains. In fact, bulkier passengers such as non-reduced ScFv (single-chain antibody) fusions are only inefficiently (i.e. 15–20%) translocated). It has previously been shown that translocation is a two step process involving: (i) insertion of the C-terminal translocation unit into the outer membrane; and (ii) translocation of the passenger (Klauser *et al.*, 1992). In this regard, seminal studies characterizing the secretion of IgA protease have come to the conclusion that translocation across the outer membrane takes place in an unfolded or translocation competent conformation (Pohlner *et al.*, 1987; Klauser *et al.*, 1990; Klauser *et al.*, 1993b). Thus, given that autotransporter secretion involves a translocation competent folding state one would predict that mechanisms exist: (i) to maintain the polypeptide in a translocation competent folding state within the periplasm (which would include providing protection from periplasmic proteases); and (ii) to promote proper and rapid folding of the passenger on the surface of the bacterium, ostensibly in the absence of chaperones. Consistent with the self-contained autotransporter theme, it is possible that the information required for folding of the passenger domain is encoded within the polypeptide itself. In this regard, a putative intramolecular chaperone region has previously been identified in PrtS, a *Serratia marcescens* autotransporter with protease activity (Ohnishi *et al.*, 1994). This region, termed the 'junction', is found in the C-terminus of the passenger domain just upstream of the β domain and functional activity of the protease is dependent on the junction region being intact. Whether the proposed intramolecular chaperone function of the junction region is a general theme for all autotransporters, including non-proteases, remains to be determined.

In this study we sought to investigate the role of the C-terminal region of the passenger domain of BrkA, an autotransporter protein with no sequence or functional identity with PrtS. BrkA is a *Bordetella pertussis* virulence factor that is one of many *B. pertussis* adhesins (Ewanowich *et al.*, 1989; Fernandez and Weiss, 1994; Locht *et al.*, 2001). It also mediates serum resistance (Fernandez and Weiss, 1994). BrkA is regulated by the Bvg two-component regulatory system and is expressed as a preproprotein of 103 kDa. Two processing sites have been identified – one that yields a 42 amino acid signal peptide (Oliver *et al.*, 2003) and one that produces a 30 kDa outer membrane resident transporter (β) domain (Passerini de Rossi *et al.*, 1999; Shannon and Fernandez, 1999). A refolded recombinant form of the β-domain has been shown to produce channels with a conductivity of 3.2 nanoSiemens (nS) in black lipid bilayers (Shannon and Fernandez, 1999). Although cleaved, the 73 kDa BrkA passenger remains tightly associated with the bacterial surface (Oliver and Fernandez, 2001; Oliver *et al.*, 2003). Using structural, functional, and sequence analysis, we show that a region in the C-terminus of the BrkA passenger domain is required for folding of the passenger. This region is conserved in a large group of autotransporters having diverse functions indicating that it serves an important function for these proteins that is related to autotransporter secretion. We propose that this conserved domain is necessary for folding of the BrkA passenger concurrent with or following translocation through the β-domain channel.

Results

BrkA Glu^{601}–Ala^{692} is necessary for passenger stability in the presence of endogenous outer membrane proteases

In an effort to dissect the mechanism of BrkA secretion we have made several in frame deletions within the BrkA passenger domain. Interestingly, mutations within the C-terminus of the passenger domain rendered the secreted form of the protein unstable in *E. coli* strain DH5α (data not shown). Based on these observations we postulated that the BrkA passenger might encode a region important for folding of its passenger domain similar to the PrtS protease junction region (Ohnishi *et al.*, 1994). Ohnishi and colleagues observed that when a junction-deleted PrtS was expressed in *E. coli*, neither the mature PrtS protein nor enzymatic activity could be detected. On the other hand, a processed form of the β-core was found in the outer membrane. They proposed that the mature protease was being degraded at the cell surface because it could not fold into an active and stable conformation. We wondered whether a similar region might exist to promote folding of BrkA thereby conferring stability to the exported protein. We hypothesized that a properly folded BrkA passenger would be stable in the presence of proteases, but

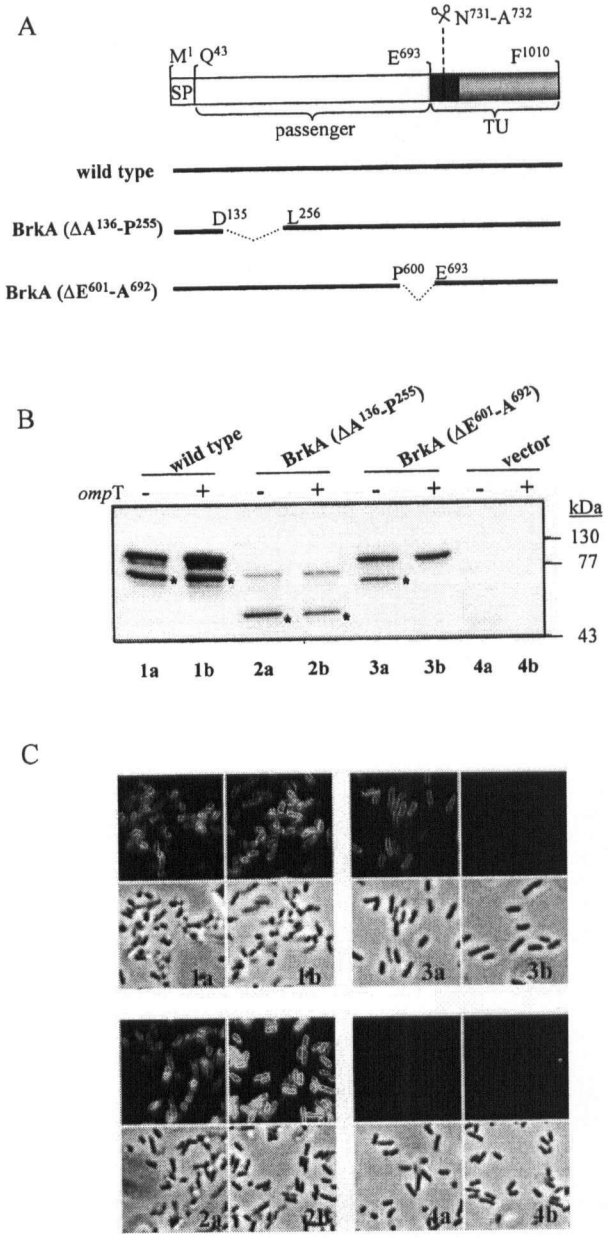

Fig. 1. Expression of mutant forms of BrkA.
A. BrkA domain organization. SP, signal peptide (residues 1–42); passenger domain (residues 43–692); shaded boxes represent the BrkA linker region (dark grey) and β-core (light grey) which form the translocation unit (TU; residues 693–1010) (Oliver *et al.*, 2003). Wild-type BrkA was expressed from pDO6935; BrkA (ΔA^{136}-P^{255}) was expressed from pDO244; and BrkA (ΔE^{601}-A^{692}) was expressed from pGH3-13.
B. Analysis of BrkA expression. Plasmids were transformed into isogenic *E. coli* strains UT2300 (*ompT*$^+$) and UT5600 (*ompT*$^-$). Bacteria were grown to 0.8 optical density units and harvested for analysis of BrkA expression by immunoblot and indirect immunofluorescence. Whole cell lysates were resolved by SDS–PAGE and blots were probed with anti-BrkA antiserum. (a) *E. coli* strain UT5600 and (b) *E. coli* strain UT2300. Band denoted by an asterisk (*), corresponds to the passenger processed between residues N^{731} and A^{732}. Plasmid pBluescript served as a vector control.
C. Indirect immunofluorecence was used to evaluate surface expression of each of the mutants.

if the BrkA passenger were unable to fold properly, it would be unstable and subject to degradation during secretion. To test this hypothesis, we developed an assay to compare the surface expression of wild-type and mutant constructs of BrkA in *E. coli* strains UT2300 and UT5600. These strains have been used routinely to study secretion of autotransporters from different bacterial species (Klauser *et al.*, 1993a; Suzuki *et al.*, 1995; Maurer *et al.*, 1997; 1999; Veiga *et al.*, 1999) including BrkA (Oliver *et al.*, 2003). UT2300 has an OmpT$^+$ and OmpP$^+$ phenotype, whereas UT5600 lacks these outer membrane proteases (Elish *et al.*, 1988). We thus compared wildtype BrkA with mutant constructs bearing deletions in either the amino (ΔAla^{136}–Pro^{255}) or carboxy (ΔGlu^{601}–Ala^{692}) termini of the BrkA passenger (α) domain; this carboxy terminus deletion would effectively represent the junction region in PrtS protease, despite a lack of sequence identity.

Expression of wild-type BrkA in both *E. coli* UT5600 and in UT2300 was detected by immunoblot (Fig. 1B, lanes 1a and 1b). The upper band migrating at approximately 103 kDa corresponds to the unprocessed BrkA precursor and the lower band migrating at 73 kDa corresponds to the cleaved BrkA passenger region. The intensity of the precursor band is variable and its nature and cellular location are not known. It has been noted that IPTG-induction of the PrtS autotransporter in *E. coli* resulted in a fraction of the PrtS precursor forming insoluble periplasmic species (Miyazaki *et al.*, 1989; Shikata *et al.*, 1993). It is possible that a proportion of the BrkA precursor may undergo a similar fate when expressed in *E. coli.* As we have previously shown, the lower band represents the surface exposed fraction of BrkA in UT5600 (Oliver *et al.*, 2003); a corresponding band is seen in the UT2300 background. Surface expression of BrkA was also detected via indirect immunofluorescence on both *E. coli* UT2300 and UT5600 (Fig. 1C, panels 1a and 1b). Taken together these data indicate that the BrkA passenger domain is surface expressed in a stable manner in *E. coli* strains UT2300 and UT5600.

When BrkA (ΔGlu^{601}–Ala^{692}) was expressed in UT5600 both the unprocessed precursor and the processed passenger were detected by immunoblot (Fig. 1B, lane 3a). In contrast, when BrkA (ΔGlu^{601}–Ala^{692}) was expressed in *E. coli* strain UT2300 only the unprocessed BrkA (ΔGlu^{601}–Ala^{692}) precursor was observed (Fig. 1B, lane 3b), suggesting that deletion of residues 601–692 rendered the processed BrkA passenger susceptible to proteolysis by the outer membrane proteases OmpT and OmpP. Consistent with this observation, immunofluorescence data showed that BrkA (ΔGlu^{601}–Ala^{692}) was detected on the surface of *E. coli* strain UT5600 but not on *E. coli* strain UT2300 (Fig. 1C, panels 3a and 3b), despite the precursor (upper band) being made. Deletions

within the N-terminal region of BrkA had a different outcome. BrkA (ΔAla^{136}–Pro^{255}) was surface expressed in a stable manner in both *E. coli* strain UT5600 and UT2300 (Fig. 1B and C, panels 2a and 2b) suggesting that the deletion of amino acids 136–255 did not influence the stability of the BrkA passenger.

A conserved domain is found within the passenger region of several autotransporters

The observations that deletion of Glu^{601}–Ala^{692} renders the BrkA passenger unstable in the presence of outer membrane proteases are consistent with the results presented by Ohnishi and colleagues characterizing the PrtS protease junction region. The functional parallels with this junction region suggest that the role of region Glu^{601}–Ala^{692} may be common to other autotransporter proteins. Therefore, to further our analysis we queried the ProDom database with the BrkA sequence (http://prodes.toulouse.inra.fr/prodom/2001.3/html/home.php) to look for proteins in the database that might have sequence identity with region Glu^{601}–Ala^{692} of BrkA. We reasoned that such an analysis might identify regions of weak homology that would provide an evolutionarily conserved function. The ProDom database (Corpet *et al.*, 2000) consists of an automatic compilation of homologous domains compiled using recursive position specific iterative BLAST (PSI-BLAST) searches of non-fragmentary sequences from SWISS-PROT 39, TrEMBL and TrEMBL update databases. ProDom (release 2001.3) analysis of the BrkA primary amino acid sequence identified a conserved domain (PD002475) at the C-terminus of the BrkA passenger spanning residues Asn^{578}–Asp^{702} (Fig. 3A). BrkA (ΔGlu^{601}–Ala^{692}) is found within this region. Domain PD002475 was found in at least 55 proteins, all of which are known to be or predicted to be autotransporters. Figure 2 depicts a subset of autotransporters bearing domain PD002475. Interestingly, domain PD002475 is consistently located near the C-terminus of the passenger domain upstream of the predicted β-domain, although the distance between domain PD002475 and the predicted β-domain varies. The observation that domain PD002475 is conserved amongst autotransporter proteins having diverse functions from multiple Gram-negative species suggests that the region may play a general role in autotransporter secretion.

As a result of the automatic compilation of the ProDom database, the boundaries of the ProDom domains can vary with each release of the database as more entries are added to it. Thus, to refine our analysis of domain PD002475, A CLUSTALW (Thompson *et al.*, 1994) alignment of domain PD002475 from the autotransporter proteins depicted in Fig. 2 was performed. As shown in Fig. 3A the highest degree of sequence conservation occurs over a region corresponding to residues Thr^{606}–Leu^{702} of BrkA. The predicted secondary structure for this region in these proteins was also highly conserved (Fig. 3A). It should be noted that sequence conservation decreases dramatically N-terminal to Thr^{606} and C-terminal to Leu^{702} (not shown).

The list of proteins bearing ProDom PD002475 includes pertactin (Prn). The structure of the pertactin passenger domain has been solved (accession number 1DAB) and shown to be a monomer folded into a single domain that is almost entirely made up of a right-handed cylindrical β-helix (Fig. 3B) (Emsley *et al.*, 1996). Given the remarkable degree of primary and secondary structural conservation within ProDom domain PD002475 we decided to examine the known structure of the pertactin passenger domain to gain insights into the tertiary structure of domain PD002475. Residues Val^{472}–Leu^{566} of the pertactin passenger, which correspond to residues Thr^{606}–Leu^{702} of BrkA, are located at the base of the β-helical structure (Fig. 3B). Interestingly, residues Glu^{463}–Phe^{470} comprise a loop located at the N-terminus of the conserved region (Fig. 3B, denoted by an arrow). This loop region corresponds to residues Ala^{597}–Tyr^{604} of BrkA (Fig. 3A).

In vivo trans *complementation of BrkA folding*

The data indicating that residues Glu^{601}–Ala^{692} are required for stability of the BrkA passenger domain suggested that this region might either serve to prevent unfolding of the passenger, or it might facilitate folding of the passenger domain during secretion. Domain PD002475 is naturally cleaved away from the mature form of some autotransporters including AIDA-1 (Benz and Schmidt, 1992), arguing against the notion that it functions to prevent unfolding of the passenger. We thus hypothesized that residues Glu^{601}–Ala^{692} are involved in promoting folding of BrkA. To test this hypothesis we developed an *in vivo* system to assess whether residues Glu^{601}–Ala^{692} are able to restore stability to BrkA (ΔGlu^{601}–Ala^{692}) when expressed in *trans*. Plasmid pDO-JB5 was constructed bearing an in frame deletion of residues Ala^{52}–Pro^{600} of BrkA. The product expressed from pDO-JB5 includes the BrkA signal peptide (Met^{1}–Ala^{42}) and the BrkA translocation unit (Glu^{693}–Phe^{1010}) (Oliver *et al.*, 2003) thus enabling export of residues Glu^{601}–Ala^{692} (the putative BrkA junction region) to the bacterial surface. Glu^{601} was chosen as the N-terminal boundary of the BrkA junction region as (i) the level of sequence conservation decreases markedly N-terminal to Thr^{606} (Fig. 3A) and (ii) because residues Ala^{597}–Tyr^{604} may represent an exposed loop (Fig. 3B) which could serve as a practical linker to construct a fusion that would avoid disrupting the core structure of the protein. Plasmid pDO-JB5 was introduced into *E. coli* strain UT5600. Immunoblot analysis of an over-exposed

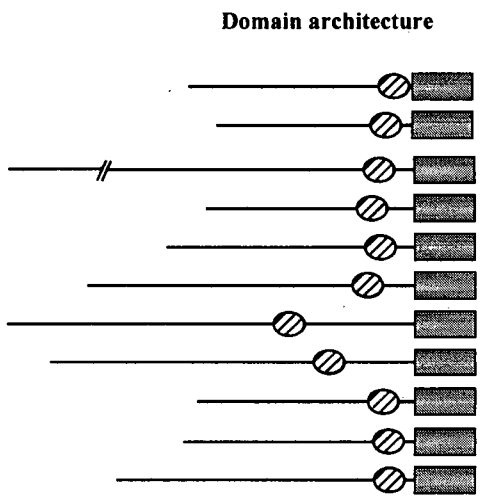

Domain architecture	Protein	Function	Organism	Accession number
	BrkA	serum^R / adherence	*B. pertussis*	U12276
	Prn	adherence	*B. pertussis*	AJ006158
	ShdA	shedding	*Salmonella sp.*	AF140550
	MisL	unknown	*S. typhimurium*	AF106566
	IcsA*	intracellular spread	*S. flexneri*	M22802
	Hap	protease	*H. influenzae*	U11024
	IgA prot.	protease	*H. influenzae*	X59800
	IgA prot.	protease	*N. gonorrhoeae*	X04835
	TibA	unknown	*E. coli*	AF109215
	Ag43	aggregation	*E. coli*	P39180
	AIDA-I	diffuse adherence	*E. coli*	X65022

Fig. 2. Identification of a conserved domain within the passenger region of several autotransporter proteins. Domain architecture of selected autotransporters. The ProDom database (version 2001.3) was searched using the BrkA primary amino acid sequence (Met^1–Phe^{1010}) and narrowed by querying domain PD002475. Ovals represent the relative position of domain PD002475 within each peptide sequence and the rectangular boxes represent the conserved β-domain (ProDom assignment PD002217). Protein name, function, bacterial host, and the GenBank accession number are noted. ShdA does not match amino acid scale, denoted by (//). *IcsA is also known as VirG.

blot using an antibody that recognizes residues 1–693 of BrkA revealed that BrkA (ΔAla^{52}–Pro^{600}) was expressed (Fig. 4B). Several forms of BrkA (ΔAla^{52}–Pro^{600}) were detected that correspond to unprocessed and processed forms of the precursor. Having demonstrated that BrkA (ΔAla^{52}–Pro^{600}) is expressed, we next asked whether coexpression of BrkA (ΔAla^{52}–Pro^{600}) could rescue the instability of BrkA (ΔGlu^{601}–Ala^{692}) (Fig. 1). We first co-transformed *E. coli* strains UT5600 and UT2300 with plasmids pDO-JB5 and pDO6935K representing BrkA (ΔAla^{52}–Pro^{600}) and wild-type BrkA respectively. Co-transformed clones were grown to an OD_{600} of ~0.8 and whole cell lysates were resolved by SDS-PAGE. BrkA expression was probed by immunoblot. As shown in Fig. 4C, processing and expression of wild-type BrkA was not affected in either *E. coli* UT5600 or UT2300 strains that were co-transformed with pDO-JB5 and pDO6935K, indicating that BrkA (ΔAla^{52}–Pro^{600}) does not interfere with the expression of wild-type BrkA.

We next co-transformed *E. coli* strains UT5600 and UT2300 with plasmids pDO-JB5 and pGH3–13K; the latter encoding the junction-deleted BrkA species. As a negative control, *E. coli* UT5600 and UT2300 were co-transformed with plasmids pBluescript (vector control) and pGH3–13K. In *E. coli* co-transformed with pDO-JB5 and pGH3–13K, a band migrating at approximately 65 kDa corresponding to the cleaved passenger region of BrkA (ΔGlu^{601}–Ala^{692}) was detected in strains UT5600 and UT2300 (Fig. 4C). In contrast, in *E. coli* co-transformed with plasmids pBluescript and pGH3–13K the band migrating at approximately 65 kDa was detected in strain UT5600 but not in UT2300. These results indicate that expression of BrkA (ΔAla^{52}–Pro^{600}) is sufficient to produce a stable form of the BrkA (ΔGlu^{601}–Ala^{692}) passenger in *E. coli* strain UT2300, although the level of complementation is not 100%.

In vivo *evidence demonstrating that residues Glu^{601}–Ala^{692} of BrkA are required for folding of the BrkA passenger*

The observation that the stability of the BrkA (ΔGlu^{601}–Ala^{692}) passenger region in *E. coli* strain UT2300 can be rescued by expressing BrkA (ΔAla^{52}–Pro^{600}) as a separate polypeptide within the same cell suggests that the BrkA junction region plays a role in folding of the BrkA passenger domain. To further investigate the role of the BrkA junction region we performed trypsin analyses of BrkA expressed on the surface of *E. coli* strain UT5600. We first performed trypsin accessibility assays to confirm that the 73 kDa and 65 kDa passengers were indeed surface expressed. Cells were exposed to trypsin, washed and whole cell lysates were analysed by immunoblot. Exposure of each clone to trypsin resulted in the removal of the band corresponding to the processed passenger domain indicating that the passenger was exported to the surface (Fig. 5A). It is worth noting, that coexpression of BrkA (ΔAla^{52}–Pro^{600}) did not affect the surface expression of either wild-type BrkA or BrkA (ΔGlu^{601}–Ala^{692}) (Fig. 5A).

Having shown that each passenger was accessible to trypsin we performed trypsin susceptibility assays on each of the clones to probe the tertiary structure of surface

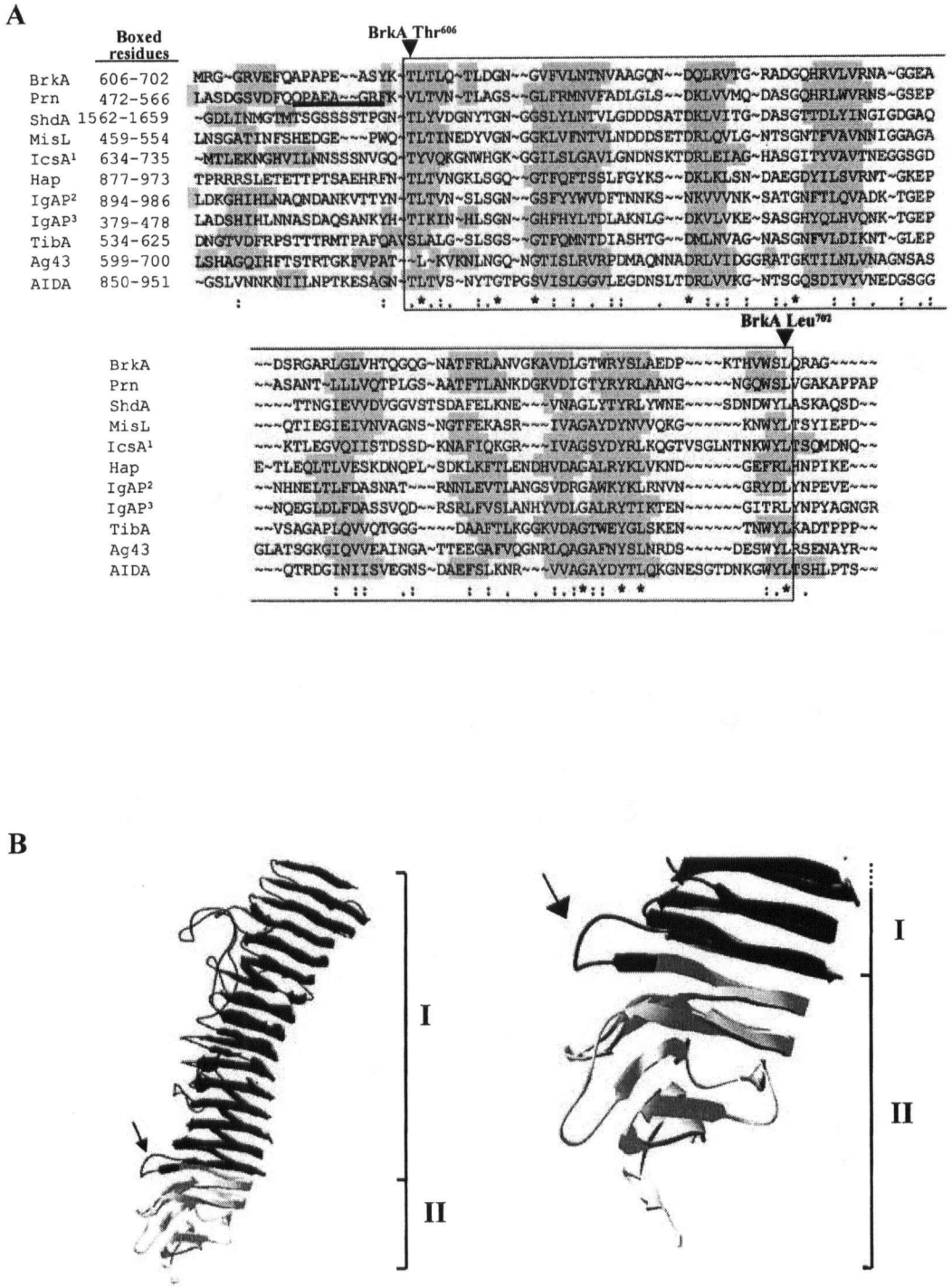

Fig. 3. Comparative analysis of the junction region found within several autotransporters.

A. CLUSTALW alignment of autotransporters depicted in Fig. 2. The position of the amino acids within the boxed region is noted for each protein. Only regions of significant amino acid conservation are shown. (*), > 80% identity; (.), > 40% identity; (:), > 60% similarity. Grey shading denotes regions predicted to form β-sheet structure by the secondary structural prediction program PSIPRED. Unshaded regions are predicted to have coil structure. PsiPred scores were assigned at a confidence level of >2. Underlined region of Prn denotes a loop region comprised of residues Gln^{463}–Phe^{470}. [1]Also known as VirG; [2]From *H. influenzae*; [3]From *N. gonorrhoeae*.

B. Ribbon representation of the 3D structure of pertactin (1DABA) illustrating the relative location and architecture of residues Asp^{35}–Pro^{573}. (I) demarks residues Asp^{35}-Arg^{452}; and (II) demarks residues Leu^{453}- Pro^{573}. Residues Val^{472}-Pro^{573} are shaded grey. Arrow denotes a loop region comprised of residues Gln^{463}-Phe^{470} of Prn. Note, amino acid numbers correspond to GenBank Accession number CAA06900 for pertactin. Left: complete 1DABA structure. Right: Close-up view of regions I and II.

expressed BrkA. Trypsin susceptibility was assayed by limited proteolysis experiments where cells were exposed to low concentrations (0.01 mg ml^{-1}) of trypsin and the stability of each passenger was monitored over time. As shown in Fig. 5B, the band corresponding to the 73 kDa processed form of the wild-type BrkA passenger domain remained stable following exposure to trypsin indicating that the protein had adopted a conformation that was resistant to low concentrations of trypsin. Similarly, when BrkA (ΔGlu^{601}–Ala^{692}) was co-expressed with BrkA (ΔAla^{52}–Pro^{600}) a band corresponding to the 65 kDa passenger was also detected after 15 min. In marked contrast, when BrkA (ΔGlu^{601}–Ala^{692}) was expressed in the absence of BrkA (ΔAla^{52}–Pro^{600}), the band corresponding to the 65 kDa passenger was not detected following exposure to trypsin. The rapid disappearance of the 65 kDa band indicates that the passenger existed in a conformation exposing multiple trypsin sensitive cleavage sites suggesting BrkA (ΔGlu^{601}–Ala^{692}) had not assumed a folded conformation.

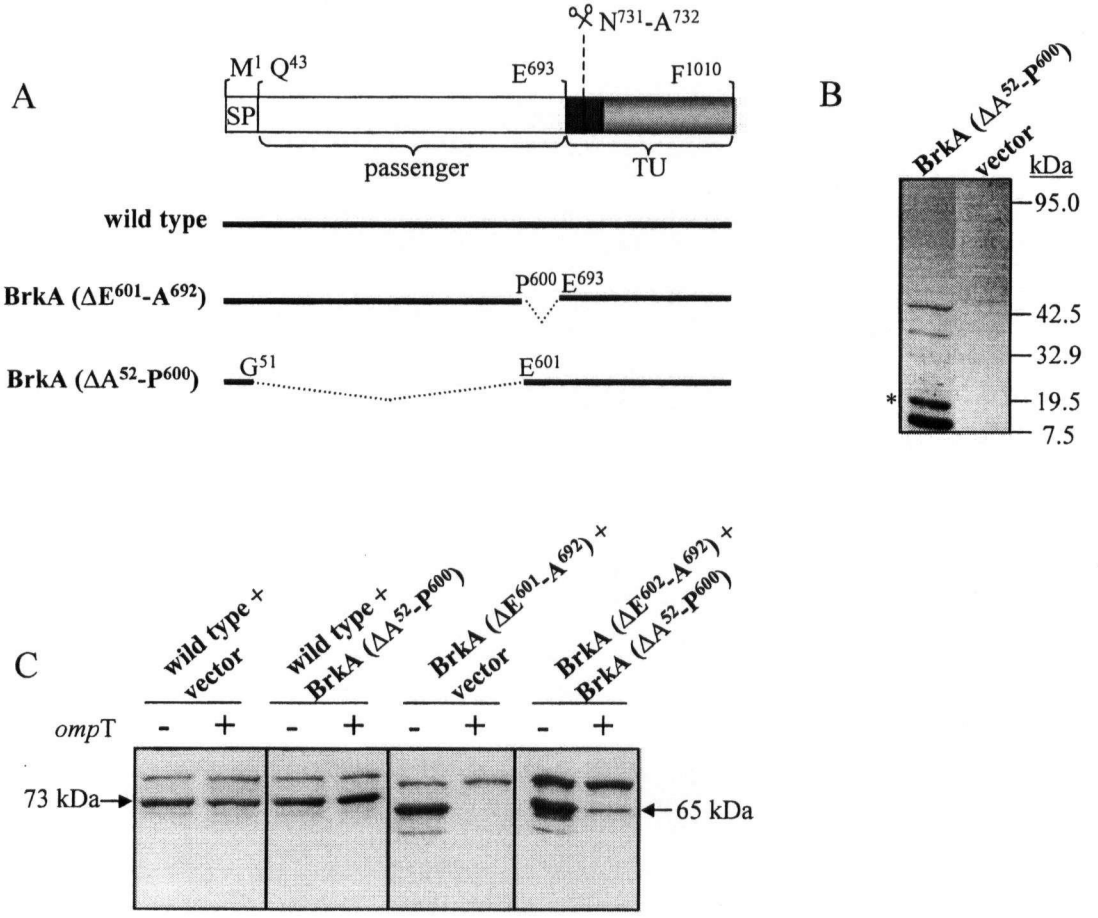

Fig. 4. *In vivo trans* complementation of BrkA stability.
A. BrkA domain organization as described in Fig. 1A.
B. Detection of BrkA (ΔA^{52}–P^{600}) expression in *E. coli* strain UT5600. *E. coli* strain UT5600 harbouring plasmid pDO-JB5 was grown to 0.8 OD units and harvested by centrifugation. Whole cell lysates were resolved by SDS-PAGE and BrkA expression was probed by immunoblot. The asterisk denotes the band corresponding to the processed passenger domain and the lowest band represents a further cleavage of the passenger. Blots were overexposed since the deleted clone has only a small fraction of the residues recognized by the antiserum.
C. Evaluating the effect of BrkA (ΔA^{52}–P^{600}) expression on the stability of wild type BrkA and BrkA (ΔE^{601}–A^{692}) in *E. coli* strains UT5600 (*ompT*$^-$) and UT2300 (*ompT*$^+$). *E. coli* were co-transformed with individual plasmids encoding BrkA variants depicted in Fig. 4A. Cells were grown to an OD of 0.8 and harvested by centrifugation. Whole cell lysates were resolved by SDS-PAGE and probed by immunoblot. When present the co-expression of BrkA (ΔA^{52}–P^{600}) was observed in overexposed blots (data not shown). Experiments were performed three times and a representative experiment is shown. Wild-type BrkA, BrkA (ΔE^{601}–A^{692}) and BrkA (ΔA^{52}–P^{600}) were expressed from plasmids pDO6935K, pGH3–13K and pDO-JB5 respectively. Plasmid pBluescript was employed as a vector control.

In vitro *evidence demonstrating that residues Ile^{535}–Val^{699} of BrkA are required for folding of the BrkA passenger*

To further investigate the role of the BrkA junction in folding of the passenger domain, we performed *in vitro* structural and functional analyses on refolded, purified recombinant forms of the protein. Expression constructs pDO418, pDO618 and pDO518 were used to over express His-tagged fusion proteins DO418P, DO618P and DO518P containing residues (Glu^{61}–Val^{699}) (Glu^{61}–Asp^{534}) (Ile^{535}–Val^{699}) of the BrkA passenger region respectively (Fig. 6A). Expression constructs pDO618, pDO518 were derived from plasmid pDO418 using a convenient *Eco*RV restriction site. Each fusion protein had an N-terminal 6 × His tag and DO618P has an additional 15 amino acids derived from the cloning vector (see *Experimental procedures*). Expressed proteins were purified from inclusion bodies under denaturing conditions (8 M urea) using nickel affinity chromatography as described (Shannon and Fernandez, 1999; Oliver and Fernandez, 2001). Each fusion protein was purified to near homogeneity insofar as no other contaminating species were observed following resolution by SDS-PAGE. Purified fusion proteins were renatured individually by dialysing them simultaneously against decreasing concentrations of urea in the presence of 0.1% Triton X-100, followed by a final dialysis against 10 mM Tris, pH 8 (Shannon and Fernandez, 1999; Oliver and Fernandez, 2001). Following dialysis, fusion proteins DO418P and DO618P remained soluble whereas fusion DO518P formed a visible precipitate indicative of protein aggregation. DO518P was thus excluded from further analyses.

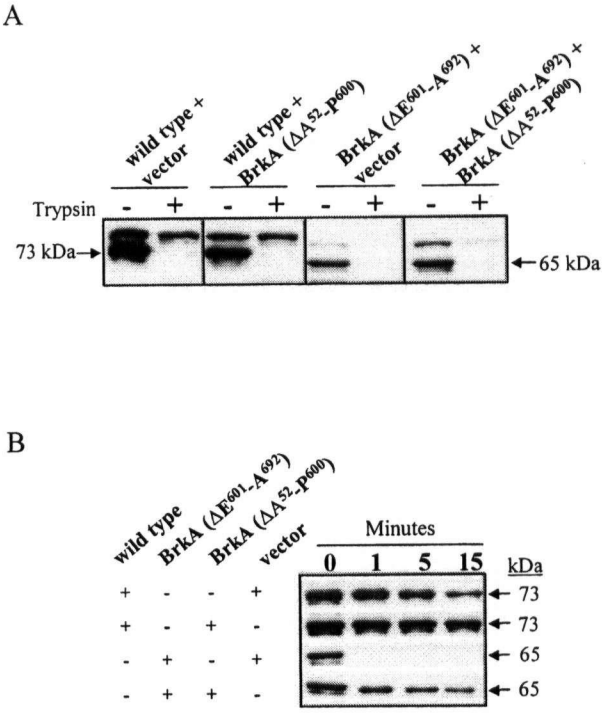

Fig. 5. Characterization of surface expressed forms of BrkA by trypsin analysis.
A. Trypsin accessibility analysis of BrkA expression. *Escherichia coli* UT5600 was co-transformed with plasmids encoding the indicated BrkA variants. Cells were grown to an OD of 0.8 and harvested by centrifugation. Surface expressed BrkA was digested with 0.1 mg ml^{-1} trypsin and washed as described in the *Experimental procedures*. Whole cell lysates were resolved by SDS-PAGE and BrkA expression was assessed by immunoblot. Arrows denote the surface exposed passenger domain of BrkA (wild type) and BrkA (ΔE^{601}–A^{692}), migrating at approximately 73 kDa and 65 kDa respectively.
B. Trypsin susceptibility analysis of surface exposed BrkA. *Escherichia coli* UT5600 were co-transformed with plasmids encoding BrkA variants indicated on the right. (+) indicates presence of plasmids and (–) indicates absence of plasmid. Cells were grown to an OD of 0.8 and harvested by centrifugation. Cells were exposed to 0.01 mg ml^{-1} trypsin and digestion was stopped at various time points (minutes) as described in the *Experimental procedures*. BrkA expression was detected by immunoblot. Arrows denote the surface exposed passenger domain of BrkA (wild type) and BrkA (ΔE^{601}–A^{692}), migrating at approximately 73 kDa and 65 kDa respectively. Experiments were performed three times and a representative experiment is shown. Wild-type BrkA, BrkA (ΔE^{601}–A^{692}) and BrkA (ΔA^{52}–P^{600}) were expressed from plasmids pDO6935K, pGH3–13K and pDO-JB5 respectively. Plasmid pBluescript was employed as a vector control.

Fusion proteins DO418P and DO618P were assayed for function. BrkA contributes to *B. pertussis* adherence to both HeLa epithelial cells (Ewanowich *et al.*, 1989) and MRC5 lung fibroblasts (Fernandez and Weiss, 1994), in addition to mediating serum resistance. To determine whether renatured DO418P or DO618P were able to bind host cells we incubated each peptide with HeLa cells and measured binding via FACS analysis using an antibody to the BrkA passenger domain. This antibody recognizes both native and denatured BrkA (Oliver and Fernandez, 2001). As shown in Fig. 6B, treatment of HeLa cells with DO418P resulted in a significant increase in fluorescence over the untreated control. In contrast, treatment with DO618P resulted in a signal that was only slightly above the background levels seen with the untreated control. These results indicate that renatured DO418P bound to HeLa cells well, whereas renatured DO618P bound poorly. Thus, the information encoded within the region bounded by residues Ile^{535}–Val^{699}, which spans the junction region, is necessary for the production of functional recombinant BrkA. It is possible that Ile^{535}–Val^{699} encodes a binding domain, however, the junction region is present in a variety of passengers with a diverse array of functions, arguing that the junction performs a more general function.

To gain insights into the structure of dialysed DO418P and DO618P we used limited proteolysis as a probe of tertiary structure. Exposure to trypsin resulted in a significant and rapid reduction in the band corresponding to DO618P over time (Fig. 6C). In contrast, DO418P remained remarkably stable in the presence of trypsin

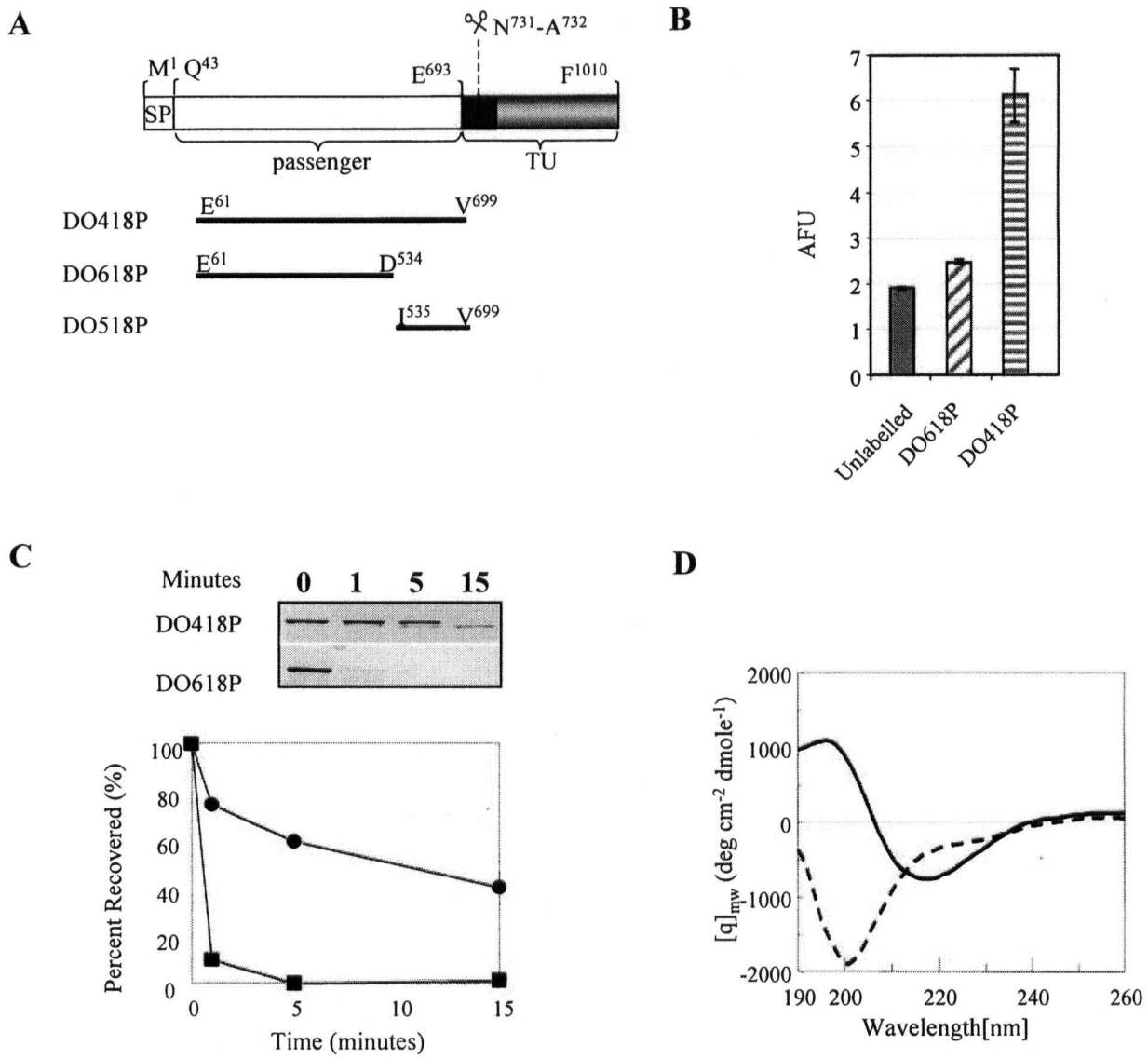

Fig. 6. Characterization of refolded BrkA fusion peptides.
A. Diagram illustrating positions of fusion constructs compared to primary BrkA sequence. BrkA domain structure is described in Fig. 1.
B. Binding assays for DO418P and DO618P. Equimolar concentrations of fusion proteins DO418P and DO618P were added to HeLa cells and binding was assessed via fluorescence activated cell sorting. Binding assays were performed as described in the *Experimental procedures* and reported as arbitrary fluorescence units (AFU).
C. Protease sensitivity analysis comparing the relative stability of renatured DO418P and DO618P. 7.5 μg of dialysed DO418P or DO618P was digested with trypsin at room temperature. Digestion was stopped at various time points and samples were resolved by SDS-PAGE and visualized by staining with Coomassie brilliant blue (top panel). Densitometry was performed on each lane at positions corresponding to the migration of undigested fusion protein. Density of each band was recorded as arbitrary units and percent recovered was calculated based on arbitrary densitometry units measured for each time point (minutes) relative to time zero.
D. Far-UV circular dichroism (CD) profiles of DO418P and DO618P. Equimolar amounts of purified DO418P and DO618P were dialysed against decreasing concentrations of urea into a final buffer of 10 mM Tris pH 8 and submitted to 10 scans between 190 nm and 260 nm. Solid line, DO418P; dashed line, DO618P.

suggesting that the protein had adopted a folded conformation. To characterize the secondary structure of fusion proteins DO418P and DO618P we employed far-UV circular dichroism spectroscopy. Fusion protein DO418P was shown to have a far-UV CD profile indicative of a protein rich in beta-structure with a minimum at 218 nm (Fig. 6D). This far-UV CD profile is consistent with PSIPRED secondary structural analysis (McGuffin *et al.*, 2000) that

predicts that the BrkA passenger domain is primarily composed of β-sheet. In contrast, fusion protein DO618P (Glu^{61}–Asp^{534}) had a non-structured far-UV CD profile with a minimum at 202 nm (Fig. 2D). It is worth noting that similar non-structured profiles were also observed for DO187P and DO417P, independent 6 × His BrkA fusion proteins consisting of residues Glu^{61}–Ser^{517} and Glu^{61}–Phe^{595} (data not shown).

Discussion

Prokaryotic and eukaryotic translocation systems exist to enable proteins to traverse biological membranes (Agarraberes and Dice, 2001). A common feature amongst the well-characterized Sec pathway of prokayotes and the mitochondrial and chloroplast import pathways of eukaryotes is that translocating proteins must be unfolded before or concurrent with translocation. In these systems the unfolding and refolding of the translocating protein on either side of the membrane is facilitated by system specific intermolecular chaperones (Agarraberes and Dice, 2001). In Gram-negative bacteria, proteins destined to be secreted must cross two membranes – the cytoplasmic membrane and the outer membrane. As reviewed by Thanassi (2002), both Sec-dependent and Sec-independent pathways exist to export proteins out of the cytoplasm, and regardless of which secretion system is employed crossing the outer membrane is reliant on a channel. Well-characterized outer membrane channels that transport proteins include ushers, secretins and TolC, having diameters of 2–3, 5–10, and 3 nm, respectively (Thanassi, 2002). The larger secretin channels are of sufficient size to accommodate oligomeric folded proteins, however, the smaller size of the ushers and TolC likely demand that their substrates be secreted in a linear (Thanassi, 2002), partially unfolded (Buchanan, 2001) translocation competent state. Autotransporter secretion can be viewed as a stepwise process in which the inner membrane, the periplasmic space and the outer membrane are traversed. Many questions remain to be answered regarding the mechanisms surrounding each of these steps including the status of the passenger folding state before, during, and following secretion. We have undertaken a structure–function analysis of the BrkA protein to gain insight into the mechanism of autotransporter secretion. BrkA is a 103 kDa protein that contains the structural hallmarks of a protein secreted via an autotransporter mechanism including: an N-terminal signal sequence, a 73 kDa passenger domain to be delivered to the bacterial surface, and a translocation unit made up of a short α-helical linker coupled to a conserved 30 kDa C-terminal autotransporter domain (Shannon and Fernandez, 1999; Oliver and Fernandez, 2001; Oliver *et al.*, 2003). In this study we identify a conserved domain located at the C-terminus of the BrkA passenger region. This junction region is found in a functionally diverse group of proteins known or predicted to be autotransporter proteins suggesting that it performs a general role in secretion.

The BrkA junction region mediates folding of the BrkA passenger domain

We have shown that the BrkA junction, defined as residues Glu^{601}–Ala^{692} confers stability to the BrkA passenger domain. Deletion of residues Glu^{601}–Ala^{692} rendered the protein susceptible to degradation by the outer membrane proteases OmpP and OmpT, and by trypsin. Consistent with this *in vivo* data, BrkA passenger domain fusion proteins bearing a deletion comprising the BrkA junction were non-functional in an adherence assay and were also highly susceptible to proteolysis by trypsin. Furthermore, we demonstrated that BrkA fusions that lacked the junction region had a far-UV CD profile indicative of an unfolded protein. Collectively, these data suggest that the BrkA junction is important for folding of the BrkA passenger domain.

An indication as to how the junction region might effect folding has come from an analysis of the folding behaviour of fusion proteins encompassing or lacking the junction region. Fusion protein DO618P, representing a junction-deleted passenger, remained soluble and unfolded following dialysis; however, fusion protein DO518P (Ile^{535}–Val^{699}) which encompasses the junction precipitated following dialysis, suggesting that folding of the protein had been initiated but resulted in an off-pathway (misfolded) aggregate. These data support the concept that information encoded within residues Ile^{535}–Val^{699} is necessary to initiate or trigger folding of the BrkA passenger.

The fact that the junction region engineered to be surface expressed, could rescue the instability of a mutant that lacked Glu^{601}–Ala^{692} when provided *in trans* (via co-transformation), is strong evidence that the junction region acts as an intramolecular chaperone. Although *in vitro* attempts to refold fusion protein DO518P resulted in the formation of insoluble aggregates, possibly by exposing reactive β-strands (Richardson and Richardson, 2002), anchoring of the junction region on the bacterial surface via the translocation unit may have served to circumvent aggregation between junction regions thereby allowing *trans* complementation to occur.

Despite the lack of sequence and functional identity with the PrtS protease, BrkA also has a similarly positioned junction region that functions as an intramolecular chaperone. Whether the PrtS junction and the BrkA junction are mechanistically similar awaits further elucidation. The junction region identified in PrtS is conserved in a number of autotransporters with serine protease activity

including the *B. pertussis* protein SphB1 (Coutte *et al.*, 2001). The junction region is cleaved from PrtS but not from BrkA suggesting that the folding mechanism(s) of the junction region may vary depending on the autotransporter. Recently, a new folding domain termed an 'intramolecular building block' has been described (Ma *et al.*, 2000). Intra-molecular building blocks are distinguished from traditional pro-peptides because they are not cleaved as they comprise a part of the core structure of the mature protein. Perhaps the BrkA junction region acts similarly.

Sequence conservation of the BrkA junction in a diverse subset of autotransporters suggests that its mechanism of action in this subset of autotransporters may also be conserved. It is tempting to speculate that the junction may function as a general chaperone to facilitate folding of any protein linked to it or more specifically, by mediating folding of a subset of proteins that have evolved to have similar structures with different functions. As such, the junction region (Fig. 3B) may act as a scaffold or platform from which folding is initiated. We are currently designing experiments to address these scenarios. It should be noted that whereas conserved domains for the junction region can be detected in most of the predicted autotransporters in the database, there are some exceptions [e.g. TcfA from *B. pertussis* (Finn and Stevens, 1995) and Hia from *H. influenzae* (St Geme and Cutter, 2000)]. It is possible that the passenger domains of these proteins have a different structure and so may not need folding assistance, or that the presence of a folding-promoting domain escapes detection by sequence analysis.

The role of the junction in BrkA secretion

Figure 7 depicts a model of BrkA secretion, taking into account previous models (Henderson *et al.*, 1998; Klauser *et al.*, 1993b; Ohnishi and Horinouchi, 1996) and incorporating the data presented in this paper. Using the mechanism of porin biogenesis as an analogy (Tamm *et al.*, 2001), it is proposed that following the Sec-dependent transit of BrkA through the inner membrane, the β-domain spontaneously folds into a β-barrel conformation as it interacts with the local non-polar environment of the outer membrane. The passenger domain remains unfolded as it transits through the channel (Shannon and Fernandez, 1999) and folding, using the junction region as a scaffold, begins vectorially in a C-terminal to N-terminal direction on the bacterial surface as the passenger emerges from the β-domain channel. Although we depict the passenger domain of BrkA as an unfolded intermediate, and the transporter domain as a monomer, we cannot exclude the possibility that BrkA could adopt a partially folded conformation within the periplasm, and that the channel could itself be a multimer (discussed below). In any case, two key questions in this model are: does protein folding occur on the bacterial surface, and if so, how does the protein maintain an unfolded or partially folded state in the periplasm?

We have shown that the junction region is necessary for folding of the BrkA passenger (Figs 5 and 6) and that surface expression can occur in its absence (Fig. 1B and C). The fact that we can detect an unfolded BrkA passenger on the surface of an OmpT-deficient strain (UT5600) (Fig. 1) indicates that folding is not a prerequisite for translocation, and that the unfolded BrkA passenger survived its stay in the periplasm.

Based on the size of the IgA protease β domain channel (Veiga *et al.*, 2002), the translocation-competent state of the passenger domain is likely to comprise an unfolded or partially folded intermediate (Pohlner *et al.*, 1987; Klauser *et al.*, 1993b). If the assumption that the BrkA passenger transits through the channel in an unfolded conformation is correct (Shannon and Fernandez, 1999), the fact that the junction is not necessary for transit implies that the junction may be responsible for initiating folding of the BrkA passenger following translocation across the outer membrane. Indeed, the susceptibility of unfolded proteins (Fig. 1) to outer membrane proteases such as OmpT (Grodberg and Dunn, 1988) makes it essential that the nascent passenger domain adopt a folded conformation while or shortly after it emerges from the channel. Evidence that passenger folding can occur on the bacterial surface has been provided by studies of the PrtS autotransporter (Ohnishi *et al.*, 1994). Ohnishi and colleagues reported that in the absence of the PrtS junction region, passengers could be surface expressed using the PrtS translocation unit but limited (i.e. 4–25%) functional activity was only evident when the junction region was supplied as an outer membrane protein extract *in trans* (Ohnishi *et al.*, 1994). Our *in vivo* complementation data corroborates the PrtS data. In our experiments, both the junction region itself and the junction-deleted passenger were engineered to be surface expressed using the BrkA signal peptide and translocation unit. As shown in Figs 1 and 5, the junction-deleted species is capable of being exported albeit in a protease-sensitive unfolded conformation. A surface-exposed, protease-resistant species (Fig. 5) would arise if complementation by the junction region occurred on the surface. In order for complementation to occur, it is reasonable to assume that the junction region and the junction-deleted proteins were in close proximity on the bacterial surface. The model put forth by Veiga and colleagues depicting the IgA protease β domain as forming a channel made of multimers supports such a scenario. In this regard, a less than optimal stoichiometry of the co-transformed products might account for the lack of complete complementation seen in Fig. 4.

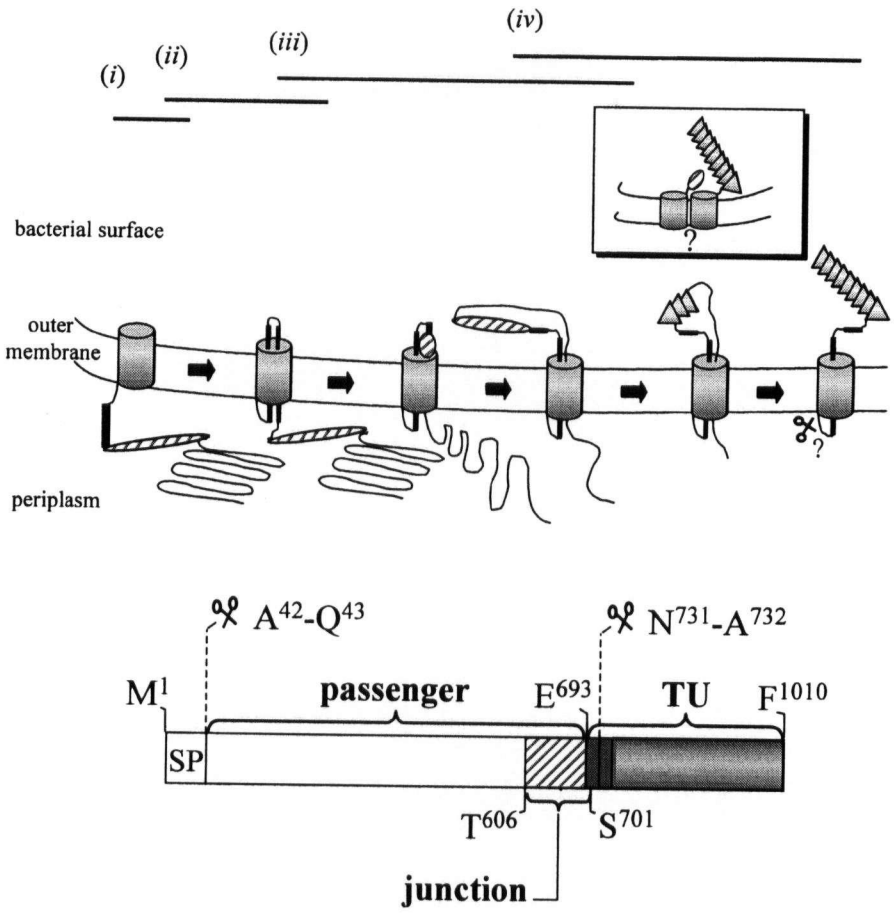

Fig. 7. Working model of BrkA translocation across the outer membrane. (*i*) Following translocation into the periplasm and cleavage of the N-terminal signal peptide, the 30 kDa β-domain folds into the outer membrane forming an amphipathic β-barrel. (*ii*) The alpha helical linker region initiates translocation of the passenger domain across the outer membrane. Although depicted as an unfolded intermediate, it is possible that the passenger domain may exist in a partially folded conformation in the periplasm. (*iii*) The passenger domain is translocated across the outer membrane in an unfolded or 'translocation-competent' state. (*iv*) Following export, or possibly concurrent with translocation onto the cell surface, the junction region acts as a scaffold to trigger folding of the passenger domain. Cleavage of the BrkA passenger is mediated by an unknown protease (in an OmpT independent manner) and the passenger remains non-covalently associated with the bacterial surface. A monomeric channel is shown but it is possible that the channel may be oligomeric. The results of the complementation experiment (inset) suggest that multiple BrkA autotransporters can interact but the exact number of interacting subunits has yet to be ascertained. Shaded boxes, translocation unit (TU), which is made up of the linker region (dark grey) and the β-core (light grey); the N-terminal boundary of the TU lies between E^{693} and S^{701} (Oliver *et al.*, 2003). Hatched area, junction region; line or white box, N-terminal passenger region. Grey triangles, folded BrkA passenger (Gln^{43}–Ala^{692}). Scissors denote cleavage site. It is not known whether cleavage takes place in the periplasm or on the surface.

We have argued that folding of the autotransporter passenger occurs on the bacterial surface, but we have not addressed the folding state of the protein in the periplasm. Indeed, how an unfolded or partially folded polypeptide is maintained during transit through the periplasm is not known. Brandon and Goldberg (2001) note that the soluble periplasmic form of the autotransporter IcsA is transient and only detectable using sensitive methods. Based on this observation it was proposed that the translocation unit inserts rapidly into the outer membrane. It is also possible that the protein may interact with an autotransporter-specific or a general periplasmic chaperone. In this regard, Purdy *et al.* (2002) have implicated the chaperone activity of DegP in the surface localization of IcsA. The status of BrkA in the periplasm is under investigation.

Autotransporters have been touted as promising systems for surface displaying heterologous proteins (Shimada *et al.*, 1994; Maurer *et al.*, 1997; Kjaergaard *et al.*, 2000; Lattemann *et al.*, 2000; Valls *et al.*, 2000; Jose *et al.*, 2001). The native passengers have evolved to be efficiently expressed using this mechanism and it stands to reason that a better understanding of the process of secretion of native passengers including the mechanism by which the junction folds passengers will allow the better design of surface display strategies for

producing functional heterologous proteins. The surface location of autotransporters has made some of them attractive candidates for vaccines (Roberts *et al.*, 1992; Hadi *et al.*, 2001; Oliver and Fernandez, 2001; van Ulsen *et al.*, 2001). We have shown that the BrkA passenger domain can be refolded *in vitro* from inclusion bodies. The conservation of the junction suggests that other autotransporters can be produced in a similar manner, at minimal cost. Finally, many autotransporters are known or proposed to be virulence factors. Inhibitors of the folding mechanism may provide a possible therapeutic approach to block colonization by limiting the ability of the autotransporter to express functional virulence factors.

Experimental procedures

Bacterial strains, plasmids and growth conditions

Bacterial strains and plasmids used in this study are listed in Table 1. *Escherichia coli* strains were cultured at 37°C on Luria broth or Luria agar supplemented with the appropriate antibiotics. UT5600 and UT2300 were a gift from L. Fernandez and V. deLorenzo (Centro Nacional de Biotecnologia, Madrid, Spain). Kanamycin was added to the media at 50 μg ml^{-1}. Ampicillin was added at 100 μg ml^{-1} for DH5α and 200 μg ml^{-1} for UT5600 and UT2300.

Recombinant DNA techniques

DNA manipulations and polymerase chain reactions (PCR) were carried out using standard techniques (Sambrook *et al.*, 1989) and reagents, as described previously (Oliver *et al.*, 2003). Plasmid pDO6935 was used as a template in all PCR reactions. Primers used in this study were obtained from Alpha DNA (Montreal, PQ) or the University of British Columbia (UBC) Nucleic Acid and Protein Services (NAPS) Unit. DNA sequencing was done by the UBC NAPS Unit.

Construct pGH3-13 was made by digesting pDO6935 with *StuI* and *Bam*HI. The resulting 6.7 kilobase pair fragment was purified and the 5′ *Bam*HI overhang was filled-in with the nucleotides dGTP, dATP, dTTP (Invitrogen, Burlington, ON) at 0.5 mM using Klenow large polymerase (Invitrogen). The remaining unpaired guanidine nucleotide was removed using mung bean endonuclease (Invitrogen) and the blunt-ended product was circularized by ligation to yield pGH3-13. Construct pDO-JB5 was made by digesting pGD7 with *Asc*I and *Xba*I. The resulting 5.0 kb product was purifed and the 5′ *Asc*I and *Xba*I overhangs were filled-in with the nucleotides dGTP and dCTP (Invitrogen, Burlington, ON) at 0.5 mM using Klenow large polymerase. The remaining unpaired nucleotides were removed using mung bean nuclease and the blunt-ended producted was circularized by ligation to yield pDO-JB5. Constructs pGH3–13K and pDO6935K were constructed by linearizing plasmids pGH3-13 and pDO6935 with *Xmn*I. A 1.4 kb *Sma*I cassette encoding resistance to kanamycin was excised from pUC4-KIXX and ligated into linearized plasmids pGH3-13 and pDO6935 to yield pGH3–13K and pDO-6935K respectively.

Expression construct pDO418 was made using primer pair G1NCO (5′-TCAGTCCATGGCGCAGGAAGGAGAGTTCG AC-3′) and G2HIND (5′- CAGTGCAAGCTTCTGCAAGCTCC AGACATG-3′) to amplify a 1.9 kb fragment representing the N-terminal passenger domain of BrkA. This product was cloned into pET30b using *Nco*I and *Hin*dIII to yield construct pDO418. Sequencing of pDO418 revealed a single base pair mutation that introduced a stop codon at the 3′ terminus of the gene fusion resulting in a translated fusion protein lacking the C-terminal His-tag. Digesting plasmid pDO418 with *Eco*RV and *Not*I and filling-in the resulting 5′ *Not*I extension using Klenow large polymerase generated a blunt ended product that was religated to yield plasmid pDO618. Digesting plasmid pDO418 with *Eco*RV and *Nco*I and filling-in the resulting 5′ *Nco*I extension with Klenow large polymerase

Table 1. Strains and plasmids.

Strain/plasmid	Relevant characteristics[a]	Reference/source
Strains		
E. coli		
UT2300	F⁻ *ara-14 leuB6 azi-6 lacYI proC14 tsx-67 entA403 trpE38 rfbD1 rpsL109 xyl-5 mtl-1 thi1*	Elish *et al.* (1988)
UT5600	UT2300 derivative, Δ*ompT-fepC266*	Elish *et al.* (1988)
DH5αF′	K-12 cloning strain	Invitrogen
Plasmids		
pET30b	Kan^r; Expression vector	Novagen
pBluescriptII SK⁻	Amp^r; cloning vector	Stratagene
pUC4-KIXX	pUC4 vector carrying a Kan^r cassette	Barany (1985)
pDO6935	Amp^r, *brk*A	Oliver *et al.* (2003)
pDO244	Amp^r, *brk*A mutant; Δ(A^{136}-P^{255})	Oliver *et al.* (2003)
pGD7	Amp^r, *brk*A mutant; Δ(S^{229}-P^{600})	Oliver *et al.* (2003)
pGH3-13	Amp^r, *brk*A mutant; Δ(E^{601}-A^{692}), derived from pDO6935	This study
pDO-JB5	Amp^r, *brk*A mutant; Δ(A^{52}-P^{600}), derived from pGD7	This study
pGH3–13K	Kan^r, pGH3-13 derivative carrying a 1.4-kb *Sma*I Kan^r cassette derived from pUC4-KIXX	This study
pDO-6935K	Kan^r, pDO-6935 derivative carrying a 1.4-kb *Sma*I Kan^r cassette derived from pUC4-KIXX	This study
pDO418	Kan^r, pET30b fusion construct; BrkA(E^{61}-V^{699})	This study
pDO518	Kan^r, pDO418 derivative, fusion construct; BrkA(I^{535}-V^{699})	This study
pDO618	Kan^r, pDO418 derivative, fusion construct; BrkA(E^{61}-D^{534})	This study

a. Kan^r, and Amp^r refer to resistance to kanamycin and ampicillin respectively.

generated a blunt ended product that was re-ligated to yield plasmid pDO518.

SDS-PAGE and immunoblot analysis

For detection of expressed BrkA via immunoblot, *E. coli* cultures were grown to 0.8 optical density (OD_{600}) units and sedimented by centrifugation. Washed pellets were resuspended finally in sample buffer and immediately boiled for 5 min before SDS-PAGE as previously described (Laemmli, 1970; Fernandez and Weiss, 1994). Samples resolved by SDS-PAGE were transferred to Immobilon-P membranes (Millipore, Etobicoke, ON) as described (Oliver and Fernandez, 2001). Staining of the SDS-PAGE gels with Coomassie blue verified that approximately equal amounts of lysates were loaded into each lane. Blots were probed using heat inactivated rabbit anti-BrkA antiserum and horseradish peroxidase-conjugated goat anti-rabbit secondary antibody (ICN Biomedicals, Costa Mesa, CA) diluted 1 : 50 000 and 1 : 10,000 respectively (Oliver and Fernandez, 2001). Kaleidoscope prestained markers (Bio-Rad, Hercules, CA) were used for estimation of molecular mass.

Immunofluorescence analysis

Indirect immunofluorescence was performed as previously described (Oliver *et al.*, 2003) using a 1 : 200 dilution of heat inactivated rabbit anti-BrkA antiserum (Oliver and Fernandez, 2001) followed by a 1 : 100 dilution of FITC-conjugated goat anti-rabbit antibody (Jackson ImmunoResearch Laboratories, West Grove, PA). Bacteria were visualized under epi-fluorescence using a Zeiss Axioscop-2 microscope. Phase contrast and fluorescent images were captured digitally.

Purification and refolding of BrkA fusion proteins

Recombinant His-tagged BrkA was expressed and purified using a protocol previously established in our laboratory (Shannon and Fernandez, 1999; Oliver and Fernandez, 2001). *Escherichia coli* strain BL21 (DE3) harbouring expression constructs (Table 1) were grown to approximately 0.6 OD_{600} units and induced with 0.1 mM isopropyl-B-D-thiogalactopyranoside (IPTG). Purification was performed under denaturing conditions using nickel Ni^{2+}-nitrilotriacetic acid (NTA)-agarose following the protocol described in the Xpress System Protein Purification manual (Invitrogen). In brief, 50 ml of induced cell culture was pelleted by centrifugation and lysed using 6 M guanidinium hydrochloride pH 7.8. Lysates were sonicated, centrifuged to remove insoluble material, and filtered through a 0.45 μm filter. Filtered lysates were bound to NTA-agarose and washed in 8 M urea at decreasing pH, and finally eluted in 8 M urea (pH 4.0). Eluted fractions were pooled, resolved by SDS-PAGE, and visualized by staining with Coomassie brilliant Blue-R250. Refolding of purified fusion proteins was performed as previously described (Oliver and Fernandez, 2001). Briefly, protein samples normalized to a concentration of 4.5 μM in 10 mM Tris buffer pH 8.0 containing 0.1% Triton X-100 were dialysed against decreasing concentrations of urea. Samples were ultimately dialysed into 10 mM Tris pH 8.0 and examined via SDS-PAGE. Protein concentration was determined using the Bio-Rad Protein Assay.

Far-UV circular dichroism spectroscopy of BrkA fusion proteins

Circular dichroism (CD) analysis was performed on dialysed BrkA fusion protein using a Jasco J-810 CD spectropolarimeter (Jasco, Easton, MD) at room temperature using a cell path length of 1 mm. Individual spectra were collected by averaging 10 scans made over a spectral window of 190 nm to 260 nm. Fusion proteins were analysed at concentration of 0.3 μg ml^{-1} in 10 mM Tris, pH 8.0 buffer.

In vitro *limited proteolysis analysis*

Limited proteolysis digestions were performed using 25 μl aliquots of DO418P (300 μg ml^{-1}) or DO618P (300 μg ml^{-1}) that had been dialysed into 10 mM Tris buffer pH 8. One microlitre of trypsin (1 μg ml^{-1}) was added to each sample and digestion was allowed to proceed at room temperature. At time intervals of 1, 5, and 15 min, reactions were stopped by the addition of 2.5 μl of 100 mM phenyl methylsulfonyl fluoride (PMSF) and stored on ice. Each sample was precipitated using 30 μl of 20% trichloroacetic acid (TCA) and sedimented by centrifugation at 4°C for 15 min. Before analysis by SDS-PAGE samples were washed with 300 μl ice-cold acetone and resuspended in 50 μl disruption buffer. Densitometry was performed using the Alpha Imager 1200 (Alpha Innotech Corporation, San Leandro, CA).

In vivo *limited proteolysis analysis*

Escherichia coli UT5600 co-transformed with the indicated plasmids were grown to an OD_{600} of 0.8 in the presence of antibiotic selection. One ml of culture was harvested by centrifugation and resuspended in 150 μl of PBS. A 15 μl aliquot was removed and added to 50 μl of SDS-PAGE disruption buffer and boiled for 5 min. Trypsin was then added to the remaining culture to a final concentration of 0.01 mg ml^{-1}. Following the addition of trypsin, 15 μl aliquots were removed at various time intervals (1, 5, 15 min) and added to 50 μl of disruption buffer and immediately boiled to stop digestion. Samples were resolved by SDS-PAGE, transferred to Immobilon-P membrane and probed for BrkA expression (as described above). Trypsin accessibility experiments were performed as previously described (Maurer *et al.*, 1997; Oliver *et al.*, 2003).

Adherence assay

HeLa cells were maintained in complete minimal essential medium (MEM) supplemented with 10% heat-inactivated fetal bovine serum, 50 U of penicillin and 50 μg ml^{-1} streptomycin. All cell culture media were purchased from Invitrogen. The adherence assay was performed in triplicate in 96-well Falcon U-bottom plates (Becton Dickinson Labware, Franklin Lakes, NJ) essentially as described by van den Berg *et al.*

(1999). Confluent monolayers were washed with PBS and the cells were detached with a 1 mM EDTA-0.25% trypsin solution (Invitrogen). A buffer control or 0.2 μg of DO418P or DO618P in 100 μl of PBS containing 0.5% BSA (PBS-BSA) were added to 100 μl of PBS-BSA containing 10^6 detached HeLa cells that had been previously fixed for 10 min with 1% formaldehyde. After incubating for 30 min at 37°C, the cells were washed twice in PBS-BSA and incubated for 30 min at room temperature with a 1 : 400 dilution of the rabbit anti-BrkA antiserum (Oliver and Fernandez, 2001). The cells were washed again, and incubated with a 1 : 200 dilution of a FITC-conjugated goat anti-rabbit antibody (Jackson ImmunoResearch Laboratories). Washed cells were then subjected to flow cytometry using a FACScan (Becton Dickinson, San Jose, Calif.) and the data from 10 000 cells were analysed using the CELLQUEST program.

Acknowledgements

Alina S. Gerrie is gratefully acknowledged for technical assistance and for critical reading of the manuscript. We thank R.E.W. Hancock and members of his lab, Jon-Paul Powers and Annete Rozek for assistance with far-UV CD spectroscopy, and Shawn Lewenza for providing valuable comments on the manuscript. D.C.O. was recipient of a University of British Columbia graduate student fellowship. This research was funded by a grant from the Natural Sciences and Engineering Research Council of Canada.

References

Agarraberes, F.A., and Dice, J.F. (2001) Protein translocation across membranes. *Biochim Biophys Acta* **1513:** 1–24.

Barany, F. (1985) Single-stranded hexameric linkers: a system for in-phase insertion mutagenesis and protein engineering. *Gene* **37:** 111–123.

Benz, I., and Schmidt, M.A. (1992) Isolation and serologic characterization of AIDA-I, the adhesin mediating the diffuse adherence phenotype of the diarrhea-associated *Escherichia coli* strain 2787 (O126: H27). *Infect Immun* **60:** 13–18.

van den Berg, B.M., Beekhuizen, H., Mooi, F.R., and van Furth, R. (1999) Role of antibodies against *Bordetella pertussis* virulence factors in adherence of *Bordetella pertussis* and *Bordetella parapertussis* to human bronchial epithelial cells. *Infect Immun* **67:** 1050–1055.

Brandon, L.D., and Goldberg, M.B. (2001) Periplasmic transit and disulfide bond formation of the autotransported *Shigella* protein IcsA. *J Bacteriol* **183:** 951–958.

Buchanan, S.K. (2001) Type I secretion and multidrug efflux: transport through the TolC channel-tunnel. *Trends Biochem Sci* **26:** 3–6.

Corpet, F., Servant, F., Gouzy, J., and Kahn, D. (2000) ProDom and ProDom-CG tools for protein domain analysis and whole genome comparisons. *Nucleic Acids Res* **28:** 267–269.

Coutte, L., Antoine, R., Drobecq, H., Locht, C., and Jacob-Dubuisson, F. (2001) Subtilisin-like autotransporter serves as maturation protease in a bacterial secretion pathway. *EMBO J* **20:** 5040–5048.

Elish, M.E., Pierce, J.R., and Earhart, C.F. (1988) Biochemical analysis of spontaneous fepA mutants of *Escherichia coli*. *J Gen Microbiol* **134:** 1355–1364.

Emsley, P., Charles, I.G., Fairweather, N.F., and Isaacs, N.W. (1996) Structure of *Bordetella pertussis* virulence factor P.69 pertactin. *Nature* **381:** 90–92.

Ewanowich, C.A., Melton, A.R., Weiss, A.A., Sherburne, R.K., and Peppler, M.S. (1989) Invasion of HeLa 229 cells by virulent *Bordetella pertussis*. *Infect Immun* **57:** 2698–2704.

Fernandez, R.C., and Weiss, A.A. (1994) Cloning and sequencing of a *Bordetella pertussis* serum resistance locus. *Infect Immun* **62:** 4727–4738.

Finn, T.M., and Stevens, L.A. (1995) Tracheal colonization factor: a *Bordetella pertussis* secreted virulence determinant. *Mol Microbiol* **16:** 625–634.

Fischer, W., Buhrdorf, R., Gerland, E., and Haas, R. (2001) Outer membrane targeting of passenger proteins by the vacuolating cytotoxin autotransporter of *Helicobacter pylori*. *Infect Immun* **69:** 6769–6775.

Grodberg, J., and Dunn, J.J. (1988) ompT encodes the *Escherichia coli* outer membrane protease that cleaves T7 RNA polymerase during purification. *J Bacteriol* **170:** 1245–1253.

Hadi, H.A., Wooldridge, K.G., Robinson, K., and Ala'Aldeen, D.A. (2001) Identification and characterization of App: an immunogenic autotransporter protein of *Neisseria meningitidis*. *Mol Microbiol* **41:** 611–623.

Henderson, I.R., and Nataro, J.P. (2001) Virulence functions of autotransporter proteins. *Infect Immun* **69:** 1231–1243.

Henderson, I.R., Navarro-Garcia, F., and Nataro, J.P. (1998) The great escape: structure and function of the autotransporter proteins. *Trends Microbiol* **6:** 370–378.

Jose, J., Bernhardt, R., and Hannemann, F. (2001) Functional display of active bovine adrenodoxin on the surface of *E. Coli* by chemical incorporation of the [2Fe-2S] cluster. *Chembiochem Europ J Chem Biol* **2:** 695–701.

Kjaergaard, K., Schembri, M.A., Hasman, H., and Klemm, P. (2000) Antigen 43 from *Escherichia coli* induces inter- and intraspecies cell aggregation and changes in colony morphology of *Pseudomonas fluorescens*. *J Bacteriol* **182:** 4789–4796.

Klauser, T., Pohlner, J., and Meyer, T.F. (1990) Extracellular transport of cholera toxin B subunit using *Neisseria* IgA protease beta-domain: conformation-dependent outer membrane translocation. *EMBO J* **9:** 1991–1999.

Klauser, T., Pohlner, J., and Meyer, T.F. (1992) Selective extracellular release of cholera toxin B subunit by *Escherichia coli*: dissection of *Neisseria* Iga beta-mediated outer membrane transport. *EMBO J* **11:** 2327–2335.

Klauser, T., Kramer, J., Otzelberger, K., Pohlner, J., and Meyer, T.F. (1993a) Characterization of the *Neisseria* Iga beta-core. The essential unit for outer membrane targeting and extracellular protein secretion. *J Mol Biol* **234:** 579–593.

Klauser, T., Pohlner, J., and Meyer, T.F. (1993b) The secretion pathway of IgA protease-type proteins in Gram-negative bacteria. *Bioessays* **15:** 799–805.

Laemmli, U.K. (1970) Cleavage of structural proteins during the assembly of the head of bacteriophage T4. *Nature* **227:** 680–685.

Lattemann, C.T., Maurer, J., Gerland, E., and Meyer, T.F. (2000) Autodisplay. functional display of active beta-lactamase on the surface of *Escherichia coli* by the AIDA-I autotransporter. *J Bacteriol* **182:** 3726–3733.

Locht, C., Antoine, R., and Jacob-Dubuisson, F. (2001) *Bordetella pertussis*, molecular pathogenesis under multiple aspects. *Curr Opin Microbiol* **4:** 82–89.

Loveless, B. J., and Saier, M.H., Jr (1997) A novel family of channel-forming, autotransporting, bacterial virulence factors. *Mol Membr Biol* **14:** 113–123.

Ma, B., Tsai, C.J., and Nussinov, R. (2000) Binding and folding: in search of intramolecular chaperone-like building block fragments. *Protein Eng* **13:** 617–627.

Maurer, J., Jose, J., and Meyer, T.F. (1997) Autodisplay: one-component system for efficient surface display and release of soluble recombinant proteins from *Escherichia coli*. *J Bacteriol* **179:** 794–804.

Maurer, J., Jose, J., and Meyer, T.F. (1999) Characterization of the essential transport function of the AIDA-I autotransporter and evidence supporting structural predictions. *J Bacteriol* **181:** 7014–7020.

McGuffin, L.J., Bryson, K., and Jones, D.T. (2000) The PSIPRED protein structure prediction server. *Bioinformatics* **16:** 404–405.

Miyazaki, H., Yanagida, N., Horinouchi, S., and Beppu, T. (1989) Characterization of the precursor of *Serratia marcescens* serine protease and COOH-terminal processing of the precursor during its excretion through the outer membrane of *Escherichia coli*. *J Bacteriol* **171:** 6566–6572.

Ohnishi, Y., and Horinouchi, S. (1996) Extracellular production of a *Serratia marcescens* serine protease in *Escherichia coli*. *Biosci Biotechnol Biochem* **60:** 1551–1558.

Ohnishi, Y., Nishiyama, M., Horinouchi, S., and Beppu, T. (1994) Involvement of the COOH-terminal pro-sequence of *Serratia marcescens* serine protease in the folding of the mature enzyme. *J Biol Chem* **269:** 32800–32806.

Oliver, D.C., and Fernandez, R.C. (2001) Antibodies to BrkA augment killing of *Bordetella pertussis*. *Vaccine* **20:** 235–241.

Oliver, D.C., Huang, G., and Fernandez, R.C. (2003) Identification of secretion determinants of the *Bordetella pertussis* BrkA autotransporter. *J Bacteriol* **185:** 489–495.

Passerini de Rossi, B.N., Friedman, L.E., Gonzalez Flecha, F.L., Castello, P.R., Franco, M.A., and Rossi, J.P. (1999) Identification of *Bordetella pertussis* virulence-associated outer membrane proteins. *FEMS Microbiol Lett* **172:** 9–13.

Pohlner, J., Halter, R., Beyreuther, K., and Meyer, T.F. (1987) Gene structure and extracellular secretion of *Neisseria gonorrhoeae* IgA protease. *Nature* **325:** 458–462.

Purdy, G.E., Hong, M., and Payne, S.M. (2002) *Shigella flexneri* DegP facilitates IcsA surface expression and is required for efficient intercellular spread. *Infect Immun* **70:** 6355–6364.

Richardson, J.S., and Richardson, D.C. (2002) Natural β-sheet proteins use negative design to avoid edge-to-edge aggregation. *Proc Natl Acad Sci USA* **99:** 2754–2759.

Roberts, M., Tite, J.P., Fairweather, N.F., Dougan, G., and Charles, I.G. (1992) Recombinant P.69/pertactin: immunogenicity and protection of mice against *Bordetella pertussis* infection. *Vaccine* **10:** 43–48.

Sambrook, J., Fritsch, E.F., and Maniatis, T. (1989) *Molecular Cloning: a Laboratory Manual*, 2nd edn. Cold Springs Harbor, NY: Cold Springs Harbor Laboratory Press.

Shannon, J.L., and Fernandez, R.C. (1999) The C-terminal domain of the *Bordetella pertussis* autotransporter BrkA forms a pore in lipid bilayer membranes. *J Bacteriol* **181:** 5838–5842.

Shikata, S., Shimada, K., Ohnishi, Y., Horinouchi, S., and Beppu, T. (1993) Characterization of secretory intermediates of *Serratia marcescens* serine protease produced during its extracellular secretion from *Escherichia coli* cells. *J Biochem* **114:** 723–731.

Shimada, K., Ohnishi, Y., Horinouchi, S., and Beppu, T. (1994) Extracellular transport of pseudoazurin of *Alcaligenes faecalis*. *Escherichia coli* using the COOH-terminal domain of *Serratia marcescens* serine protease. *J Biochem* **116:** 327–334.

St Geme, J.W. 3rd, and Cutter, D. (2000) The *Haemophilus influenzae* Hia adhesin is an autotransporter protein that remains uncleaved at the C terminus and fully cell associated. *J Bacteriol* **182:** 6005–6013.

Suhr, M., Benz, I., and Schmidt, M.A. (1996) Processing of the AIDA-I precursor. removal of AIDAc and evidence for the outer membrane anchoring as a beta-barrel structure. *Mol Microbiol* **22:** 31–42.

Suzuki, T., Lett, M.C., and Sasakawa, C. (1995) Extracellular transport of VirG protein in *Shigella*. *J Biol Chem* **270:** 30874–30880.

Tamm, L.K., Arora, A., and Kleinschmidt, J.H. (2001) Structure and assembly of B-barrel membrane proteins. *J Biol Chem* **276:** 32399–32402.

Thanassi, D.G. (2002) Ushers and secretins. Channels for the secretion of folded proteins across the bacterial outer membrane. *J Mol Microbiol Biotechnol* **4:** 11–20.

Thanassi, D.G., and Hultgren, S.J. (2000) Multiple pathways allow protein secretion across the bacterial outer membrane. *Curr Opin Cell Biol* **12:** 420–430.

Thompson, J.D., Higgins, D.G., and Gibson, T.J. (1994) CLUSTAL W: improving the sensitivity of progressive multiple sequence alignment through sequence weighting, position-specific gap penalties and weight matrix choice. *Nucleic Acids Res* **22:** 4673–4680.

van Ulsen, P., van Alphen, L., Hopman, C.T., van der Ende, A., and Tommassen, J. (2001) In vivo expression of *Neisseria meningitidis* proteins homologous to the *Haemophilus influenzae* Hap and Hia autotransporters. *FEMS Immunol Med Microbiol* **32:** 53–64.

Valls, M., Atrian, S., de Lorenzo, V., and Fernandez, L.A. (2000) Engineering a mouse metallothionein on the cell surface of *Ralstonia eutropha* CH34 for immobilization of heavy metals in soil. *Nat Biotechnol* **18:** 661–665.

Veiga, E., de Lorenzo, V., and Fernandez, L.A. (1999) Probing secretion and translocation of a beta-autotransporter using a reporter single-chain Fv as a cognate passenger domain. *Mol Microbiol* **33:** 1232–1243.

Veiga, E., Sugawara, E., Nikaido, H., de Lorenzo, V., and Fernandez, L.A. (2002) Export of autotransported proteins proceeds through an oligomeric ring shaped by C-terminal domains. *EMBO J* **21:** 2122–2131.

Yanagida, N., Uozumi, T., and Beppu, T. (1986) Specific excretion of *Serratia marcescens* protease through the outer membrane of *Escherichia coli*. *J Bacteriol* **166:** 937–944.